06/23/2011

TD-11-008

HIGH ORDER MODES IN 650 MHZ SECTIONS OF THE PROJECT X LINAC

A. Vostrikov, V. Yakovlev, N. Solyak, A. Lunin, A. Saini, T. Khabiboulline, A. Sukhanov.
Fermilab, Batavia IL 60510, U.S.A.

Abstract

Results of calculations are presented for losses caused by longitudinal high order modes (HOM) excitation in the acceleration RF system of the CW linac of the Project X facility. Emittance dilution due to both longitudinal and transversal HOMs is calculated. Collective effects are considered. 650 MHz sections of the linac are considered. HOMs with frequencies below beam-pipe cutoff frequency are considered.

Introduction

The Project X is a multi-MW proton source which is under development at Fermilab [1]. The facility is based on 3 GeV CW linac [2]. The main portion of the H^- beam from the linac is directed to three different experiments: Mu2e, Kaon, and other. Separation scheme is shown on the Figure 1. Beam is accelerated from $160\ MeV$ to $2\ GeV$ by superconducting 650 MHz cavities. Power of losses in these cavities and emittance dilution due to HOMs are the subject of calculations.

Current Spectrum Calculation

The beam in the Project X Linac contains three components which go to Mu2e, Kaon, and other experiments. One whole period of the beam structure are shown on the Figure 2. One can find its spectrum considering each component separately. The vector sum of the spectrum of these components is the spectrum of the beam. Nevertheless one can notice that the beam components for Kaon and other experiments have similar structure. These components have the same bunch frequency, but they are shifted in time. It means that they have similar spectrum with different complex phase. That is why we will consider them together. In contradiction to the components for Kaon and other experiments the beam component for Mu2e experiment has chopping. It means that the spectrum of this component is completely different. Therefore we will consider it separately and then sum it with other components.

Before starting calculations let's introduce some basic parameters of the beam, which are the same for all components of the beam. Basic frequency is $f_0 = 325 \cdot 10^6\ Hz$. Number of particles in a bunch is $N_H = 9 \cdot 10^7$. Charge of the bunch in the beam is

$$q = N_H e = 9 \cdot 10^7 \cdot 1.6 \cdot 10^{-19}\ C = 1.44 \cdot 10^{-11}\ C.$$

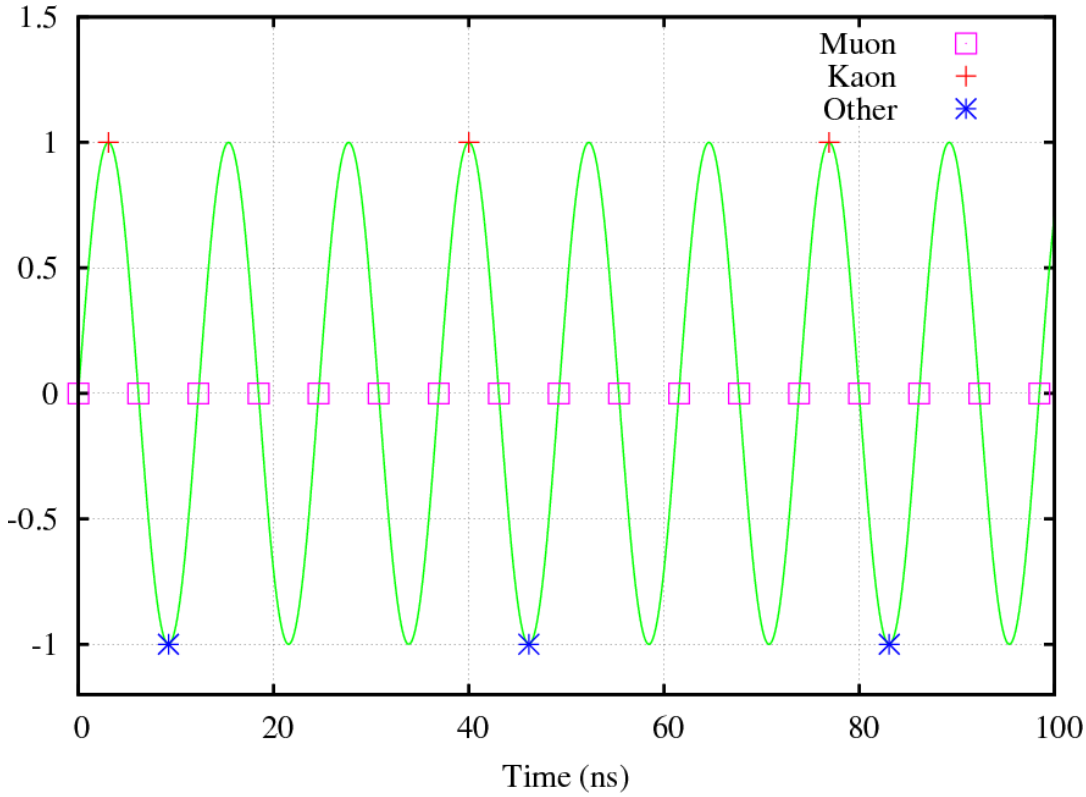

Figure 1: Beam separation scheme

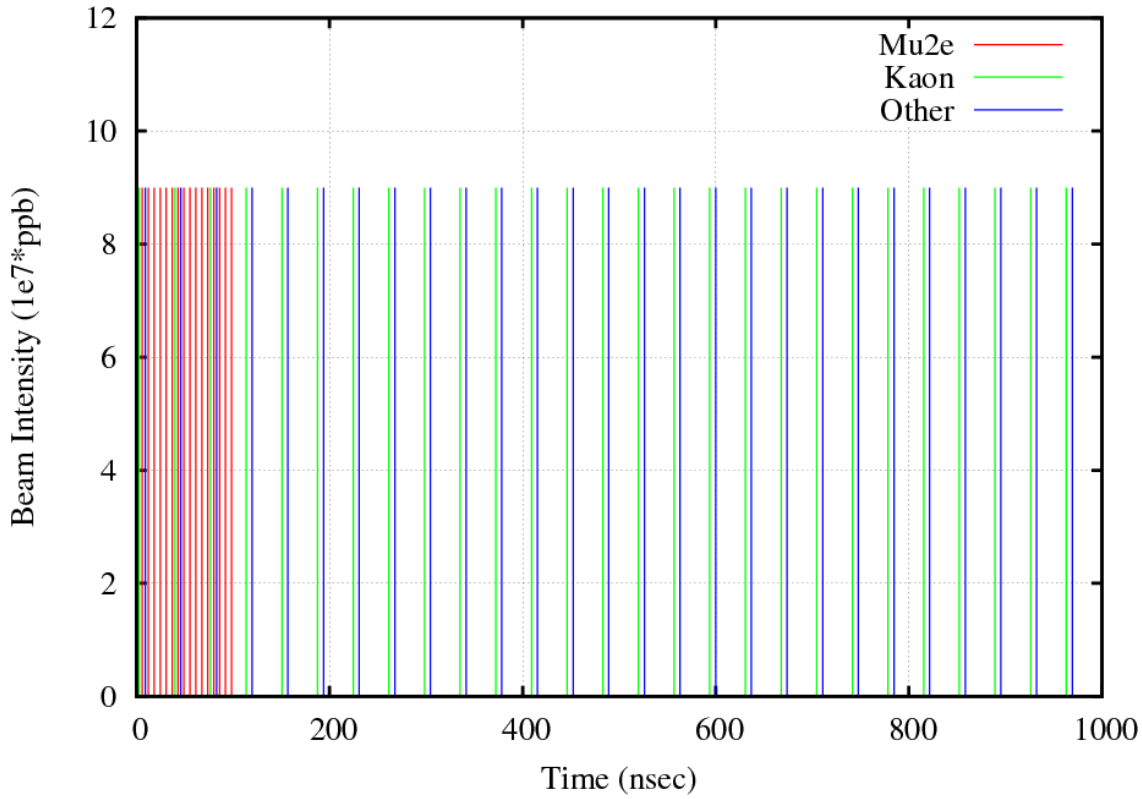

Figure 2: Beam structure [3]

Beam components for Kaon and other experiments

Time of the first bunch is

$$t_0 = \frac{a}{f_0},$$

where $a = 1$ for the component for Kaon experiment, $a = 3$ for the component for other experiments. Components bunch frequency is

$$f = \frac{f_0}{12} \approx 27.08\ MHz.$$

As there is no matching, period can be written like

$$T = \frac{1}{f} = \frac{12}{f_0} \approx 36.9\ nsec,$$

and Fourier components have circular frequencies

$$\omega_k = 2\pi k f = \frac{\pi k f_0}{6}.$$

Current function of a component can be written as

$$I(t) = \sum_{n=-\infty}^{+\infty} q\delta(t - nt_0),$$

and one can write Fourier coefficients for one component like

$$C_k^{(a)} = \frac{2}{T}\int_0^T \sum_{n=-\infty}^{+\infty} q\delta(t - nt_0)\, e^{-i\omega_k t} dt = \frac{2}{T}\int_0^T q\delta(t - t_0) e^{-i\omega_k t} dt =$$

$$= 2qf \int_0^T \delta(t) e^{-i\omega_k (t+t_0)} dt = \frac{qf_0}{6} e^{-i\omega_k t_0} = \frac{qf_0}{6} e^{-i\frac{a\pi k}{6}}.$$

Remember that the components for Kaon and other experiments have different value of a, but the same other parameters so the vector sum of these components is

$$C_k = C_k^{(1)} + C_k^{(3)} = \frac{qf_0}{6}\left(e^{-i\frac{\pi k}{6}} + e^{-i\frac{3\pi k}{6}}\right) = \frac{qf_0}{6} e^{-i\frac{\pi k}{3}}\left(e^{i\frac{\pi k}{6}} + e^{-i\frac{\pi k}{6}}\right),$$

$$C_k = \frac{qf_0}{3} e^{-i\frac{\pi k}{3}} \cos\frac{\pi k}{6}, \qquad f_k = \frac{kf_0}{12}.$$

Beam component for Mu2e experiment

Number of not chopped bunches per chopping period for the beam component for Mu2e experiment is $N = 16$, chopping rate is $\alpha = 10$. The beam component for Mu2e experiment has bunch frequency

$$f = \frac{f_0}{2} = 162.5\ MHz,$$

so time period between two bunches is

$$\Delta t = \frac{1}{f}.$$

Taking into account the number of not chopped bunches per chopping period and chopping rate, one can find period of this component $T = \Delta t \alpha N$, and Fourier components have circular frequencies

$$\omega_m = \frac{2\pi m}{T}.$$

Idealized current function of the component on a chopping period can be written as

$$I(t) = \sum_{p=0}^{N-1} q\delta(t - p\Delta t),$$

then one can write Fourier coefficients for the component like

$$C_m = \frac{2}{T}\int_0^T \sum_{p=0}^{N-1} q\delta(t - p\Delta t)\, e^{-i\omega_m t} dt = \frac{2q}{T}\sum_{p=0}^{N-1} e^{-i\omega_m p\Delta t} = \frac{2q}{T}\sum_{p=0}^{N-1}\left(e^{-i\omega_m \Delta t}\right)^p =$$

$$= \frac{2q}{T}\sum_{p=0}^{N-1}\left(e^{-2\pi i\frac{m\Delta t}{T}}\right)^p = \frac{2q}{T}\sum_{p=0}^{N-1}\left(e^{-2\pi i\frac{m}{\alpha N}}\right)^p.$$

We have to consider two cases here:

1. If
$$\frac{m}{\alpha N} \in \mathbb{Z}, \qquad \text{then } C_m = \frac{2qN}{T}, \qquad f_m = \frac{mf_0}{2\alpha N}.$$
2. If
$$\frac{m}{\alpha N} \notin \mathbb{Z}, \qquad \text{then } C_m = \frac{2q}{T}\cdot\frac{1 - e^{-2\pi i\frac{m}{\alpha}}}{1 - e^{-2\pi i\frac{m}{\alpha N}}}, \qquad f_m = \frac{mf_0}{2\alpha N}.$$

Coincidence of frequencies

Fourier coefficients for the whole beam are the vector sum of coefficients for each component at each value of frequency. It is necessary to find common frequencies for both types of components. For doing this we have to solve an equation:

$$f_m = f_k \Rightarrow \frac{mf_0}{2\alpha N} = \frac{kf_0}{12} \Rightarrow \frac{m}{\alpha N} = \frac{k}{6} \Rightarrow m = \frac{80}{3}k,$$

where k and m are both integer numbers. It is clear that k has to be multiple of 3. Let's consider two possible cases:

1. $k = 6n$, and n is integer then
$$m = 160n \Rightarrow \frac{m}{\alpha N} \in \mathbb{Z},$$
and total amplitude and frequency:
$$C_n = \frac{qf_0}{3}e^{-2\pi n i}\cos\pi n + \frac{2qN}{T} = (-1)^n\frac{qf_0}{3} + \frac{qf_0}{\alpha} = qf_0\left(\frac{1}{\alpha} + \frac{(-1)^n}{3}\right), \qquad f_n = \frac{nf_0}{2}.$$
2. $k = 6n - 3$, then amplitude of the beam components for Kaon and other experiments is
$$C_k = \frac{qf_0}{3}e^{-i\frac{\pi k}{3}}\cos\left(\pi n - \frac{\pi}{2}\right) = 0$$

so in spite of the frequency coincidence total amplitude depends on the component for Mu2e experiment only.

All other frequencies are contained by one spectrum only (the component for Mu2e experiment or Kaon and other experiment) so they do not have to be summed.

Total Fourier coefficients

All Fourier coefficients for whole beam are the follow:

- Sum component:

$$|C_n| = qf_0 \left| \frac{1}{\alpha} + \frac{(-1)^n}{3} \right|, \qquad f_n = \frac{nf_0}{2}, \qquad n \in \mathbb{N}.$$

- The beam components for Kaon and other experiments only:

$$|C_n| = \frac{qf_0}{3} \left| \cos \frac{\pi n}{6} \right|, \qquad f_n = \frac{nf_0}{12}, \qquad n \in \mathbb{N}, \qquad \frac{n}{3} \notin \mathbb{N}.$$

- The component for Mu2e experiment only:

$$|C_n| = \frac{qf_0}{\alpha N} \left| \frac{\sin \frac{\pi n}{\alpha}}{\sin \frac{\pi n}{\alpha N}} \right|, \qquad f_n = \frac{nf_0}{2\alpha N}, \qquad n \in \mathbb{N}, \qquad \frac{n}{\alpha N} \notin \mathbb{N}.$$

The idealized spectrum of the beam is shown on the Figure 3. The beam imperfectness like finite time of bunches and jitter effects are not taken into account. One can see that it has spectral components with large amplitude every $325\ MHz$, components with smaller amplitudes about every $27\ MHz$, and sidebands about every $1\ MHz$.

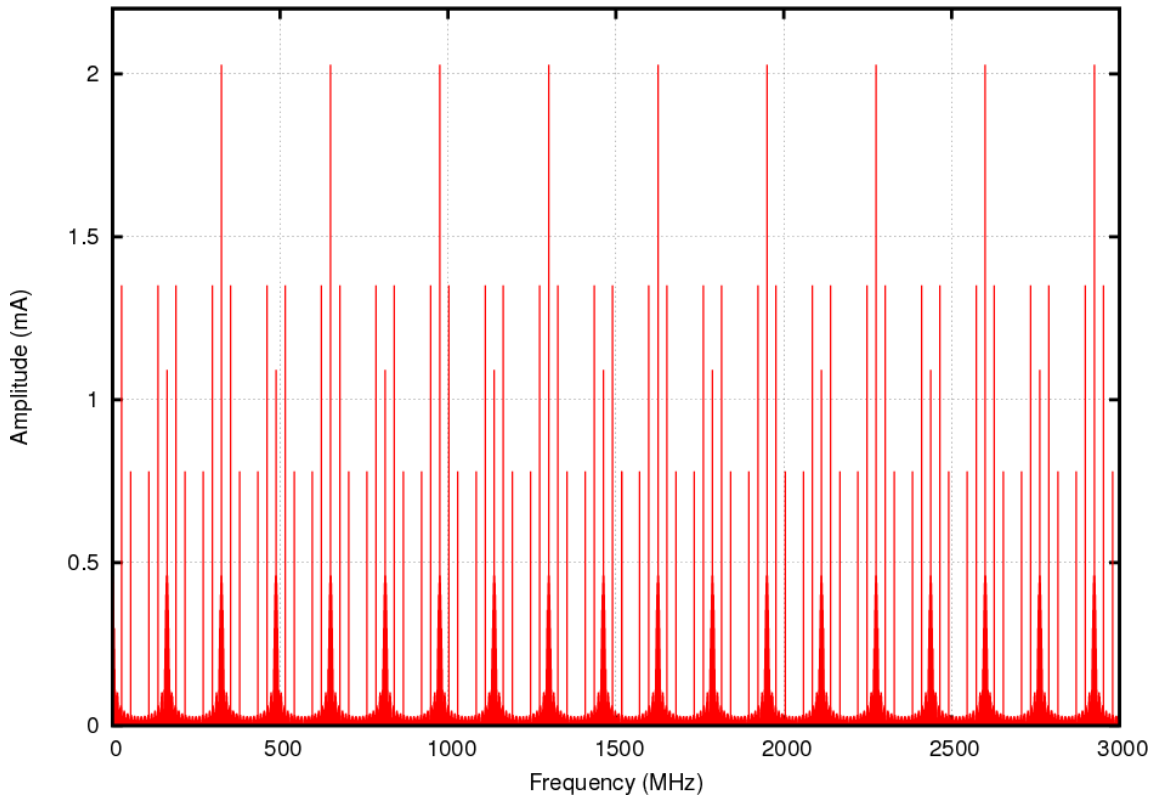

Figure 3: Beam spectrum

Quality Factor Assumptions

The quality factor of the fundamental accelerating mode is equal to $1.5 \cdot 10^{10}$ for Low Energy section (LE650) section and it is equal to $2 \cdot 10^{10}$ for High Energy section (HE650) section [4]. This mode is connected to feeding line (this is necessary for acceleration of particles), that is why it is important to know its external quality factor. Maximum value of the external quality factor can be estimated as

$$Q_0 = \frac{R_{bunch}}{(R/Q)_0} = \frac{U/\bar{I}}{(R/Q)_0},$$

where $(R/Q)_0$ is impedance of the mode (accelerator definition is used, see below), U is amplitude on a cavity, $\bar{I} = 1\ mA$ is the average current. Maximum value of amplitude is $12\ MV$ at LE650 and $20\ MV$ at HE650. The main mode impedance at optimal beta equals to $378\ \Omega$ at LE650 and $638\ \Omega$ at HE650. So external quality factors of the accelerating modes at these sections are following:

$$Q_{0ext}^{LE650} = 3.2 \cdot 10^7, \qquad Q_{0ext}^{HE650} = 3.1 \cdot 10^7.$$

Actual value of the quality factor is smaller because of microphonics, but this approximation is enough for our estimations.

HOMs quality factors have connection with external load. Their values are defined by leak to main coupler, Ohmic losses in walls of a cavity, and leak to HOM damper if one has it. Due to high frequencies of HOMs their quality factors are smaller than the quality factor of the accelerating mode. The following values of quality factors of HOMs are considered: 10^7, 10^8, 10^9, 10^{10}.

Losses Calculation

The beam going through a cavity excites eigenmodes of the cavity. The main accelerating mode is compensated, but there are also high order modes (HOM) in the cavity. Excitation of HOMs leads to losses of beam power. It is necessary to know which modes the cavity has to evaluate these losses. Magnetic field of these modes on the surface is necessary too. As we know shapes of cavities, we can get all needed information using CLANS code [5]. After that we can calculate losses as it is described below.

Before start the calculation let us introduce notations which we are going to use. $\tilde{I}_n$ is a harmonic of alternating current, $\vec{J}_n$ is density of current of this harmonic, ω_n is its circular frequency. Circular frequencies of cavity modes are ω_m and ω_p. Q_m and Q_p are quality factors of the modes. $\{\vec{E}_m, \vec{H}_m\}$ are normalized eigenmodes, $\vec{E}_{nm}$ and $\vec{H}_{nm}$ are electric and magnetic fields of the mode on a certain harmonic of current. $\vec{E}^{(n)}$ and $\vec{H}^{(n)}$ are total electric and magnetic fields on a certain harmonic of current. W_m is normalized value of stored energy, W_{nm} is energy stored by the mode due to a certain harmonic of current. U_m is normalized induced voltage, U_{nm} is induced voltage of the mode due to a certain harmonic of current.

As it is shown in [6] if there is electric current with density $\vec{J}_n$ and circular frequency ω_n in a cavity with eigenmodes $\{\vec{E}_m, \vec{H}_m\}$, the fields in the cavity will be expressed as

$$\vec{E}^{(n)} = \sum_m \vec{E}_{nm} = \sum_m A_m \vec{E}_m\,, \qquad \vec{H}^{(n)} = \sum_m \vec{H}_{nm} = \sum_m B_m \vec{H}_m, \tag{1}$$

where

$$A_m = \frac{-\omega_n}{i\left(\omega_n^2 - \omega_m^2 - i\frac{\omega_n\omega_m}{Q_m}\right)} \frac{\oint_V \vec{J}_n \vec{E}_m^* dV}{\oint_V \vec{H}_m \vec{H}_m^* dV},$$

$$B_m = \frac{-\omega_m}{i\left(\omega_n^2 - \omega_m^2 - i\frac{\omega_n\omega_m}{Q_m}\right)} \frac{\oint_V \vec{J}_n \vec{E}_m^* dV}{\oint_V \vec{H}_m \vec{H}_m^* dV}.$$

Q_m is quality factor of the mode here.

Now let's consider each term in the sums separately. In case of thin beam, electric field $\vec{E}_m$ can be considered constant in its cross-section, then

$$\oint_V \vec{J}_n \vec{E}_m^* dV = \int_L \vec{E}_m^* \oint_S \vec{J}_n dS\, dl = \int_L \vec{E}_m^* \vec{\tilde{I}}_n dl = \tilde{I}_n \int_{-\infty}^{+\infty} E_{mz}^*(x,y,z) e^{i\left(\frac{kz}{\beta}+\varphi\right)} dz = -\tilde{I}_n U_m^*.$$

where phase φ is optimal so U_m^* is a real number.

Energy stored by the mode can be written as

$$\oint_V \vec{H}_m \vec{H}_m^* dV = 2W_m.$$

That is why the fields' coefficients look like

$$A_m = \frac{\omega_n}{i\left(\omega_n^2 - \omega_m^2 - i\frac{\omega_n\omega_m}{Q_m}\right)} \frac{\tilde{I}_n}{2} \frac{U_m^*}{W_m},$$

$$B_m = \frac{\omega_m}{i\left(\omega_n^2 - \omega_m^2 - i\frac{\omega_n\omega_m}{Q_m}\right)} \frac{\tilde{I}_n}{2} \frac{U_m^*}{W_m}.$$

Taking into account the equation $\vec{E}_{nm} = A_m \vec{E}_m$ and integrating it along the beam through the cavity one can write the formula for the voltage which beam excites on the cavity at mode $\vec{E}_m$:

$$U_{nm} = A_m U_m = \frac{\omega_n}{i\left(\omega_n^2 - \omega_m^2 - i\frac{\omega_n\omega_m}{Q_m}\right)} \frac{\tilde{I}_n}{2} \frac{U_m U_m^*}{W_m}. \tag{2}$$

Using the accelerator definition of mode impedance (in contrast to the circuit definition)

$$\left(\frac{R}{Q}\right)_m = \frac{U_m U_m^*}{\omega_m W_m} = \frac{U_{nm} U_{nm}^*}{\omega_m W_{nm}},$$

one can write the formula (2) like

$$U_{nm} = \frac{\omega_n\omega_m}{i\left(\omega_n^2 - \omega_m^2 - i\frac{\omega_n\omega_m}{Q_m}\right)} \frac{\tilde{I}_n}{2} \left(\frac{R}{Q}\right)_m, \tag{3}$$

and one can get the ratio

$$\frac{|U_{nm}|}{|U_m|} = \sqrt{\frac{W_{nm}}{W_m}} = \sqrt{\frac{U_{nm}^2}{\omega_m \left(\frac{R}{Q}\right)_m W_m}}. \tag{4}$$

Now let's rewrite magnetic field like

$$\vec{H}_{nm} = \left|\vec{H}_{nm}\right| e^{i\arg(\vec{H}_{nm})} \vec{a},$$

where $\vec{a}$ is a unit vector.

For the magnitude of magnetic field it can be written from (1)

$$\left|\vec{H}_{nm}\right| = \left|B_m \vec{H}_m\right| = \left| \frac{\omega_m}{\omega_n^2 - \omega_m^2 - i\frac{\omega_n \omega_m}{Q_m}} \frac{\tilde{I}_n}{2} \frac{U_m^*}{W_m} \vec{H}_m \right|.$$

From the equation (2) follows

$$\left| \frac{\omega_m}{\omega_n^2 - \omega_m^2 - i\frac{\omega_n \omega_m}{Q_m}} \frac{\tilde{I}_n}{2} \frac{U_m^*}{W_m} \right| = \left| \frac{U_{nm}}{\omega_n U_m} \right|.$$

Then also taking into account the equation (4), one can write

$$\left|\vec{H}_{nm}\right| = \left| \frac{\omega_m}{\omega_n} \frac{U_{nm}}{U_m} \vec{H}_m \right| = \frac{\omega_m}{\omega_n} \sqrt{\frac{U_{nm}^2}{\omega_m \left(\frac{R}{Q}\right)_m W_m}} \left|\vec{H}_m\right| = \frac{1}{\sqrt{\left(\frac{R}{Q}\right)_m W_m}} \frac{\sqrt{\omega_m}}{\omega_n} |U_{nm}| \left|\vec{H}_m\right|.$$

As U_m and U_m^* are real numbers,

$$\arg(\vec{H}_{nm}) = \arg\left(\frac{1}{i\left(\omega_n^2 - \omega_m^2 - i\frac{\omega_n \omega_m}{Q_m}\right)} \right) = \arg(U_{nm}).$$

Finally,

$$\vec{a} = \frac{\vec{H}_m}{\left|\vec{H}_m\right|}.$$

Now one can write the equation for magnetic field:

$$\vec{H}_{nm} = \frac{1}{\sqrt{\left(\frac{R}{Q}\right)_m W_m}} \frac{\sqrt{\omega_m}}{\omega_n} |U_{nm}| |\vec{H}_m| e^{i\arg(U_{nm})} \frac{\vec{H}_m}{|\vec{H}_m|} = \frac{1}{\sqrt{\left(\frac{R}{Q}\right)_m W_m}} \frac{\sqrt{\omega_m}}{\omega_n} U_{nm} \vec{H}_m.$$

Applying the equation (3) for HOM voltage to the magnetic field equation, one can get

$$\vec{H}_{nm} = \frac{\omega_m \sqrt{\omega_m}}{i\left(\omega_n^2 - \omega_m^2 - i\frac{\omega_n \omega_m}{Q_m}\right)} \frac{\tilde{I}_n}{2\sqrt{W_m}} \sqrt{\left(\frac{R}{Q}\right)_m} \vec{H}_m.$$

Note that there is a factor $\sqrt{\omega_m}$ because of normalization on stored energy.

We already calculated current spectrum:

$$\tilde{I}(\omega) = \sum_n \tilde{I}_n \delta(\omega - \omega_n),$$

where ω_n is current frequency. Monopole high-order mode spectrum for both LE650 and HE650 cavities are also known (see Figures 4 – 7). We have magnetic field of each mode on the surface of the cavity $H_m(z)$ for stored energy $W_m = W_0 = 1\ mJ$ for each mode from CLANS.

Let's separate terms which depend on HOM frequency, longitudinal coordinate in the cavity, and terms which do not depend on these parameters. For doing this one can write magnetic field on the surface of the cavity as

$$H_{nm}(z) = -iH_m(z) \frac{\tilde{I}_n}{2\sqrt{W_0}} \sqrt{\left(\frac{R}{Q}\right)_m} \cdot \frac{\omega_m \sqrt{\omega_m}}{\omega_n^2 - \omega_m^2 - i\frac{\omega_n \omega_m}{Q_m}} = -iC_{nm} f_{nm} H_m(z),$$

where there are notations

$$C_{nm} = \frac{\tilde{I}_n}{2\sqrt{W_0}} \sqrt{\left(\frac{R}{Q}\right)_m}, \qquad f_{nm} = \frac{\omega_m \sqrt{\omega_m}}{\omega_n^2 - \omega_m^2 - i\frac{\omega_n \omega_m}{Q_m}}.$$

One can see that only term f_{nm} depends on HOM frequency, and only $H_m(z)$ depends on longitudinal coordinate. Taking into account all modes (equation (1)) and whole current spectrum, power of losses can be expressed like

$$P = \sum_n \frac{1}{2} R_n \oint \vec{H}^{(n)} \vec{H}^{(n)*} ds = \sum_n \frac{1}{2} R_n \oint \left(\sum_m -iC_{nm} f_{nm} H_m(z)\right)\left(\sum_p -iC_{np} f_{np} H_p(z)\right)^* ds,$$

where R_n is surface resistance. It consists of two terms: residual and BCS resistance.

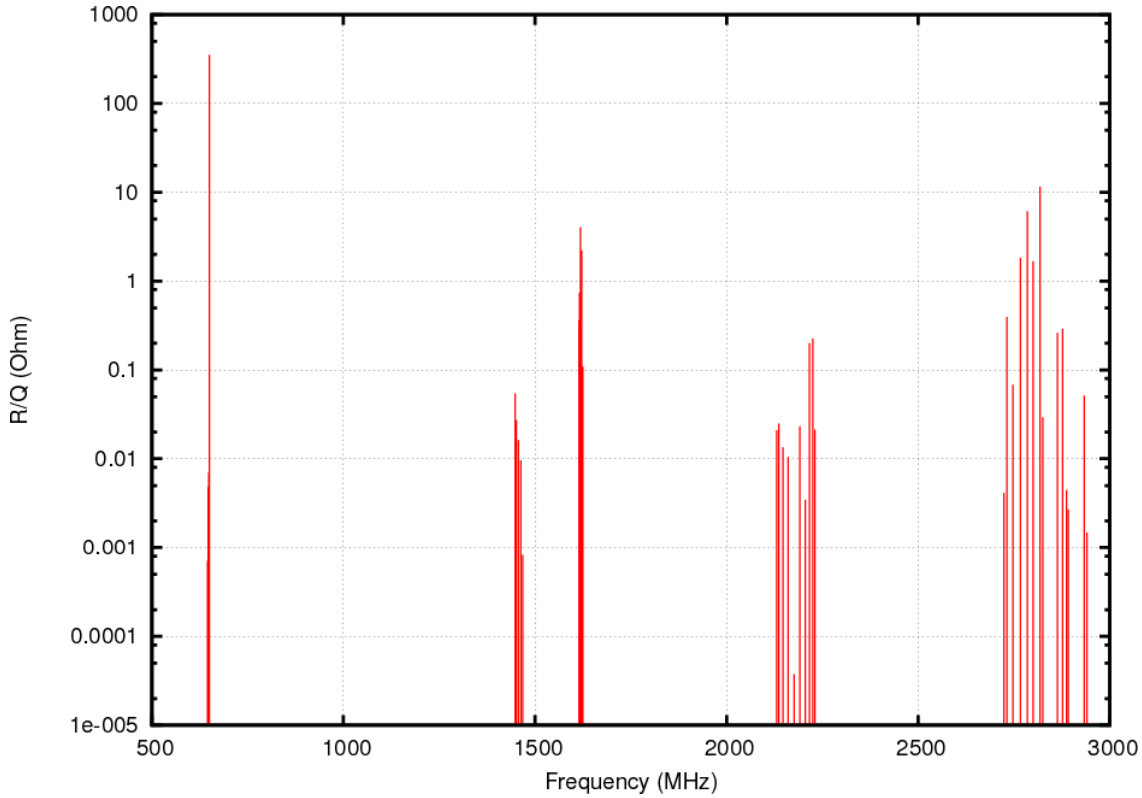

Figure 4: LE650 section monopole HOM spectrum at geometrical beta

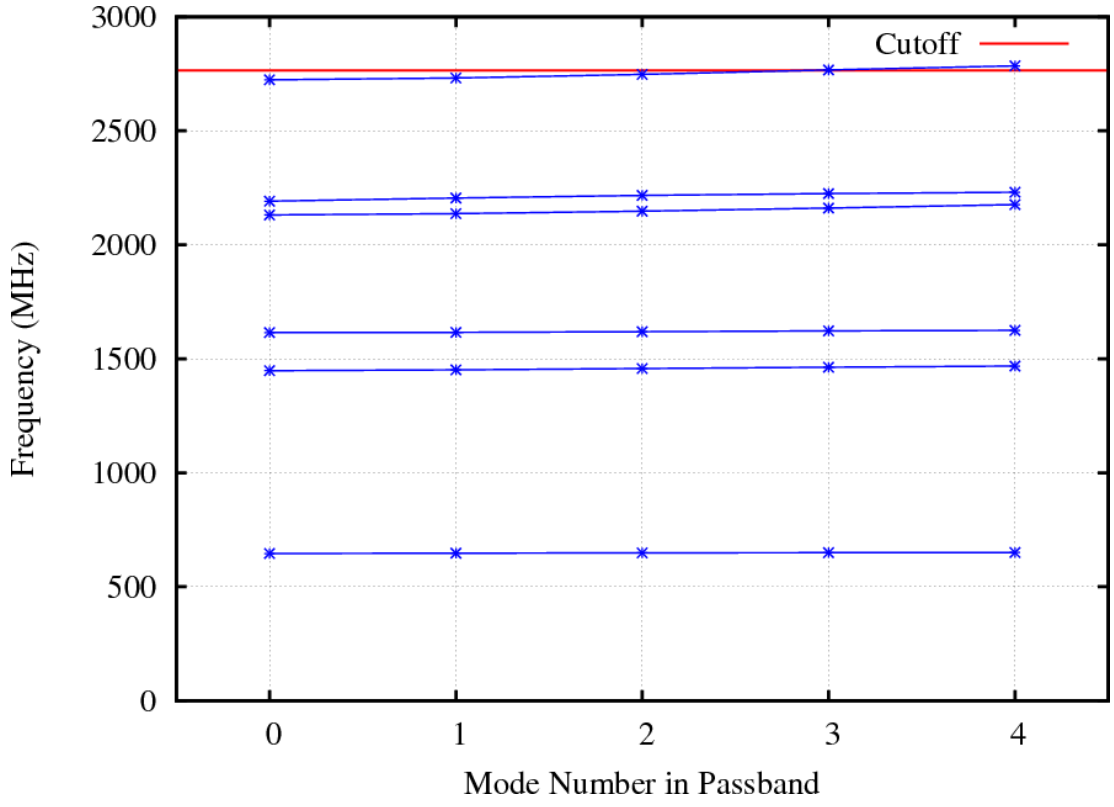

Figure 5: Dispersion curves for LE650

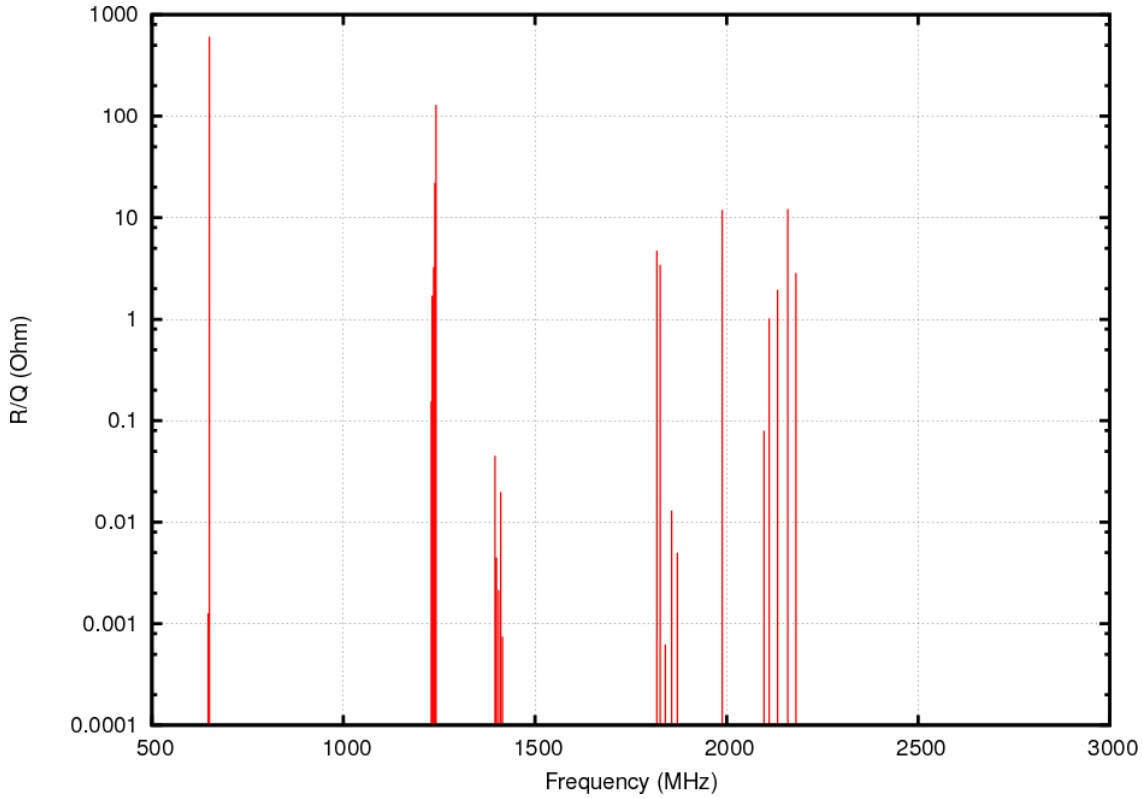

Figure 6: HE650 section monopole HOM spectrum at geometrical beta

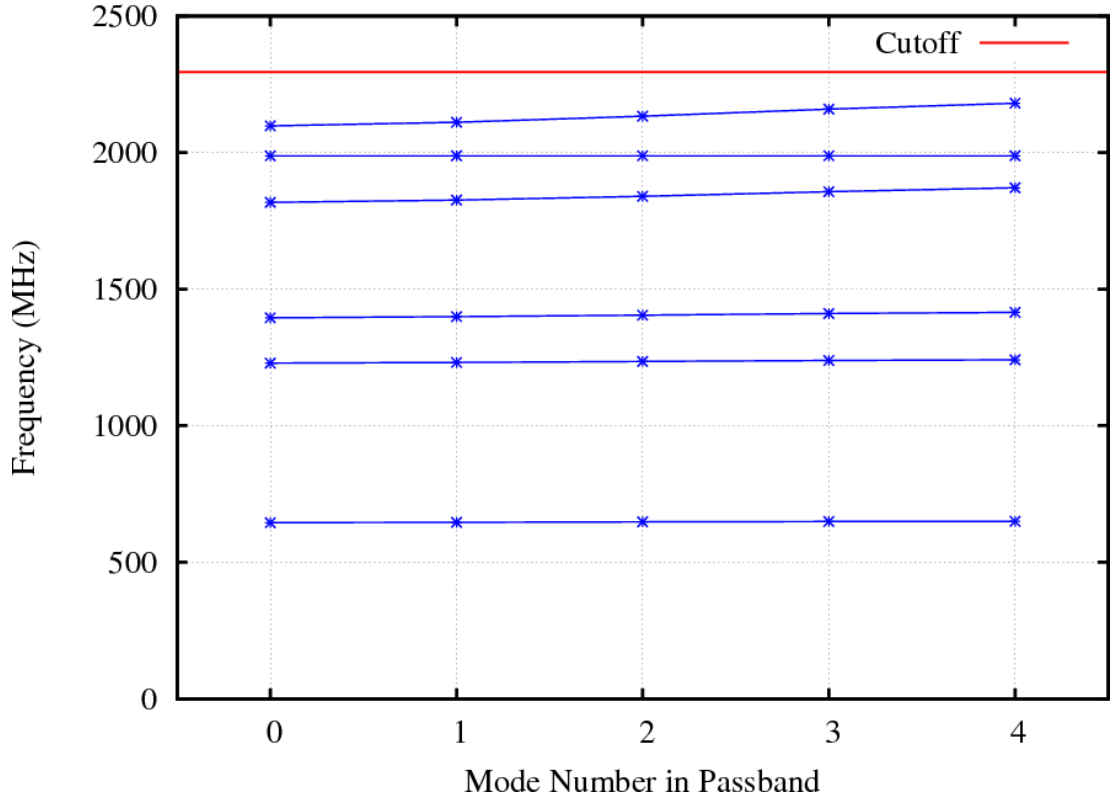

Figure 7: Dispersion curves for HE650

$$R_n = R_{residual} + R_{BCS}^n.$$

For calculations we use a conservative value of residual resistance

$$R_{residual} = 10\ n\Omega,$$

and the average value of BCS resistance [4]

$$R_{BCS}^n[\Omega] = 2 \cdot 10^{-4} \frac{1}{T[K]} \left(\frac{f_n[GHz]}{1.5}\right)^2 e^{-\frac{17.67}{T[K]}},$$

where f_n is frequency of the current spectral line, T is temperature and

$$T = 2\ K.$$

If $f_n = 650\ MHz$, then $R_{BCS}^n = 2.7\ n\Omega$.

Now as C_{nk} and f_{nk} do not depend on longitudinal coordinate, one can rewrite the integral:

$$P = \sum_n \frac{1}{2} R_n \oint \sum_m C_{nm} f_{nm} H_m(z) \cdot \sum_p C_{np} f_{np}^* H_p(z)\, ds =$$

$$= \sum_n \frac{1}{2} R_n \oint \sum_m \sum_p C_{nm} C_{np} f_{nm} f_{np}^* H_m(z) H_p(z)\, ds =$$

$$= \sum_n \frac{1}{2} R_n \sum_m \sum_p C_{nm} C_{np} f_{nm} f_{np}^* \oint H_m(z) H_p(z) ds.$$

Let's introduce new notations to simplify the equation:

$$C_{nm} C_{np} = B_{nmp} = \left(\frac{\tilde{I}_n}{2}\right)^2 \frac{1}{W_0} \sqrt{\left(\frac{R}{Q}\right)_m \left(\frac{R}{Q}\right)_p},$$

$$\oint H_m(z) H_p(z) ds = A_{mp},$$

then the formula for losses power will look like

$$P = \sum_n \frac{1}{2} R_n \sum_m \sum_p B_{nmp} A_{mp} \cdot f_{nm} f_{np}^* = \sum_n \sum_m \sum_p \frac{1}{2} R_n B_{nmp} A_{mp} \cdot f_{nm} f_{np}^*,$$

$$P = \sum_n \sum_m \sum_p a_{nmp} f_{nm} f_{np}^*,$$

where we introduced a new parameter

$$a_{nmp} = \frac{1}{2} R_n B_{nmp} A_{mp}.$$

This parameter depends on beam spectrum, modes impedances and magnetic field on the surface of the cavity. Let's consider mode frequency dependent term:

$$f_{nm} f_{np}^* = \frac{\omega_m^{3/2} \omega_p^{3/2}}{\left(\omega_n^2 - \omega_m^2 - i\frac{\omega_n \omega_m}{Q_m}\right)\left(\omega_n^2 - \omega_p^2 + i\frac{\omega_n \omega_p}{Q_p}\right)}.$$

If $m = p$ then

$$f_{nm} f_{np}^* = f_{nm} f_{nm}^* = \frac{\omega_m^3}{(\omega_n^2 - \omega_m^2)^2 + \frac{\omega_n^2 \omega_m^2}{Q_m^2}},$$

otherwise

$$f_{nm} f_{np}^* + f_{np} f_{nm}^* = 2\mathrm{Re}\left(f_{nm} f_{np}^*\right) = 2\mathrm{Re}\left(\frac{\omega_m^{3/2} \omega_p^{3/2}}{\left(\omega_n^2 - \omega_m^2 - i\frac{\omega_n \omega_m}{Q_m}\right)\left(\omega_n^2 - \omega_p^2 + i\frac{\omega_n \omega_p}{Q_p}\right)}\right).$$

One can notice that $a_{nmp} = a_{npm}$, then power of losses:

$$P = \sum_n \sum_m a_{nmm} f_{nm} f_{nm}^* + \sum_n \sum_m \sum_{p<m} 2 a_{nmp} \mathrm{Re}\left(f_{nm} f_{np}^*\right). \tag{5}$$

Now let's go back to A_{mp} definition. Cavities in LE650 and HR650 are axial symmetric so integration on the surface can be replaced by integration on the length of the border of cavity's cross-section by introducing

$$ds = 2\pi r(l) dl,$$

where l is a new integration variable. Applying this change of variables to the equation for A_{mp} one can write

$$A_{mp} = \oint H_m(z) H_p(z) ds = \int_0^L 2\pi r(l) H_m(l) H_p(l) dl,$$

where $r(l)$ is the cavity radius, L is length of the border of cavity's cross-section.

Finally we have the equation (5) for power of losses calculation, and we know how to calculate all terms in this equation.

Simulation

Let's say one has a set of current spectrum frequencies and amplitudes

$$\{\omega_n, \tilde{I}_n : \omega_n < \omega_{n+1}, 1 \le n \le +\infty\},$$

and a set of modes frequencies, impedances and quality factors

$$\left\{\omega_m, \left(\frac{R}{Q}\right)_m, Q_m : \omega_m < \omega_{m+1}, 0 \le m \le +\infty\right\},$$

where ω_0 is the accelerating mode. All frequencies have to be less than cutoff frequency, which we define as cutoff frequency of the TM_{01} mode in a waveguide of circular cross-section, which is given by

$$\omega_c = c\frac{\chi_{01}}{r} \approx \frac{2.4048c}{r},$$

where c is speed of light, χ_{01} is the first root of the Bessel function of the first kind of order 1, and r is the radius of the waveguide (which is the radius of the tube in our case). $r = 4.15\ cm$ for LE650 cavities, and $r = 5\ cm$ for HE650 cavities, so

$$f_c^{LE650} = 2765\ MHz,$$

$$f_c^{HE650} = 2295\ MHz.$$

This condition gives us limitations on the sets sizes: N and $M + 1$ correspondingly.

Remember that losses on excitation of the accelerating mode are compensated, that is why there are no terms

$$\sum_{n=1}^{N} a_{n00} f_{n0} f_{n0}^*$$

in the formula for power of losses:

$$P = \sum_{n=1}^{N}\sum_{m=1}^{M} a_{nmm} f_{nm} f_{nm}^* + \sum_{n=1}^{N}\sum_{m=1}^{M}\sum_{p=0}^{m-1} 2a_{nmp} Re\left(f_{nm} f_{np}^*\right) =$$

$$= \sum_{n=1}^{N}\sum_{m=1}^{M} a_{nmm} f_{nm} f_{nm}^* + \sum_{n=1}^{N}\sum_{m=1}^{M}\sum_{p=1}^{m-1} 2a_{nmp} \mathrm{Re}\left(f_{nm} f_{np}^*\right) + \sum_{n=1}^{N}\sum_{m=1}^{M} 2a_{nm0} \mathrm{Re}(f_{nm} f_{n0}^*).$$

Let's introduce new parameters:

$$P_2 = \sum_{n=1}^{N} \sum_{m=1}^{M} a_{nmm} f_{nm} f_{nm}^*,$$

$$P_1 = \sum_{n=1}^{N} \sum_{m=1}^{M} \sum_{p=1}^{m-1} 2a_{nmp} \mathrm{Re}\left(f_{nm} f_{np}^*\right), \qquad P_0 = \sum_{n=1}^{N} \sum_{m=1}^{M} 2a_{nm0} \mathrm{Re}(f_{nm} f_{n0}^*).$$

P_2 includes diagonal terms. It shows value of losses due to a mode itself. P_0 includes cross-terms with the accelerating mode. P_1 includes the rest of cross-terms. These are integrals of product of eigen functions of different modes. It is clear that $P = P_2 + P_1 + P_0$, but calculation of the term P_1 is CPU-time consuming. That is why first we start with some test runs to compare values of these terms.

Losses contributions one can define as

$$\delta_i = \frac{P_i}{P}, \qquad i = 0, 1, 2.$$

Results for sections LE650 and HE 650 and values of quality factor of HOMs 10^7, 10^8, 10^9, and 10^{10} are shown on the Figures 8 – 15. About 350 runs are made for each value of beta. Losses contributions are calculated for each run. Maximum values of contributions by cross-terms with the accelerating mode and the rest of cross-terms are shown on the figures in green and blue lines. For diagonal terms minimum value is calculated. It is shown on the figures in red line.

One can see that even the maximum value of losses contribution by cross-terms is always less than 0.01, and the minimum value of δ_2 is equal to 1 with very good accuracy. It means that

$$P_2 \gg P_1, \qquad \text{and } P_2 \gg P_0,$$

that is why power of losses can be calculated as

$$P = P_2 + P_1 + P_0 \approx P_2 = \sum_{n=1}^{N} \sum_{m=1}^{M} a_{nmm} f_{nm} f_{nm}^* \tag{6}$$

with error less than 1%.

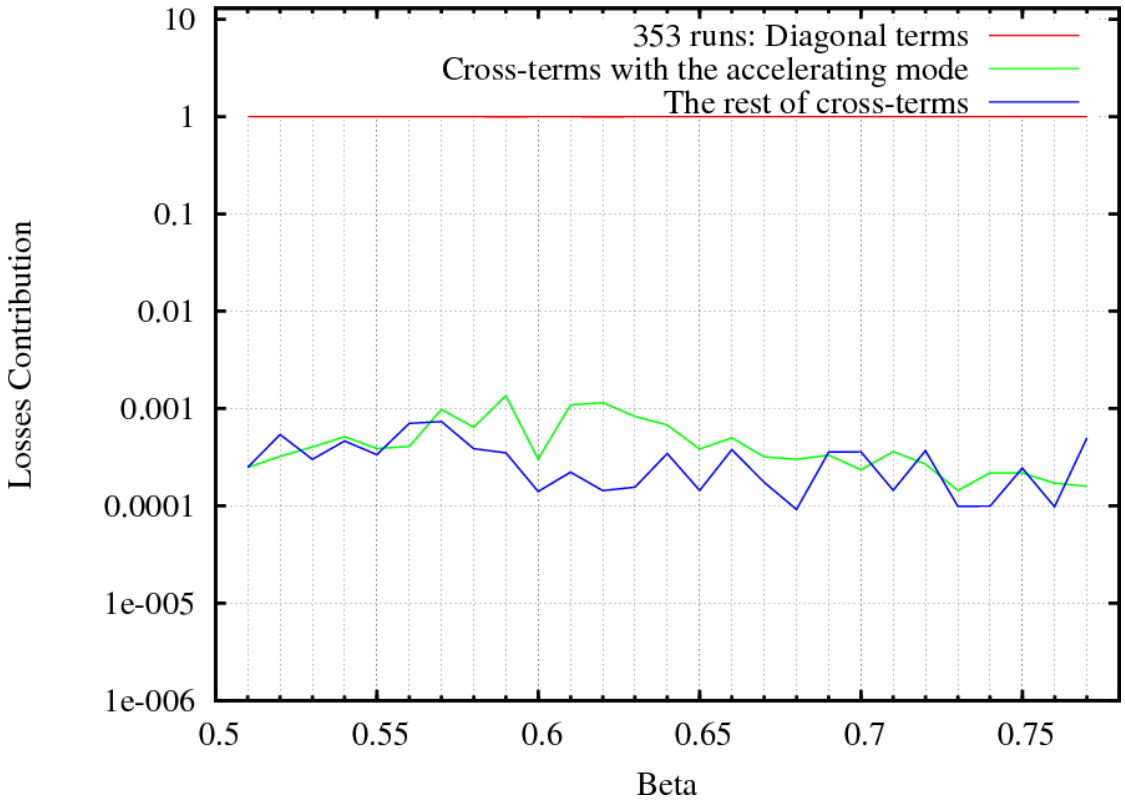

Figure 8: Losses contributions from terms P_2, P_0, P_1 at LE650, $Q = 10^7$

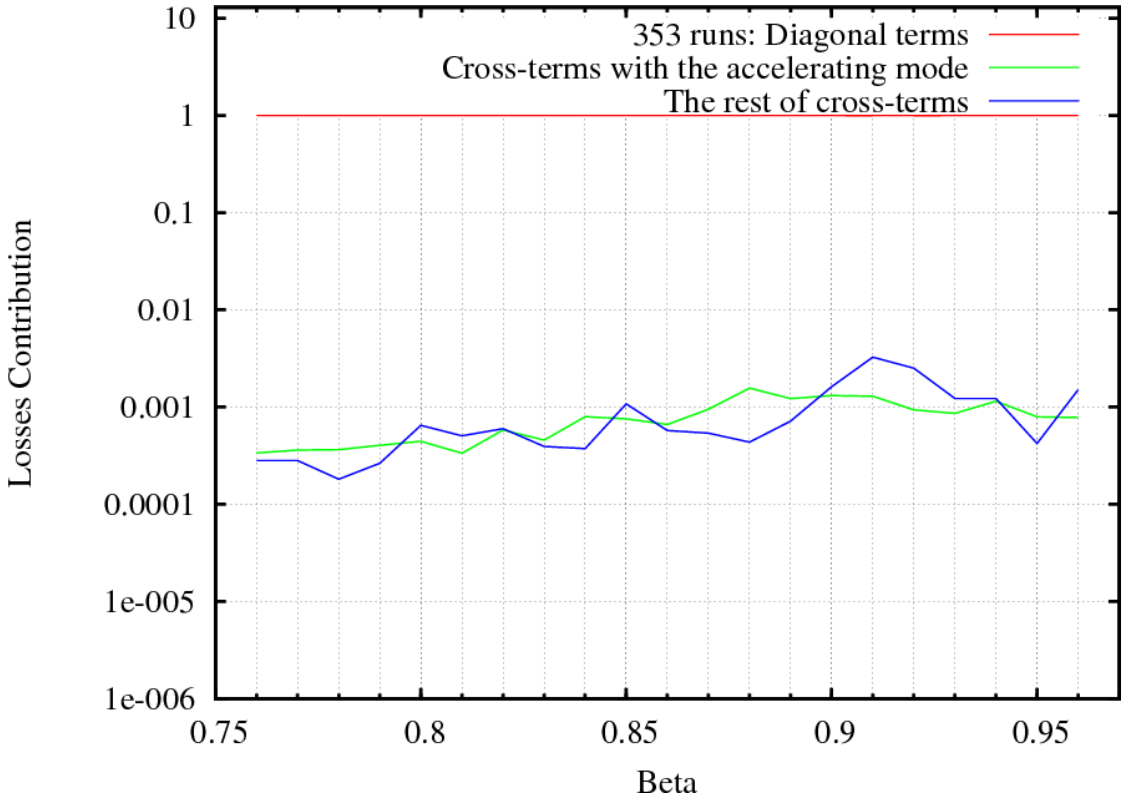

Figure 9: Losses contributions from terms P_2, P_0, P_1 at HE650, $Q = 10^7$

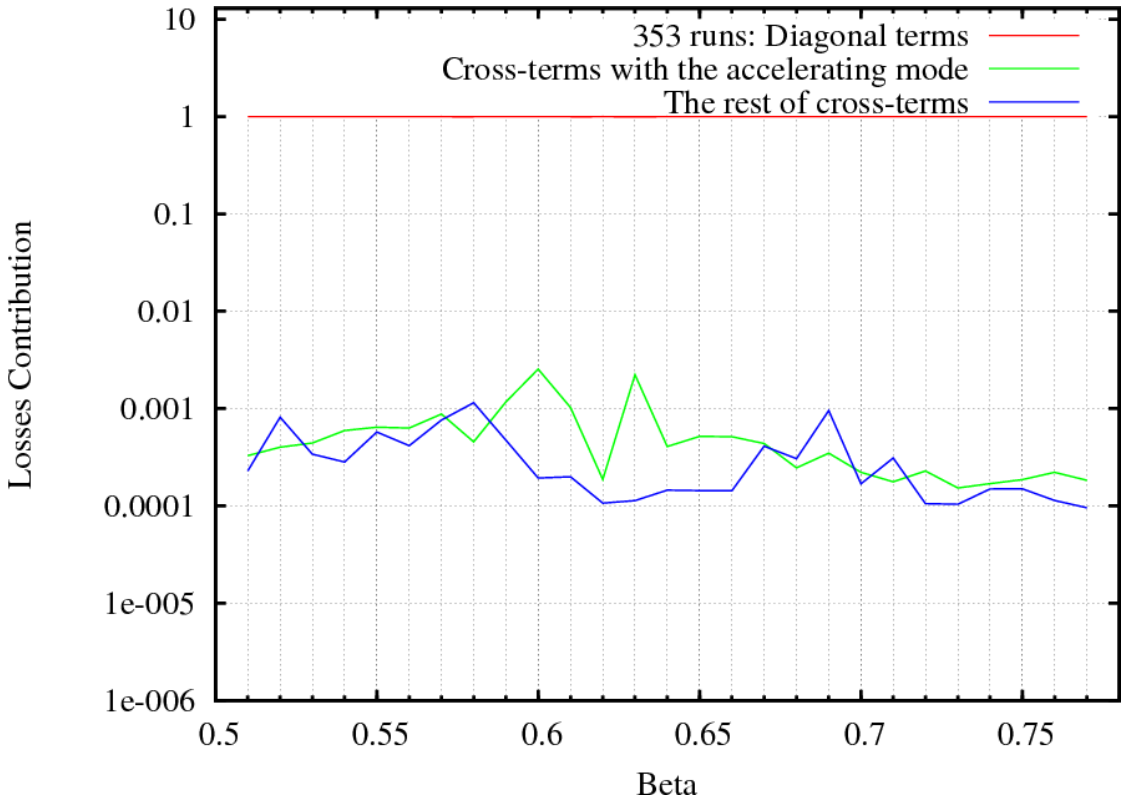

Figure 10: Losses contributions from terms P_2, P_0, P_1 at LE650, $Q = 10^8$

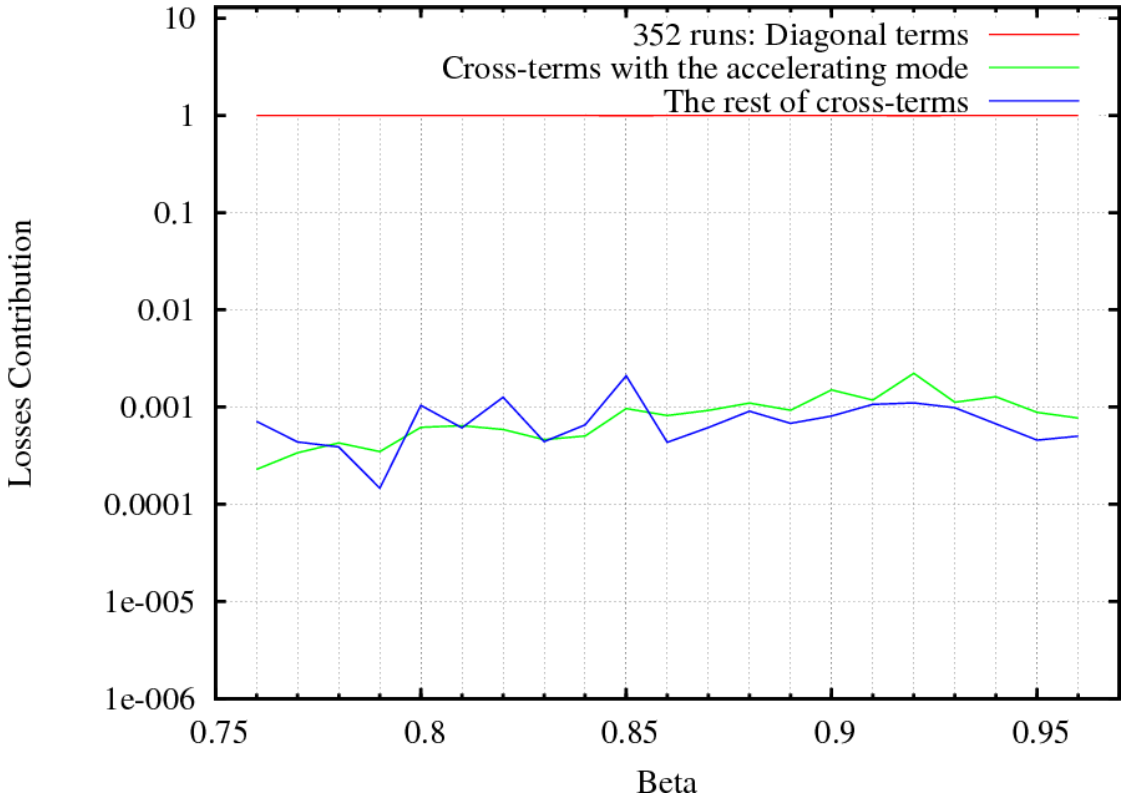

Figure 11: Losses contributions from terms P_2, P_0, P_1 at HE650, $Q = 10^8$

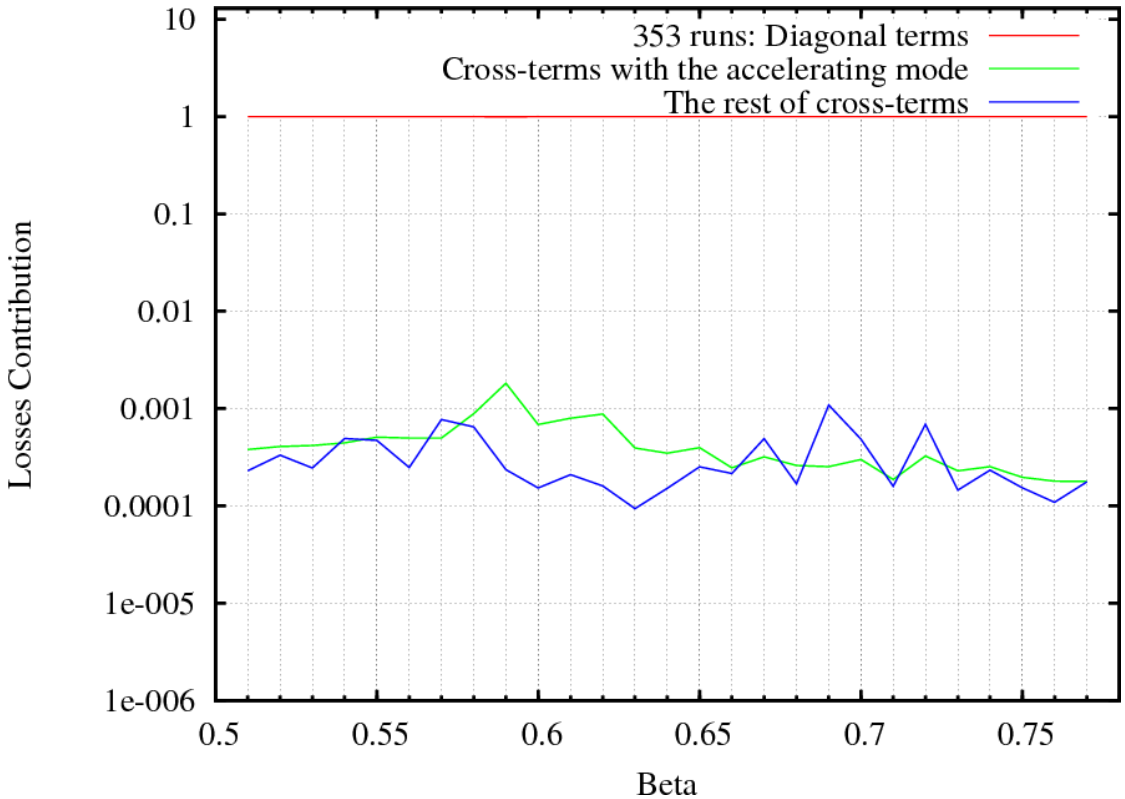

Figure 12: Losses contributions from terms P_2, P_0, P_1 at LE650, $Q = 10^9$

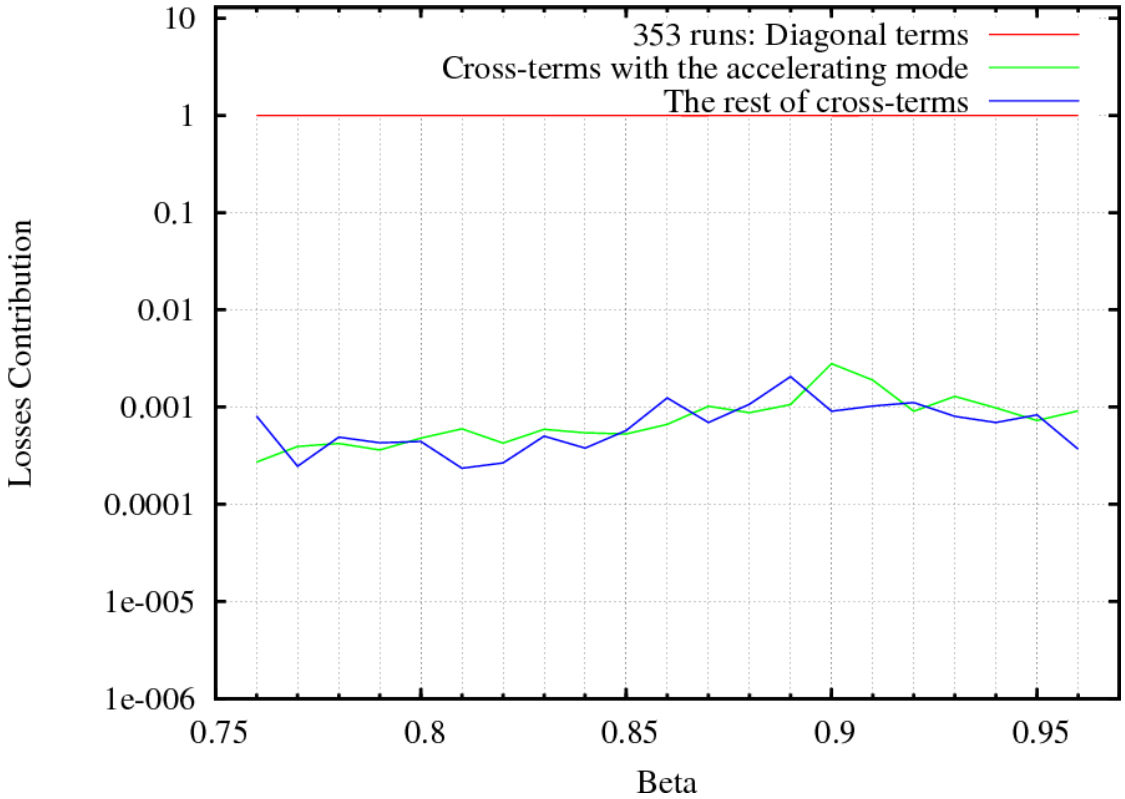

Figure 13: Losses contributions from terms P_2, P_0, P_1 at HE650, $Q = 10^9$

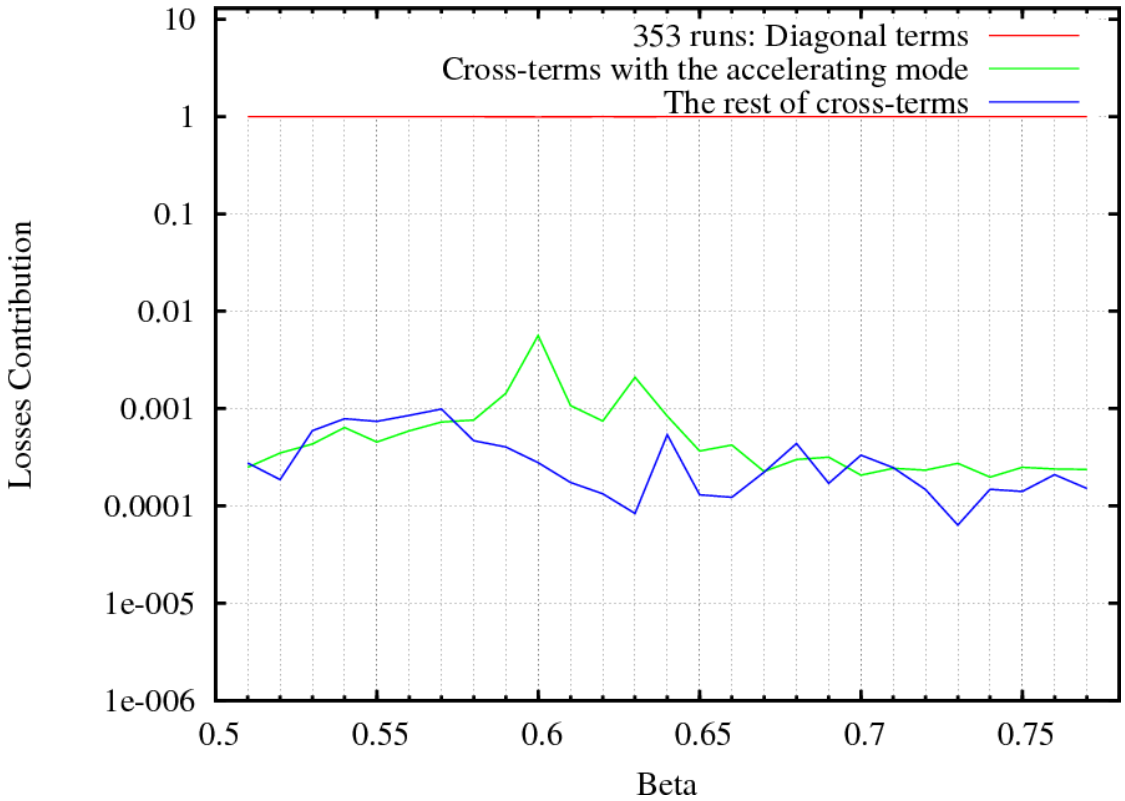

Figure 14: Losses contributions from terms P_2, P_0, P_1 at LE650, $Q = 10^{10}$

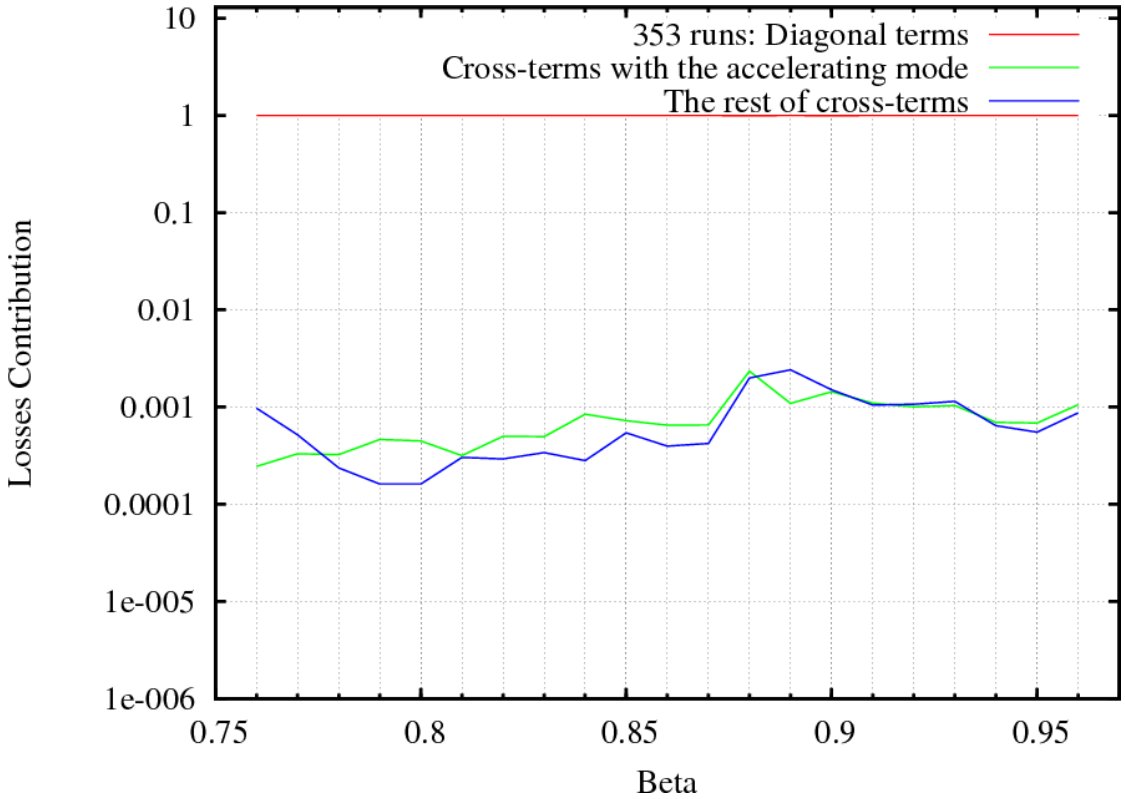

Figure 15: Losses contributions from terms P_2, P_0, P_1 at HE650, $Q = 10^{10}$

Results

650 MHz sections of the Project X Linac are considered: LE650 and High Energy (HE650) sections. The range of beta from 0.51 to 0.77 is studied for LE650. The range of beta from 0.76 to 0.96 is studied for HE650. Every single cavity is considered separately. Acceleration mode is supposed to be perfectly adjusted so its frequency exactly $650\,MHz$ is used in calculations. HOMs frequencies have spread $1\,MHz$. About 3,000 runs are made for each cavity. Power of losses per cavity is calculated by the formula (6).

For each value of beta the logarithmic average value of power is calculated:

$$\langle P\rangle_L = 10^{\langle \lg P\rangle}, \qquad \langle \lg P\rangle = \frac{1}{N}\sum_{n=1}^{N} \lg P_n.$$

Besides the value of power $P_{99\%}$ is defined that 99% of cases have power of losses less than $P_{99\%}$. Dependences these values on beta for both sections and values of quality factor of HOMs 10^7, 10^8, 10^9, and 10^{10} are shown on the Figures 16 – 23. Power of losses distributions for selected values of beta are shown on the Figures 24 - 31. Average power of losses dependences on quality factor are shown on the Figures 32 and 33.

It is shown that 99% of cases have less than $0.1\,mW$ losses on HOMs excitation in both $650\,MHz$ sections. Losses mostly do not depend on quality factors of HOMs.

One can see that losses are smaller around the value of geometrical beta for both sections. It is explained by probability for HOM to be in resonance with a beam spectrum line. This probability will be discussed in the next section.

The same calculations were done for the alternative spectrum (see Appendix). The following values of quality factor were considered: 10^8, 10^9, and 10^{10}. The average value of losses and 99% level were calculated for these cases. These values are shown the Figures 34 – 39 for LE650 and HE650 sections. Power of losses distributions for selected values of beta are shown on the Figures 40 - 45. Average power of losses dependences on quality factor are shown on the Figures 46 and 47.

Losses Reduction

Low level of losses is explained by relatively large distance between lines of HOM spectrum and main lines of beam spectrum. In spite of there is spread in HOMs frequencies, probability of HOM beam spectrum line frequency coincidence is extremely small (see Figures 48 and 49). Nevertheless we should consider the situation when we have a cavity with HOM in resonance. There is no point to consider a cavity with more than one HOM in resonance as probability of this is depreciatingly small.

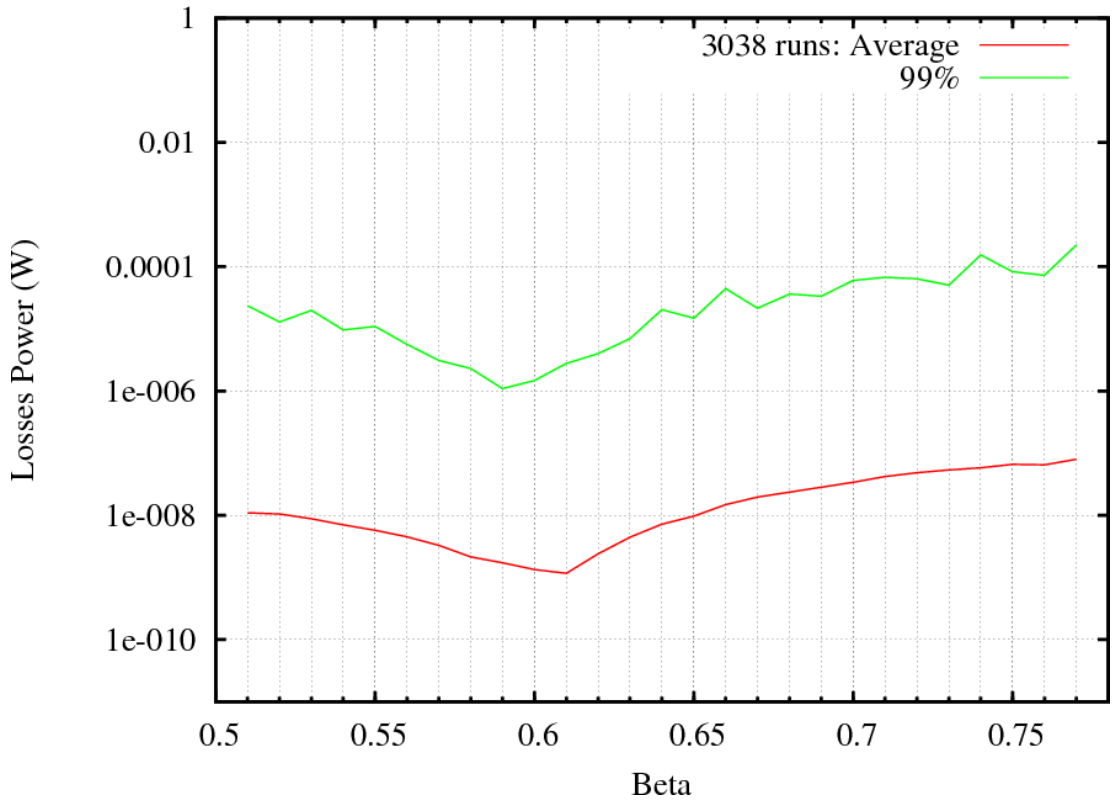

Figure 16: Power of losses vs. beta for LE650, $Q = 10^7$

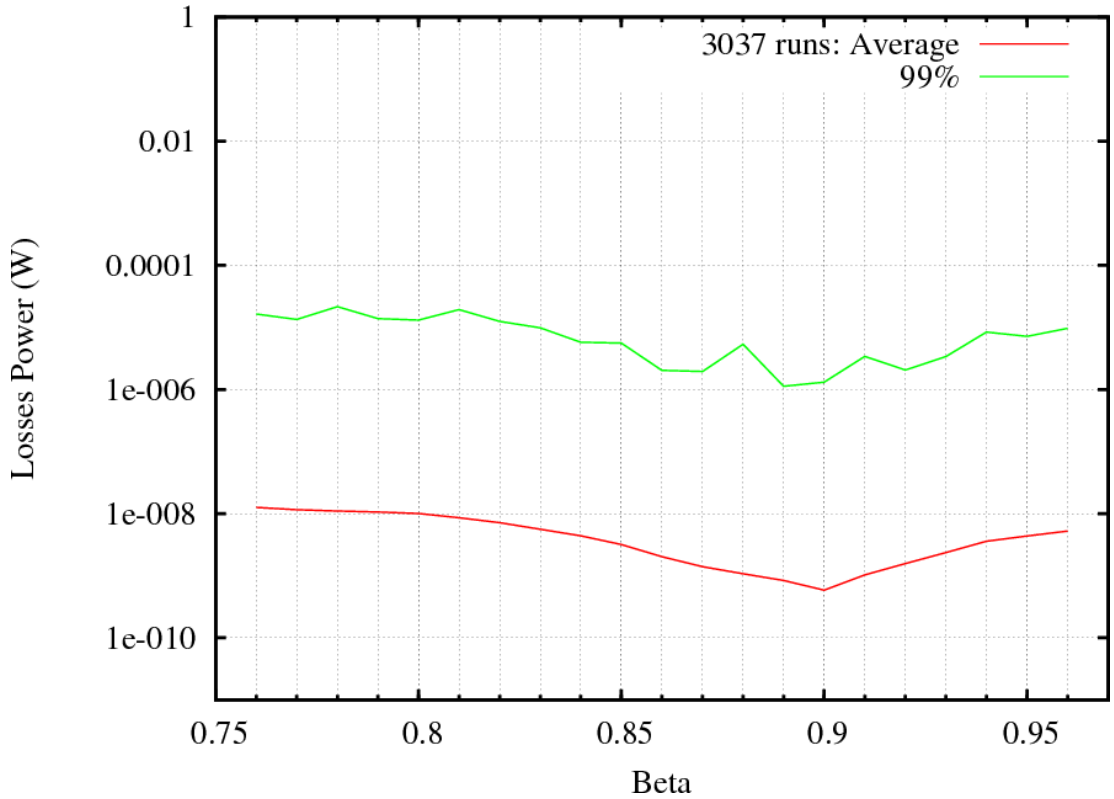

Figure 17: Power of losses vs. beta for HE650, $Q = 10^7$

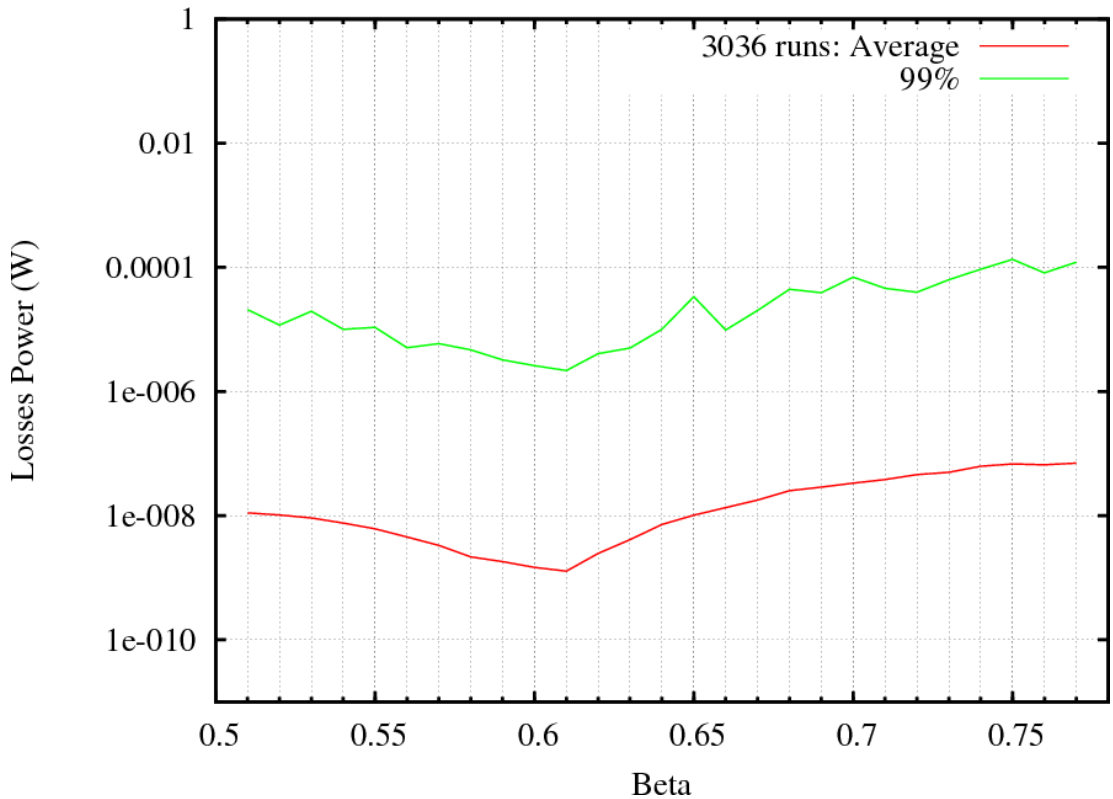

Figure 18: Power of losses vs. beta for LE650, $Q = 10^8$

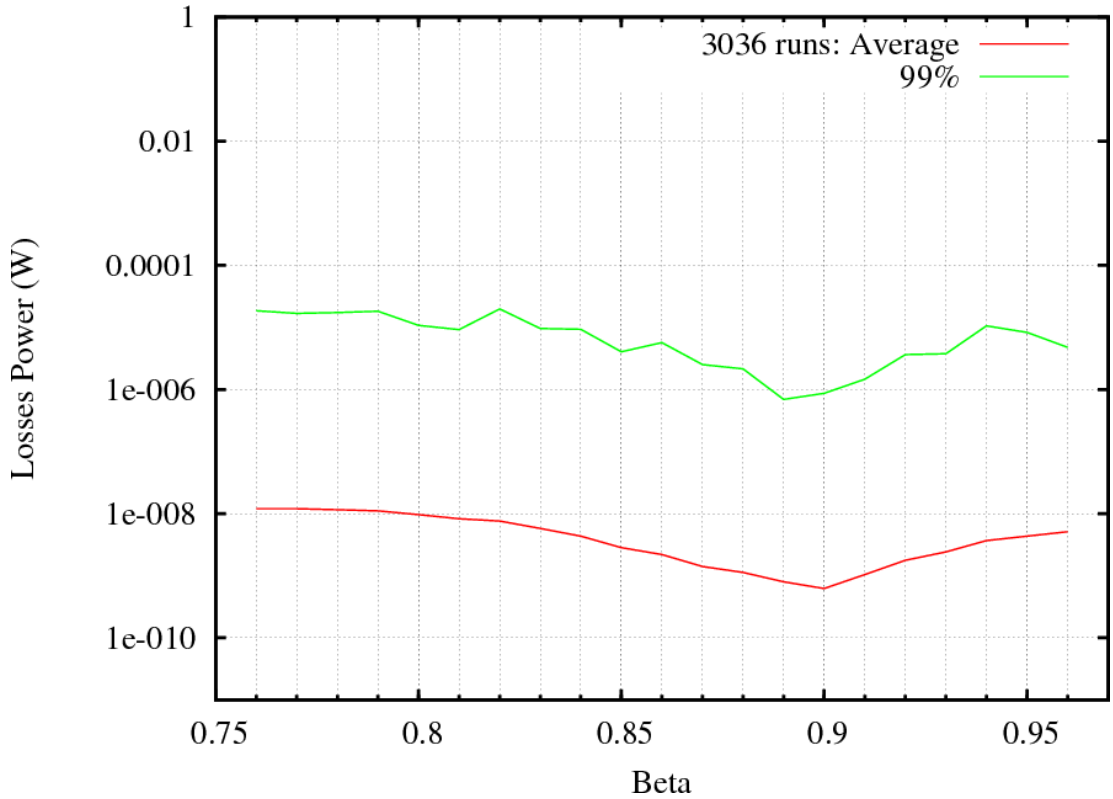

Figure 19: Power of losses vs. beta for HE650, $Q = 10^8$

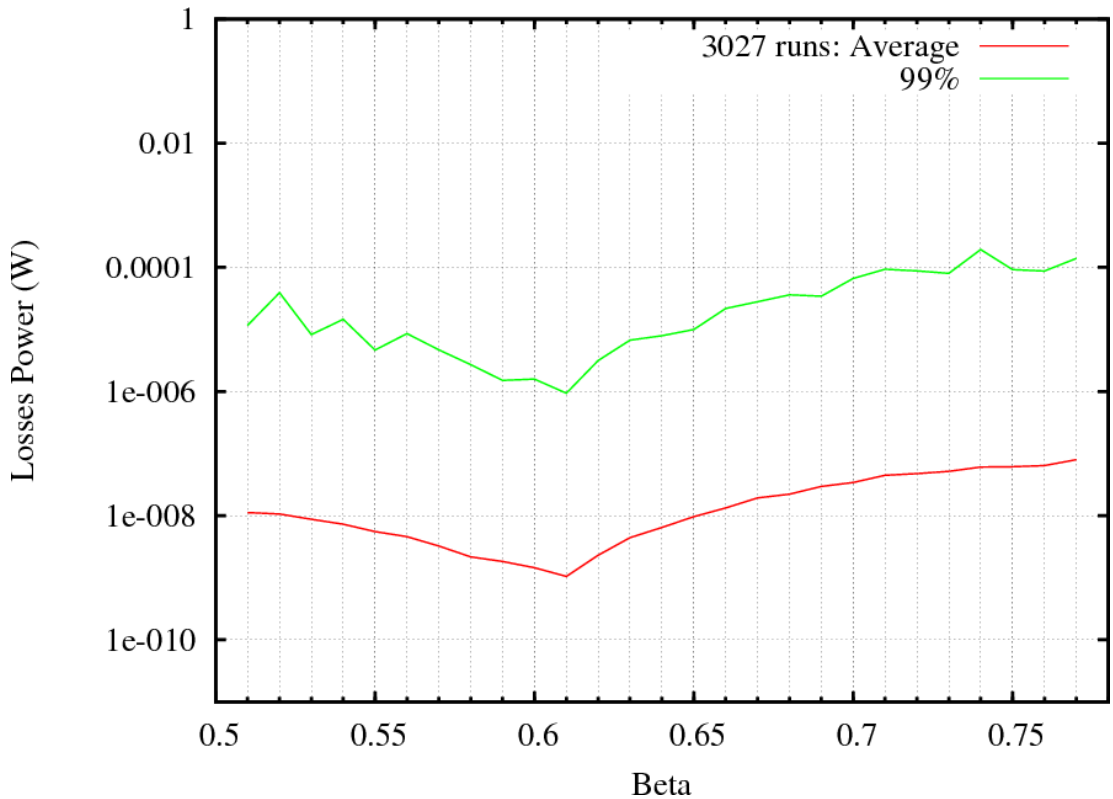

Figure 20: Power of losses vs. beta for LE650, $Q = 10^9$

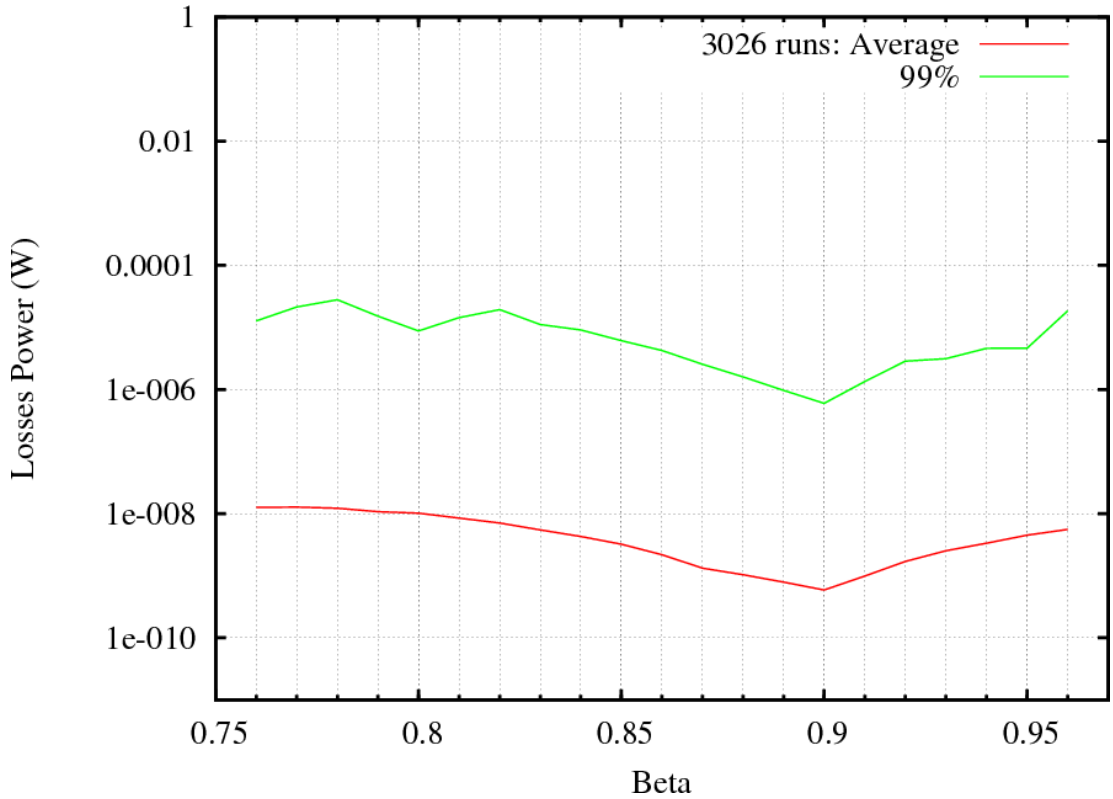

Figure 21: Power of losses vs. beta for HE650, $Q = 10^9$

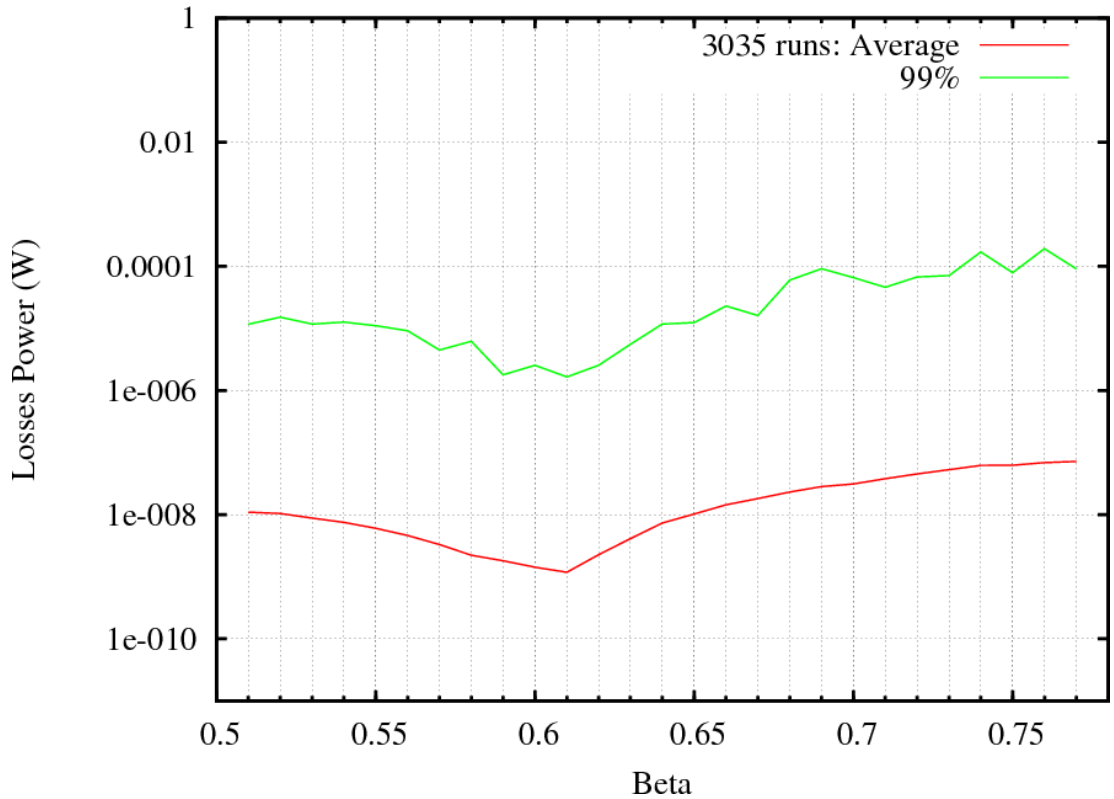

Figure 22: Power of losses vs. beta for LE650, $Q = 10^{10}$

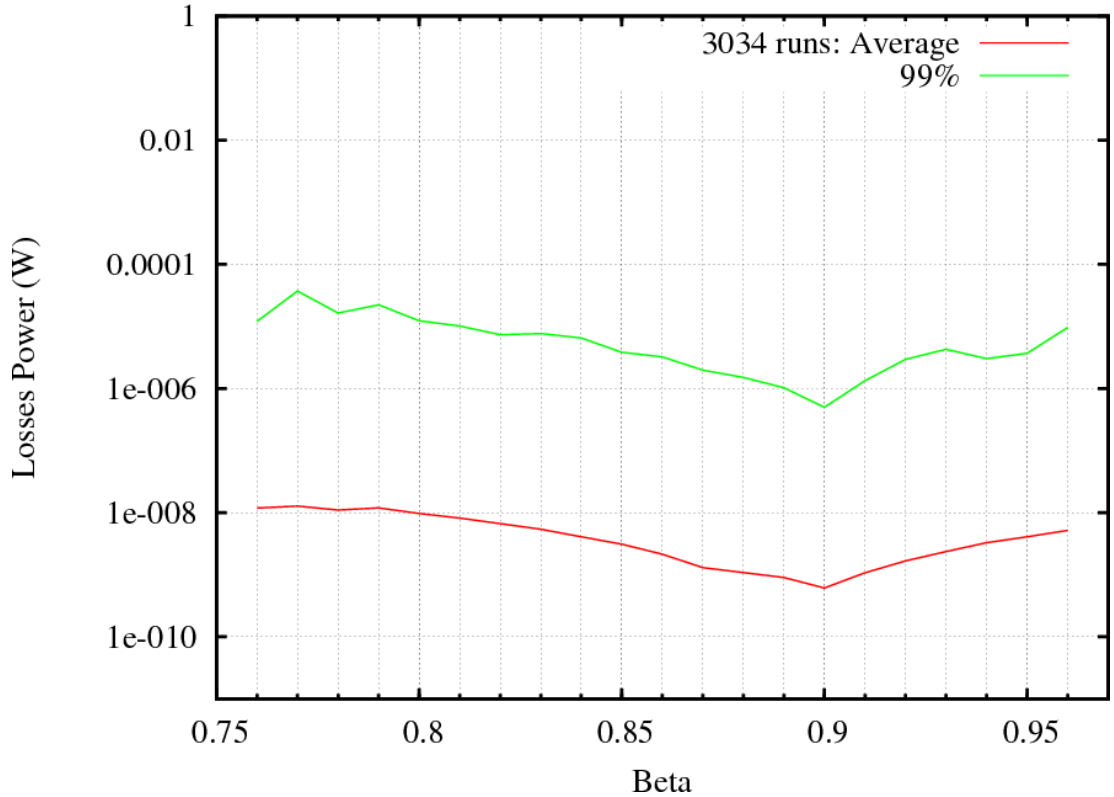

Figure 23: Power of losses vs. beta for HE650, $Q = 10^{10}$

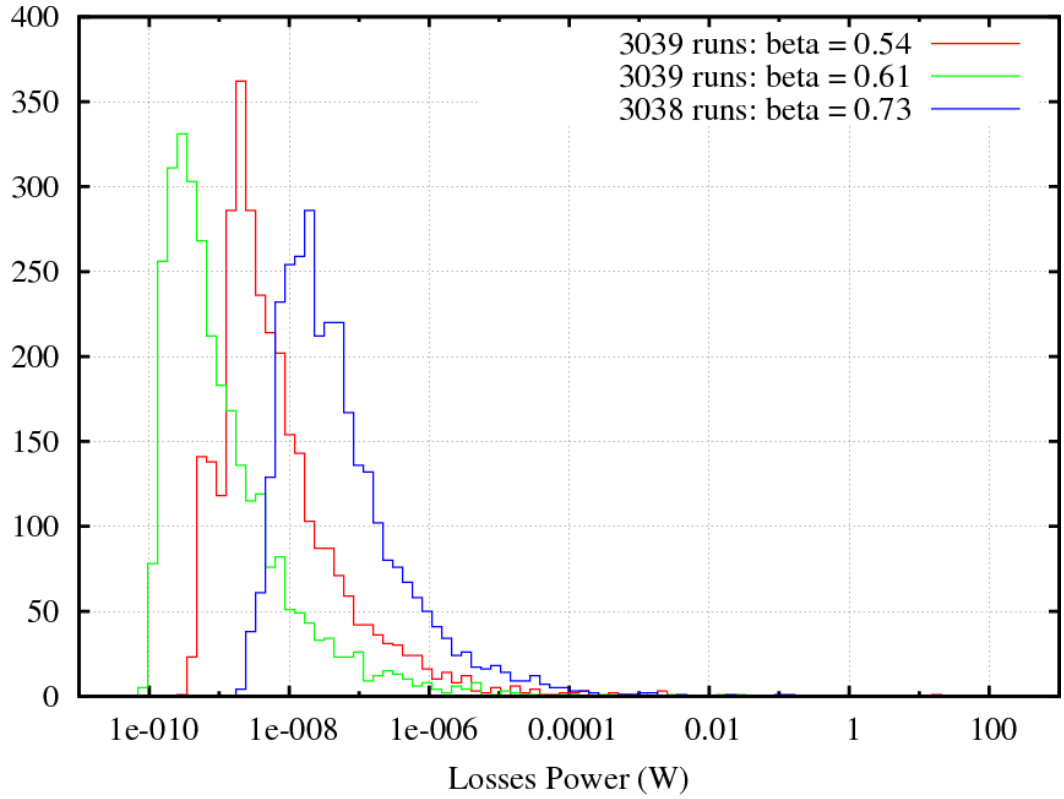

Figure 24: Power of losses distribution for LE650, $Q = 10^7$

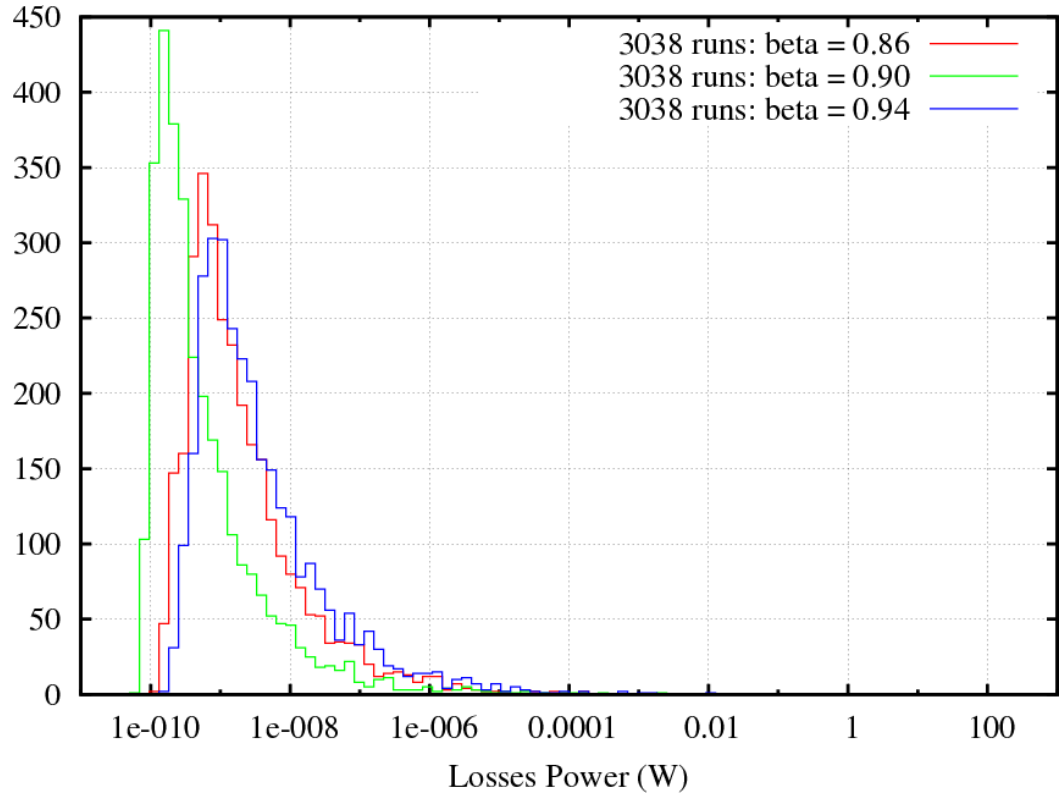

Figure 25: Power of losses distribution for HE650, $Q = 10^7$

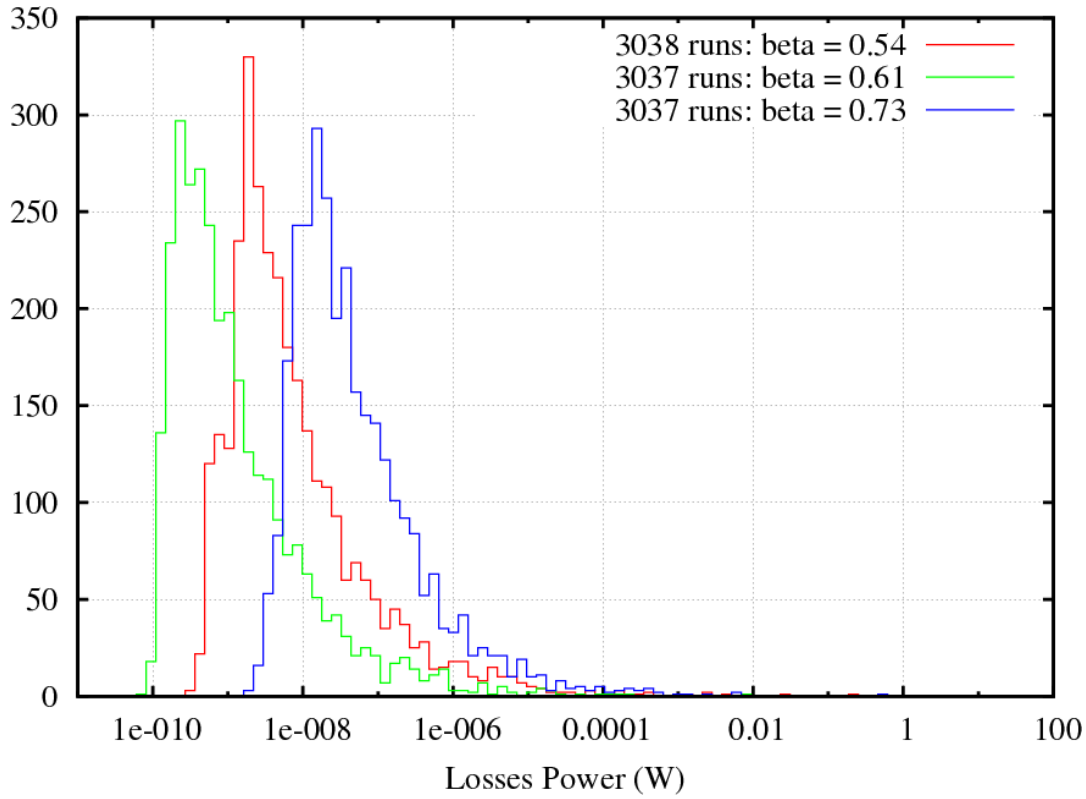

Figure 26: Power of losses distribution for LE650, $Q = 10^8$

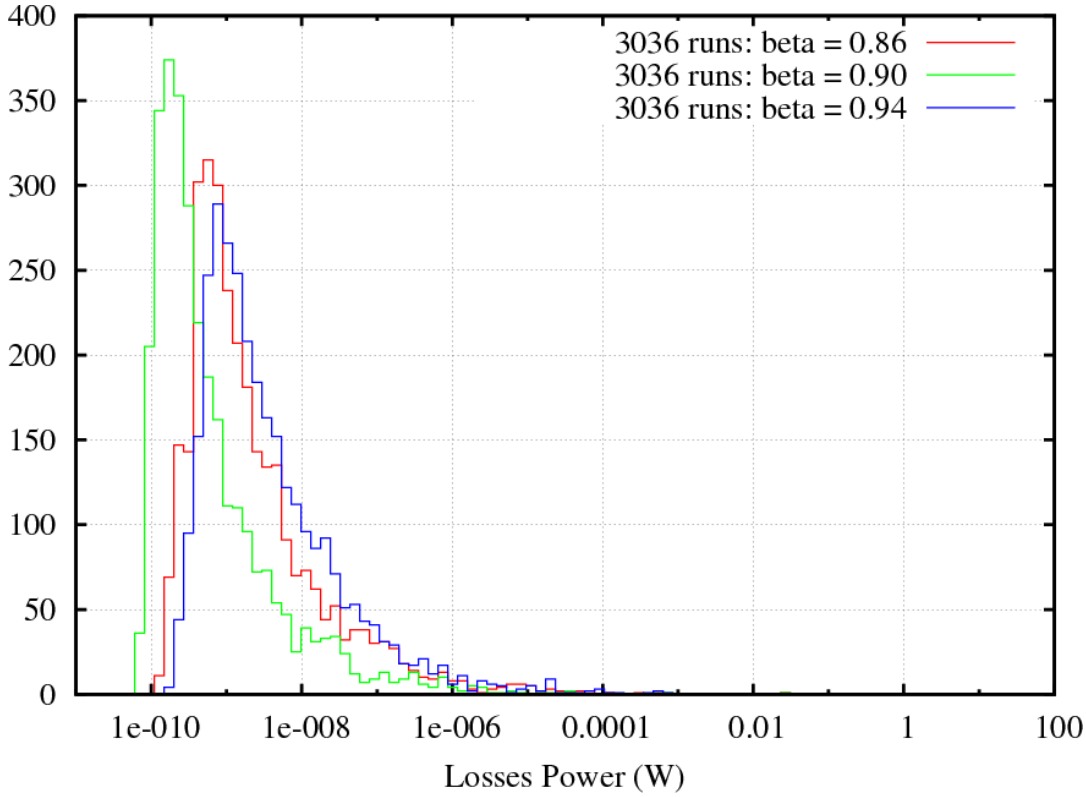

Figure 27: Power of losses distribution for HE650, $Q = 10^8$

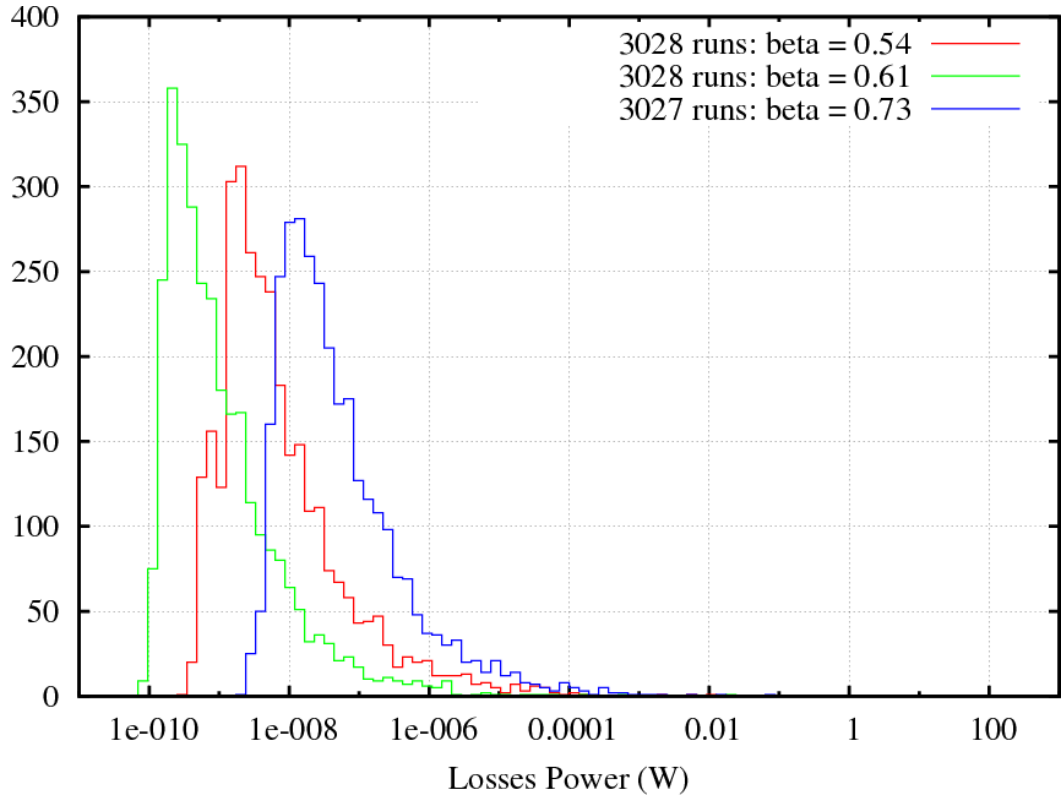

Figure 28: Power of losses distribution for LE650, $Q = 10^9$

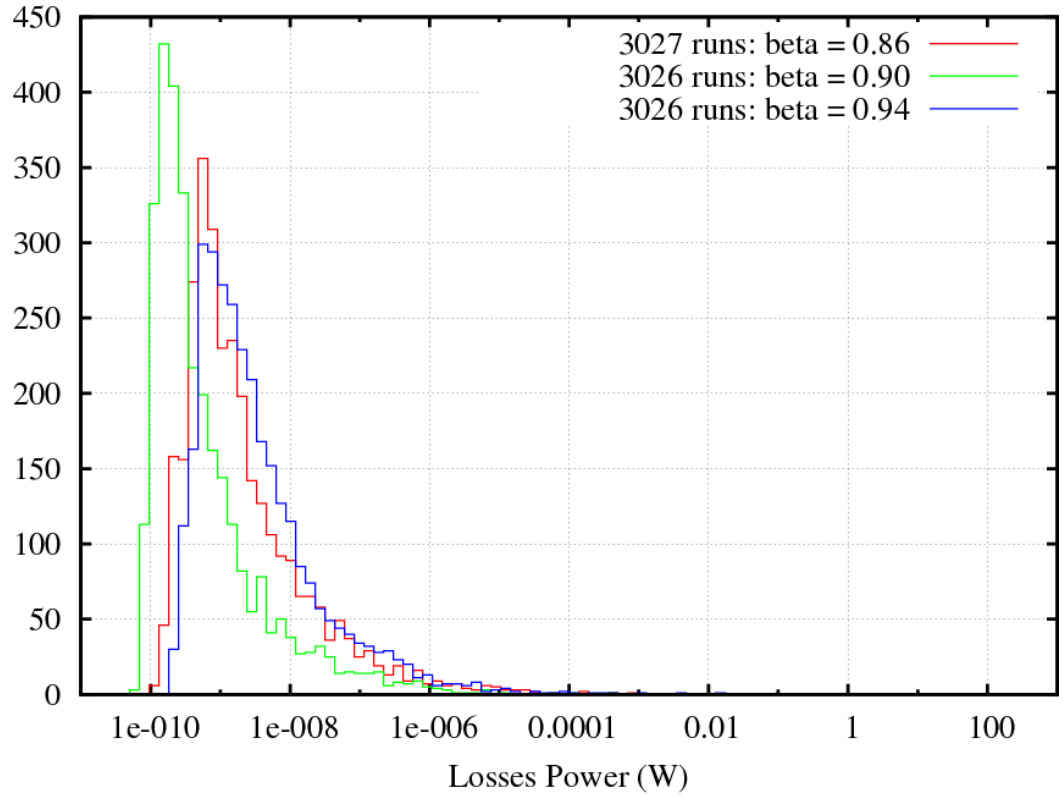

Figure 29: Power of losses distribution for HE650, $Q = 10^9$

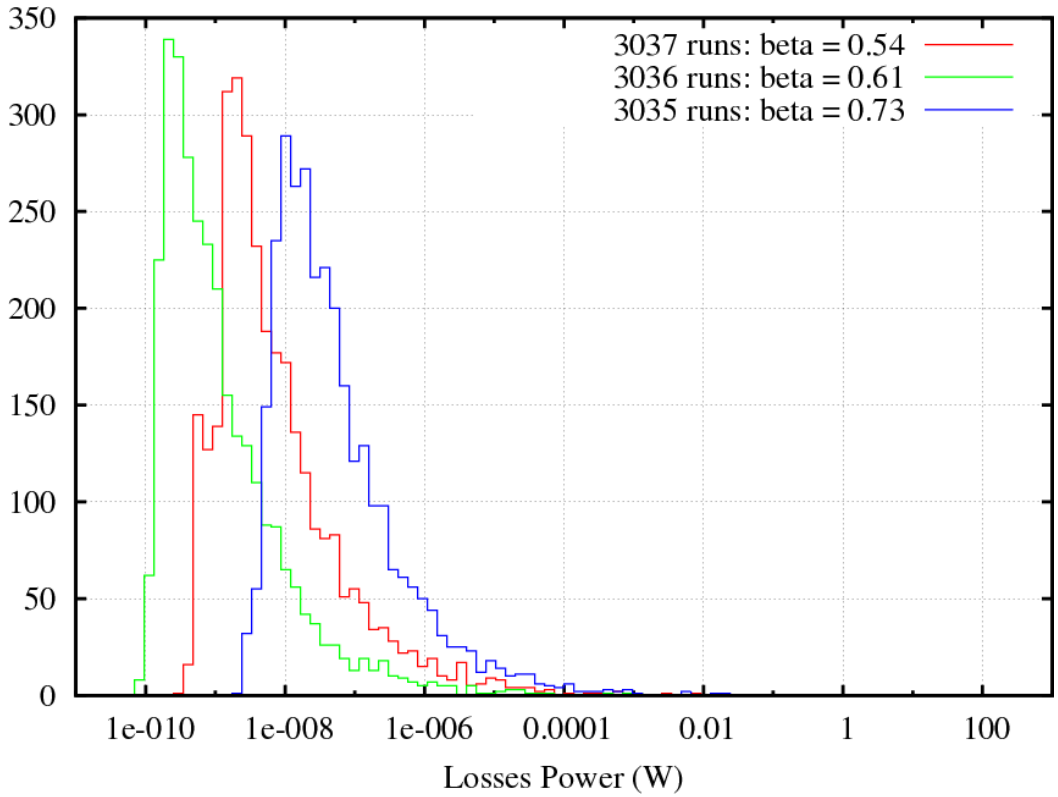

Figure 30: Power of losses distribution for LE650, $Q = 10^{10}$

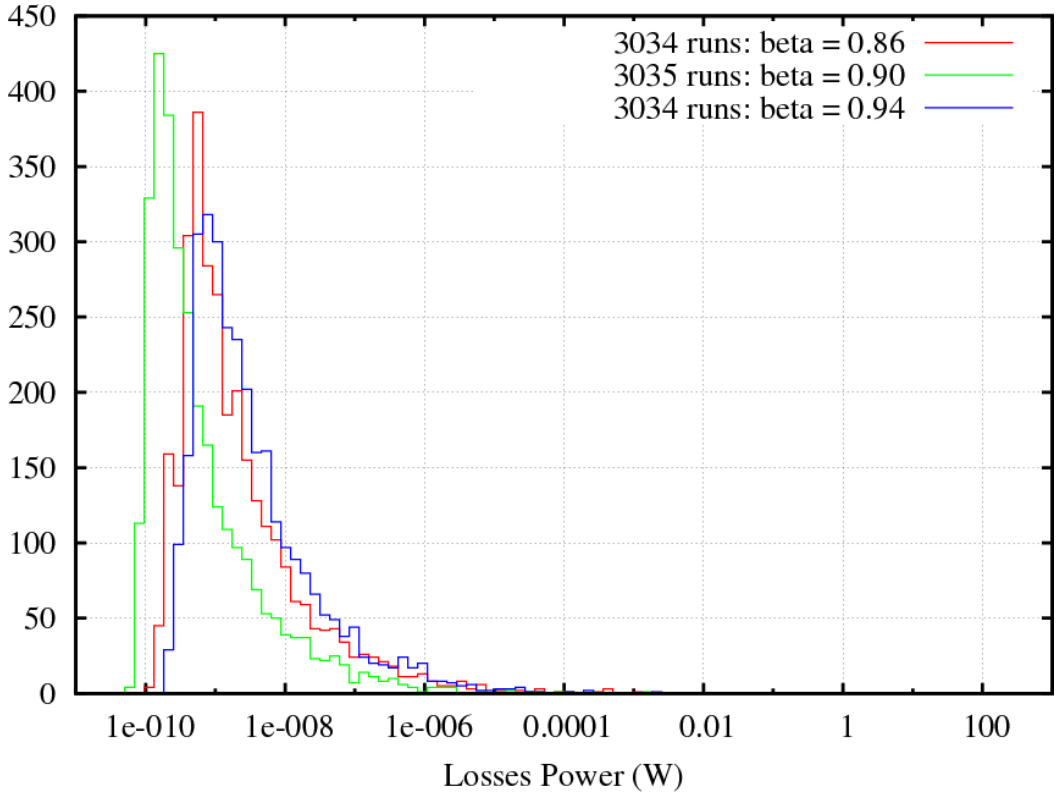

Figure 31: Power of losses distribution for HE650, $Q = 10^{10}$

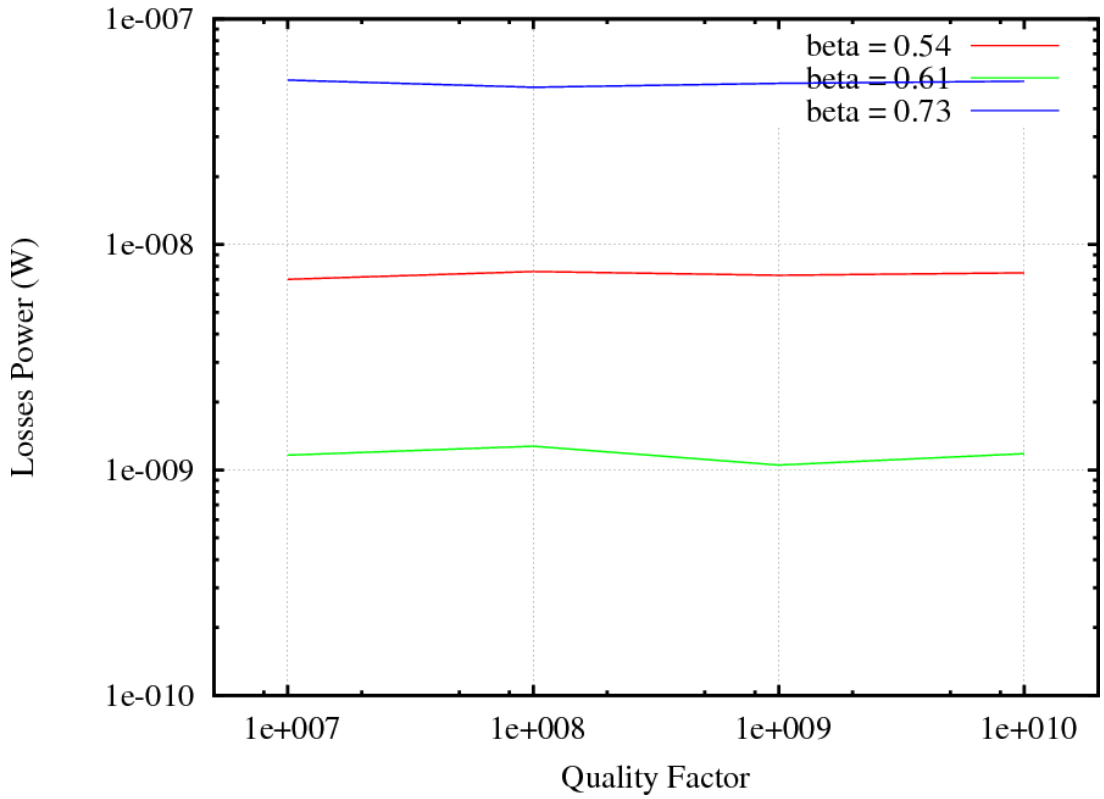

Figure 32: Power of losses vs. quality factor for LE650

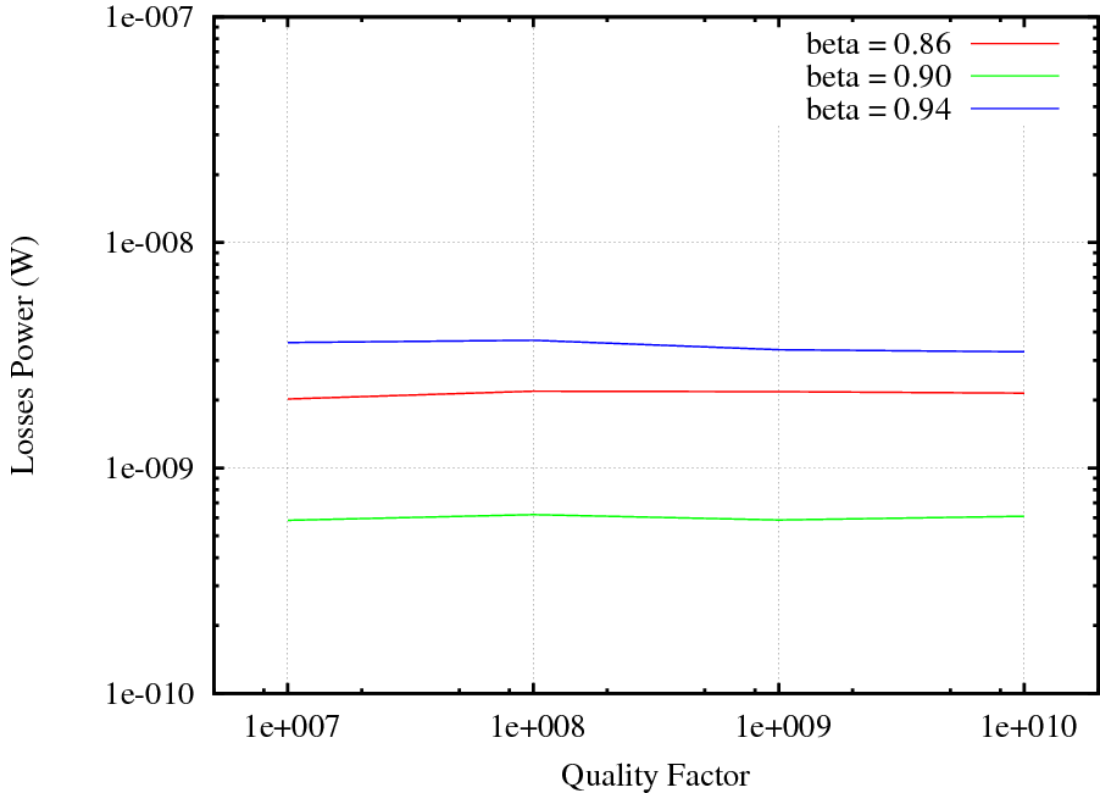

Figure 33: Power of losses vs. quality factor for HE650

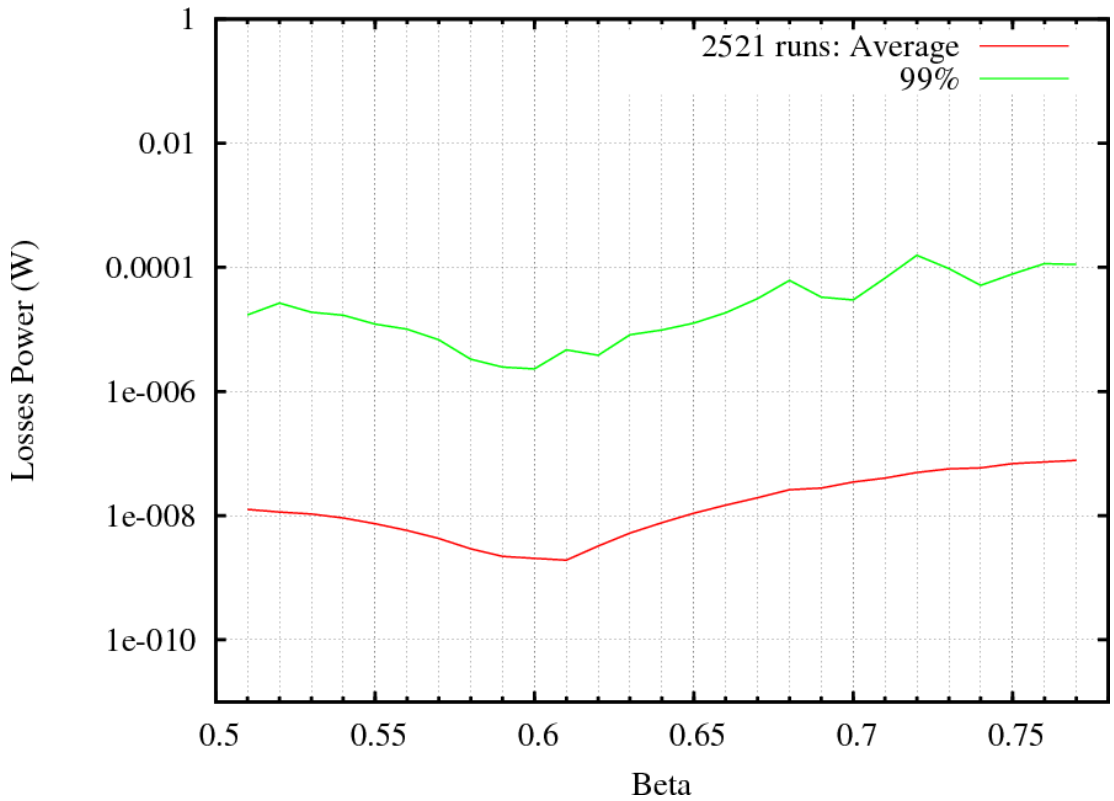

Figure 34: Power of losses vs. beta for LE650, $Q = 10^8$

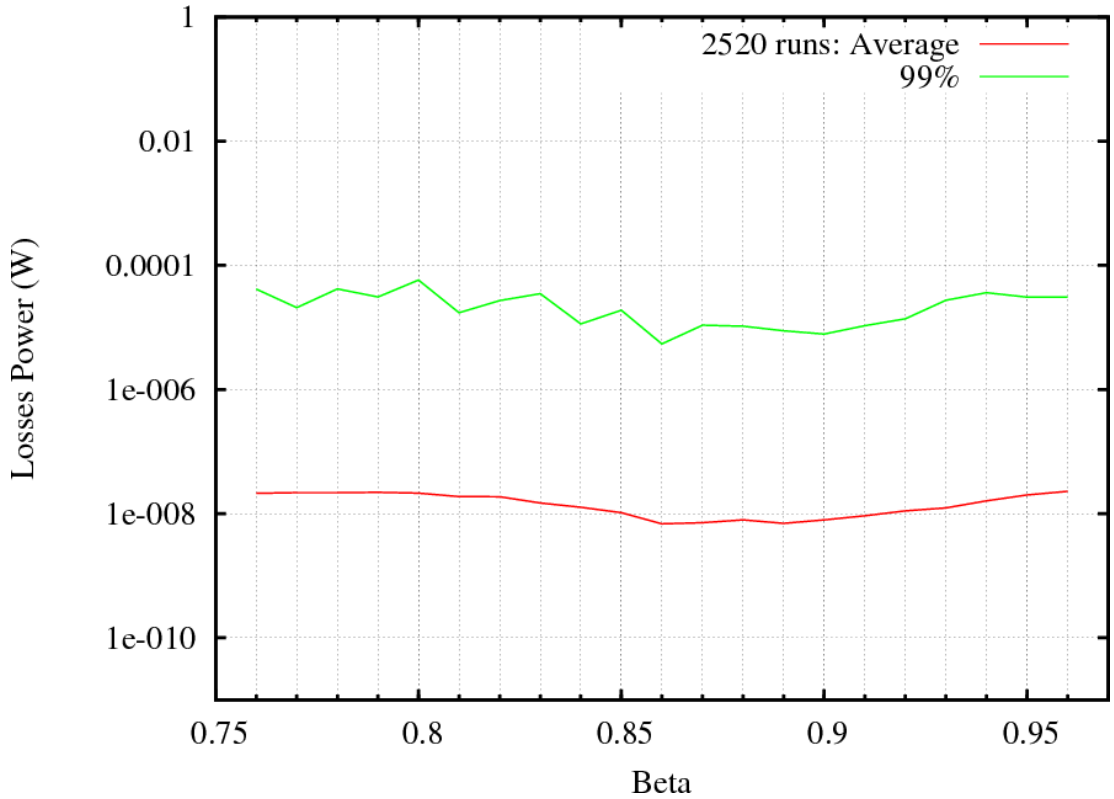

Figure 35: Power of losses vs. beta for HE650, $Q = 10^8$

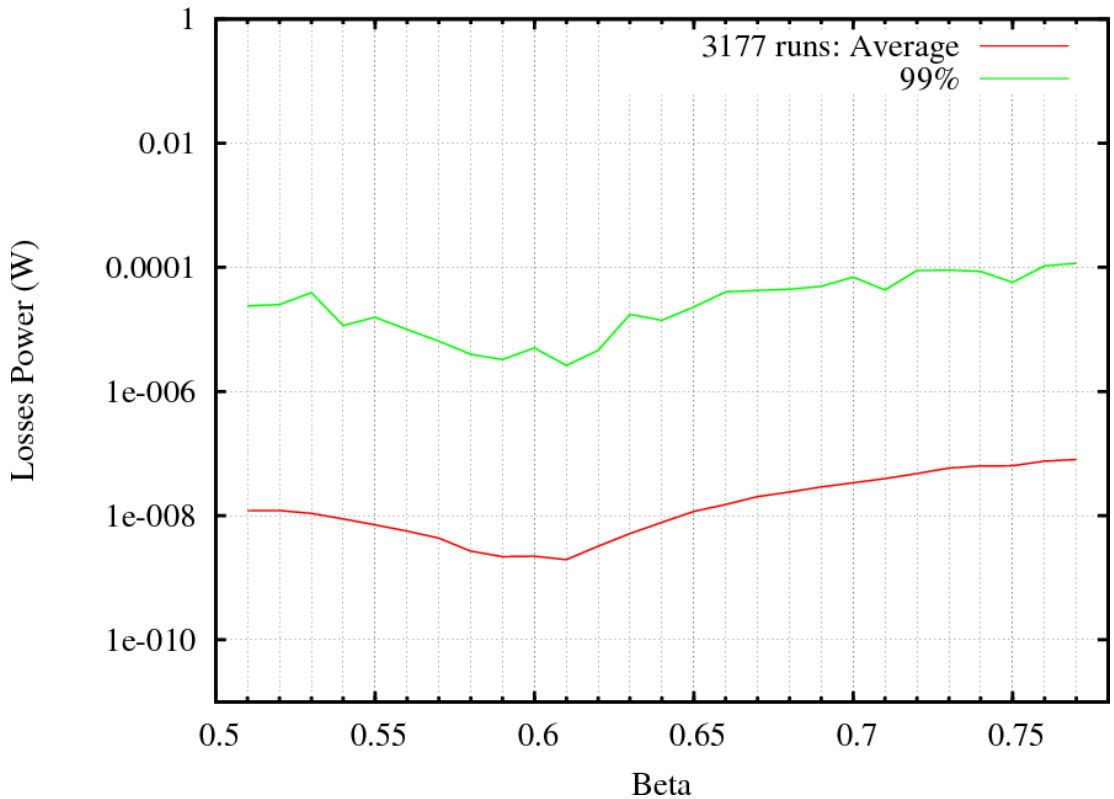

Figure 36: Power of losses vs. beta for LE650, $Q = 10^9$

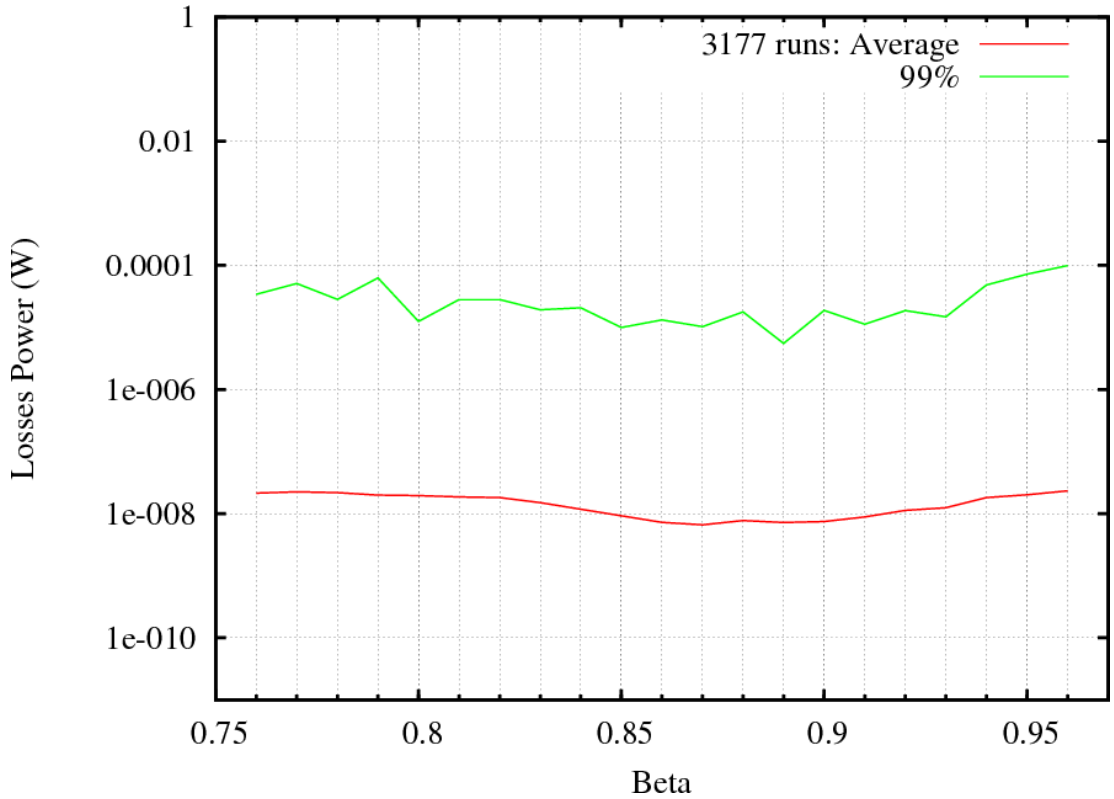

Figure 37: Power of losses vs. beta for HE650, $Q = 10^9$

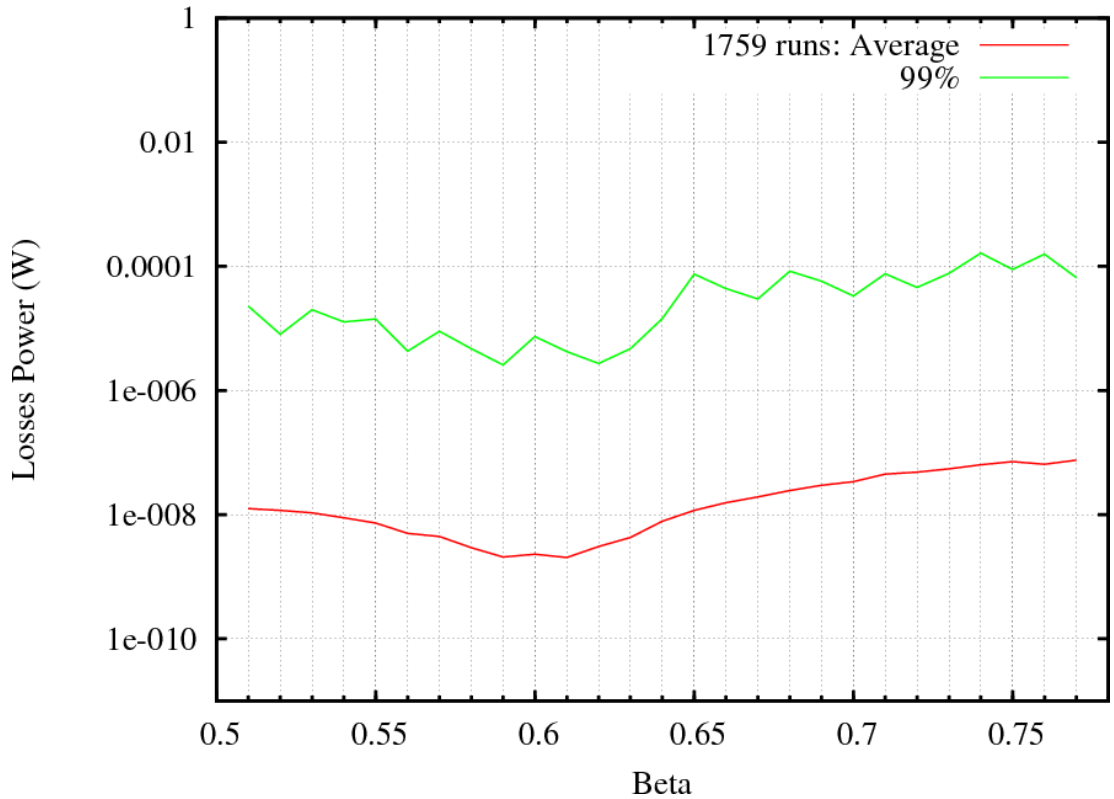

Figure 38: Power of losses vs. beta for LE650, $Q = 10^{10}$

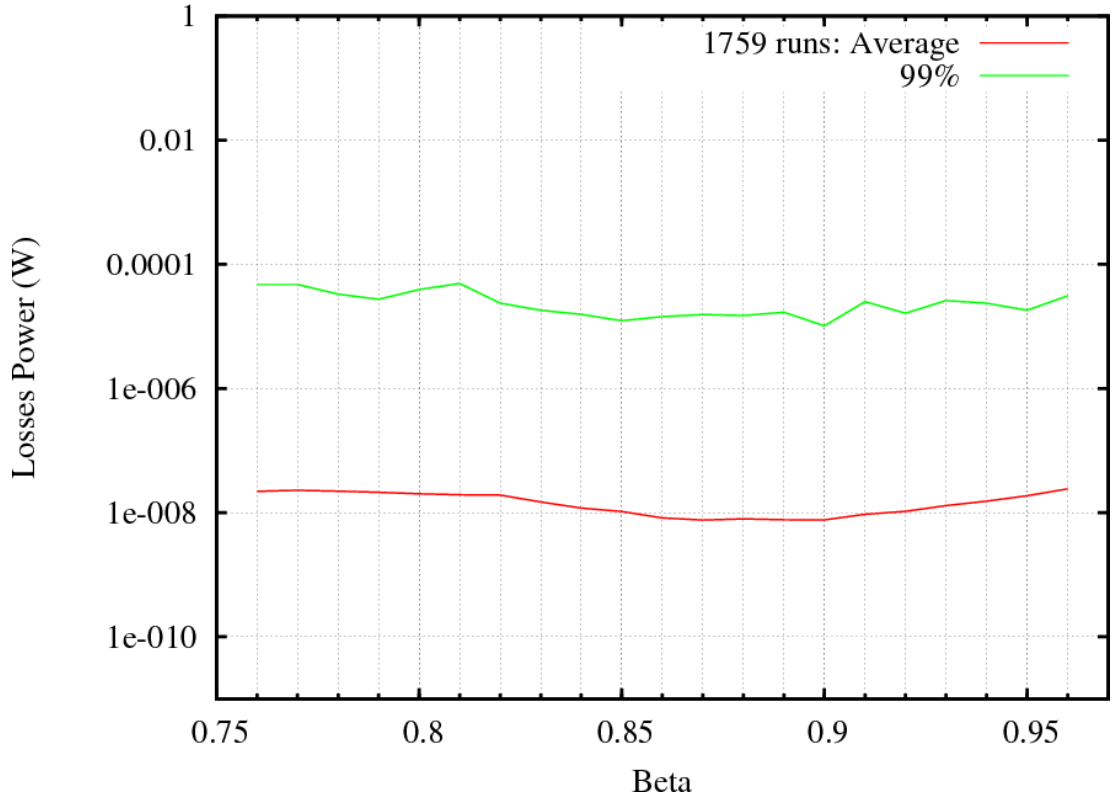

Figure 39: Power of losses vs. beta for HE650, $Q = 10^{10}$

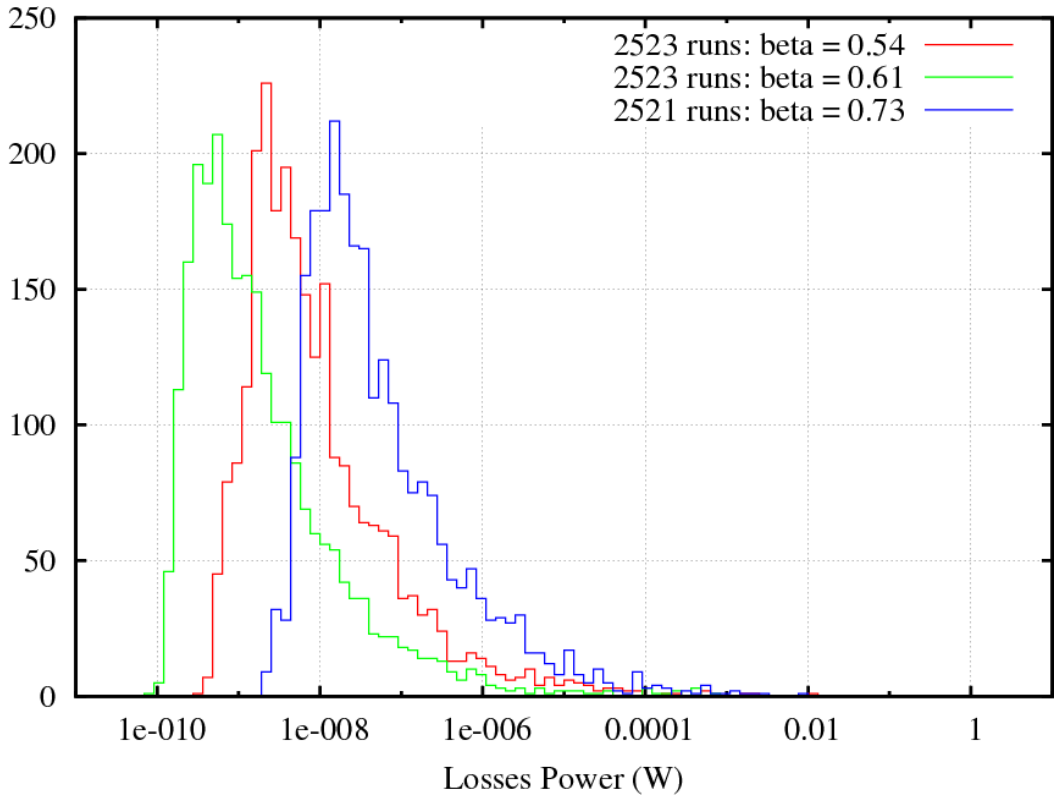

Figure 40: Power of losses distribution for LE650, $Q = 10^8$

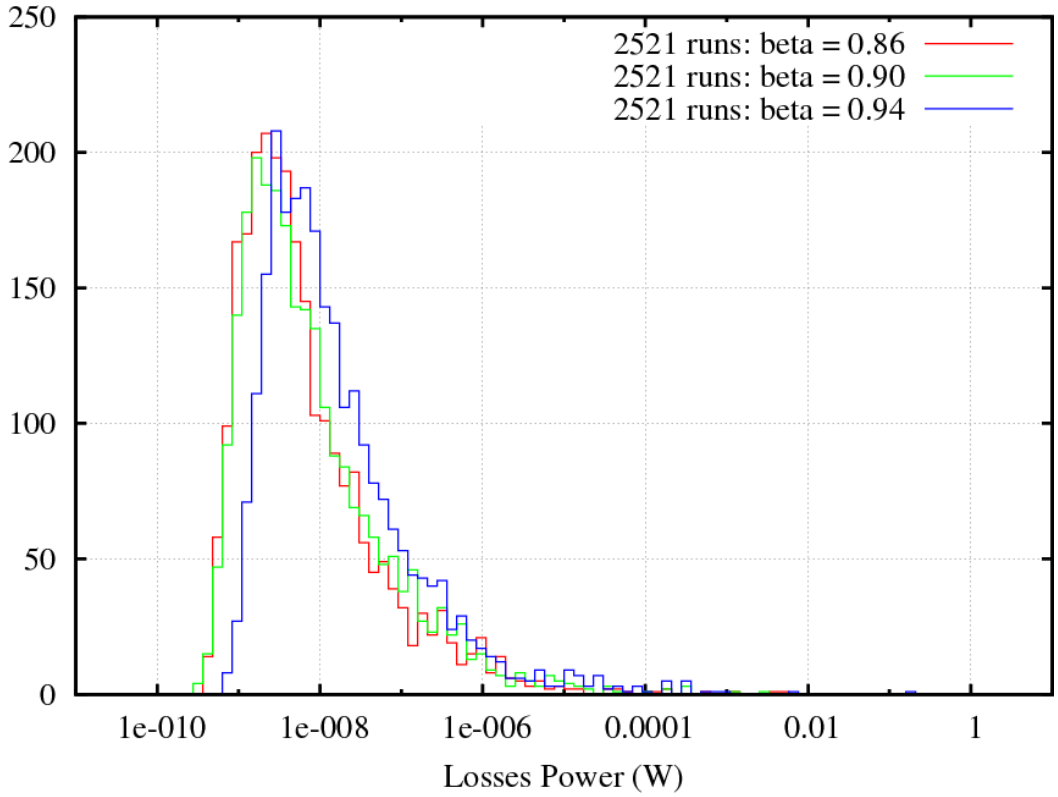

Figure 41: Power of losses distribution for HE650, $Q = 10^8$

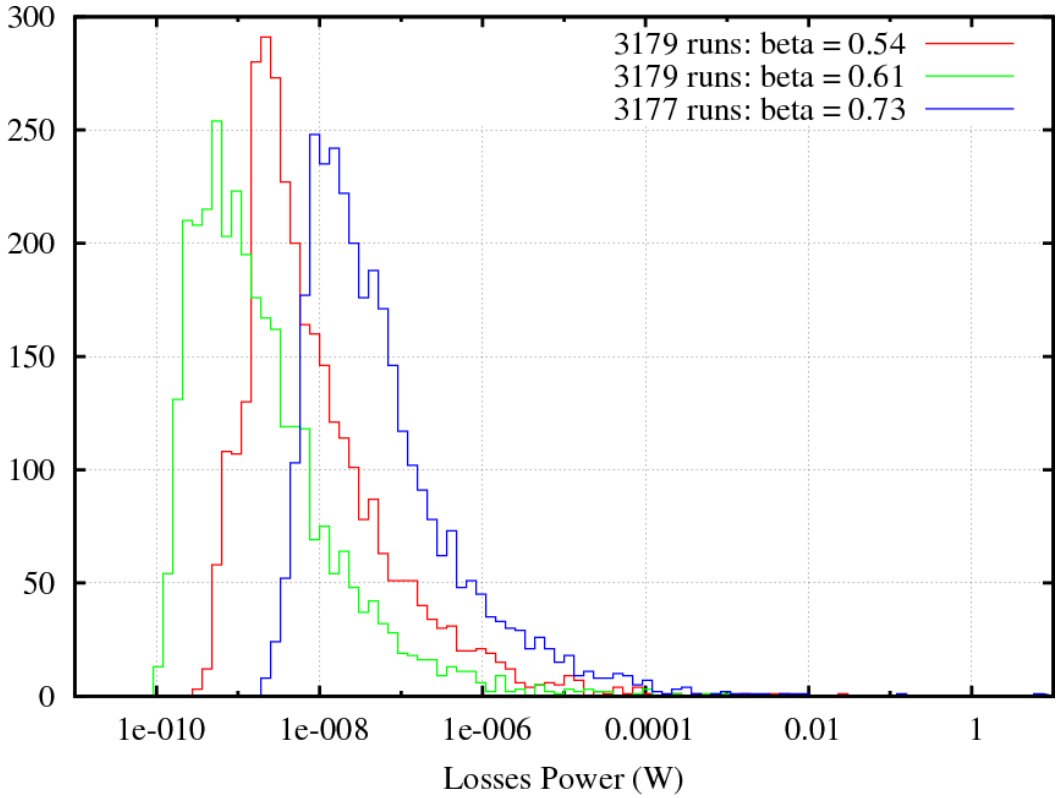

Figure 42: Power of losses distribution for LE650, $Q = 10^9$

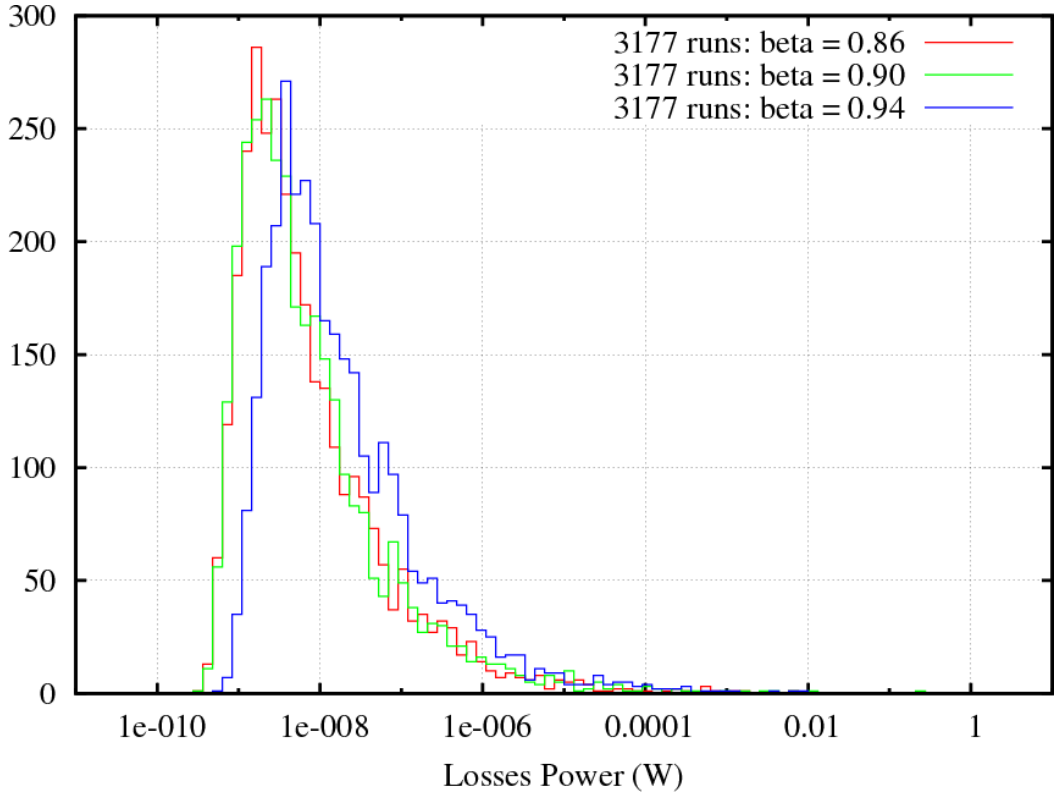

Figure 43: Power of losses distribution for HE650, $Q = 10^9$

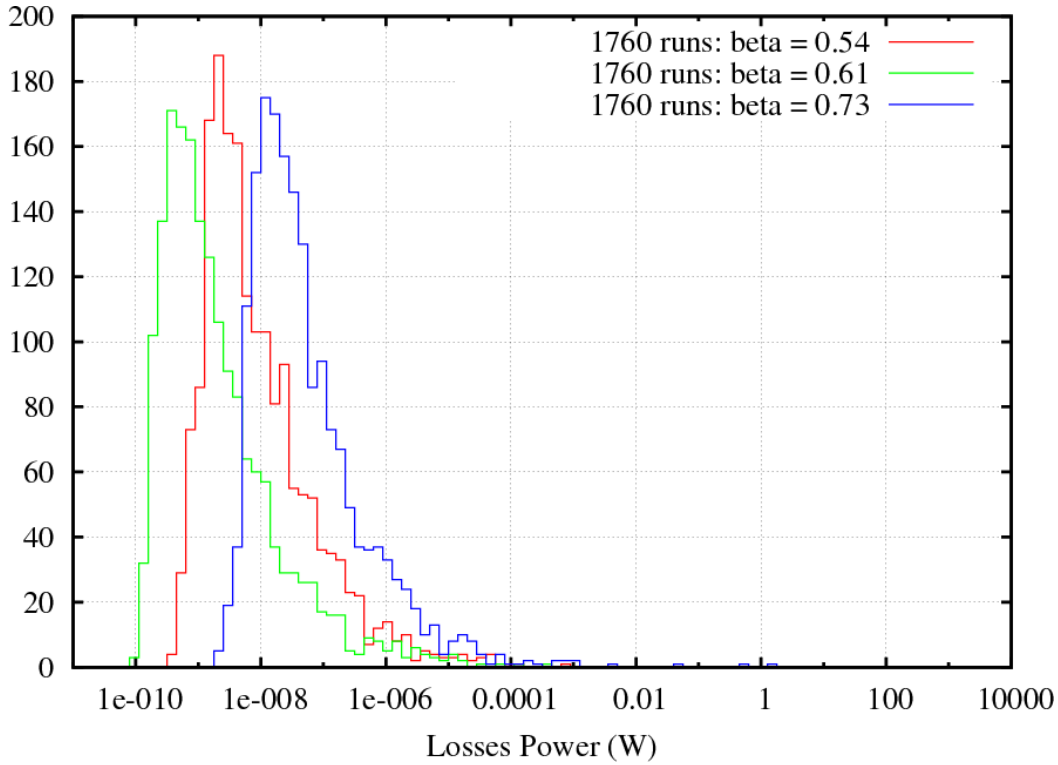

Figure 44: Power of losses distribution for LE650, $Q = 10^{10}$

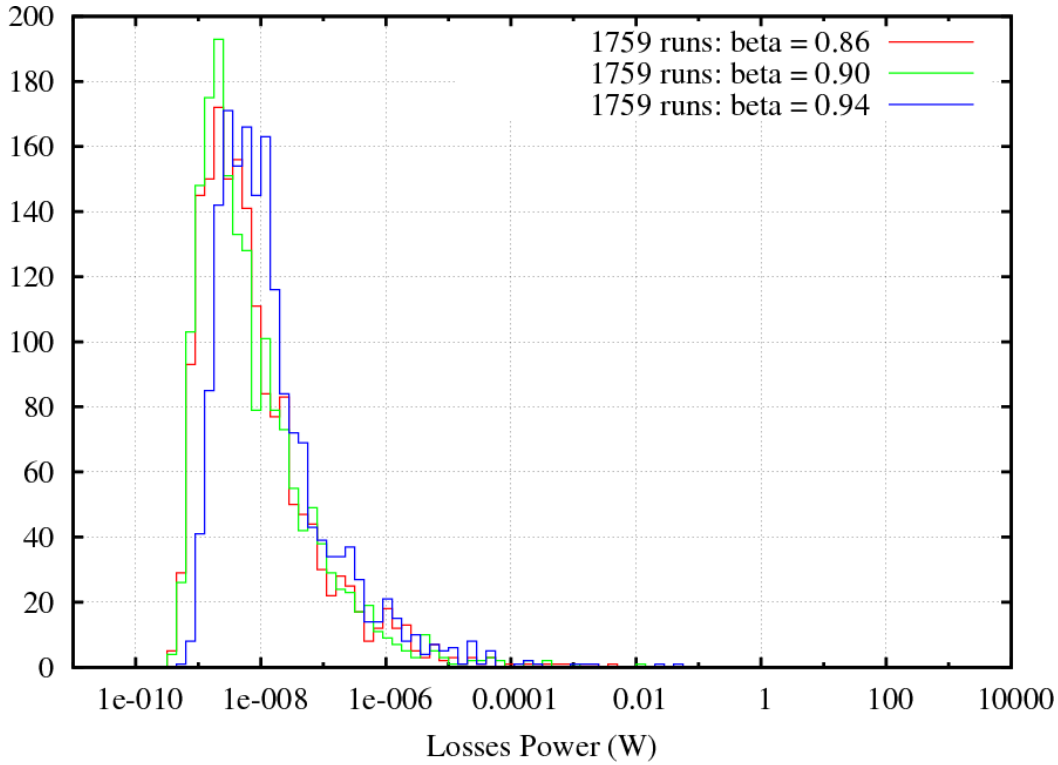

Figure 45: Power of losses distribution for HE650, $Q = 10^{10}$

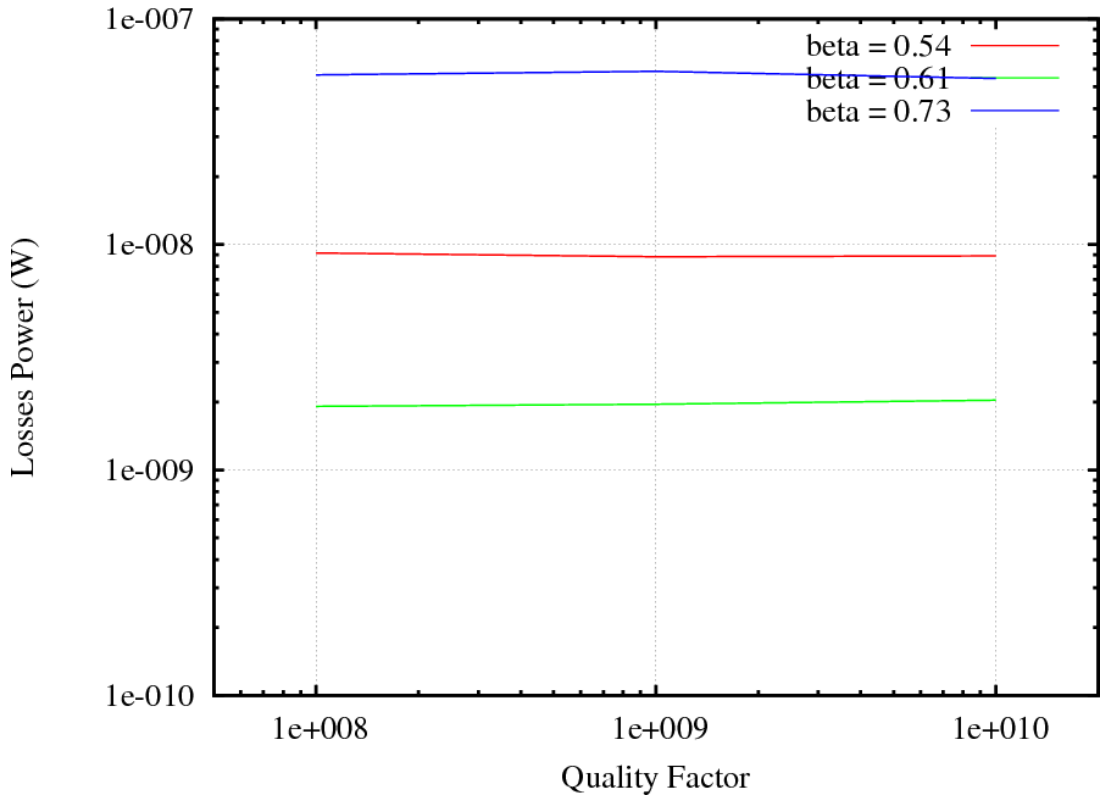

Figure 46: Power of losses vs. quality factor for LE650

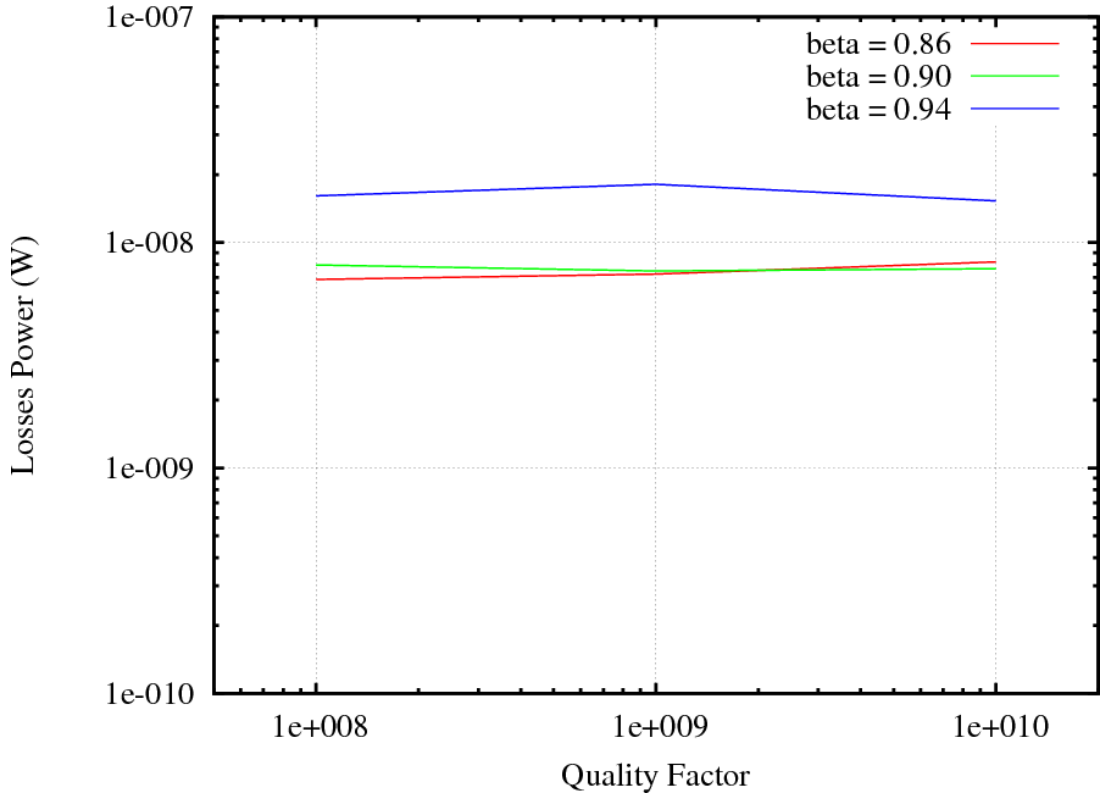

Figure 47: Power of losses vs. quality factor for HE650

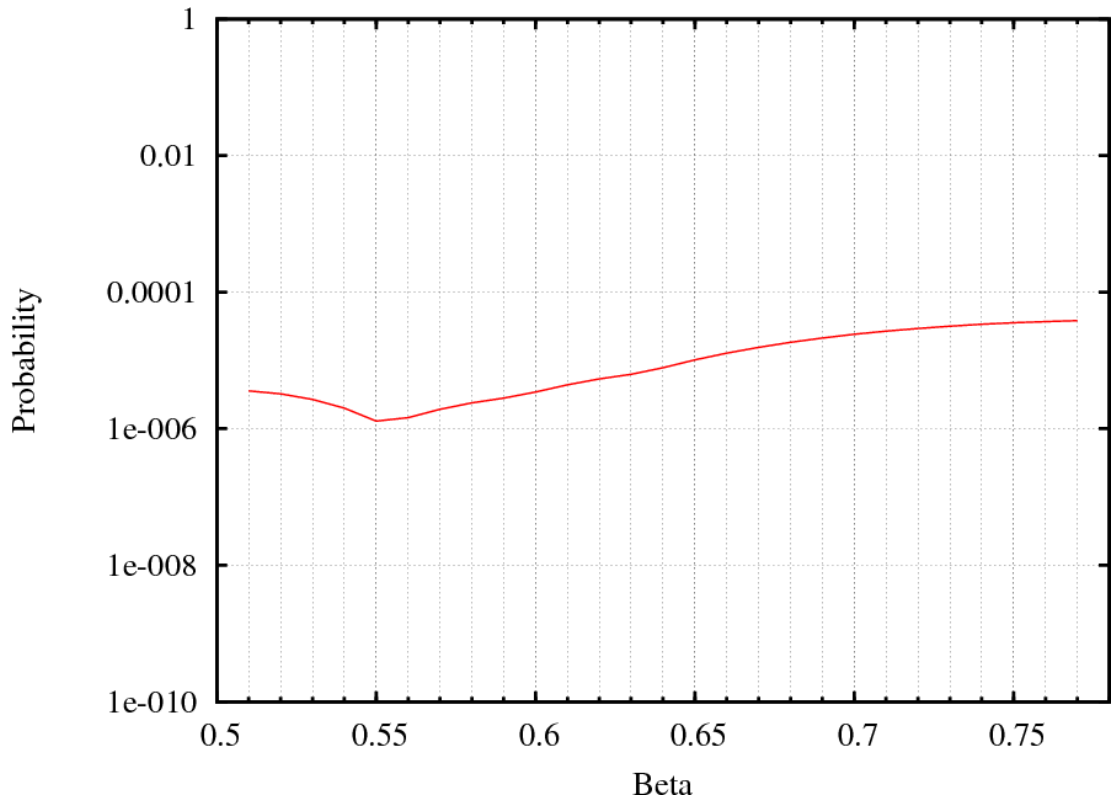

Figure 48: Probability of HOM to cause losses more than 1 W at LE650, $Q = 10^{10}$

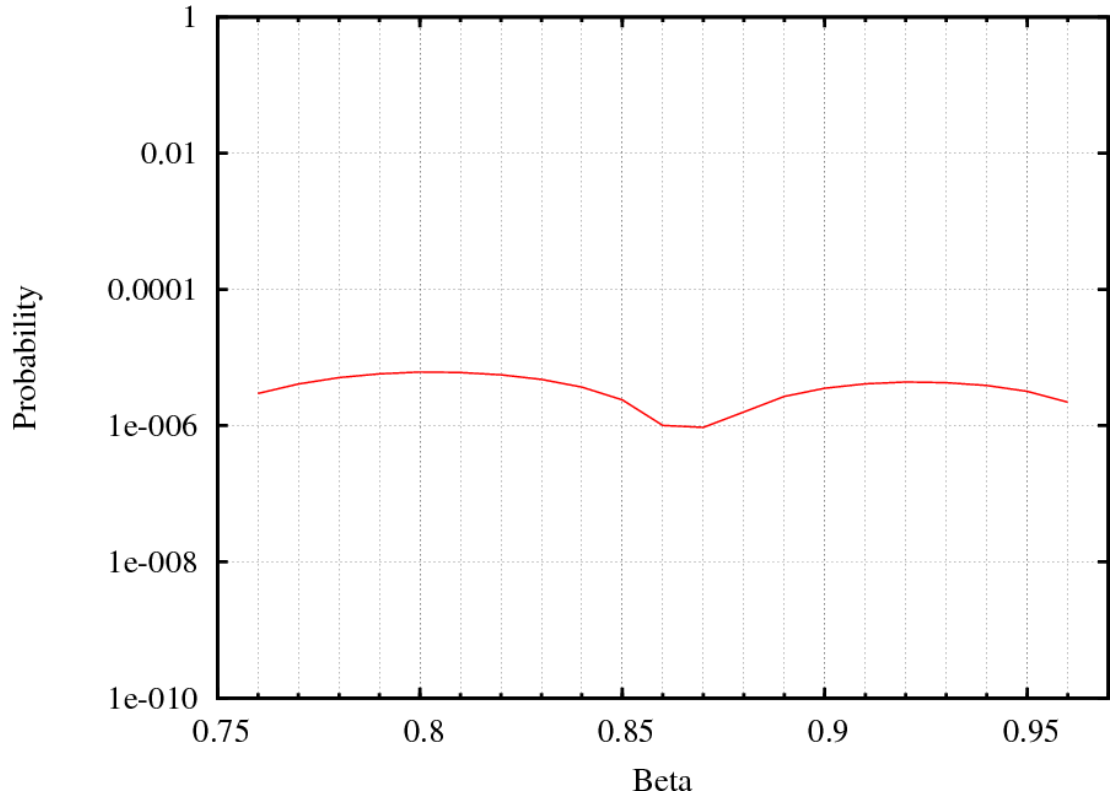

Figure 49: Probability of HOM to cause losses more than 1 W at HE650, $Q = 10^{10}$

As we already know power of losses by one HOM excited by one spectrum line of current can be written like

$$P_{nm} = \frac{1}{2} R_n \oint \vec{H}_{nm} \vec{H}_{nm}^* ds = a_{nmm} f_{nm} f_{nm}^* = a_{nmm} \frac{\omega_m^3}{(\omega_n^2 - \omega_m^2)^2 + \frac{\omega_n^2 \omega_m^2}{Q_m^2}}.$$

If the case is close to resonant one, HOM frequency is close to current frequency. Let's define

$$Q_L = Q_m, \qquad \omega_0 = \omega_n, \qquad \Delta\omega = \omega_n - \omega_m \ll \omega_0,$$

where Q_L is a loaded quality factor. Then one can say that

$$\omega_m \approx \omega_0, \qquad \text{and } \omega_n^2 - \omega_m^2 \approx (\omega_n - \omega_m)(\omega_n + \omega_m) = 2\omega_0 \Delta\omega.$$

Under this conditions the equation for power of losses can be rewritten as

$$P_{nm} \approx a_{nmm} \frac{\omega_0^3}{(2\omega_0 \Delta\omega)^2 + \frac{\omega_0^4}{Q^2}} = a_{nmm} \frac{Q_L^2}{\omega_0} \frac{1}{1 + 4Q_L^2 \left(\frac{\Delta f}{f_0}\right)^2},$$

where $\Delta\omega = 2\pi\Delta f$, and $\omega_0 = 2\pi f_0$. Going back to a_{nmm} definition one can write

$$\frac{a_{nmm}}{\omega_0} = \frac{1}{2} R_n \left(\frac{\tilde{I}_n}{2}\right)^2 \left(\frac{R}{Q}\right)_m \frac{1}{W_0} A_{mm} \frac{1}{\omega_0}.$$

Now remember that $A_{mm} = \oint \left|\vec{H}_m\right|^2 ds$, $2W_0 = \oint \left|\vec{H}_m\right|^2 dV$, and the expression for resistance:

$$\frac{a_{nmm}}{\omega_0} = \frac{1}{2} \frac{G}{Q_0} \left(\frac{\tilde{I}_n}{2}\right)^2 \left(\frac{R}{Q}\right)_m \frac{1}{W_0} \oint \left|\vec{H}_m\right|^2 ds \cdot \frac{1}{\omega_0} = \left(\frac{\tilde{I}_n}{2}\right)^2 \left(\frac{R}{Q}\right)_m \frac{1}{Q_0} G \oint \left|\vec{H}_m\right|^2 ds \frac{1}{2W_0 \omega_0} =$$

$$= \left(\frac{\tilde{I}_n}{2}\right)^2 \left(\frac{R}{Q}\right)_m \frac{1}{Q_0} \frac{\omega_0 \oint \left|\vec{H}_m\right|^2 dV}{\oint \left|\vec{H}_m\right|^2 ds} \oint \left|\vec{H}_m\right|^2 ds \frac{1}{\omega_0 \oint \left|\vec{H}_m\right|^2 dV} = \left(\frac{\tilde{I}_n}{2}\right)^2 \left(\frac{R}{Q}\right)_m \frac{1}{Q_0}.$$

That is why considering the situation when all other HOMs are far from resonance, one can say that

$$P \approx P_{nm} \approx \left(\frac{\tilde{I}_n}{2}\right)^2 \left(\frac{R}{Q}\right)_m \frac{Q_L^2}{Q_0} \frac{1}{1 + 4Q_L^2 \left(\frac{\Delta f}{f_0}\right)^2}.$$

One can see that

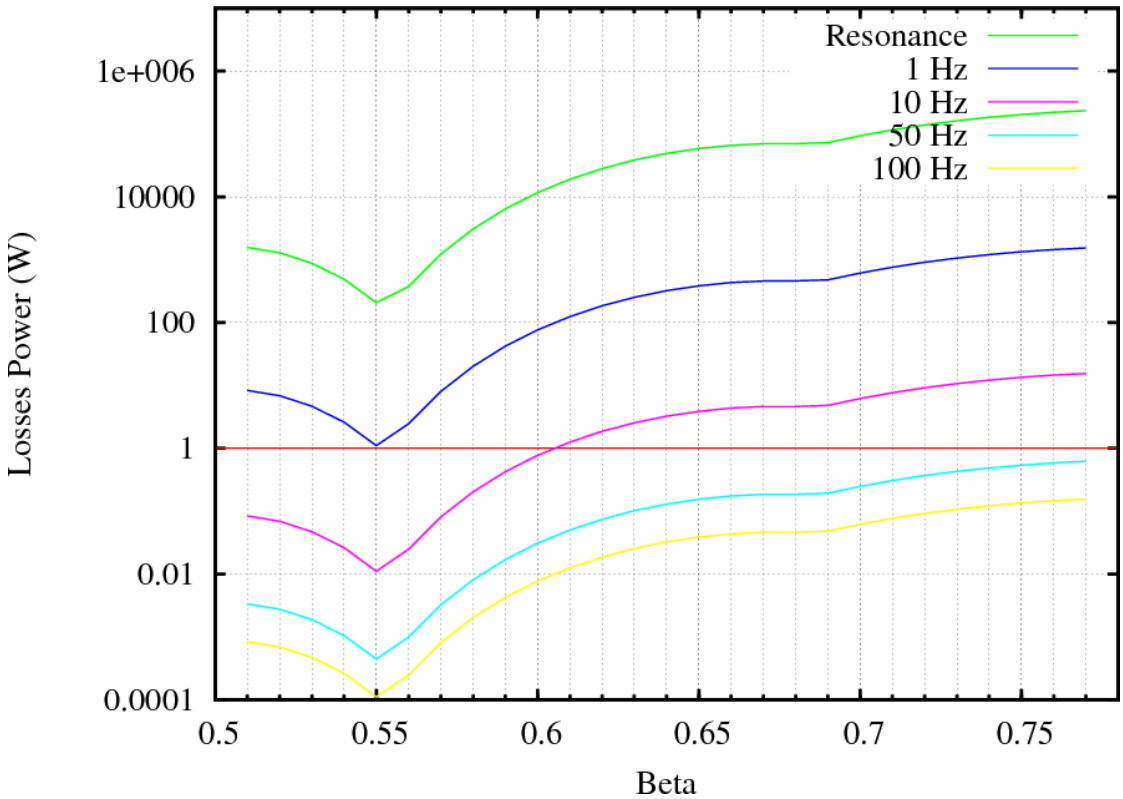

Figure 50: Power of losses reduction with HOM frequency shift at LE650, $Q = 10^{10}$

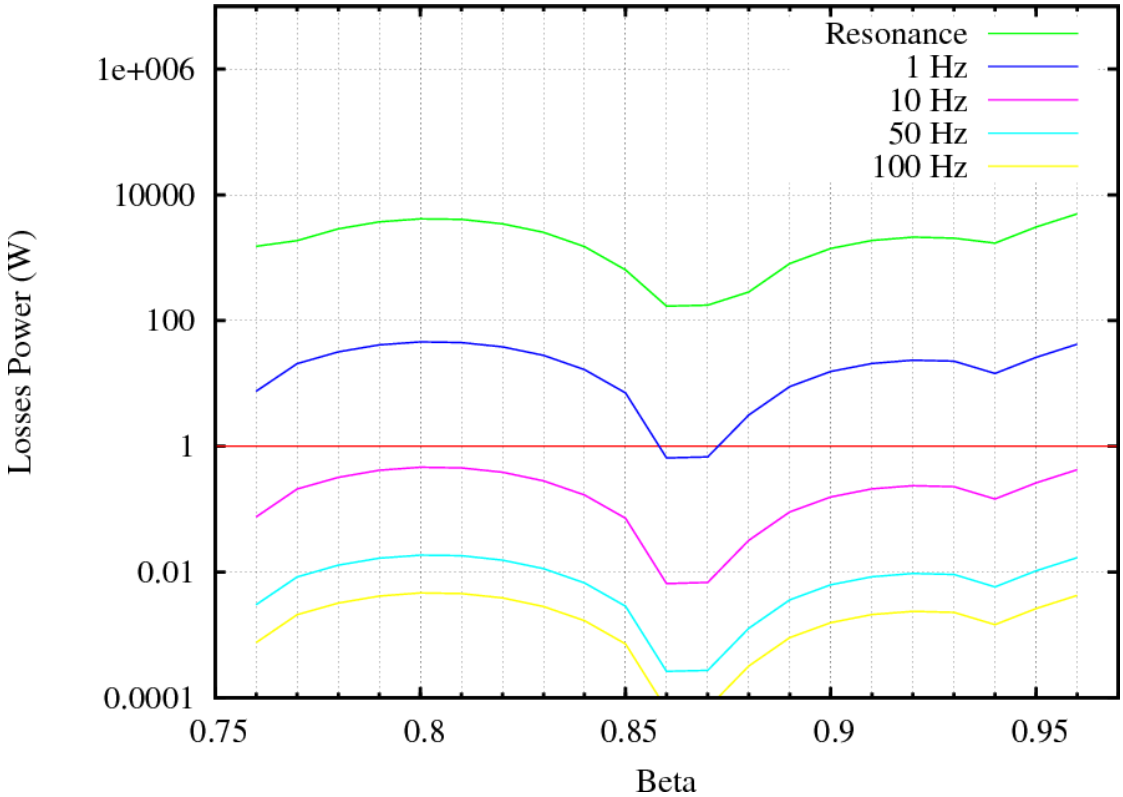

Figure 51: Power of losses reduction with HOM frequency shift at HE650, $Q = 10^{10}$

$$\frac{Q_L^2}{1+4Q_L^2\left(\frac{\Delta f}{f_0}\right)^2}=\frac{1}{\frac{1}{Q_L^2}+4\left(\frac{\Delta f}{f_0}\right)^2}$$

is a decreasing function of Q_L. That is why it is enough to consider the worst case – the largest value of quality factor ($Q = 10^{10}$). Power of losses in a resonant case ($\Delta f = 0$) can be expressed as

$$P_{res}=\left(\frac{\tilde{I}}{2}\right)^2\left(\frac{R}{Q}\right)\frac{Q^2}{Q_0},$$

where we got rid of indexes to simplify notation.

Maximum values of resonant losses in LE650 and HE650 are shown on the Figures 50 and 51. Beam spectrum lines inside three standard deviations distance from HOM frequency are considered (see Figure 3). As we can see, resonant losses are huge, but if there is even small distance between HOM frequency and beam spectrum line, losses are going down significantly. One can see that 50 Hz detune is already enough to decrease losses to acceptable level less than 1 W per cavity.

Table 1: HOM frequencies shift after the cavity detuning and tuning back [7]

F, MHz	$\Delta F, kHz$	$\delta F, Hz$	Passband
1300	90	0	1Monopole
1600.093	−218	360	1Dipole
1604.536	−215	240	1Dipole
1607.951	−214	360	1Dipole
1612.189	−210	360	1Dipole
1621.344	−211	240	1Dipole
1625.458	−208	370	1Dipole
1830.836	−185	370	2Dipople
1859.882	−36	120	2Dipople
2298.807	−278	480	1Quadrupole
2299.346	−278	490	1Quadrupole
2372.333	−224	490	2Monopole
2377.333	−221	490	2Monopole
2383.575	−213	240	2Monopole
2399.289	−210	490	2Monopole

It is possible to move the HOM frequency away from the spectrum line simply detuning the cavity by tens of kHz, and then tune the accelerating mode back. A special test was made with the 1.3 GHz 9-cell ILC cavity. The accelerating mode was detuned by

$$\Delta F = 90\ kHz$$

(see Table 1), and then was tuned back. The accelerating mode frequency remained the same, but the frequencies of HOMs moved after this procedure by $\delta F > 100\ Hz$ because of small inelastic deformations of the cavity.

Going back to plots of probability of HOM to cause losses more than 1 W dependence on beta, one can notice that, as we have already noticed for power of losses dependences, this probability is smaller around the value of geometrical beta. Remember that power of losses can be expressed as

$$P = P_{res}\frac{1}{1+4Q^2\left(\frac{\Delta f}{f_0}\right)^2},$$

where f_0 is the resonant frequency – frequency of the nearest highest beam spectrum line. If one is looking for probability to cause losses more than $P = 1\,W$, it will be the same as probability for HOM frequency to at a distance less than

$$\Delta f = \frac{f_0}{2Q}\sqrt{\frac{P_{res}}{P} - 1}$$

from a beam spectrum line. It means that first of all HOM has to have a large harmonic of current inside three standard deviation vicinity. As we consider HOMs to have normal distributions around their mean value, the probability also depends on distance from HOM frequency to the nearest highest beam spectrum line δf:

$$\wp = \rho(\delta f)\cdot 2\Delta f = \frac{1}{\sqrt{2\pi}\sigma}e^{-\frac{\delta f^2}{2\sigma^2}}\cdot\frac{f_0}{Q}\sqrt{\frac{P_{res}}{P} - 1}.$$

Since we are interested in $P_{res} \gg P$ one can write

$$\wp \approx \frac{1}{\sqrt{2\pi}\sigma}e^{-\frac{\delta f^2}{2\sigma^2}}\cdot\frac{f_0}{Q}\sqrt{\frac{P_{res}}{P}} = \frac{1}{\sqrt{2\pi}\sigma}e^{-\frac{\delta f^2}{2\sigma^2}}\cdot\frac{f_0}{Q}\sqrt{\left(\frac{\tilde{I}}{2}\right)^2\left(\frac{R}{Q}\right)\frac{Q^2}{Q_0}\frac{1}{P}} = \left(\frac{\tilde{I}}{2}\right)\sqrt{\frac{(R/Q)}{PQ_0}}\frac{f_0}{\sqrt{2\pi}\sigma}e^{-\frac{\delta f^2}{2\sigma^2}}.$$

Probability dependences on beta for the dangerous HOMs are shown on the Figures 52 and 53. There are four dangerous modes in LE650 and two dangerous modes in HE650 (see Table 2). One can see from the equation for the probability that it depends on R/Q which depends on beta. That is why a plot of probability to cause losses more than 1 W for a single mode has the same shape as its R/Q dependence on beta. The shape of total probability is defined as maximum probability among all HOMs, because probability to have more than one HOM near a high beam spectrum line is extremely small.

Table 2: The most dangerous monopole HOMs in terms of losses

f_{HOM}, MHz	f_0, MHz	$\delta f, MHz$	$\frac{\tilde{I}}{2}, mA$[1]	Q_0	$\frac{R}{Q}$
LE650					
1462.94	1462.5	0.44	0.546	$1.9\cdot 10^{10}$	Figure 138
1618.81	1620.9	2.13	0.177	$1.2\cdot 10^{10}$	Figure 142
1622.04	1625.0	2.96	1.014	$1.2\cdot 10^{10}$	Figure 143
1624.45	1625.0	0.55	1.014	$1.2\cdot 10^{10}$	Figure 144
HE650					
1241.14	1243.13	1.99	0.016	$1.8\cdot 10^{10}$	Figure 199
2110.80	2112.50	1.70	0.546	$2.2\cdot 10^{10}$	Figure 216

[1] Note that induced HOM voltage in resonant case is defined as

$$U_{HOM} = \frac{\tilde{I}}{2}\left(\frac{R}{Q}\right)Q_0$$

because of accelerator definition of R/Q.

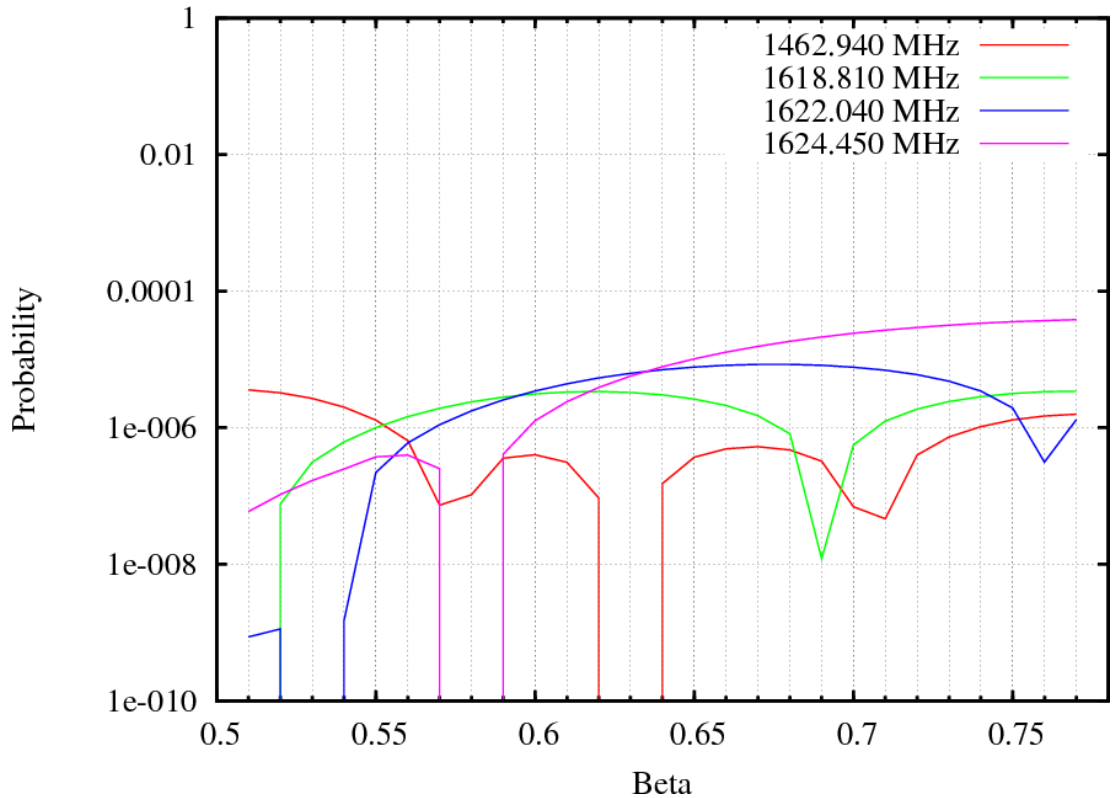

Figure 52: Probability of certain HOMs to cause losses more than 1 W at LE650, $Q = 10^{10}$

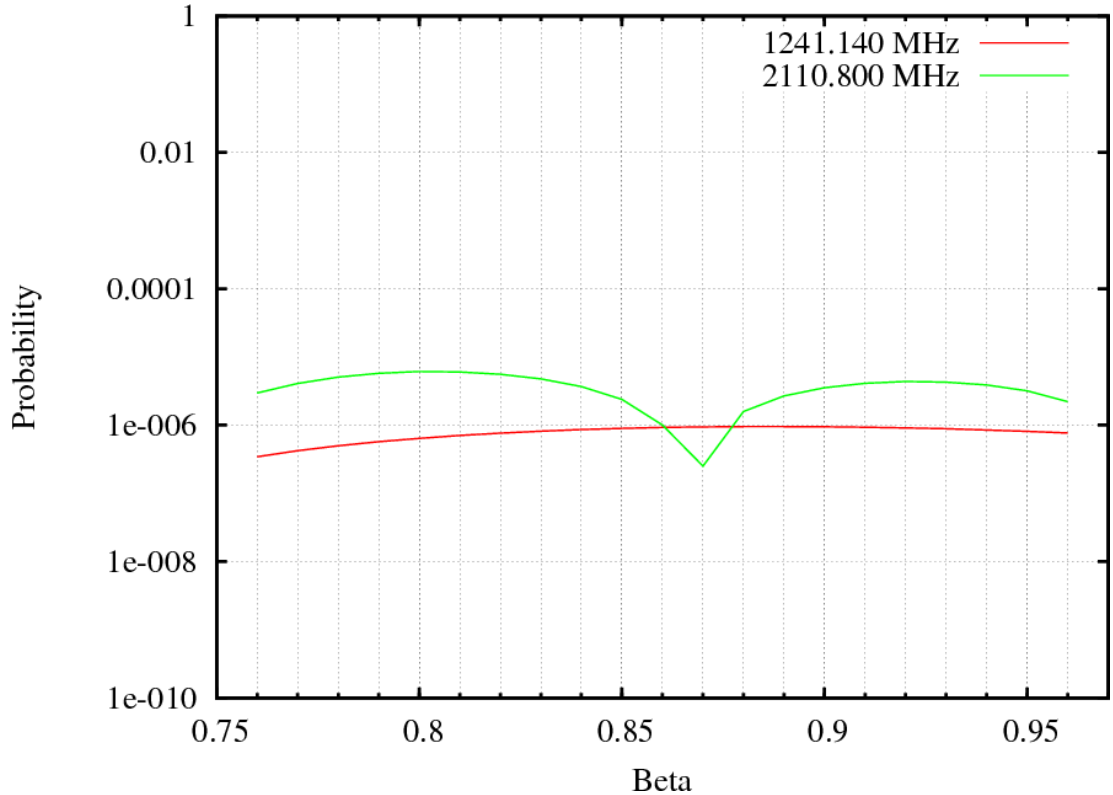

Figure 53: Probability of certain HOMs to cause losses more than 1 W at HE650, $Q = 10^{10}$

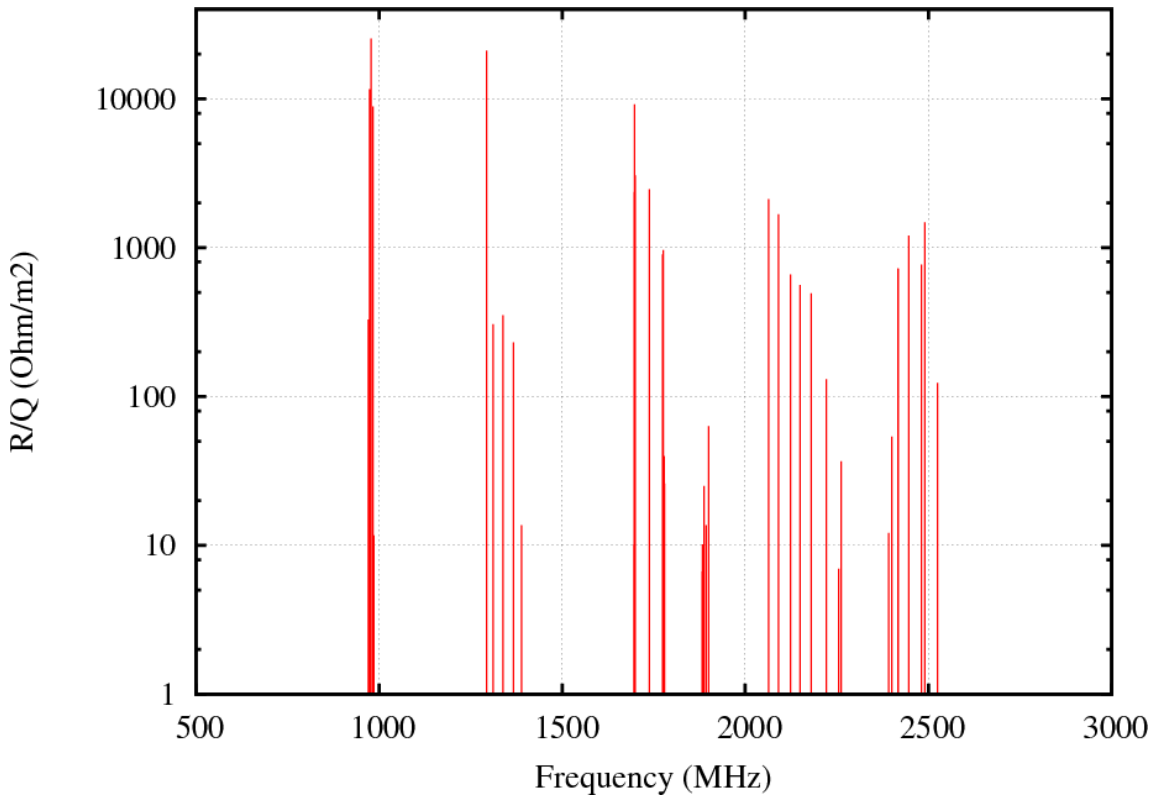

Figure 54: LE650 section dipole HOM spectrum at geometrical beta

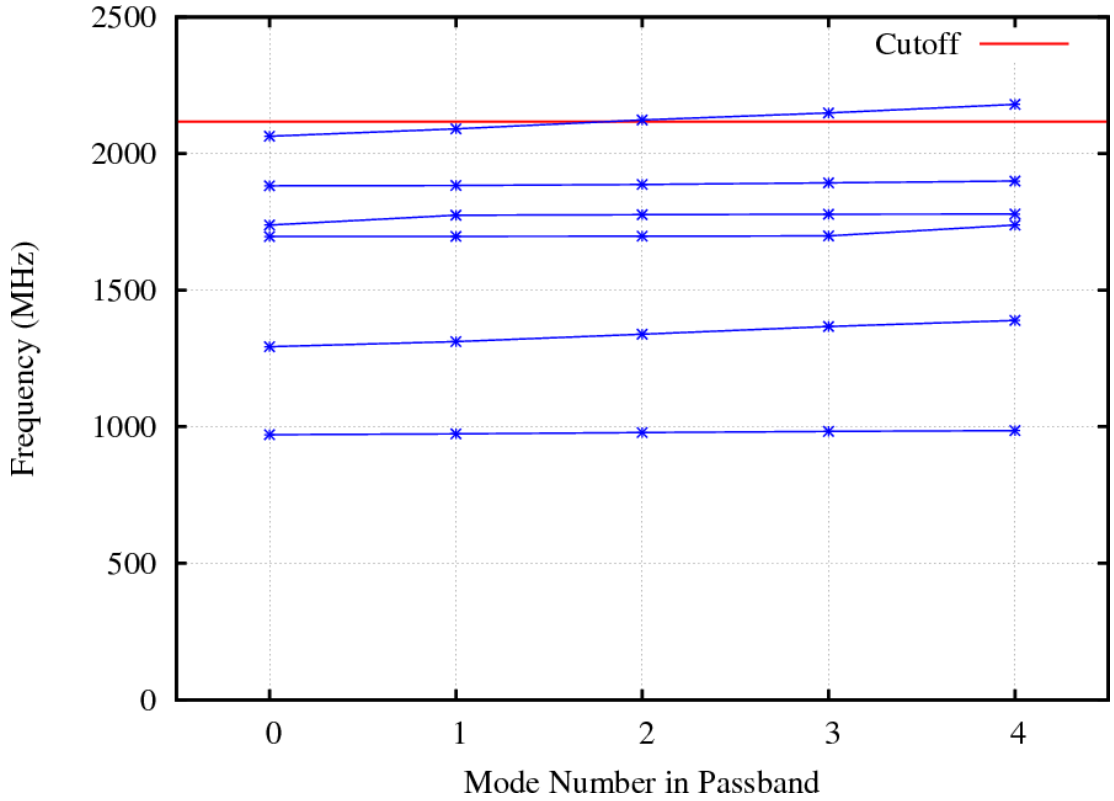

Figure 55: Dispersion curves for LE650

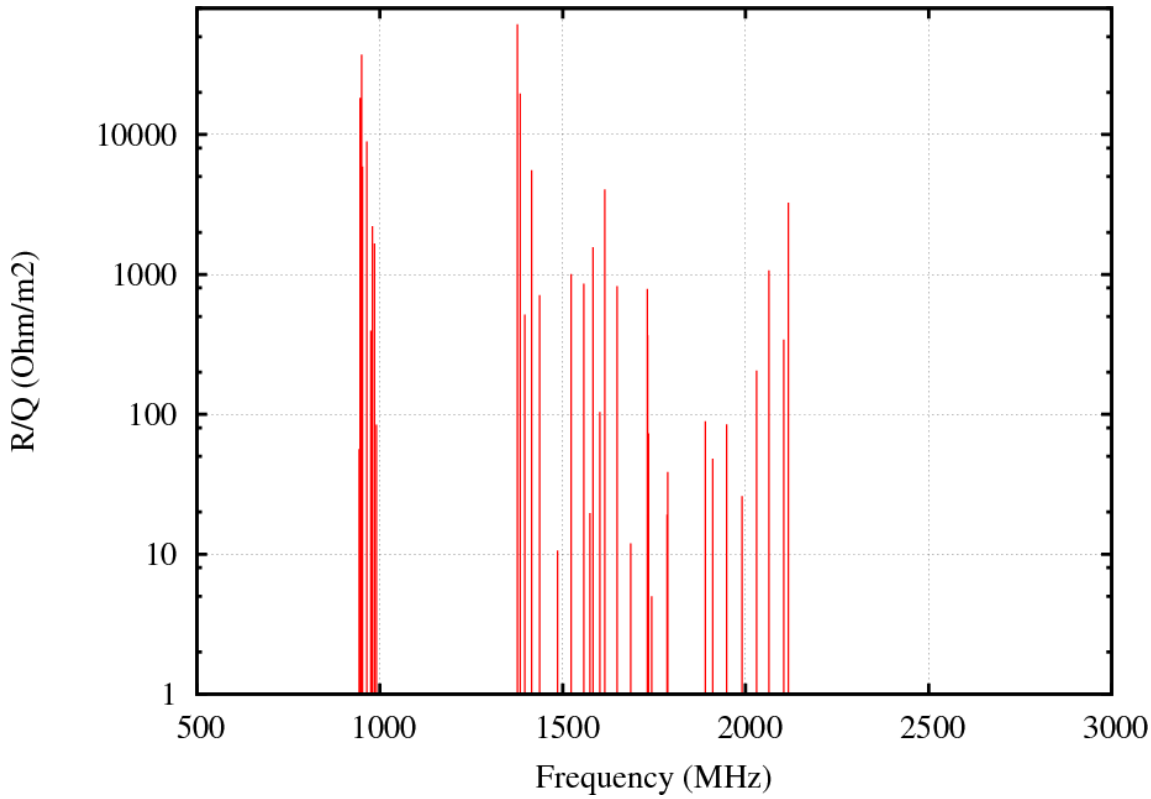

Figure 56: HE650 section dipole HOM spectrum at geometrical beta

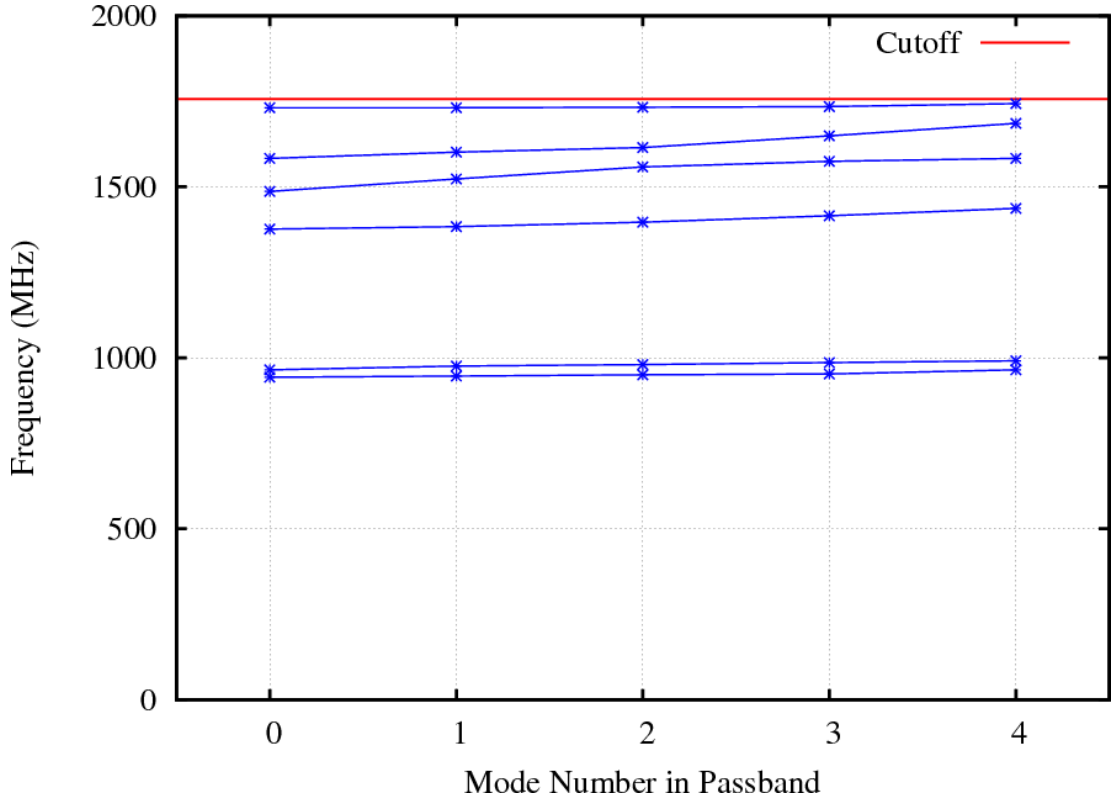

Figure 57: Dispersion curves for HE650

HOMs of the Fundamental Passband

The accelerating mode is going to be tuned exactly at $650\ MHz$. In the result of this distance between frequencies of modes in the fundamental passband will be kept constant with good accuracy. It means that HOMs of the fundamental passband do not have the same frequency spread as all other HOMs do.

Besides these HOMs are connected with the same feeding line as the accelerating mode. That is why they have loaded quality factor which value is going to be about $3 \cdot 10^7$ (as it is shown above). This value is much smaller than the considering value of HOMs quality factor (10^{10}).

These reasons allow us do not take into account HOMs of the fundamental passband for estimating of extreme cases of losses in the previous section and emittance dilution in the next section.

Estimations of the Emittance Growth

One can estimate emittance growth caused by BBU effect using a one cavity model. In this model it is assumed that only one cavity has kick voltage. This model can be used for estimation of the maximum value of the emittance dilution in the situation when collective effects do not occur. If the cavity has transverse misalignment x_0; excited HOM has frequency $\omega = 2\pi f$, transverse impedance $(r_\parallel/Q)_1$ and quality factor Q; alternating current component is $\tilde{I}$, its frequency $\omega_0 = 2\pi f_0$, then similar to the formula (3) one can write

$$V_{kick} = \frac{\omega\omega_0}{\omega^2 - \omega_0^2 - i\frac{\omega\omega_0}{Q}} x_0 \frac{\tilde{I}}{2}\left(\frac{r_\parallel}{Q}\right)_1 \cdot \frac{1}{k} = \frac{f f_0}{f^2 - f_0^2 - i\frac{f f_0}{Q}} x_0 \frac{\tilde{I}}{2}\left(\frac{r_\parallel}{Q}\right)_1 \cdot \frac{c}{2\pi f_0} =$$

$$= \frac{c}{4\pi}\left(\frac{r_\parallel}{Q}\right)_1 \cdot \frac{x_0 \tilde{I} f}{f^2 - f_0^2 - i\frac{f f_0}{Q}}.$$

If $\Delta f = f - f_0 \ll f_0 \approx f$ and $\Delta f / f_0 \gg 1/Q$ then kick voltage can be approximated by

$$V_{kick} = \frac{c}{4\pi}\left(\frac{r_\parallel}{Q}\right)_1 \cdot \frac{x_0 \tilde{I}}{2\Delta f}.$$

Emittance dilution can be estimated as

$$\varepsilon = \beta\gamma\sigma_x\sigma_{x'},$$

where

$$\sigma_{x'} = \frac{e\sigma_{V_{kick}}}{pc} = \frac{eV_{kick}}{\sqrt{2}pc},$$

since HOM gives a kick for the bunch that is equal for all the particles inside the bunch (because $\sigma_z \ll \lambda_{HOM}$), but different for different bunches. Thus, this HOM does not increase emittance of an individual bunch, but gives kicks in different phase for different bunches increasing total phase space occupied by the bunches. That is why $\sigma_{V_{kick}} = V_{kick}/\sqrt{2}$ because of integration of $\sin^2\varphi$. β and γ are Lorentz parameters. $\sigma_x = \beta_f \sigma_{x'}$, where β_f is beta function. So taking into account $p = \beta\gamma mc$, emittance dilution can be written like

$$\varepsilon = \frac{\beta_f}{\beta\gamma}\left(\frac{ex_0\tilde{I}}{8\sqrt{2}\pi mc\Delta f}\left(\frac{r_\parallel}{Q}\right)_1\right)^2 \ll \varepsilon_{initial} = 2.5 \cdot 10^{-7}\ m \cdot rad.$$

It gives us a limitation on HOM frequency deviation from a beam spectrum line:

$$\Delta f \gg \frac{ex_0\tilde{I}}{8\sqrt{2}\pi mc}\left(\frac{r_\parallel}{Q}\right)_1 \sqrt{\frac{\beta_f}{\beta\gamma\varepsilon_{initial}}} = \delta f_\varepsilon.$$

Assuming HOM frequency normal distributed one can find probability to cause emittance dilution more or equal to initial emittance as

$$\wp = \frac{\delta f_\varepsilon}{\sqrt{2\pi}\sigma} e^{-\frac{\Delta f^2}{2\sigma^2}} = \frac{ex_0\tilde{I}}{16\pi\sqrt{\pi}mc\sigma}\left(\frac{r_\parallel}{Q}\right)_1 \cdot \sqrt{\frac{\beta_f}{\beta\gamma\varepsilon_{initial}}} e^{-\frac{\Delta f^2}{2\sigma^2}},$$

where Δf is distance between HOM frequency and a beam spectrum line. The value of beta function at 650 MHz sections can be considered as $15\,m$. Maximum misalignment can be estimated by $1\ mm$, m is mass of H^-.

δf_ε dependence on beta is shown on the Figures 58 and 59 for both LE650 and HE650 sections. One can see that its value is extremely small compare with distances between HOM and beam spectrum lines and HOM frequency spread. It defines the probability $\wp$ dependence on beta which is shown on the Figures 60 and 61 for LE650 and HE 650.Its maximum value is about 10^{-6} what is extremely small. It is necessary to mention that the technique described for losses reduction can be applied here too. There are three most dangerous HOMs in LE650 (see Table 3), which form total probability in different ranges of beta (see Figures 62 and 63). There is only one HOM in HE650 section which dominates on all range of beta (see Table 3).

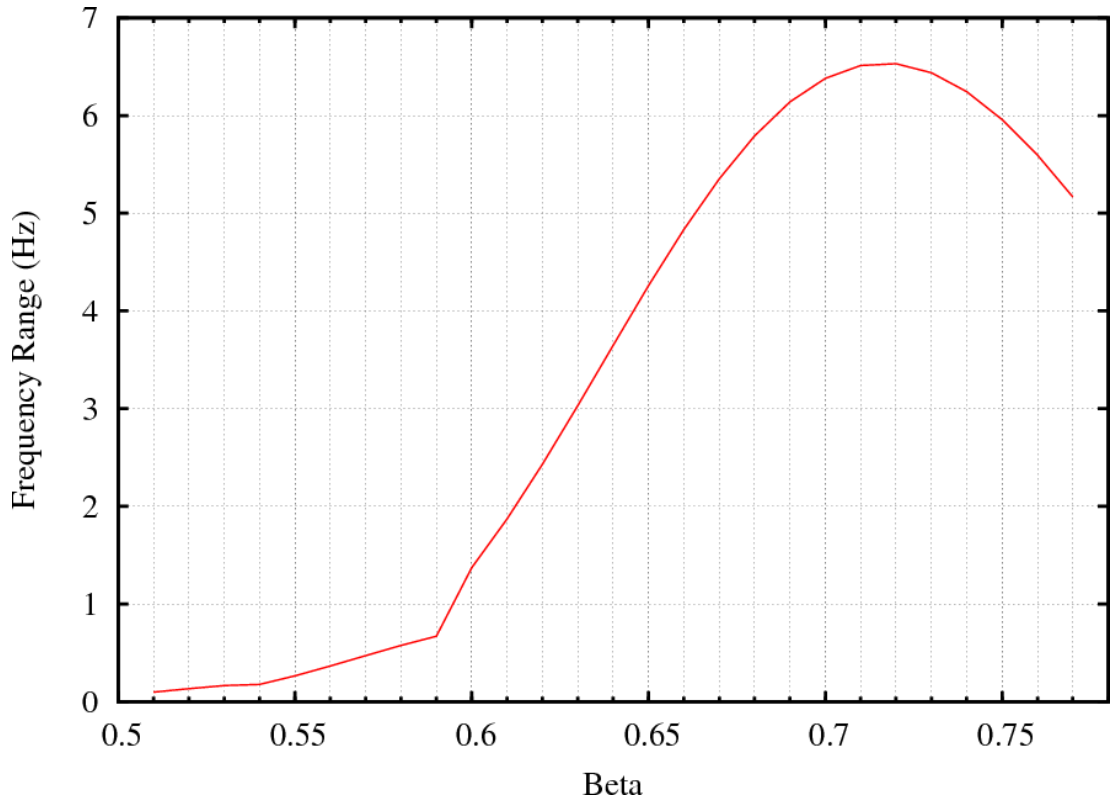

Figure 58: δf_{ε} dependence on beta at LE650 for dipole HOMs

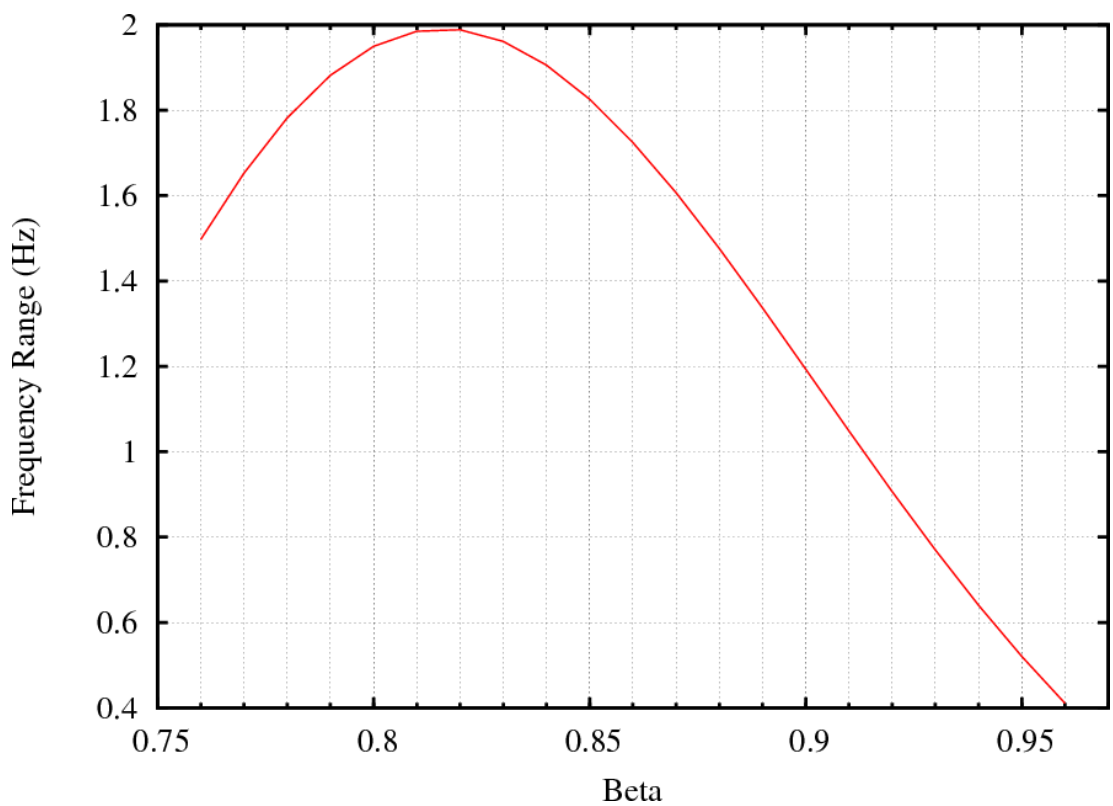

Figure 59: δf_{ε} dependence on beta at HE650 for dipole HOMs

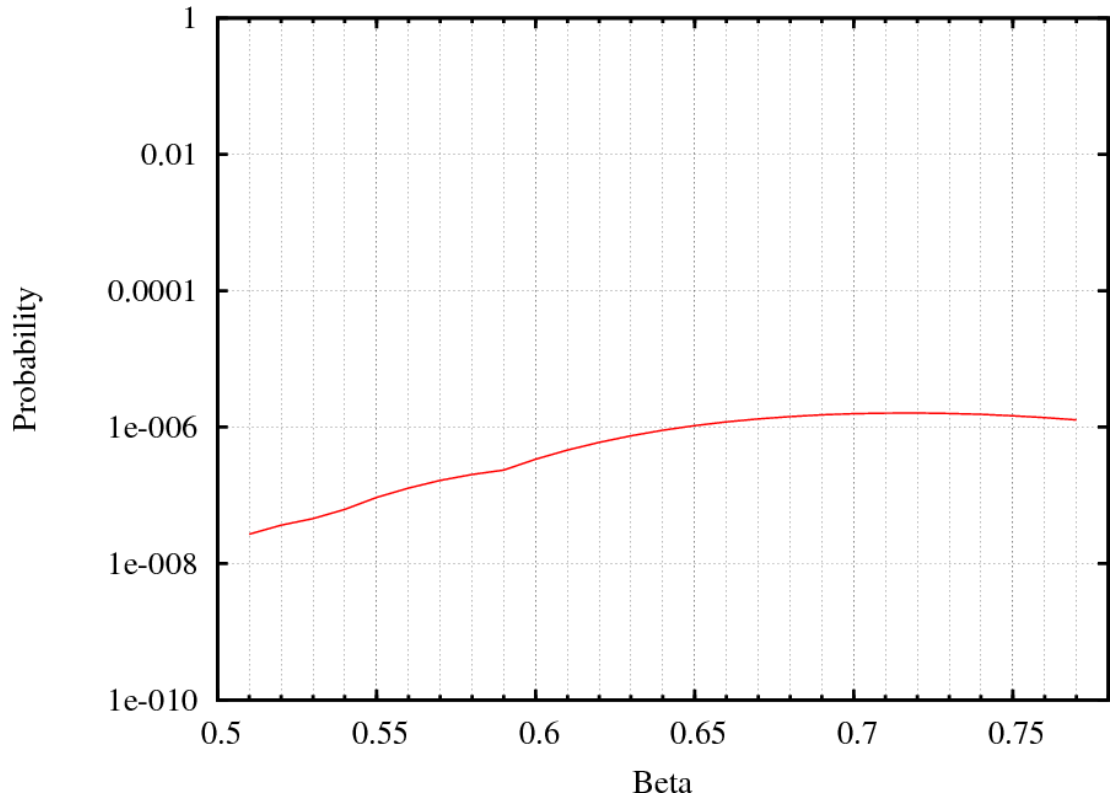

Figure 60: Probability to cause significant emittance dilution at LE650 for dipole HOMs

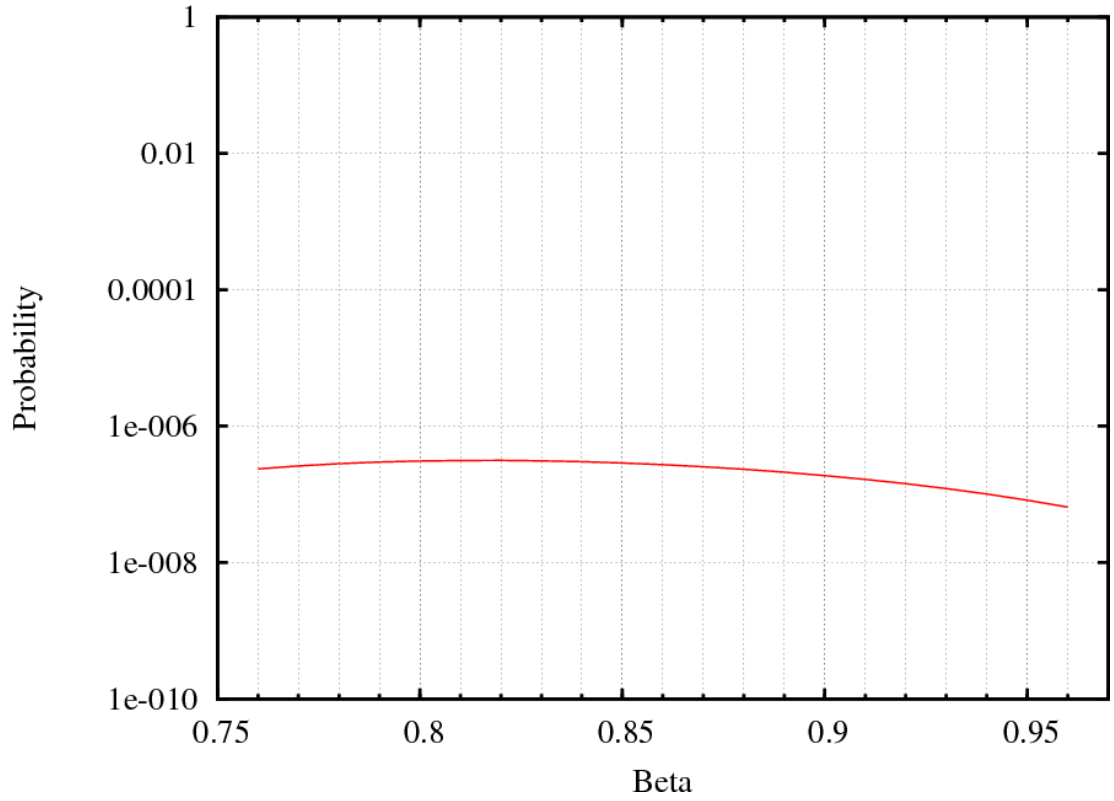

Figure 61: Probability to cause significant emittance dilution at HE650 for dipole HOMs

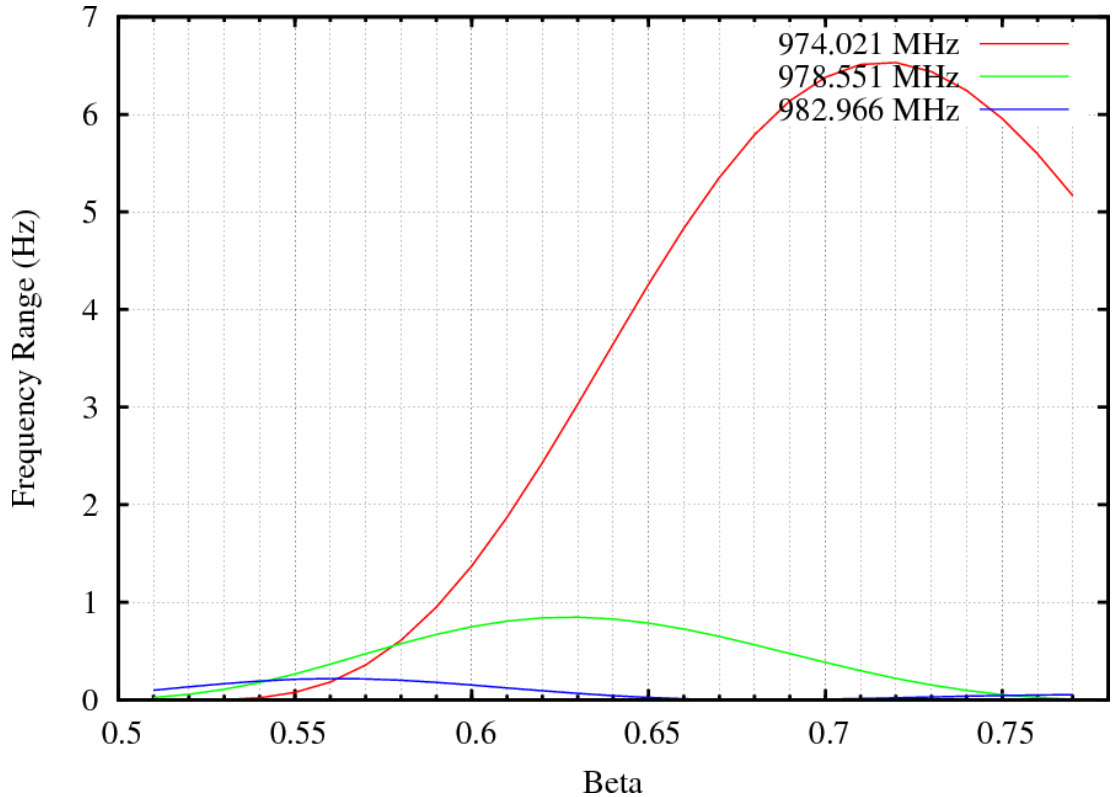

Figure 62: δf_{ε} dependence on beta at LE650 for the most dangerous dipole HOMs

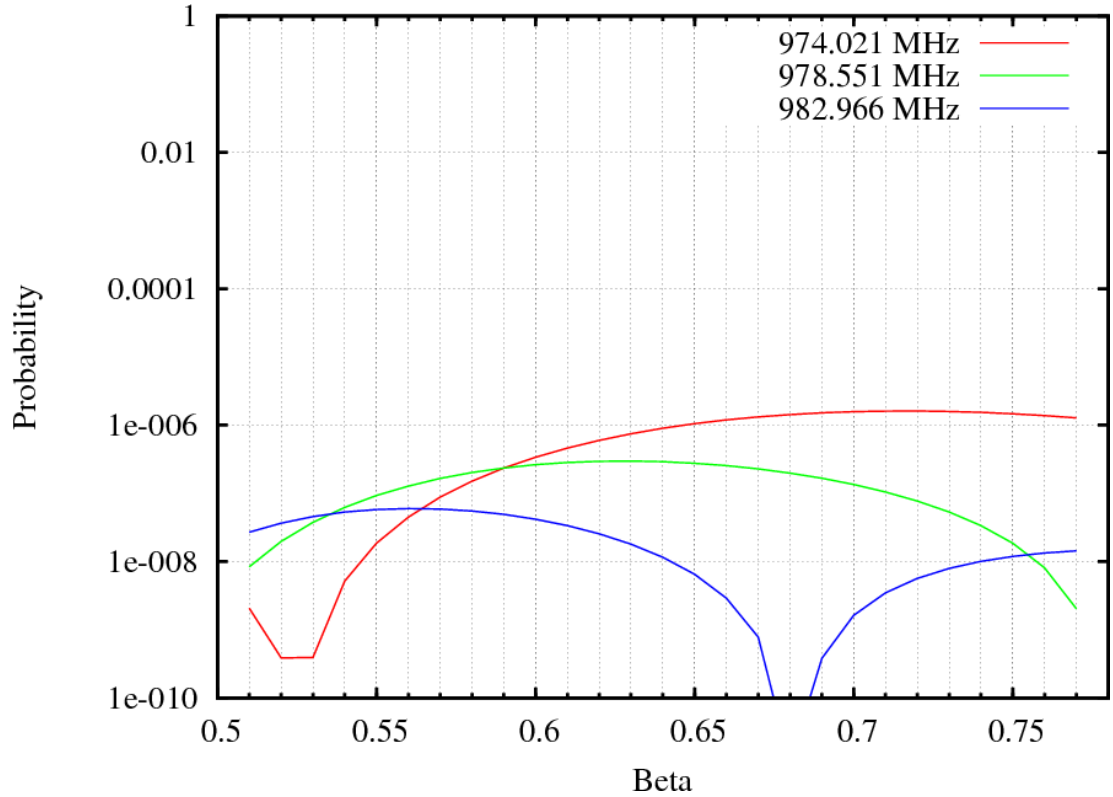

Figure 63: Probability to cause significant emittance dilution at LE650 for the most dangerous dipole HOMs

Table 3: The most dangerous dipole HOMs in terms of emittance dilution

f_{HOM}, MHz	f_0, MHz	$\Delta f, kHz$	$\frac{\tilde{I}}{2}, mA$	$\left(\frac{r_\parallel}{Q}\right)_{1max}, \frac{k\Omega}{m^2}$	β	$\wp$	$\delta f_\varepsilon, Hz$
LE650							
974.021	975.000	979	1.014	47.15	0.72	$1.6 \cdot 10^{-6}$	6.5
978.551	978.047	504	0.201	27.27	0.63	$3.0 \cdot 10^{-7}$	0.8
982.966	982.109	857	0.086	14.85	0.56	$6.0 \cdot 10^{-8}$	0.2
HE650							
946.556	947.917	1361	0.675	25.33	0.82	$3.1 \cdot 10^{-7}$	2.0

Similar estimation can be made for emittance dilution due to resonant excitation of the longitudinal HOMs. If ε is initial longitudinal emittance ($\varepsilon = 1.5 \cdot 10^3\ nsec \cdot eV$), σ_t is bunch length ($0.011\ nsec$) and U_{HOM} is energy gain caused by HOM, then it is necessary to have

$$U_{HOM}\sigma_t \ll \varepsilon.$$

Energy gain in eV with the same assumptions as in transversal HOM case can be written like

$$U_{HOM} = \sigma_{V_{HOM}} = \frac{1}{\sqrt{2}} \frac{f f_0}{f^2 - f_0^2 - i f f_0/Q} \frac{\tilde{I}}{2}\left(\frac{R}{Q}\right) \approx \frac{1}{\sqrt{2}} \frac{f_0 \tilde{I}}{4\Delta f}\left(\frac{R}{Q}\right).$$

That is why the limitation on Δf looks like

$$\Delta f \gg \frac{f_0 \tilde{I} \sigma_t}{4\sqrt{2}\varepsilon}\left(\frac{R}{Q}\right) = \delta f_\varepsilon,$$

and probability to cause significant emittance growth can be estimated as

$$\wp = \frac{\delta f_\varepsilon}{\sqrt{2\pi}\sigma} e^{-\frac{\Delta f^2}{2\sigma^2}} = \frac{f_0 \tilde{I} \sigma_t}{8\sqrt{\pi}\sigma\varepsilon}\left(\frac{R}{Q}\right) e^{-\frac{\Delta f^2}{2\sigma^2}}.$$

Table 4: The most dangerous monopole HOMs in terms of emittance dilution

f_{HOM}, MHz	f_0, MHz	$\Delta f, kHz$	$\frac{\tilde{I}}{2}, mA$	$\left(\frac{R}{Q}\right)_{max}, \Omega$	β	$\wp$	$\delta f_\varepsilon, Hz$
LE650							
1462.94	1462.50	440	0.546	1.011	0.51	$7.6 \cdot 10^{-7}$	2.1
1618.81	1618.91	96	0.118	4.308	0.77	$8.5 \cdot 10^{-7}$	2.1
1622.04	1621.95	87	0.201	8.164	0.68	$2.7 \cdot 10^{-6}$	6.9
1624.45	1625.00	550	1.014	27.340	0.77	$4.0 \cdot 10^{-5}$	116.8
2747.25	2747.27	16	0.050	2.200	0.73	$3.1 \cdot 10^{-7}$	0.8
HE650							
1241.14	1241.09	46	0.009	130.920	0.89	$1.6 \cdot 10^{-6}$	4.0
1840.26	1841.67	1407	0.390	5.662	0.96	$1.6 \cdot 10^{-6}$	10.5
2110.80	2110.47	331	0.219	3.016	0.80	$1.4 \cdot 10^{-6}$	3.6

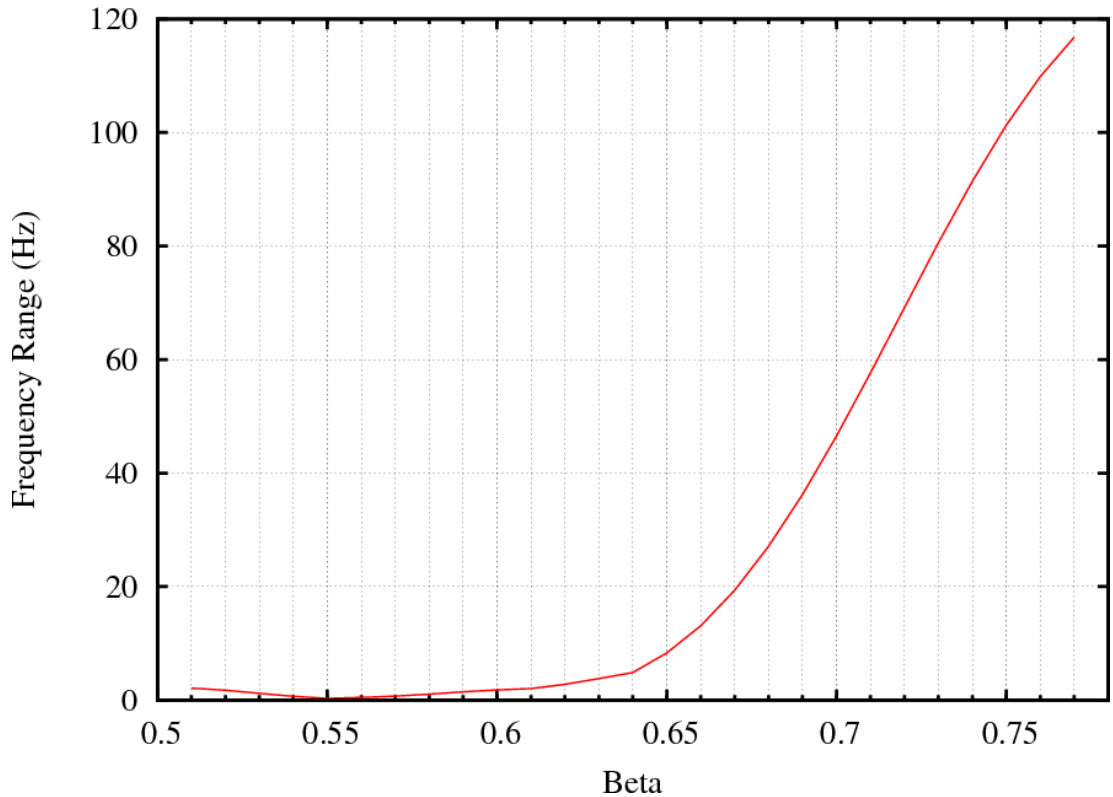

Figure 64: δf_{ε} dependence on beta at LE650 for monopole HOMs

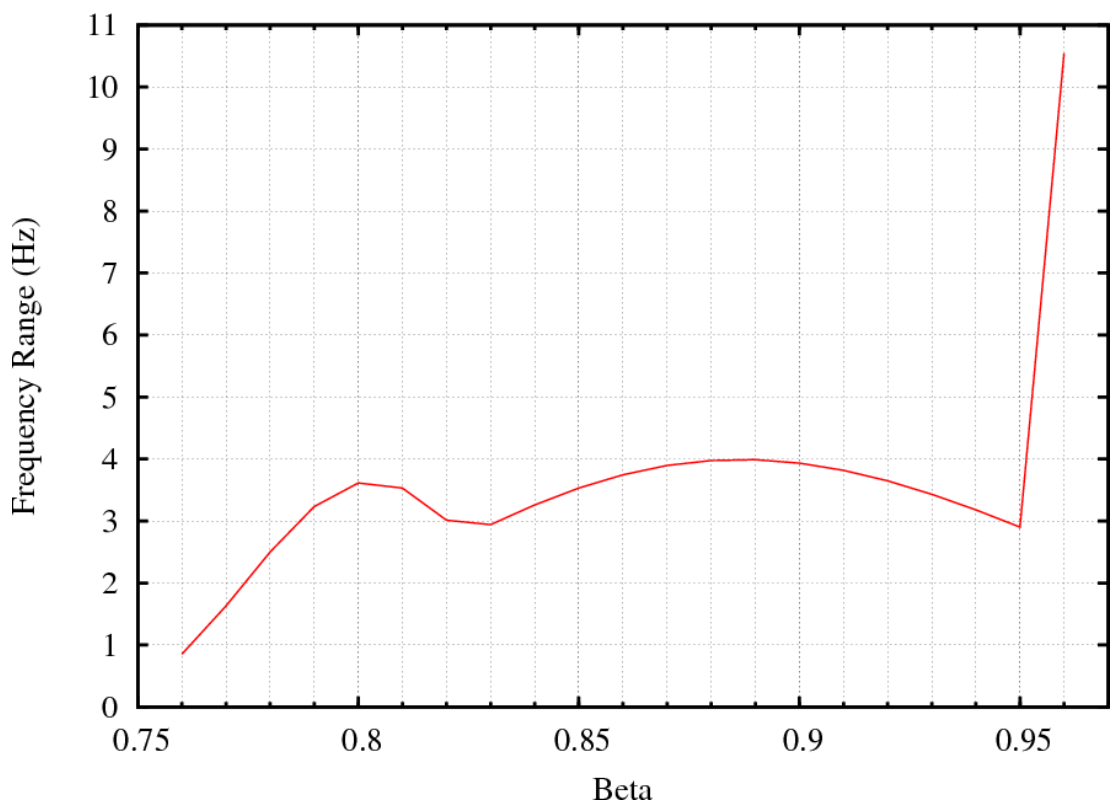

Figure 65: δf_{ε} dependence on beta at HE650 for monopole HOMs

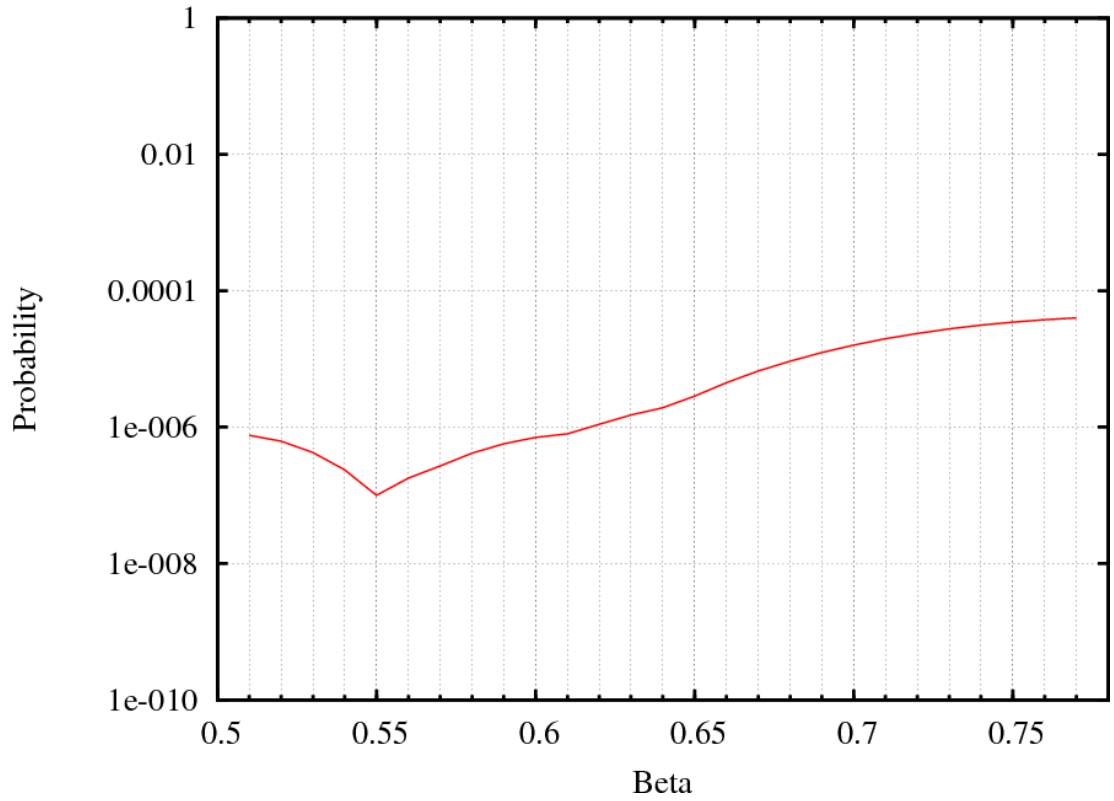

Figure 66: Probability to cause significant emittance dilution at LE650 for dipole HOMs

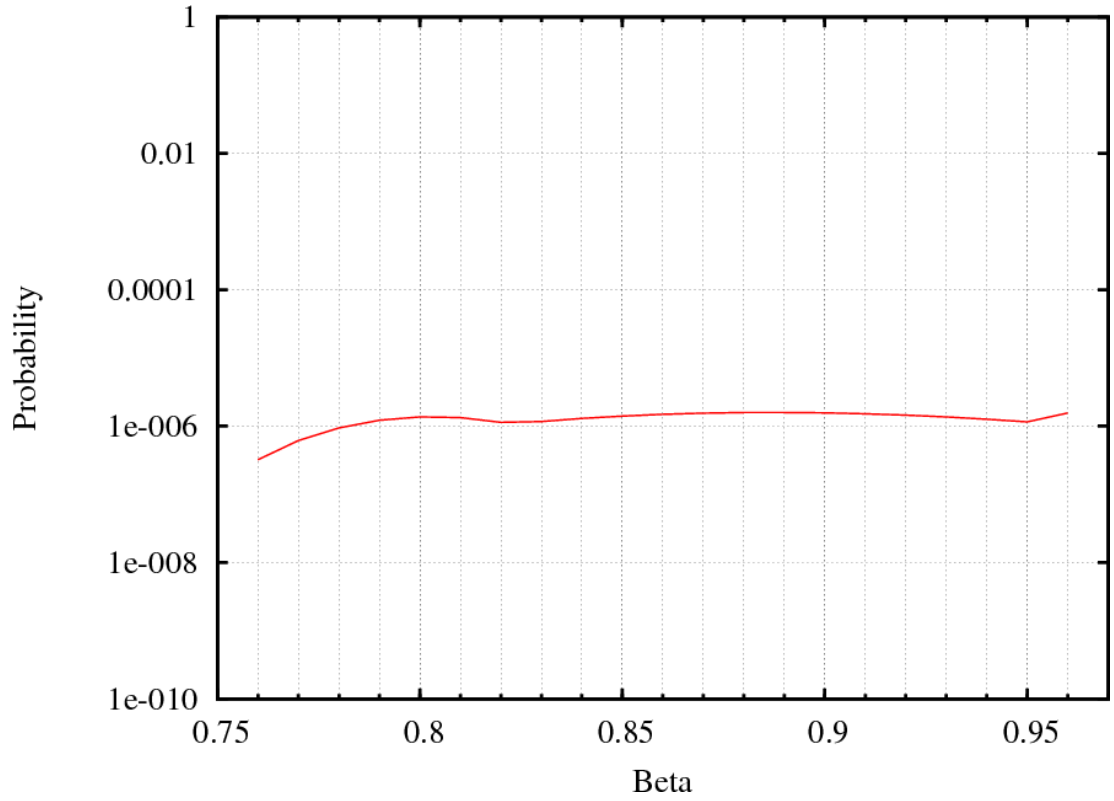

Figure 67: Probability to cause significant emittance dilution at HE650 for dipole HOMs

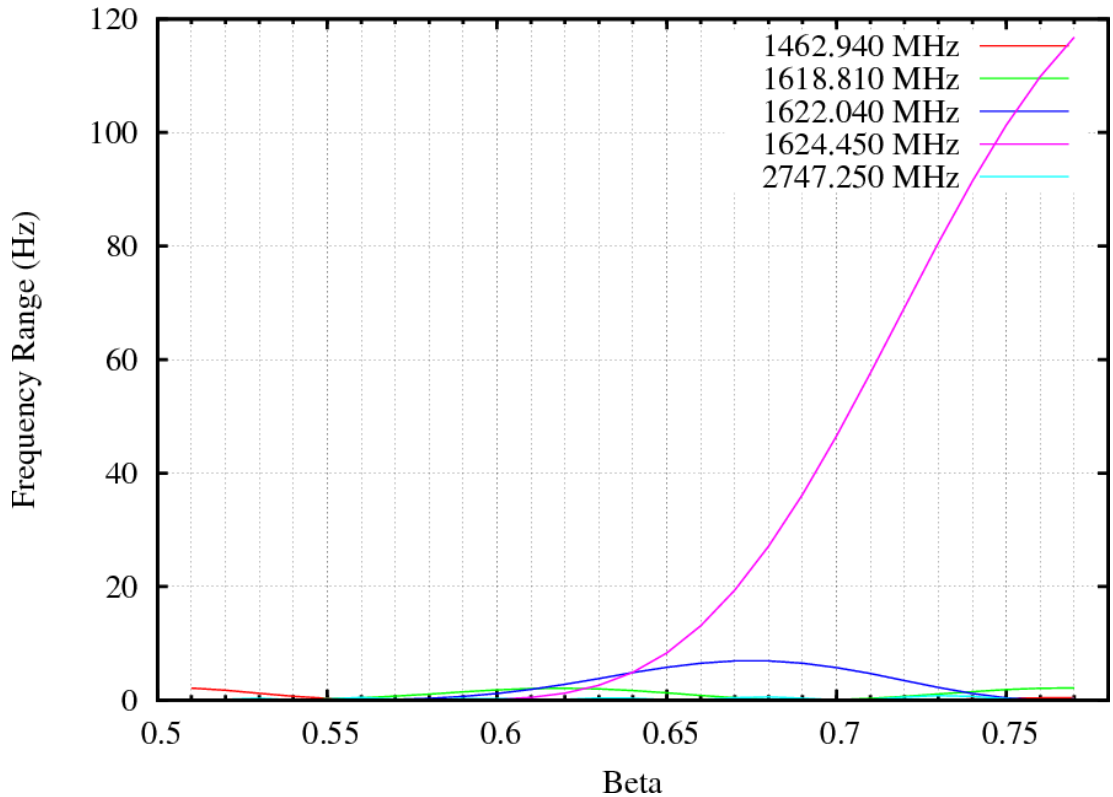

Figure 68: δf_{ε} dependence on beta at LE650 for the most dangerous monopole HOMs

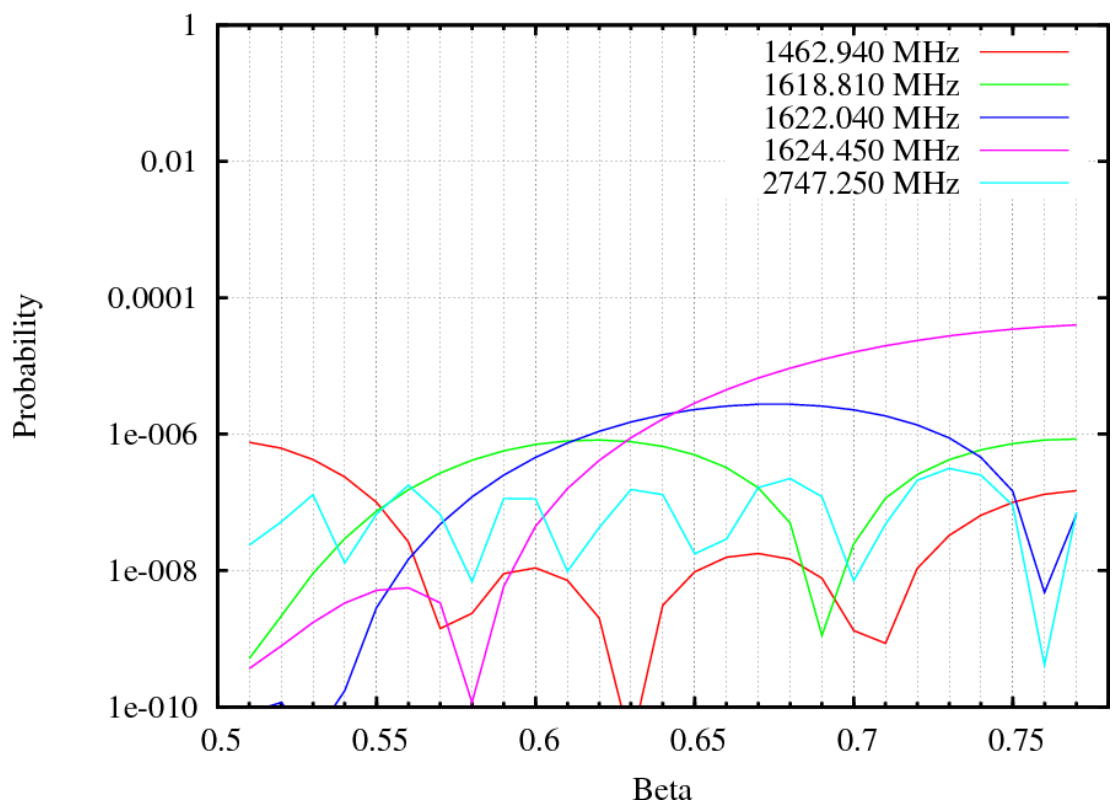

Figure 69: Probability to cause significant emittance dilution at LE650 for the most dangerous monopole HOMs

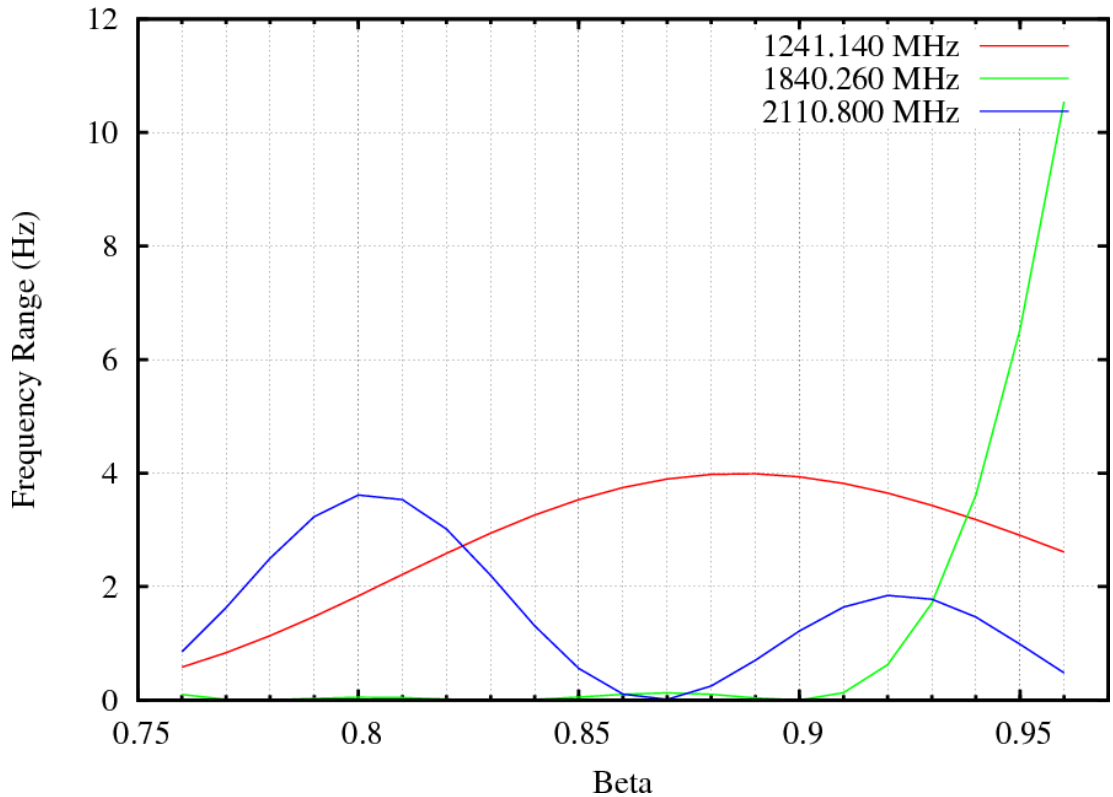

Figure 70: δf_{ε} dependence on beta at HE650 for the most dangerous monopole HOMs

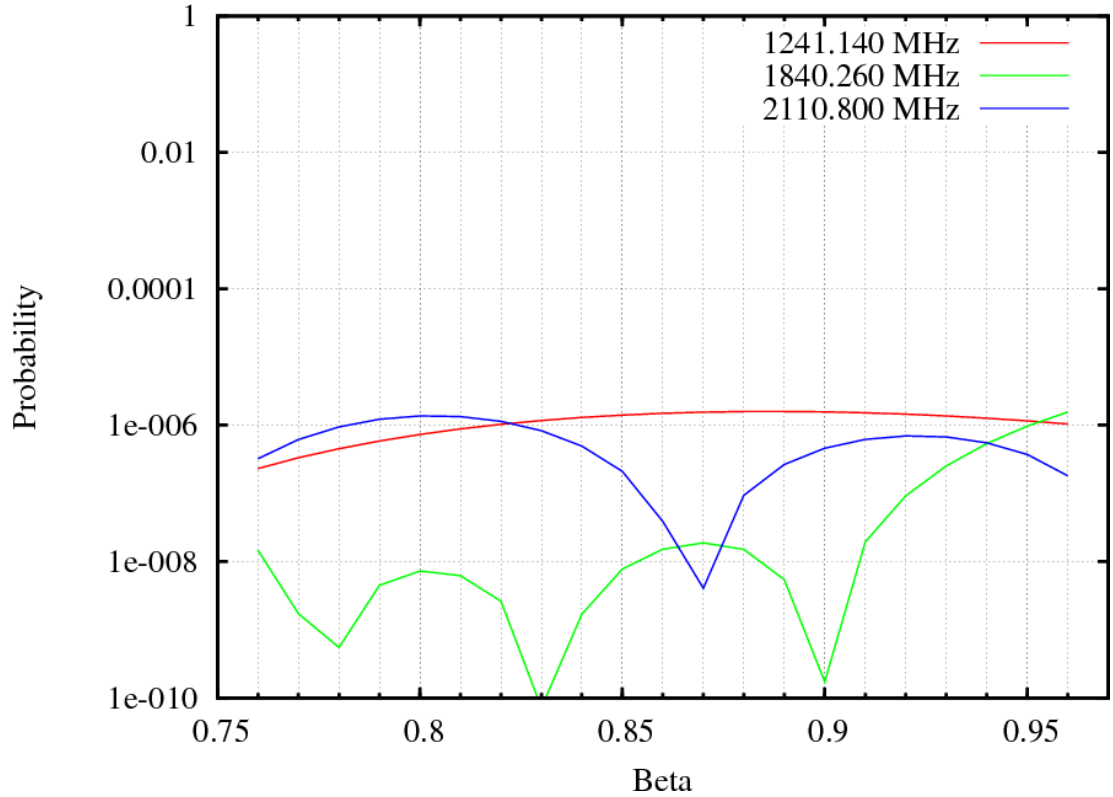

Figure 71: Probability to cause significant emittance dilution at HE650 for the most dangerous monopole HOMs

There are five dangerous modes in LE650 and three dangerous modes in HE650 (see Table 4). One can see their δf_ε and $\wp$ dependences on beta on the Figures 68 – 71. Total δf_ε and the probability dependences on beta are shown on the Figures 64 – 67. One can see that the largest value of the probability is smaller than 10^{-4}.

Comparison with SNS

The same model of losses calculation was applied to operating machine SNS. Two sections of SNS are considered: $\beta = 0.61$ and $\beta = 0.81$. Operating mode frequency is 805 MHz. Average current is 1 mA. RMS HOM frequency spread is 2 MHz. This machine operates in pulse regime. Beam structure is shown on the Figure 72. Macro-pulses are considered synchronized. That allows us to consider the same values of quality factor as for Project X case. The following values were studied: 10^8, 10^9 and 10^{10}. One can calculate idealized spectrum of the beam, which is shown on the Figure 73.

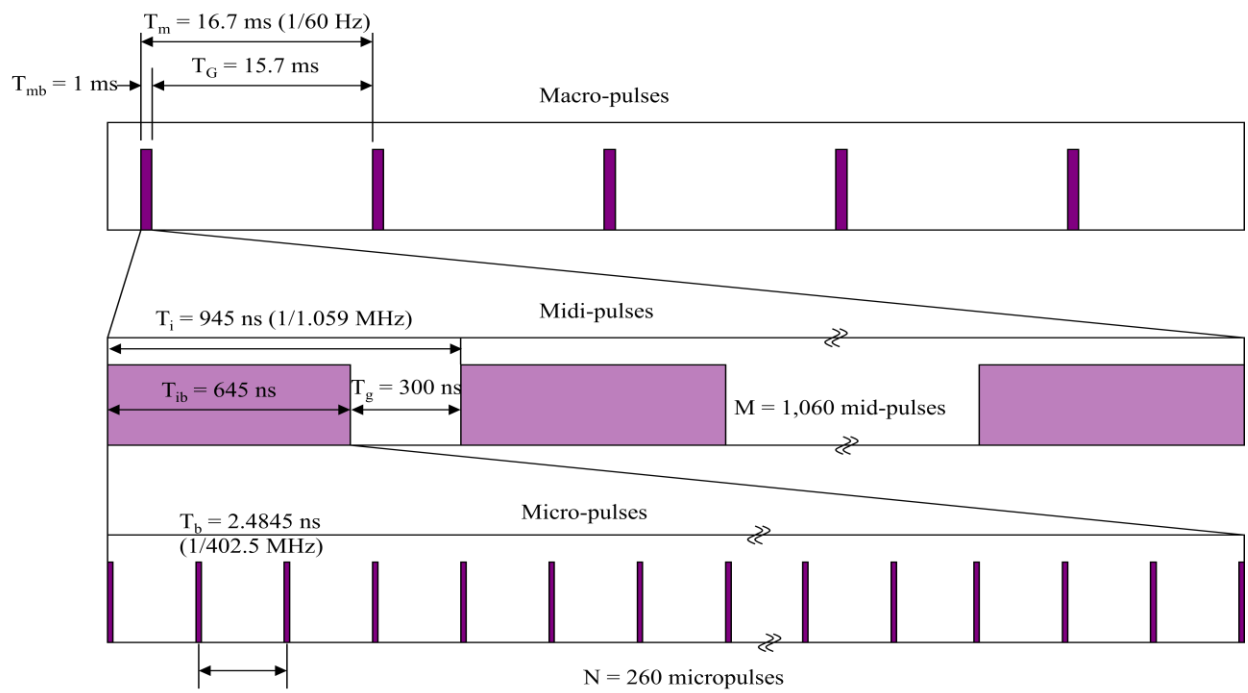

Figure 72: SNS beam structure

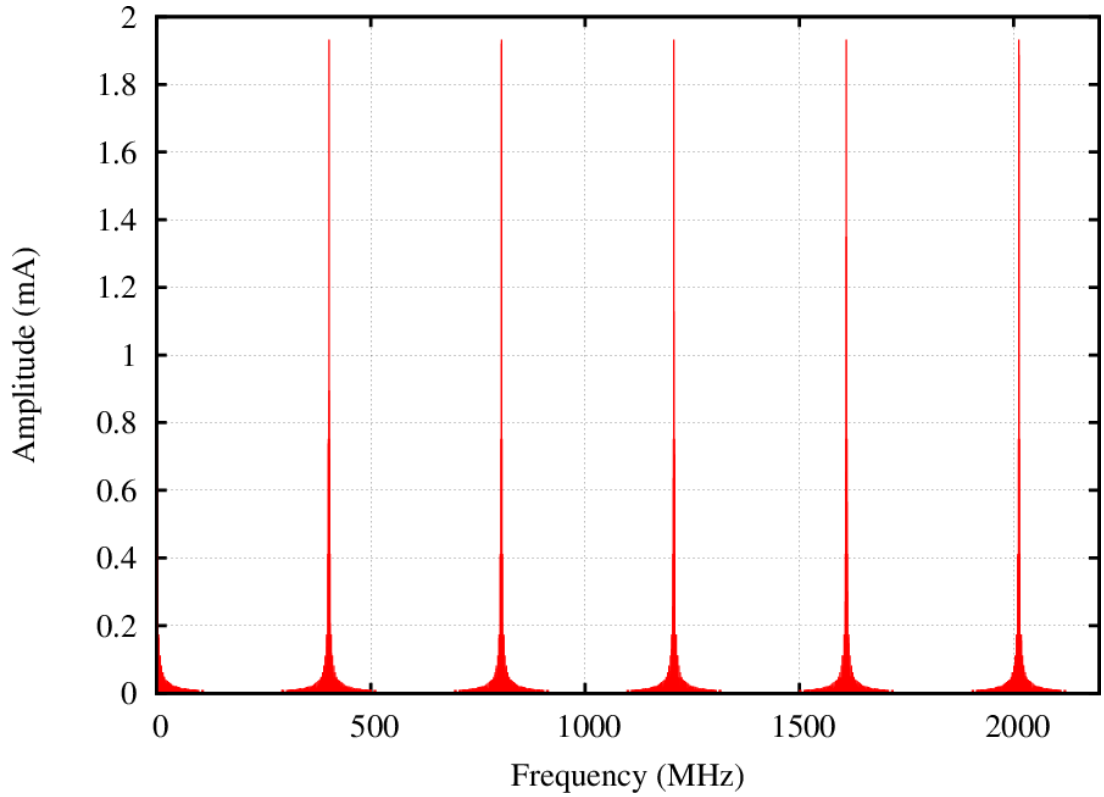

Figure 73: SNS idealized beam spectrum

The following assumptions are used in the model. Bunch size is considered to be zero. For example, actual beam size in Project X is less than $10\ psec$. It affects only high frequency part of the spectrum (more than $100\ GHz$), which is much bigger than beam-pipe cut-off frequency. Lorentz force detuning is neglected. It causes HOM frequency shift about few kHz which is much smaller than the average distance to a strong beam spectrum line.

SNS use 6-cell cavities (see Figures 74 – 75). HOM spectrums for low and high beta cavities are shown on the Figures 76 – 77. Dispersion curves are shown on the Figures 78 – 79. Results of the losses calculations are shown on the Figures 80 – 85. The average losses and $P_{99\%}$ defined as for Project X dependences on beta are shown on the figures. Power of losses distributions at geometrical beta for SNS and Project X are shown on the Figures 86 – 91. One can see that for all cases Project X has less loss than SNS. Power of losses at geometrical beta dependences on quality factor for Project X and SNS are shown on the Figures 92 – 93. Losses do not depend on the value of quality factor for both cases. Power of losses is bigger for SNS case at both low and high energy sections.

SNS experience shows that HOM effects on beam dynamics are not detected. These calculations show that losses in Project X due to HOMs are smaller than these losses in SNS. This fact supports the approach of not using HOM dumpers in Project X.

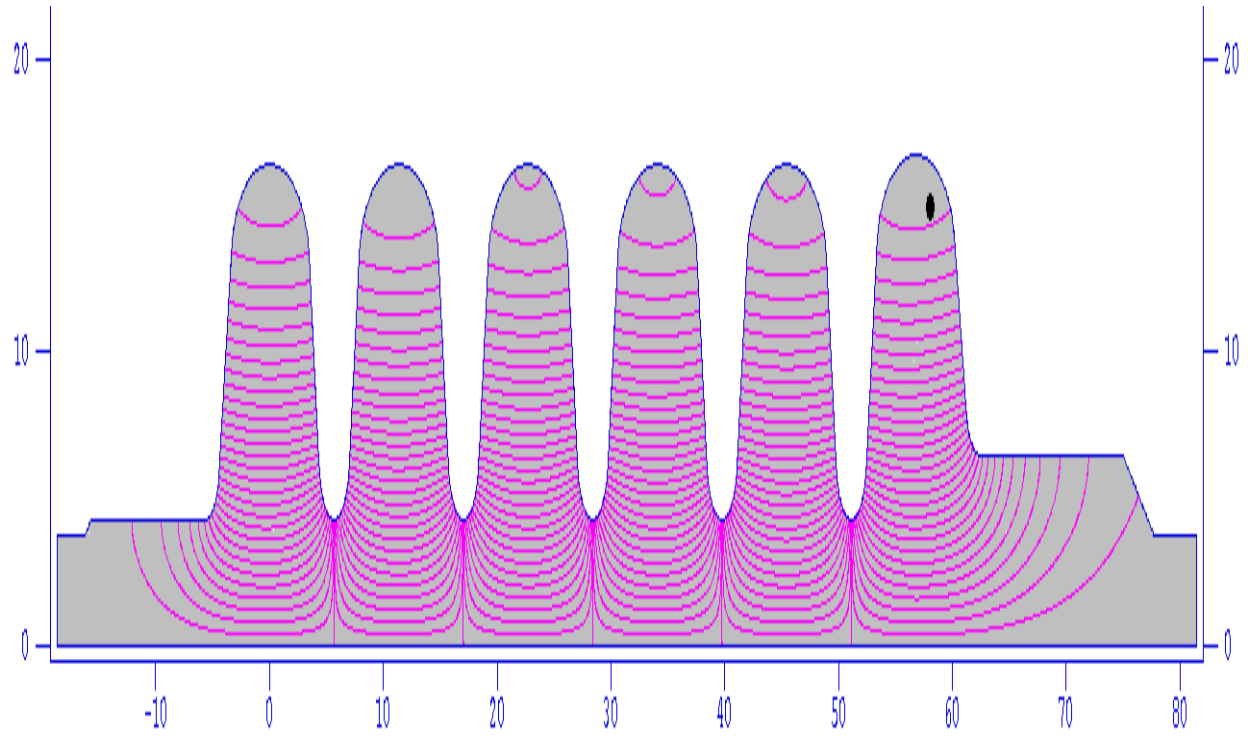

Figure 74: SNS cavity (low beta)

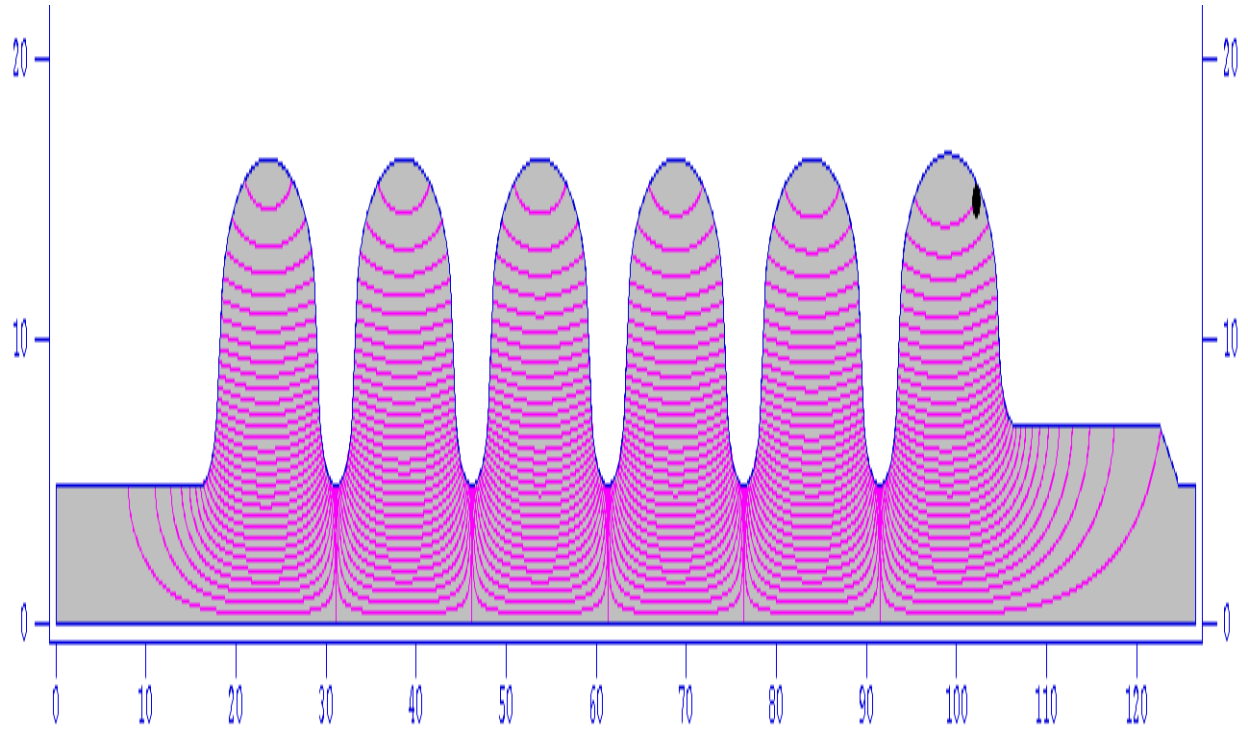

Figure 75: SNS cavity (high beta)

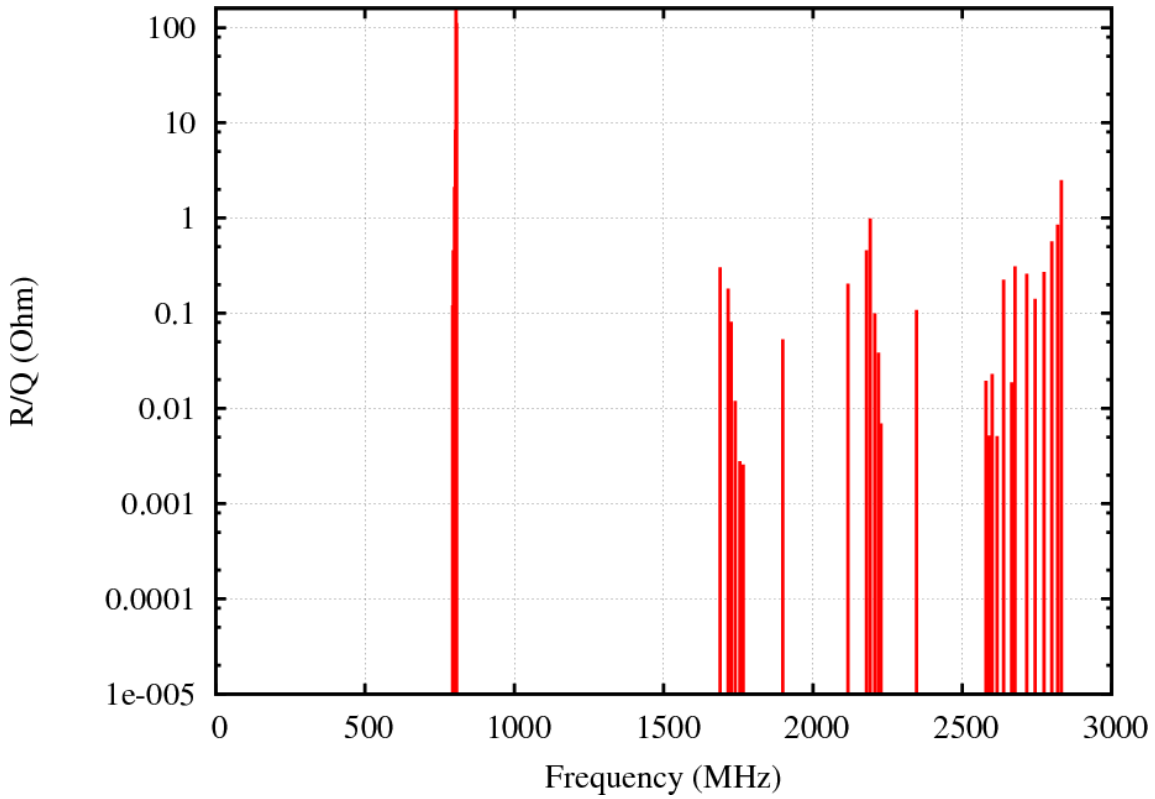

Figure 76: HOM spectrum SNS low beta cavity

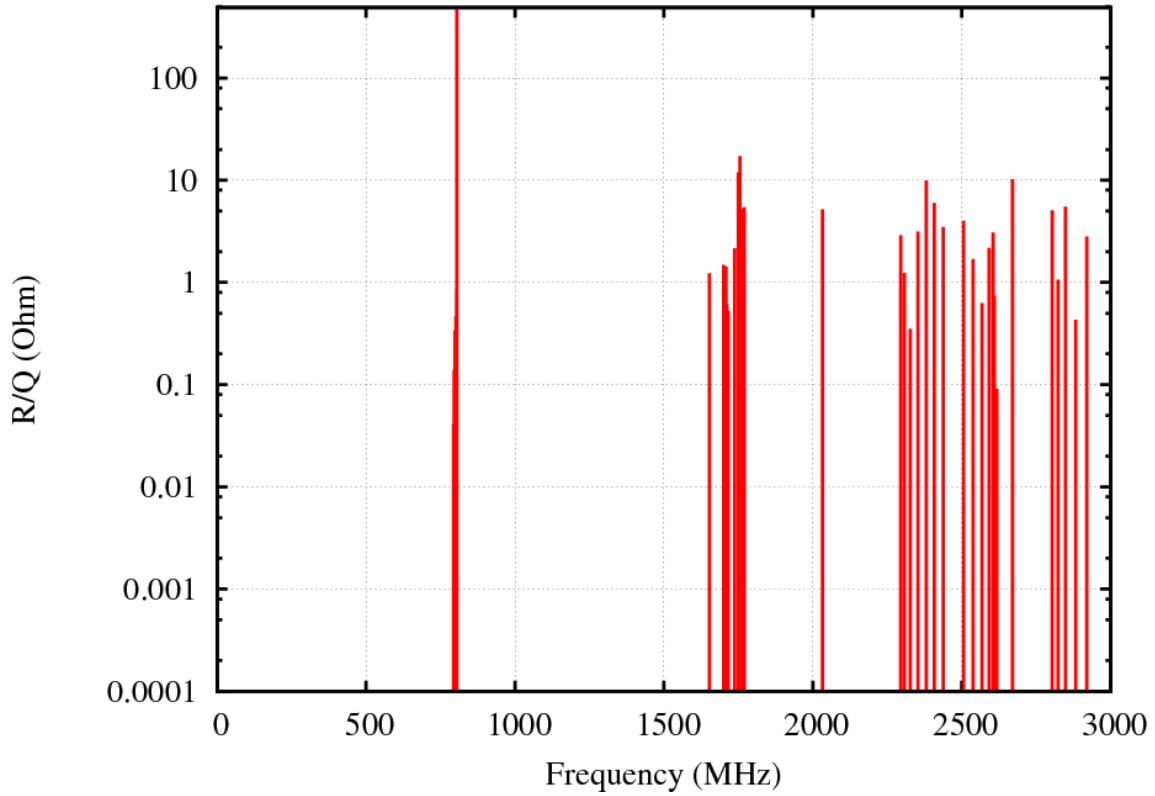

Figure 77: HOM spectrum SNS high beta cavity

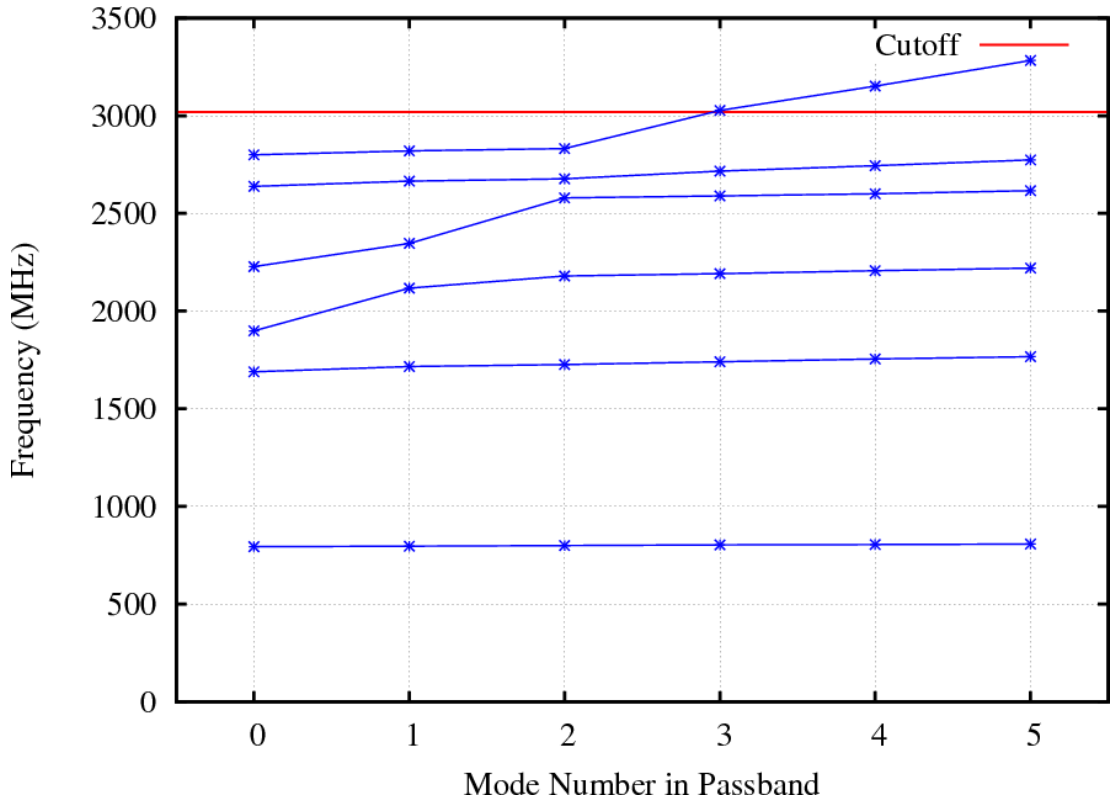

Figure 78: Dispersion curves for SNS low beta cavity

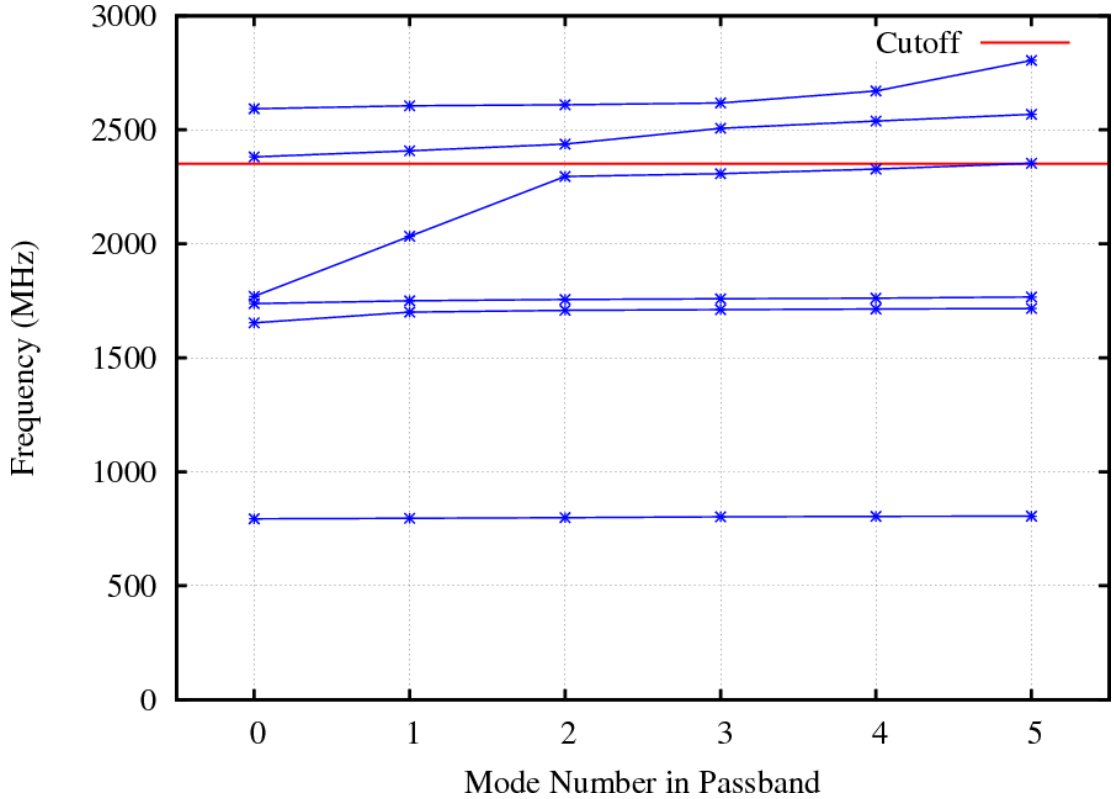

Figure 79: Dispersion curves for SNS high beta cavity

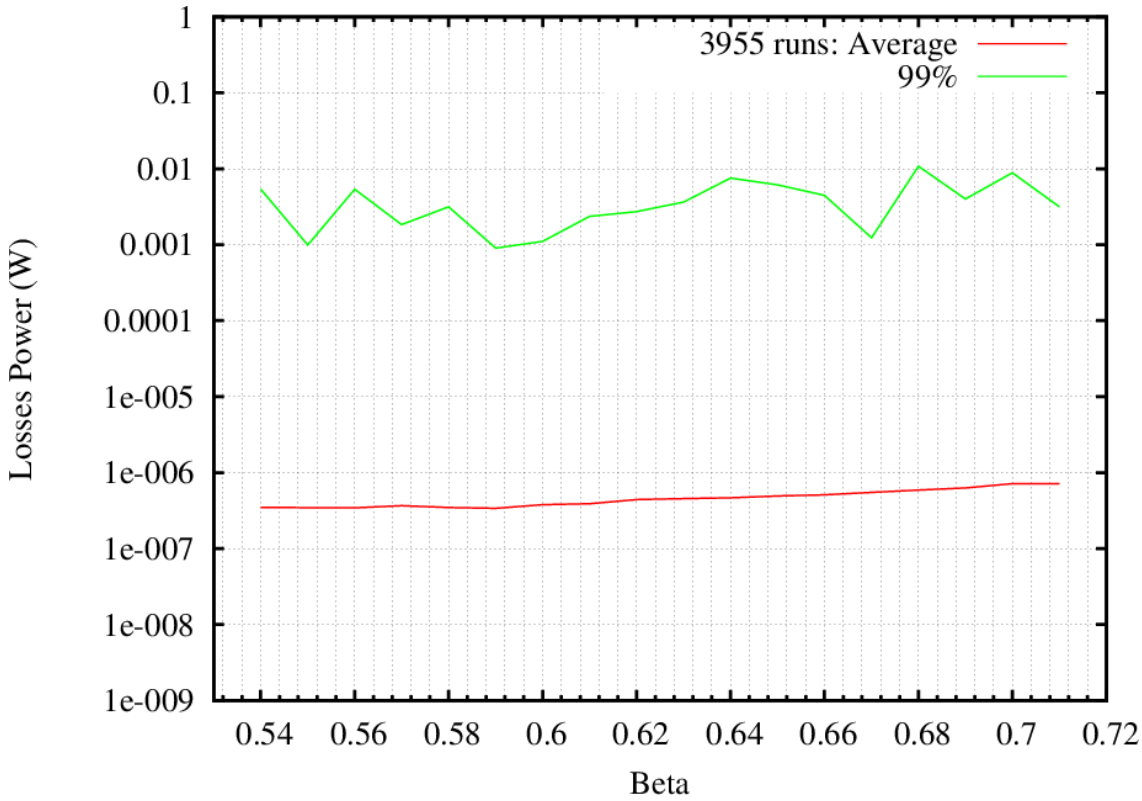

Figure 80: Power of losses vs. beta for SNS low beta cavity, $Q = 10^8$

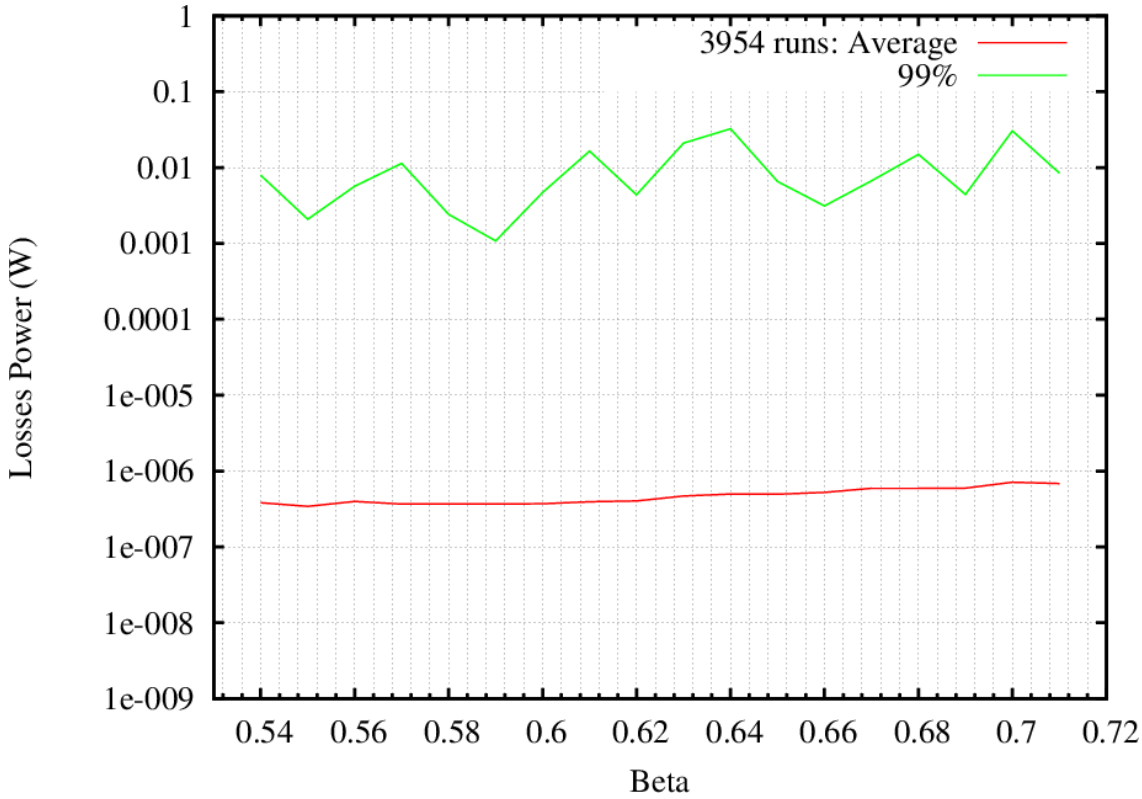

Figure 81: Power of losses vs. beta for SNS low beta cavity, $Q = 10^9$

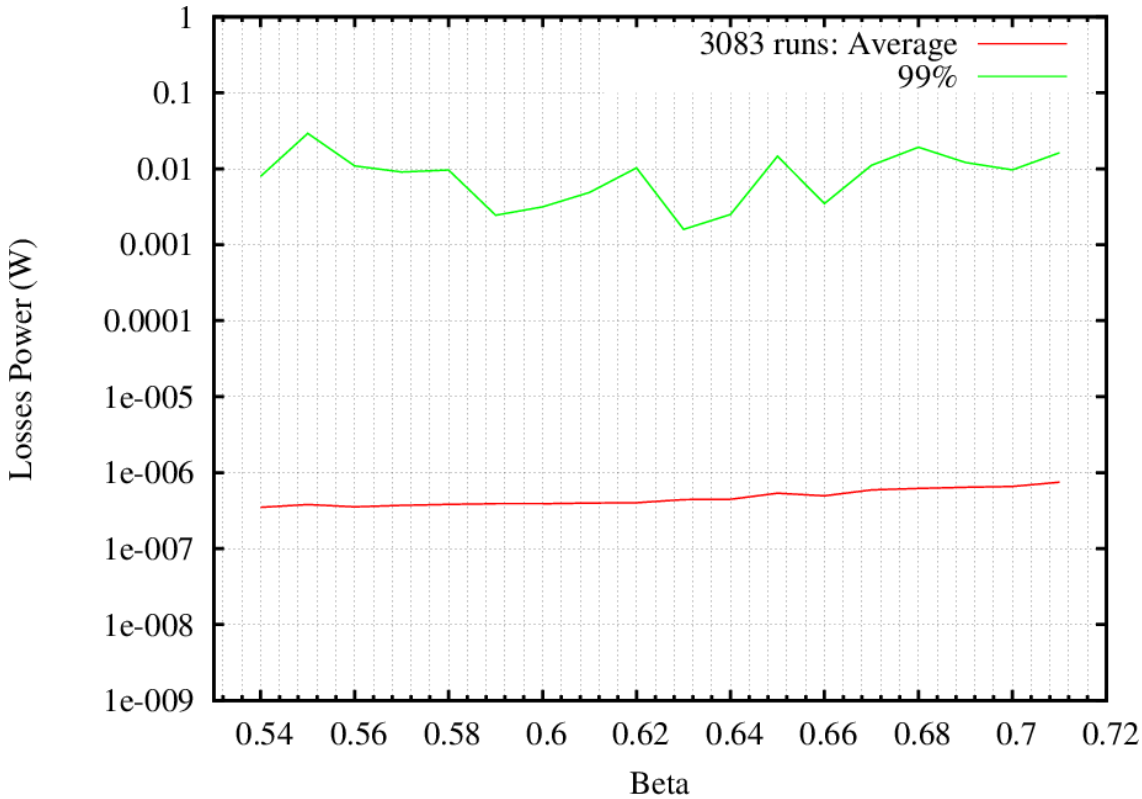

Figure 82: Power of losses vs. beta for SNS low beta cavity, $Q = 10^{10}$

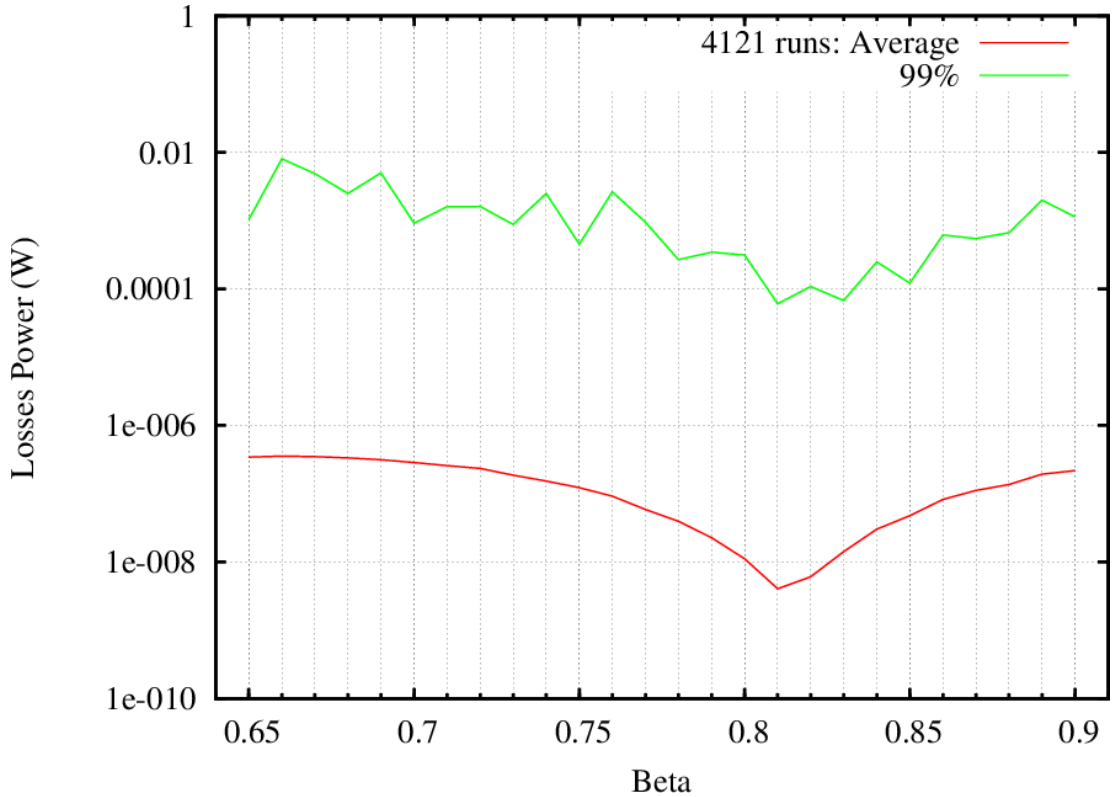

Figure 83: Power of losses vs. beta for SNS high beta cavity, $Q = 10^{8}$

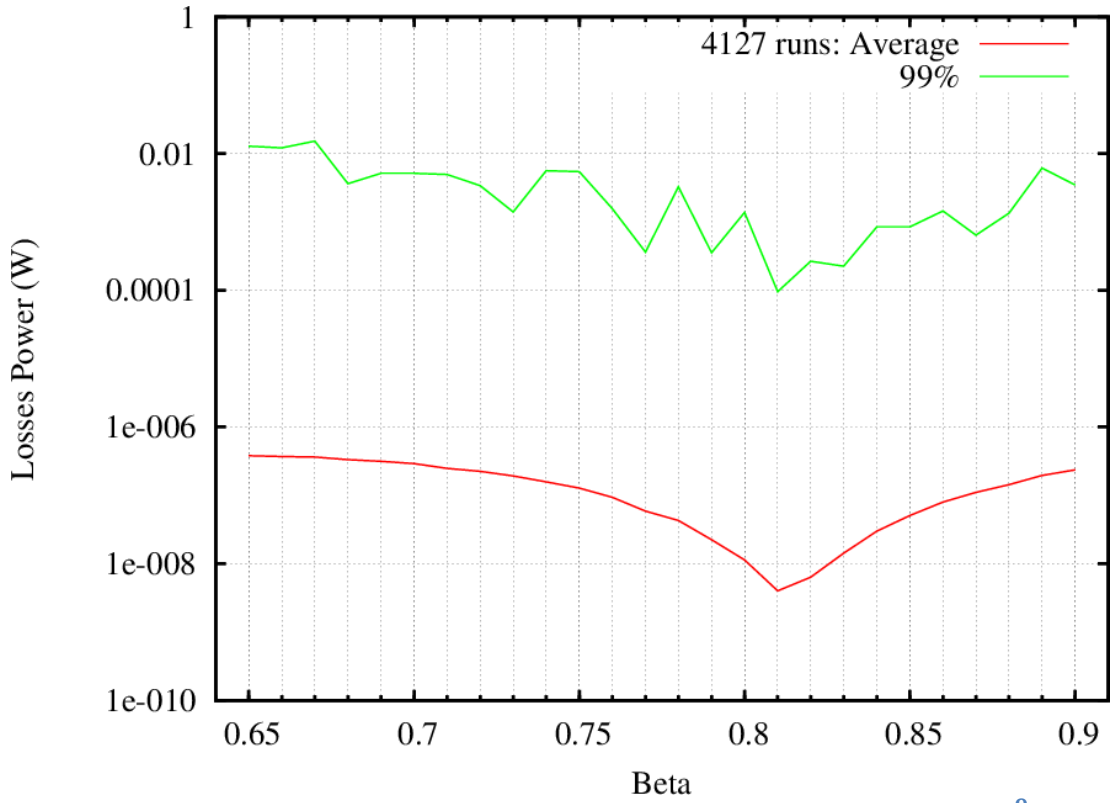

Figure 84: Power of losses vs. beta for SNS high beta cavity, $Q = 10^9$

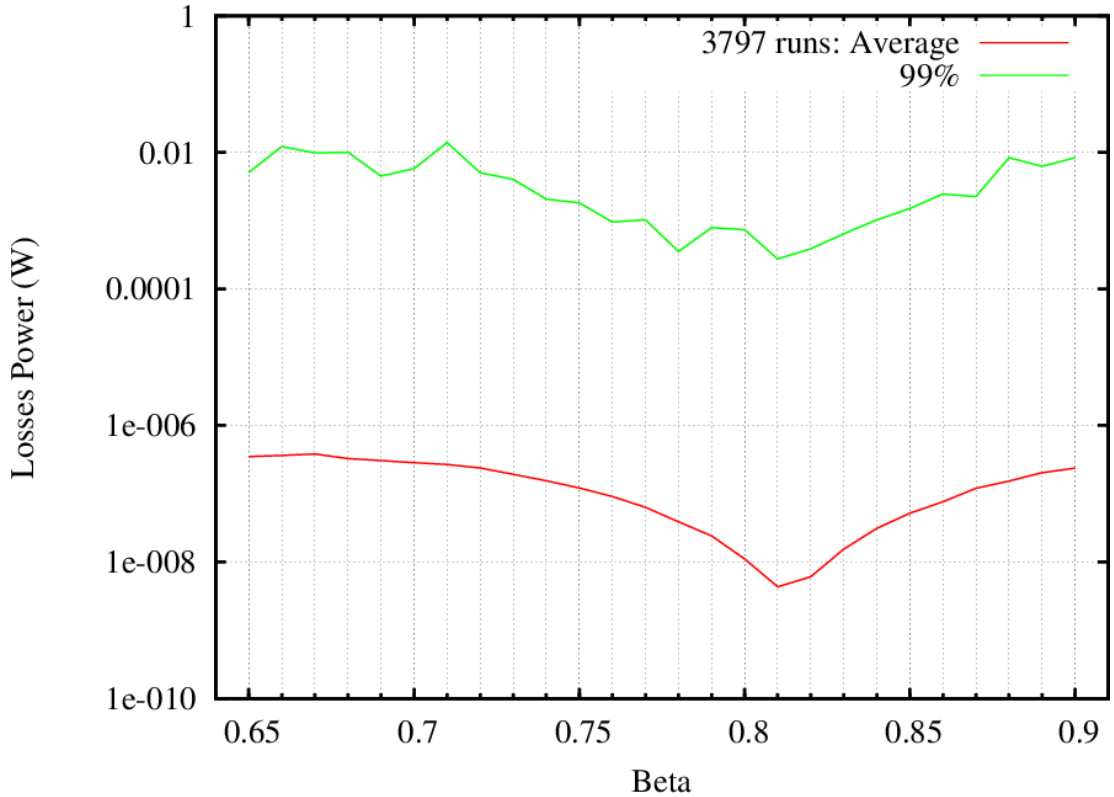

Figure 85: Power of losses vs. beta for SNS high beta cavity, $Q = 10^{10}$

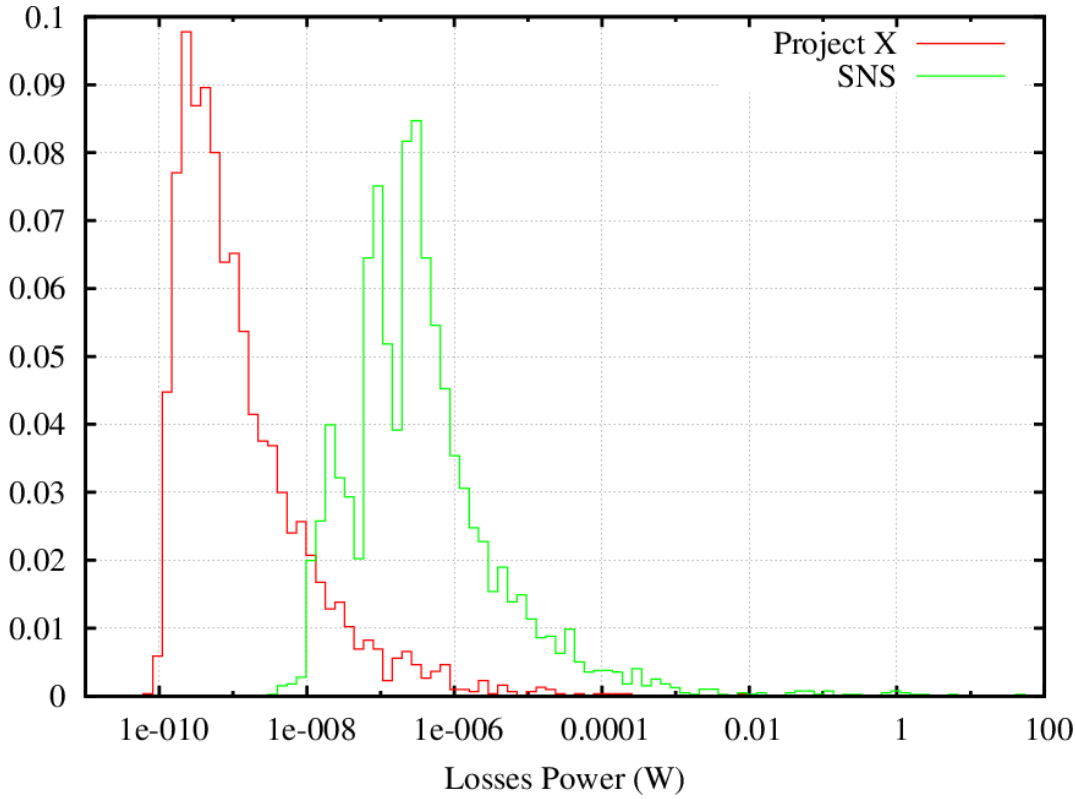

Figure 86: Power of losses distribution for low energy cavity, $Q = 10^8$

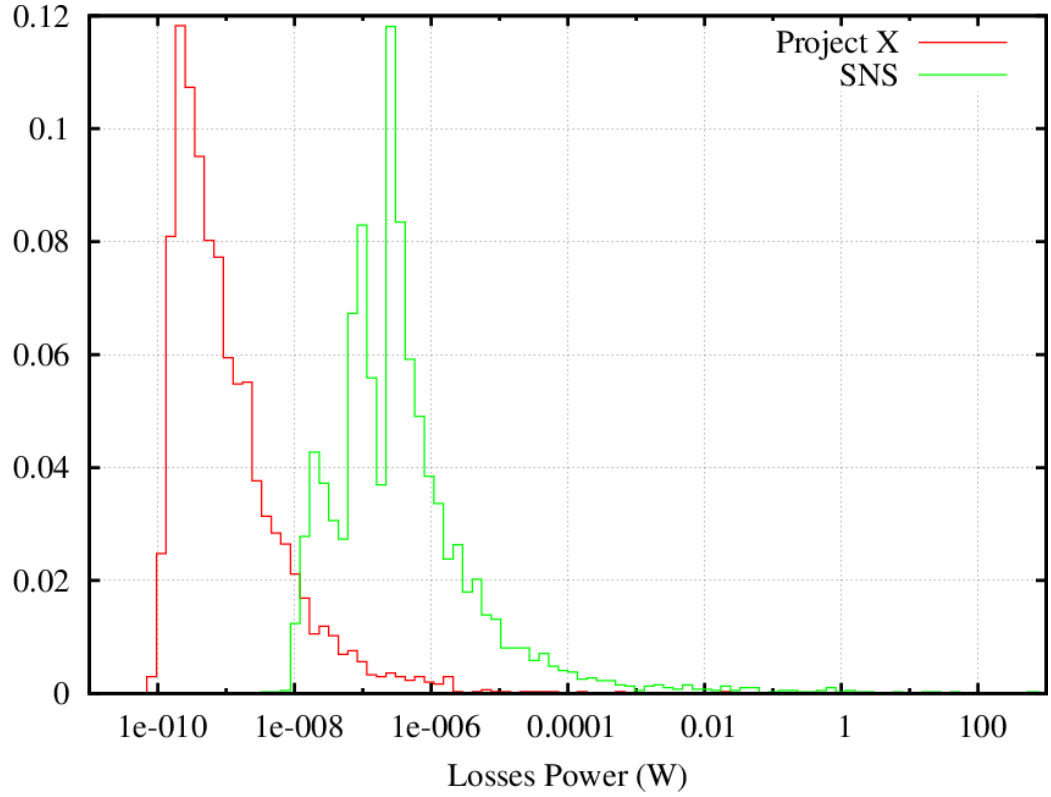

Figure 87: Power of losses distribution for low energy cavity, $Q = 10^9$

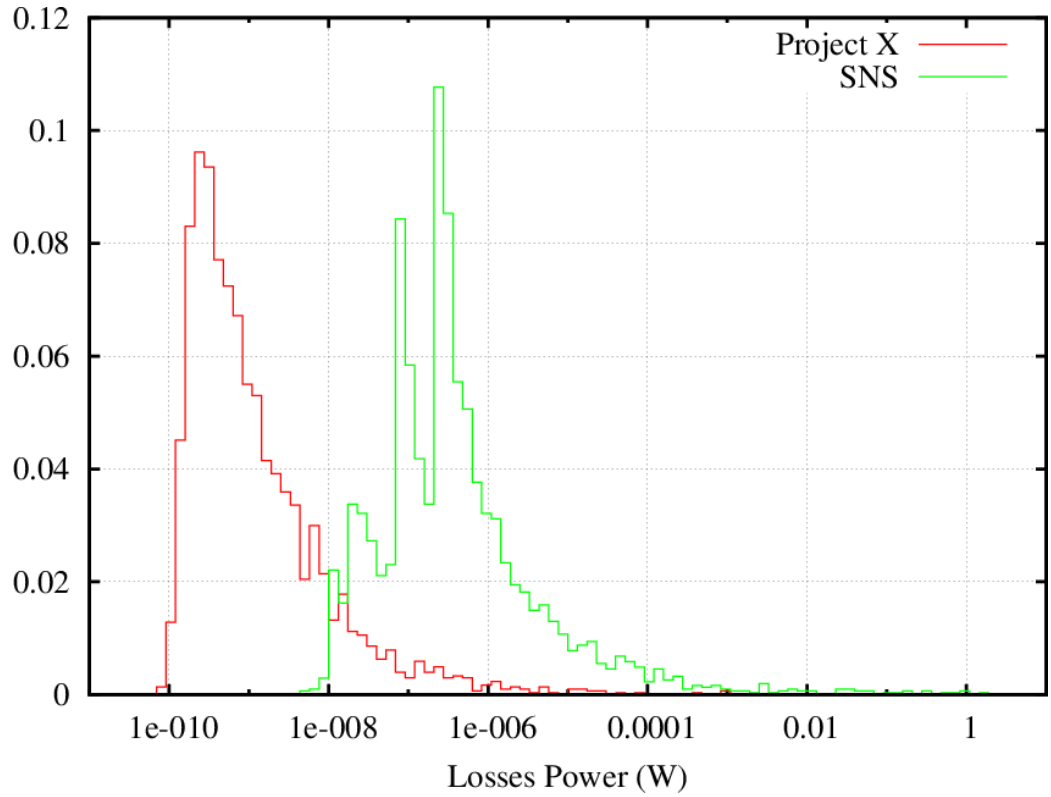

Figure 88: Power of losses distribution for low energy cavity, $Q = 10^{10}$

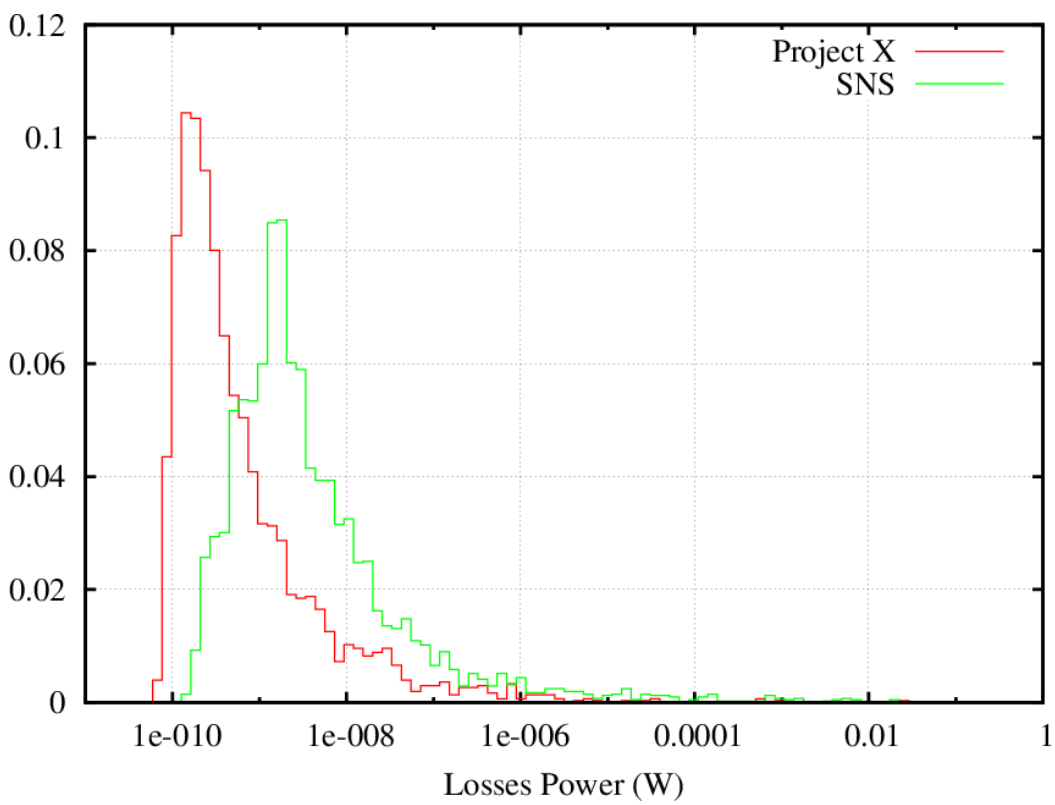

Figure 89: Power of losses distribution for high energy cavity, $Q = 10^{8}$

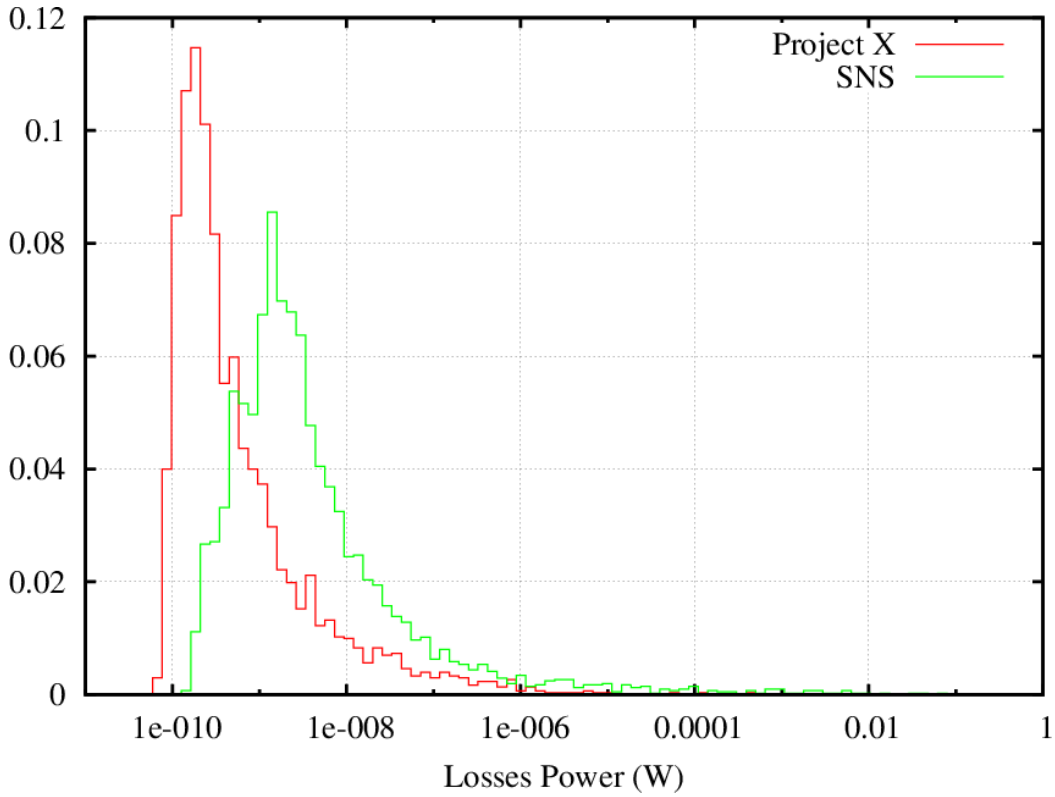

Figure 90: Power of losses distribution for high energy cavity, $Q = 10^9$

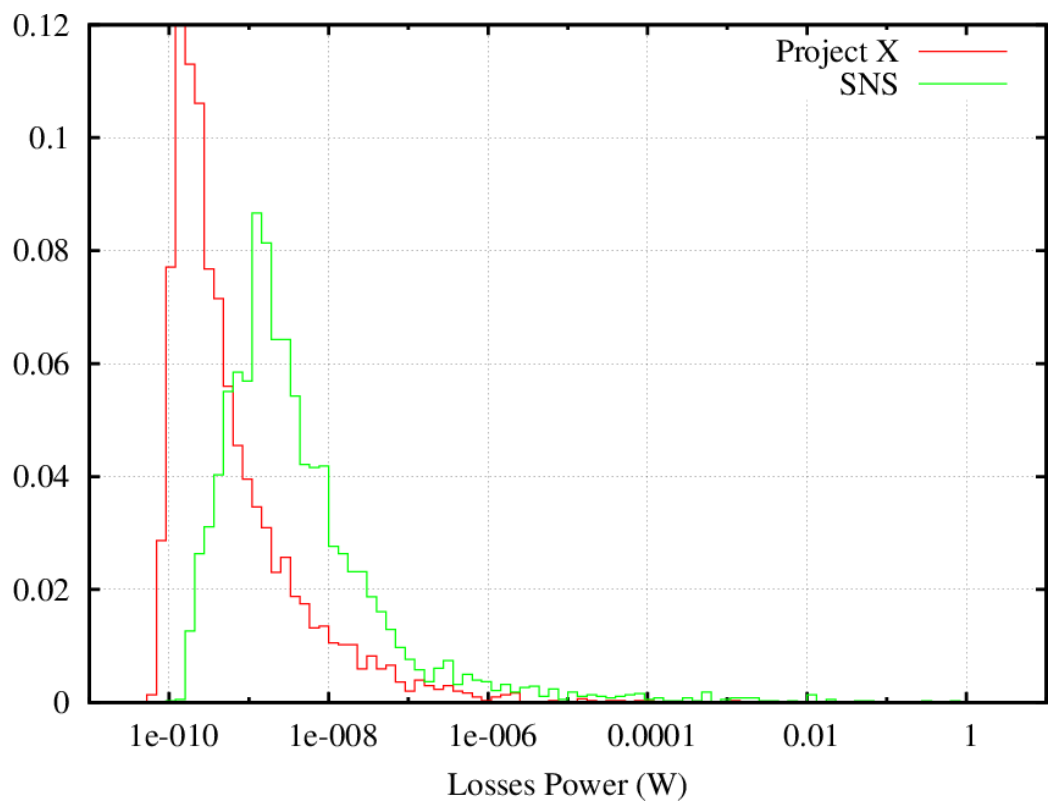

Figure 91: Power of losses distribution for high energy cavity, $Q = 10^{10}$

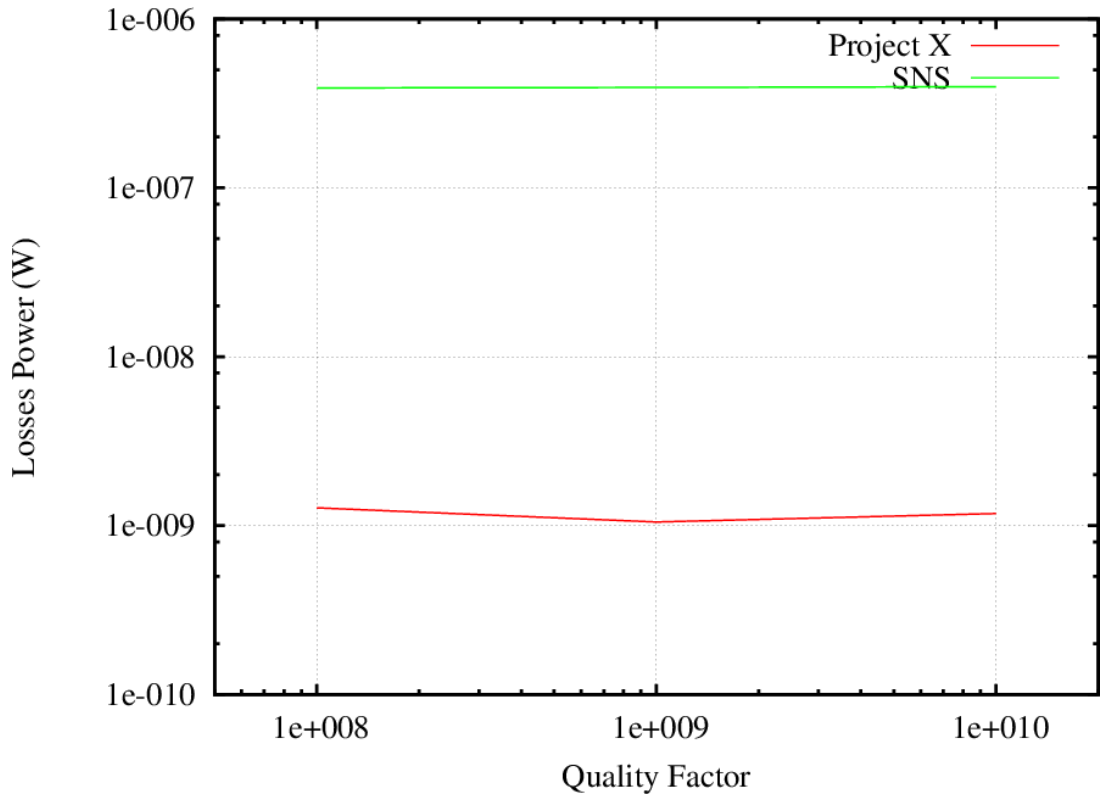

Figure 92: Power of losses vs. quality factor for low energy cavity

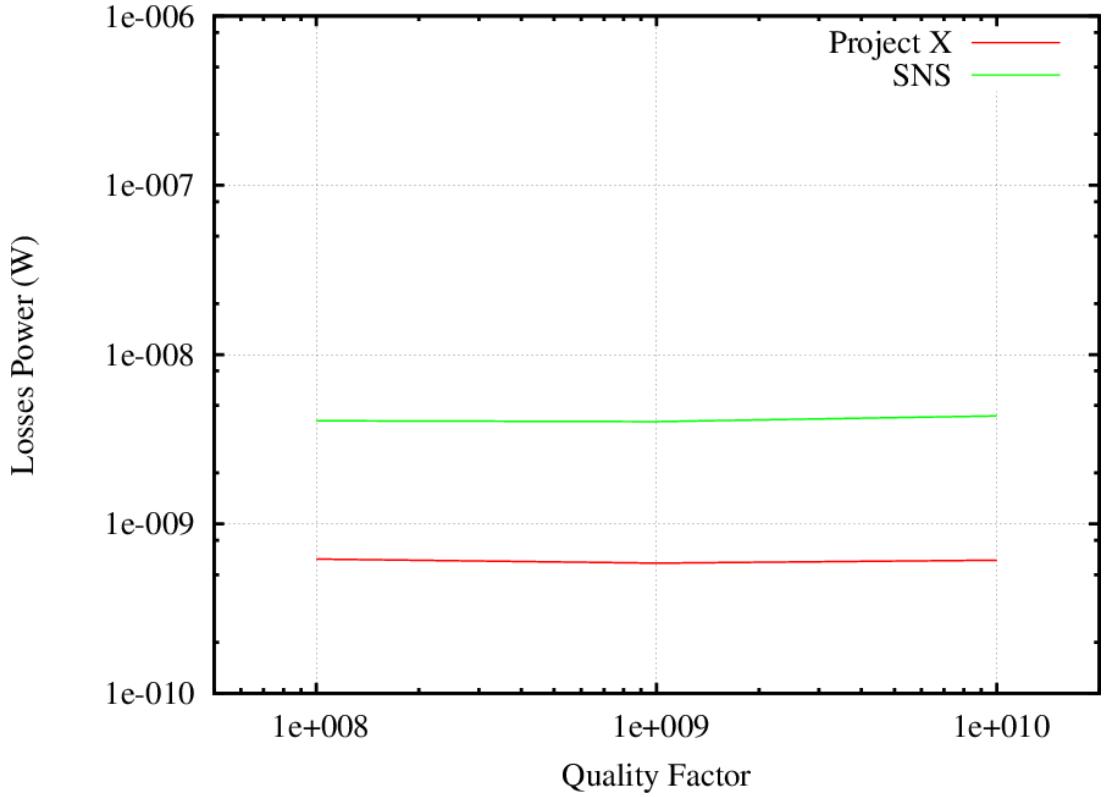

Figure 93: Power of losses vs. quality factor for high energy cavity

Cumulative Effects

Another possible problem caused by HOMs is cumulative beam break-up (BBU). The beam going through the cavity excites both longitudinal and transversal HOMs. That is why both monopole and dipole modes are important for this effect.

To excite a transversal HOM a bunch has to have a displacement relative to the axis of a cavity. In this case the bunch interacts with electric field of the cavity and induces kick voltage. If q is the charge of the bunch, Δx is its displacement relative to the axis, $(r_{\parallel}/Q)_1$ is transverse impedance of HOM (accelerator definition), induced kick voltage can be defined by the formula

$$\Delta V_{kick} = \frac{i}{2} cq \left(\frac{r_{\parallel}}{Q}\right)_1 \Delta x,$$

where c is speed of light, and i is imaginary unit. Error in the cavities axis positions is considered equals $0.5\ mm$.

If a bunch passes a cavity with kick voltage on it, it has transverse kick by magnetic field of the cavity. If x' is the ratio between x and z components of the bunch momentum, p is the momentum of the bunch, transverse kick can be expressed as

$$\Delta x' = \frac{eRe(V_{kick})}{pc},$$

where e is the charge of a particle in the bunch.

Excitation of a longitudinal HOM can be described as follow. When a bunch of charge q passes a cavity with a HOM of angular frequency ω_H and longitudinal impedance (R/Q) (accelerating definition) it induces the decelerating voltage [8]

$$\Delta V_{ind} = -\frac{q}{2}\omega_H \left(\frac{R}{Q}\right).$$

If the bunch has time lag dt, then it increases HOM voltage according to the formula

$$\Delta V_H = \Delta V_{ind} e^{-i\omega_H dt}.$$

When a bunch passes through a cavity with HOM voltage on it, it has additional energy gain

$$dU_H = e\left(\mathrm{Re}V_H \cos\omega_H dt - \mathrm{Im}V_H \sin\omega_H dt - \frac{\Delta V_{ind}}{2}\right).$$

Both kick and HOM voltage are changing in time:

$$V(t) = V(0)e^{i\omega_H t - \frac{t}{\tau}}, \qquad \text{where } \tau = \frac{2Q}{\omega_H},$$

where Q is quality factor of HOM.

The spectrum of longitudinal HOMs described above (see Figures 4 – 7) is used. The spectrum of transversal HOMs is calculated by CLANS code [5] for all range of beta and it is shown on the Figures 54 and 56 for geometrical values of beta. Real lattice of the Project X linac is simulated and the beam emittance dilution is studied. Different HOM frequencies spreads are considered.

Simulation

The case of the value of quality factor of HOMs $Q = 10^7$ was studied more detailed. Different cases which were simulated are described in the Table 5. Results of the simulation are shown on the Figures 94 – 111. The value shown on the figures is the ratio of emittance dilution caused by BBU effect or klystron type instability and initial emittance at the beginning of SSR0 section of the Project X linac. The values of normalized initial emittances are $\varepsilon_x = 0.25\, mm \cdot mrad$ and $\varepsilon_z = 180\, deg \cdot keV$. One hundred different accelerators were simulated for each case. The average, maximum and minimum values are shown on the figures.

Table 5: Cases simulated for HOM quality factor value $Q = 10^7$

#	Number of HOMs	HOM frequency value	Impedances dependence on beta	Sections
1	1	resonance	OFF	LE650
2	1	resonance	OFF	HE650
3	1	resonance	ON	LE650
4	1	resonance	ON	HE650
5	1	real	OFF	LE650
6	1	real	ON	LE650
7	1	real	OFF	LE650 and HE650
8	All	real	OFF	LE650
9	All	real	ON	LE650 and HE650

One can see that emittance dilution in the resonant case can be considerably large at some values of HOM frequency spread, but when impedances dependence on beta, real values of HOM frequencies and different sections are taken into account emittance dilution becomes significantly smaller. Monopole HOM voltage distribution for the real case is shown on the Figure 112 for different values of HOM frequency spread. One can see that even maximum values of voltage are small.

HOM quality factor values 10^8 and 10^9 were also considered. Comparison of different values of quality factor for resonant and real cases is shown on the Figures 113 – 116. It is shown that there is no emittance dilution dependence on quality factor. For all cases emittance dilution is about 10^8 times smaller than emittance at the beginning of SSR0 section. It can tell us that BBU effect and klystron instabilities do not look like an issue for the Project X linac.

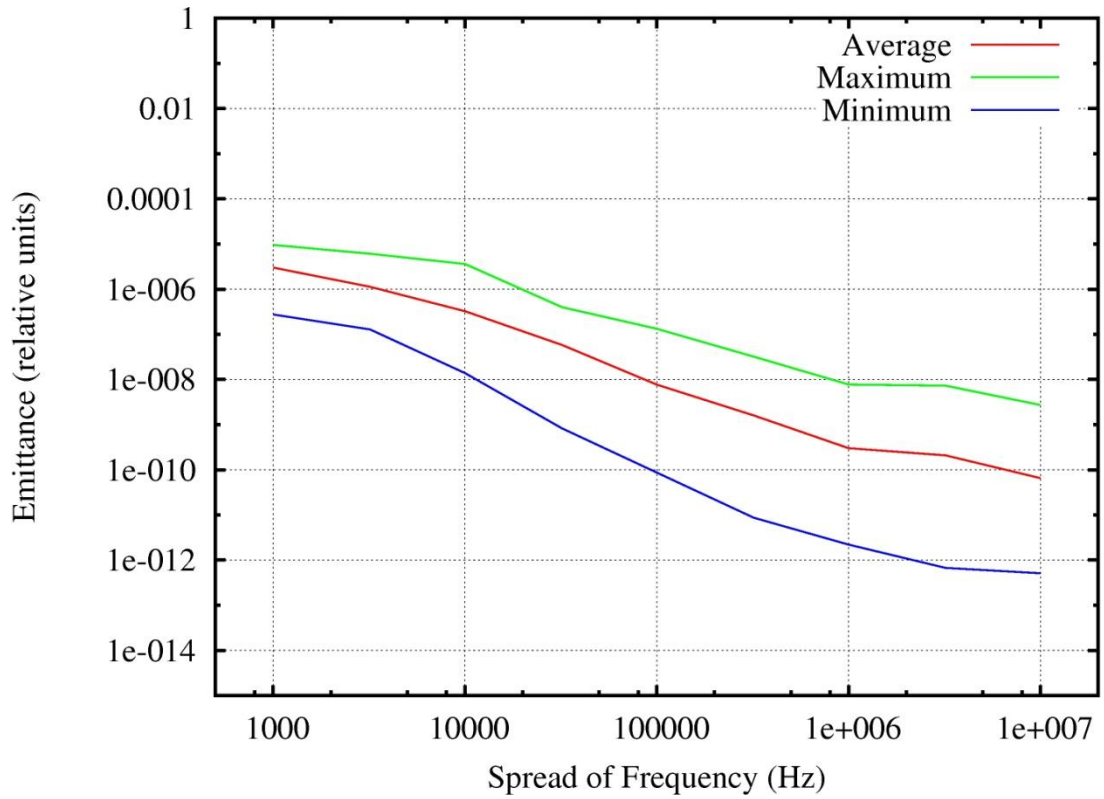

Figure 94: Transverse emittance dilution for $Q = 10^7$: case #1 (see Table 3)

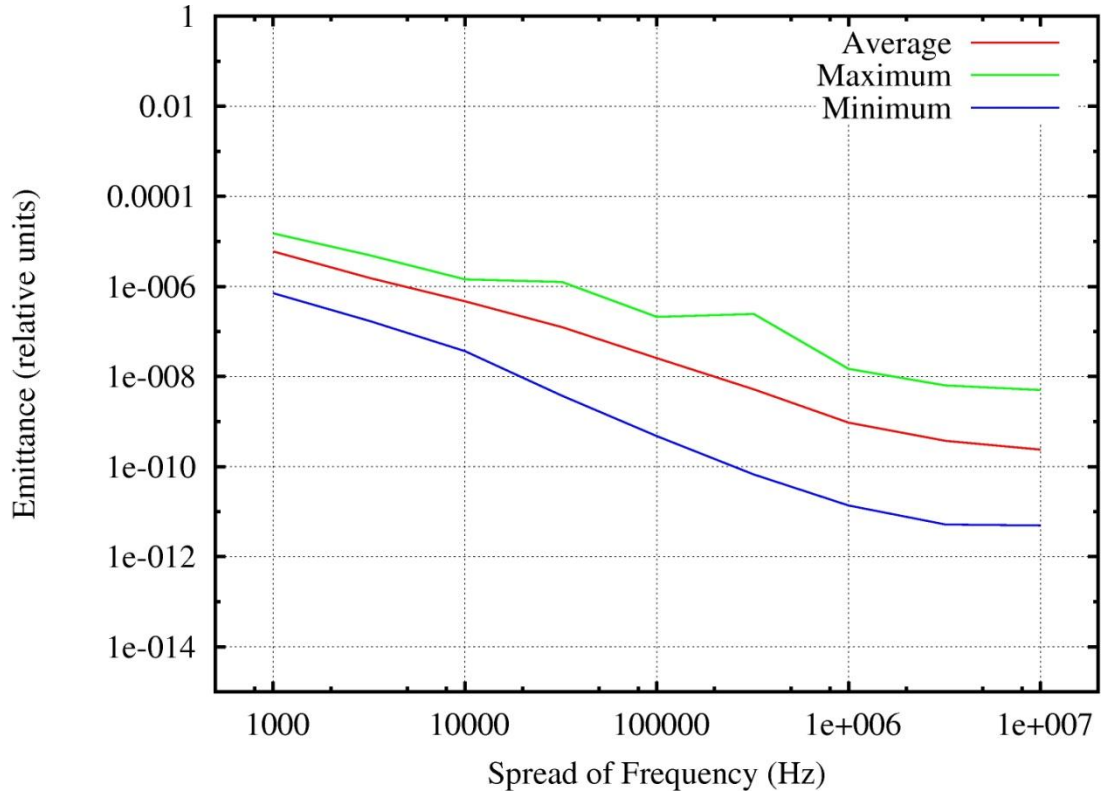

Figure 95: Transverse emittance dilution for $Q = 10^7$: case #2 (see Table 3)

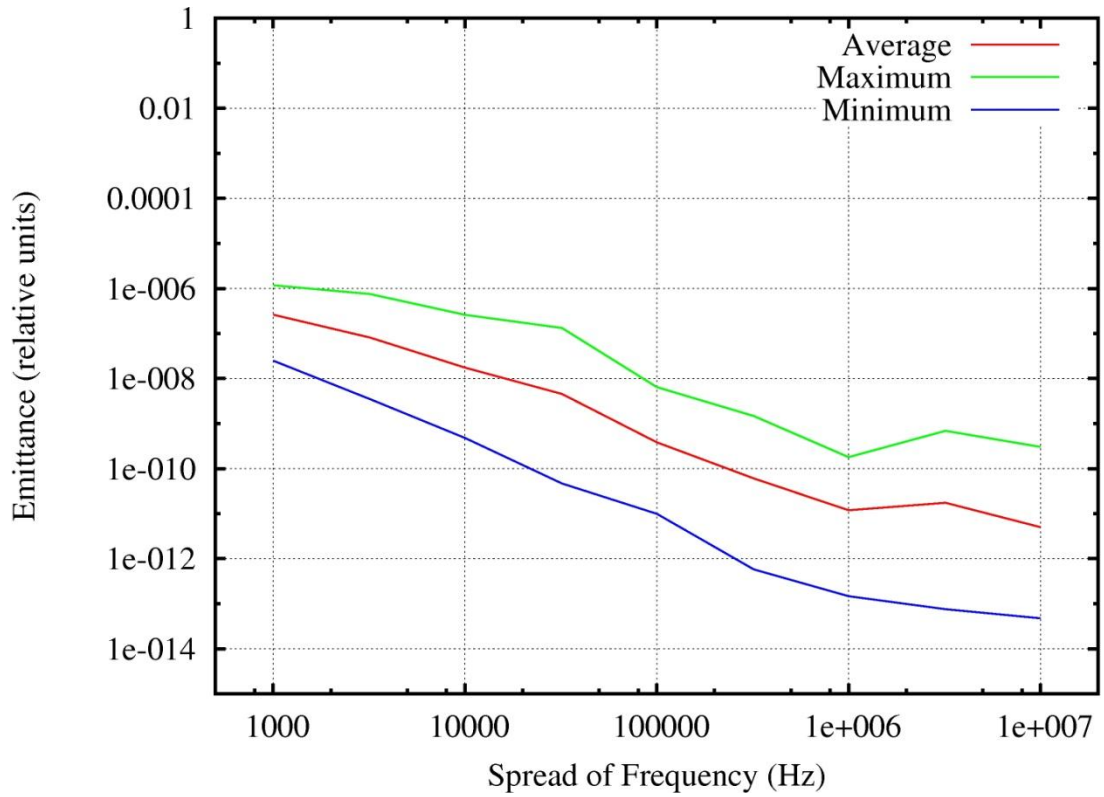

Figure 96: Transverse emittance dilution for $Q = 10^7$: case #3 (see Table 3)

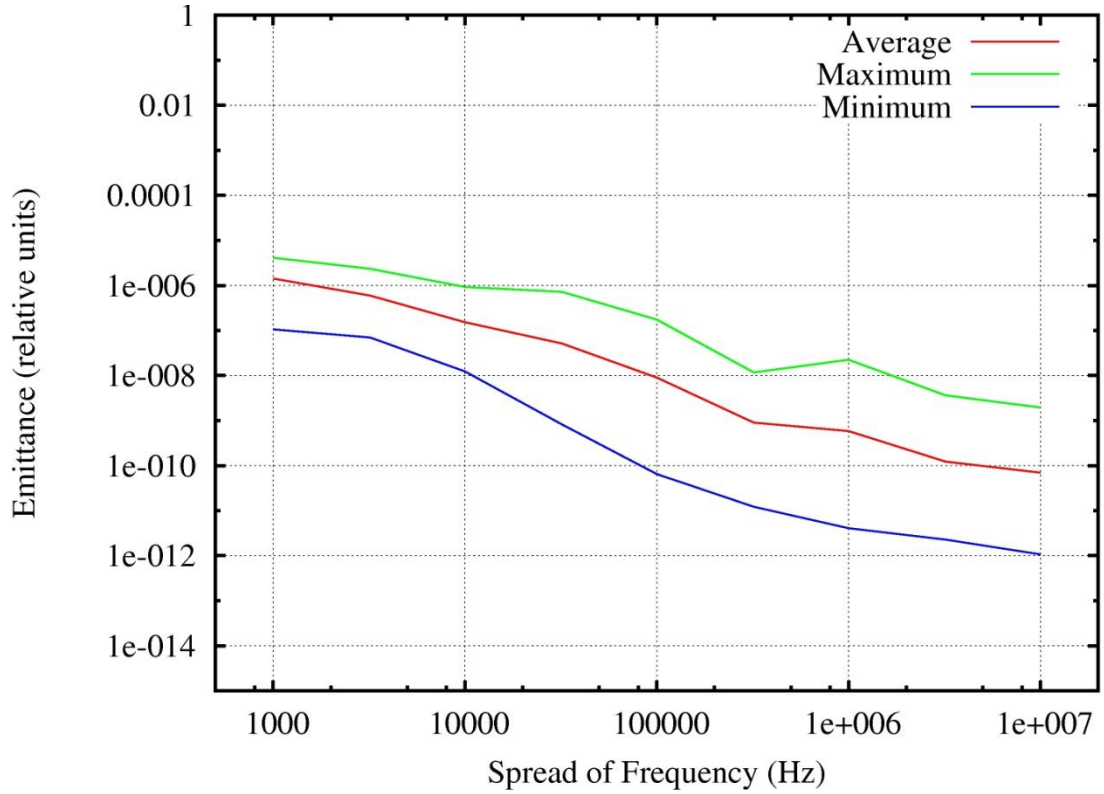

Figure 97: Transverse emittance dilution for $Q = 10^7$: case #4 (see Table 3)

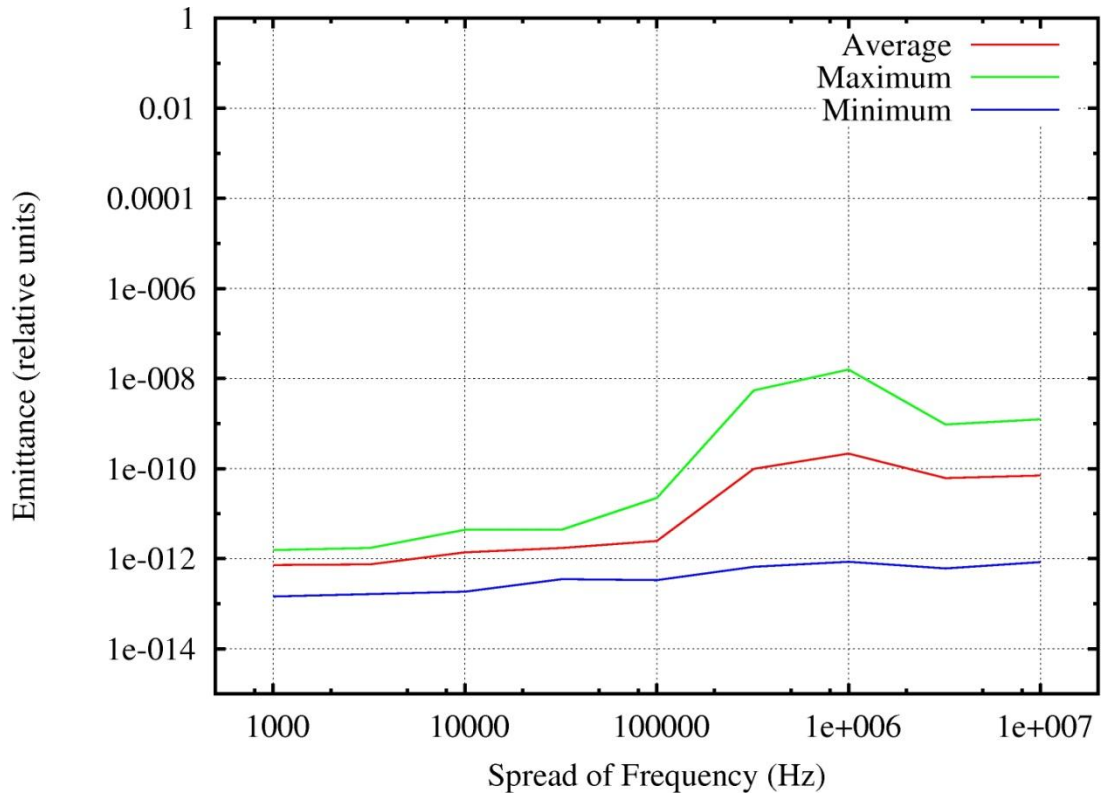

Figure 98: Transverse emittance dilution for $Q = 10^7$: case #5 (see Table 3)

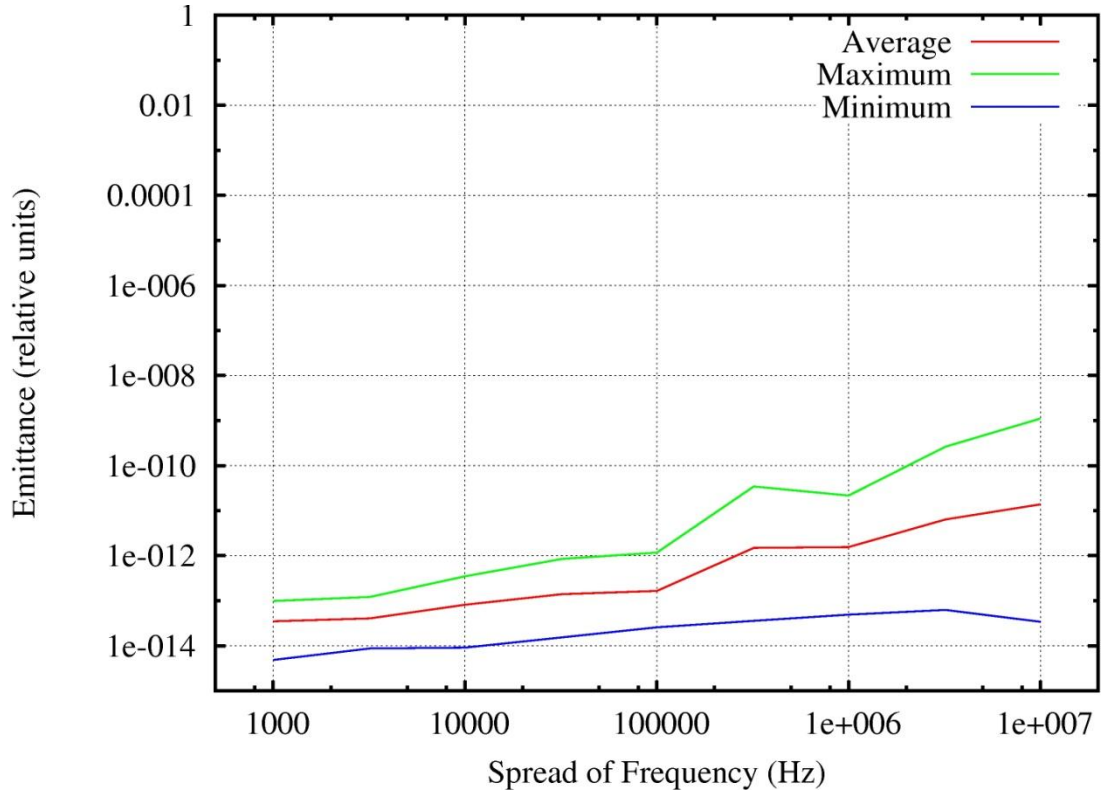

Figure 99: Transverse emittance dilution for $Q = 10^7$: case #6 (see Table 3)

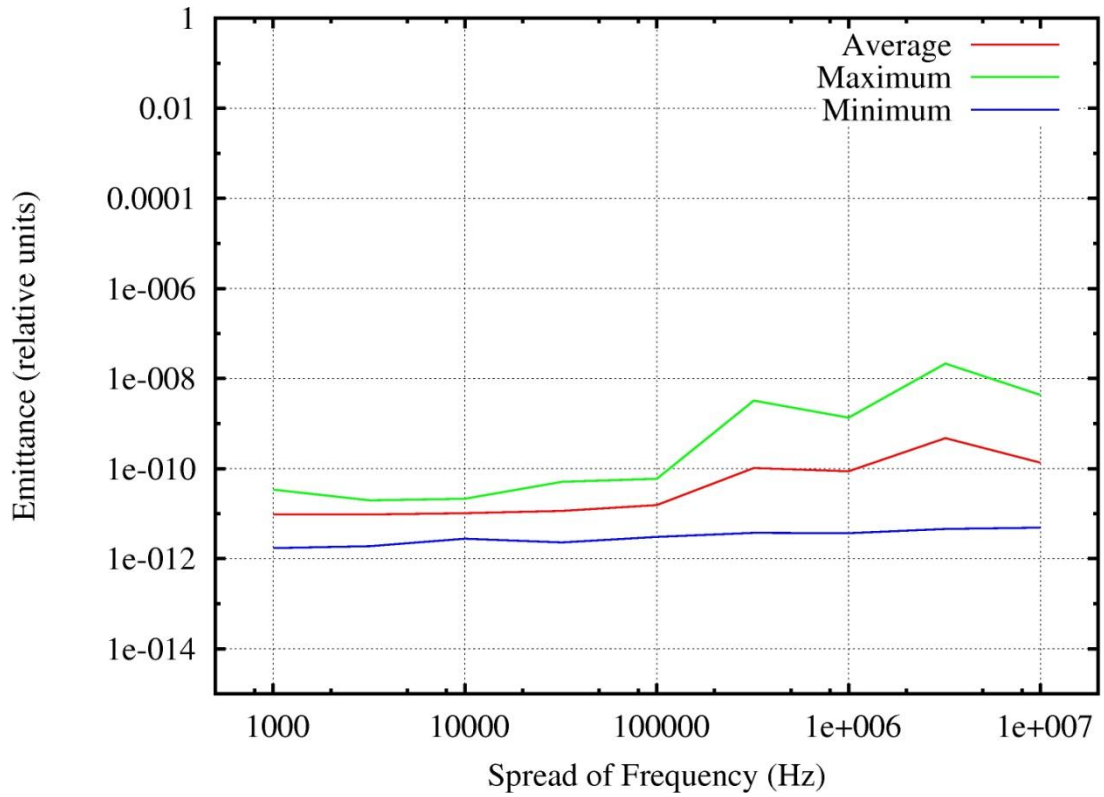

Figure 100: Transverse emittance dilution for $Q = 10^7$: case #7 (see Table 3)

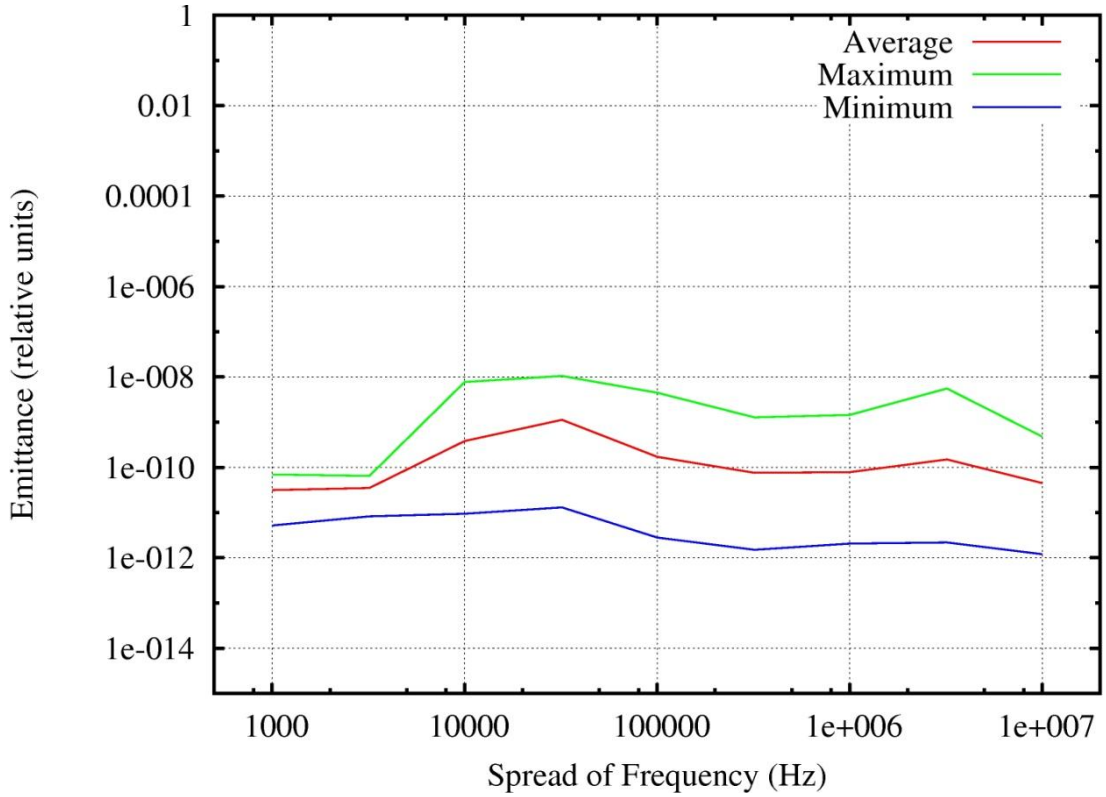

Figure 101: Transverse emittance dilution for $Q = 10^7$: case #8 (see Table 3)

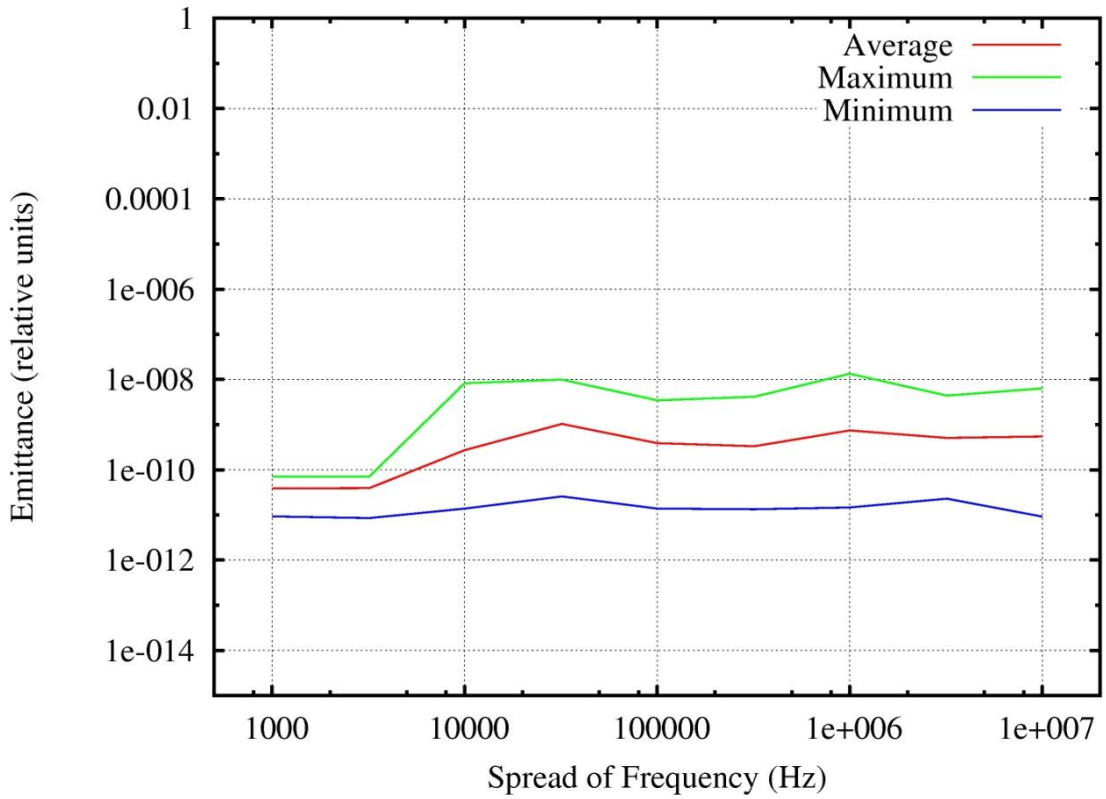

Figure 102: Transverse emittance dilution for $Q = 10^7$: real case

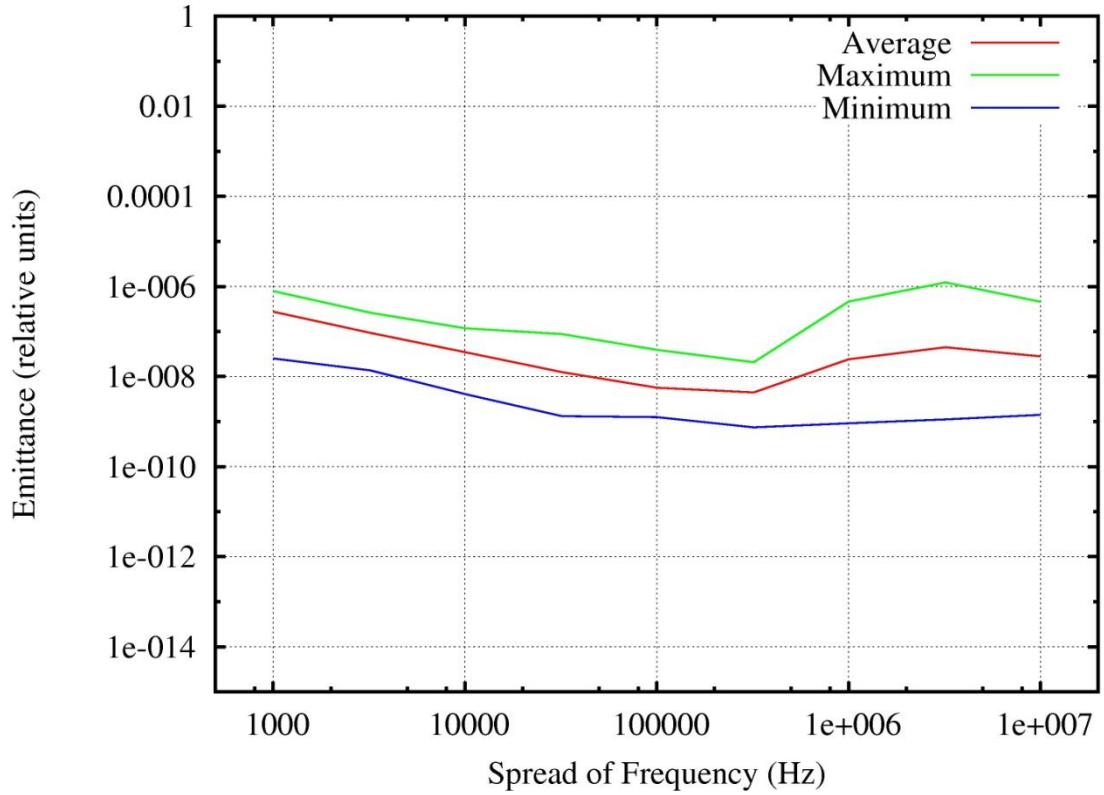

Figure 103: Longitudinal emittance dilution for $Q = 10^7$: case #1 (see Table 3)

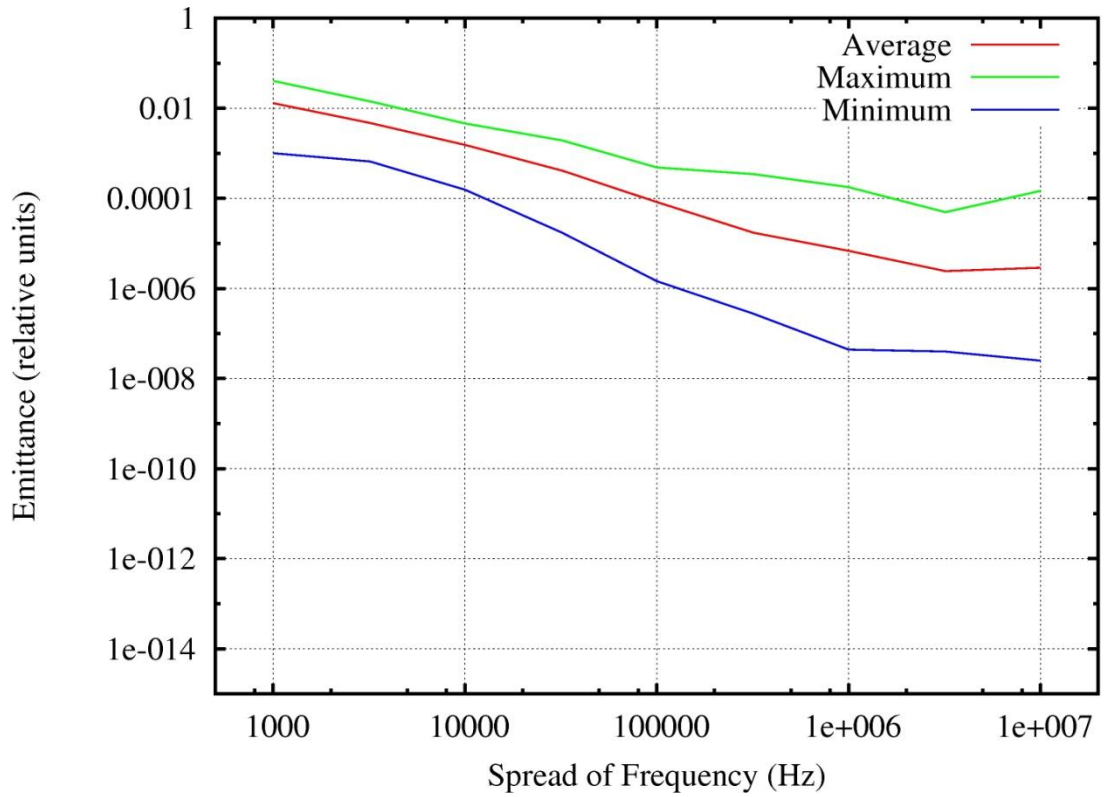

Figure 104: Longitudinal emittance dilution for $Q = 10^7$: case #2 (see Table 3)

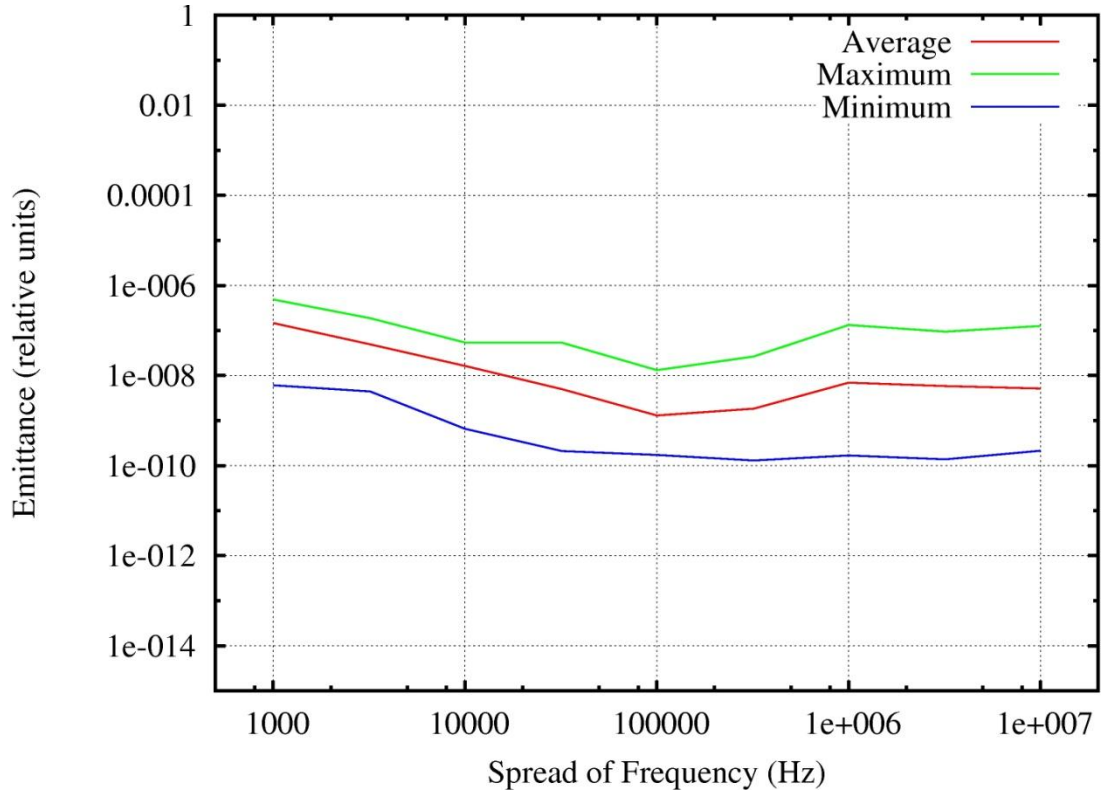

Figure 105: Longitudinal emittance dilution for $Q = 10^7$: case #3 (see Table 3)

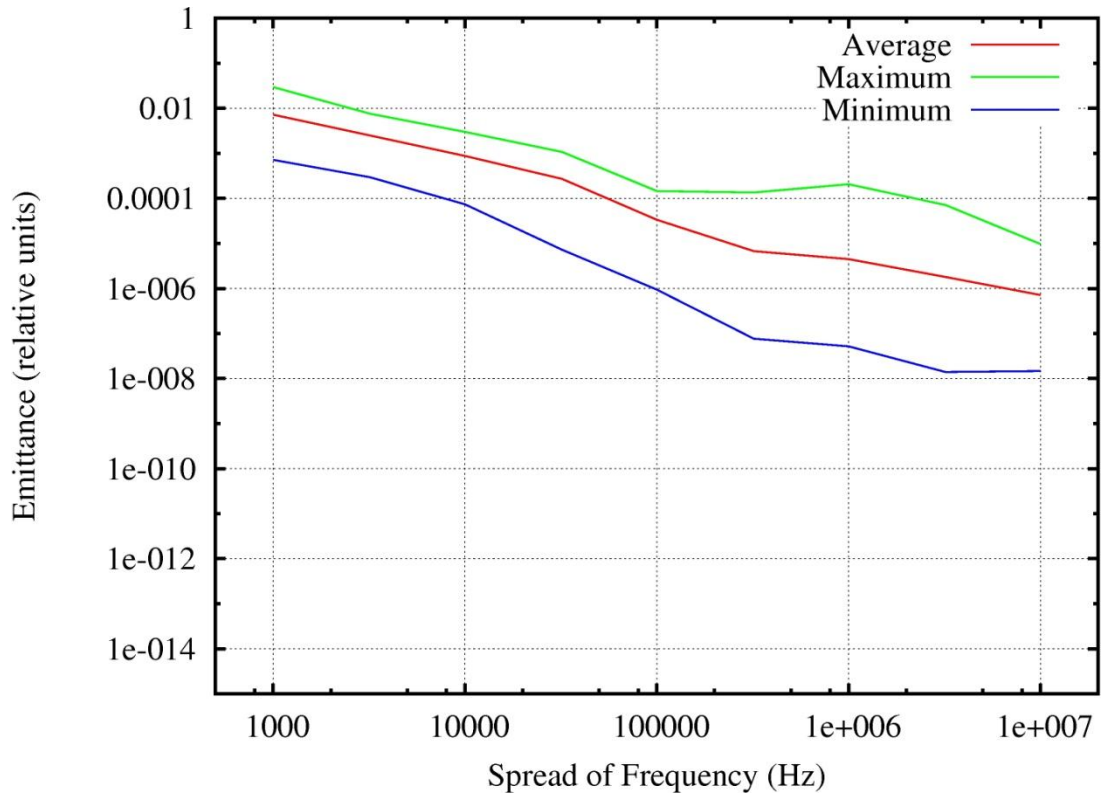

Figure 106: Longitudinal emittance dilution for $Q = 10^7$: case #4 (see Table 3)

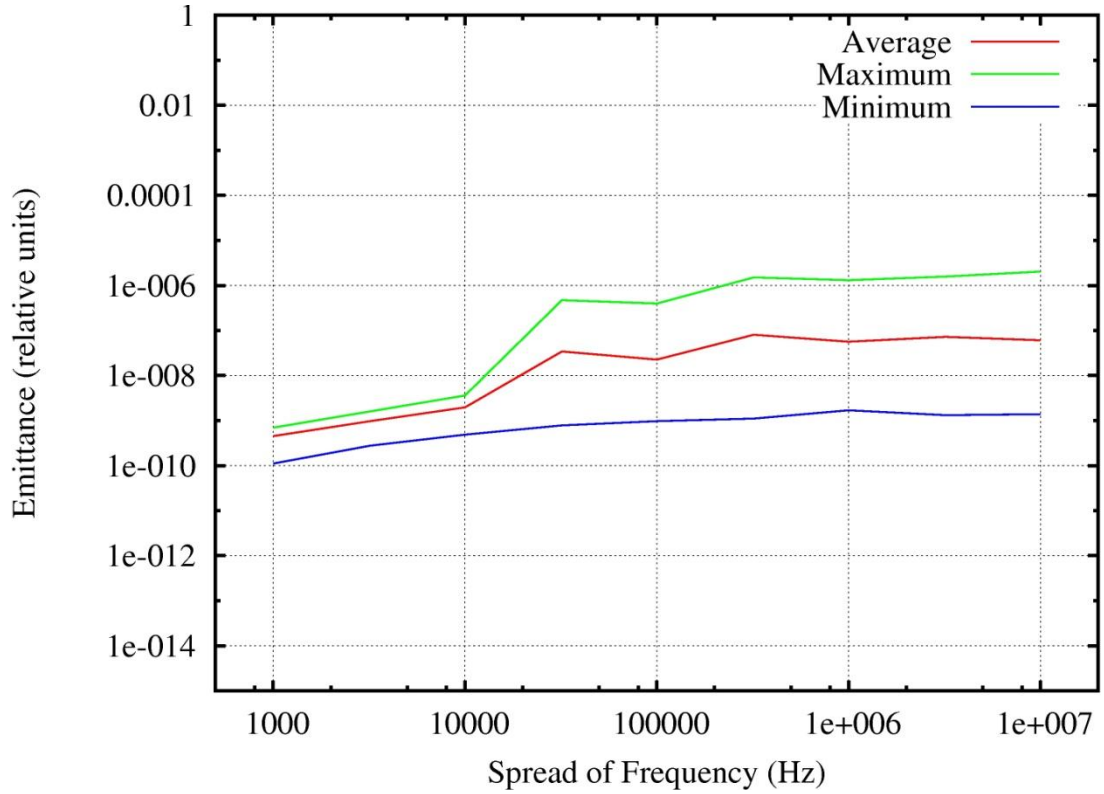

Figure 107: Longitudinal emittance dilution for $Q = 10^7$: case #5 (see Table 3)

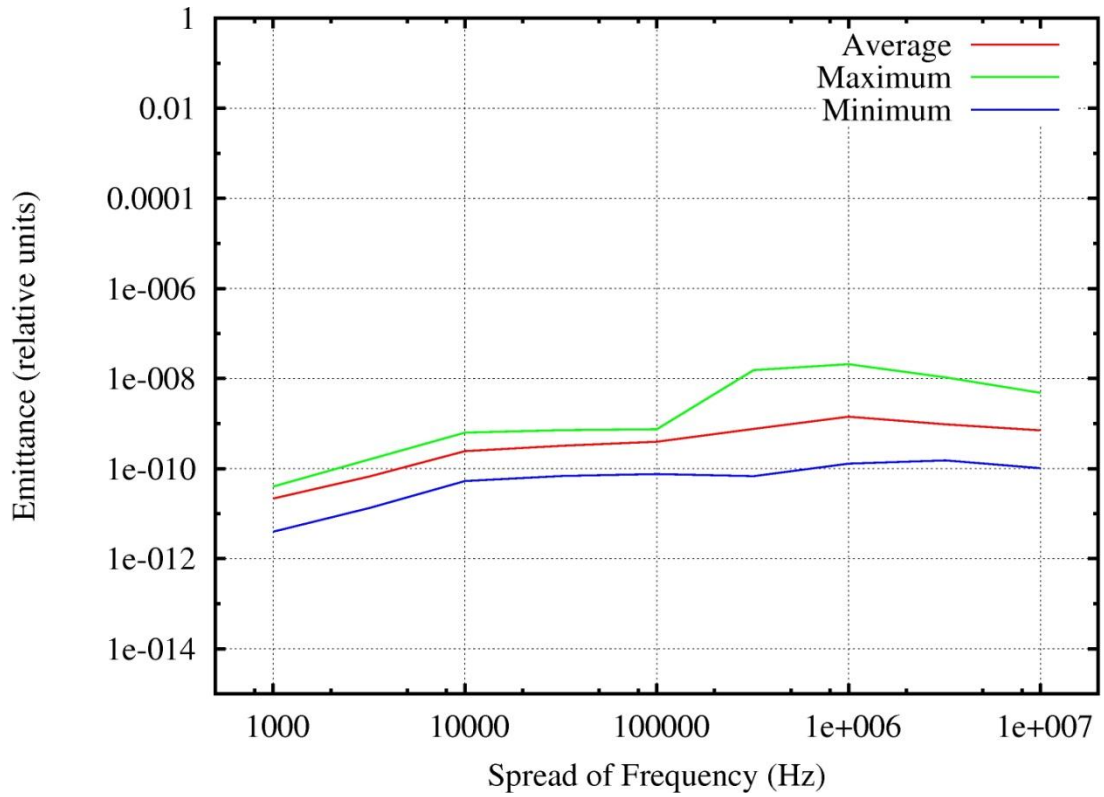

Figure 108: Longitudinal emittance dilution for $Q = 10^7$: case #6 (see Table 3)

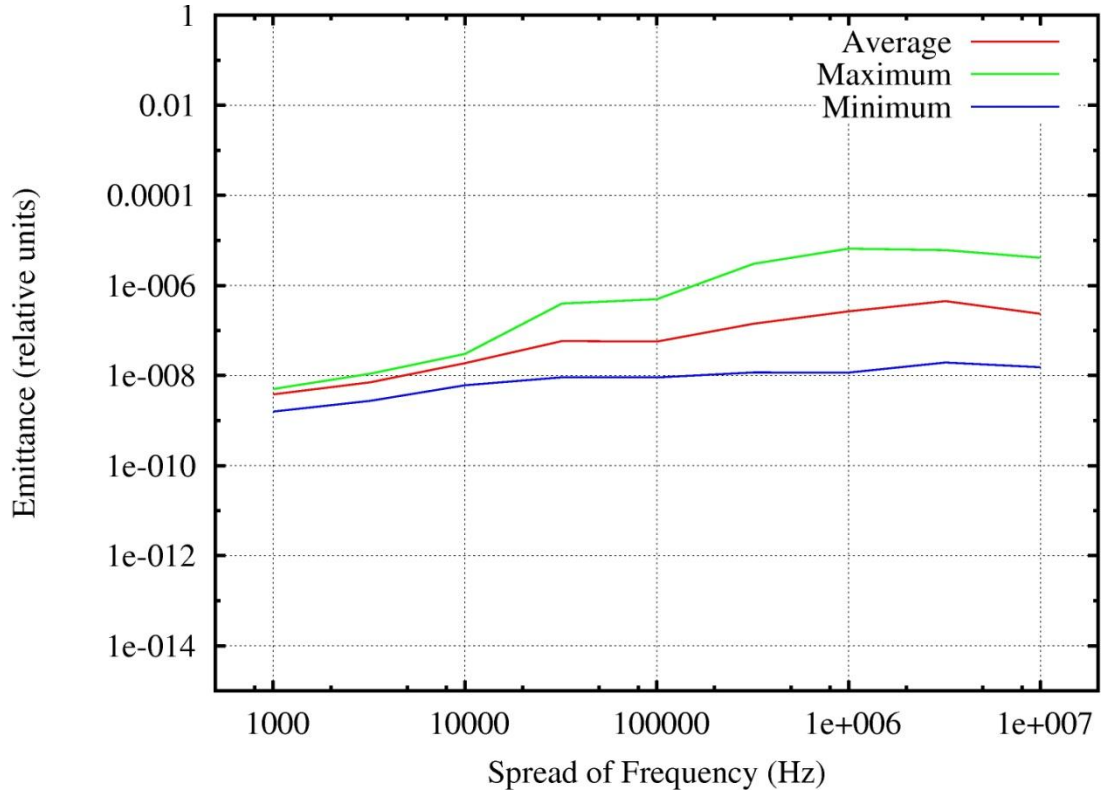

Figure 109: Longitudinal emittance dilution for $Q = 10^7$: case #7 (see Table 3)

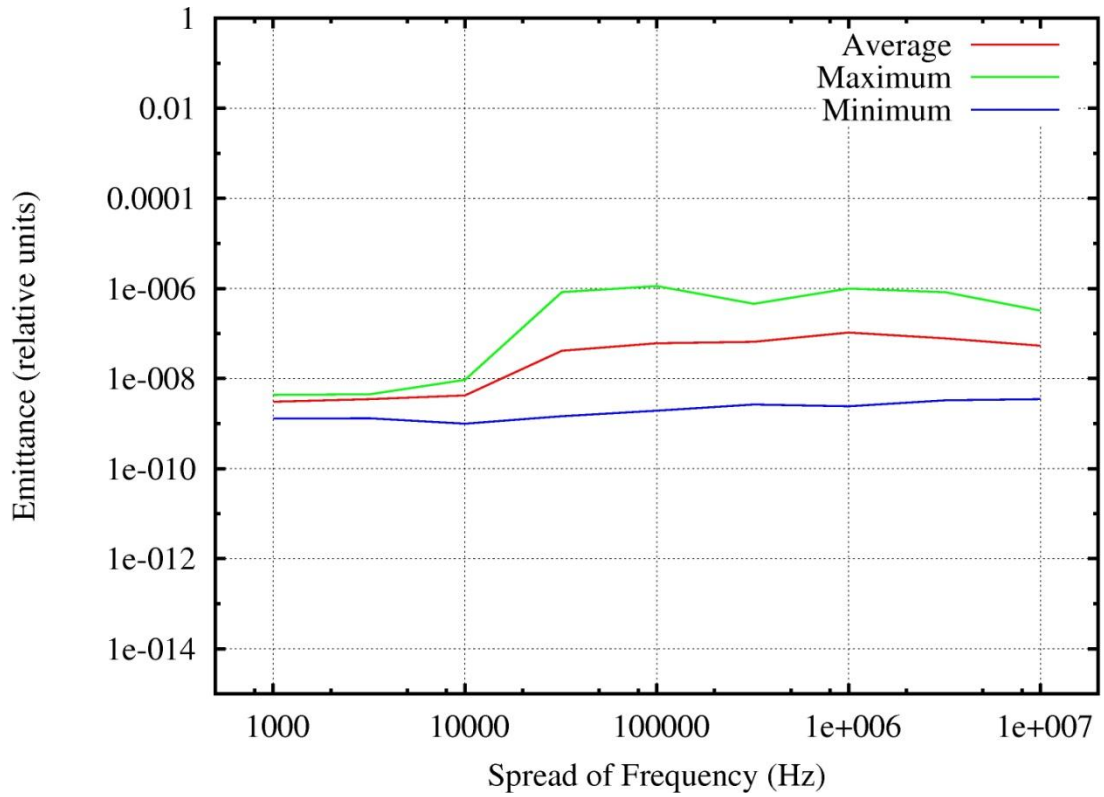

Figure 110: Longitudinal emittance dilution for $Q = 10^7$: case #8 (see Table 3)

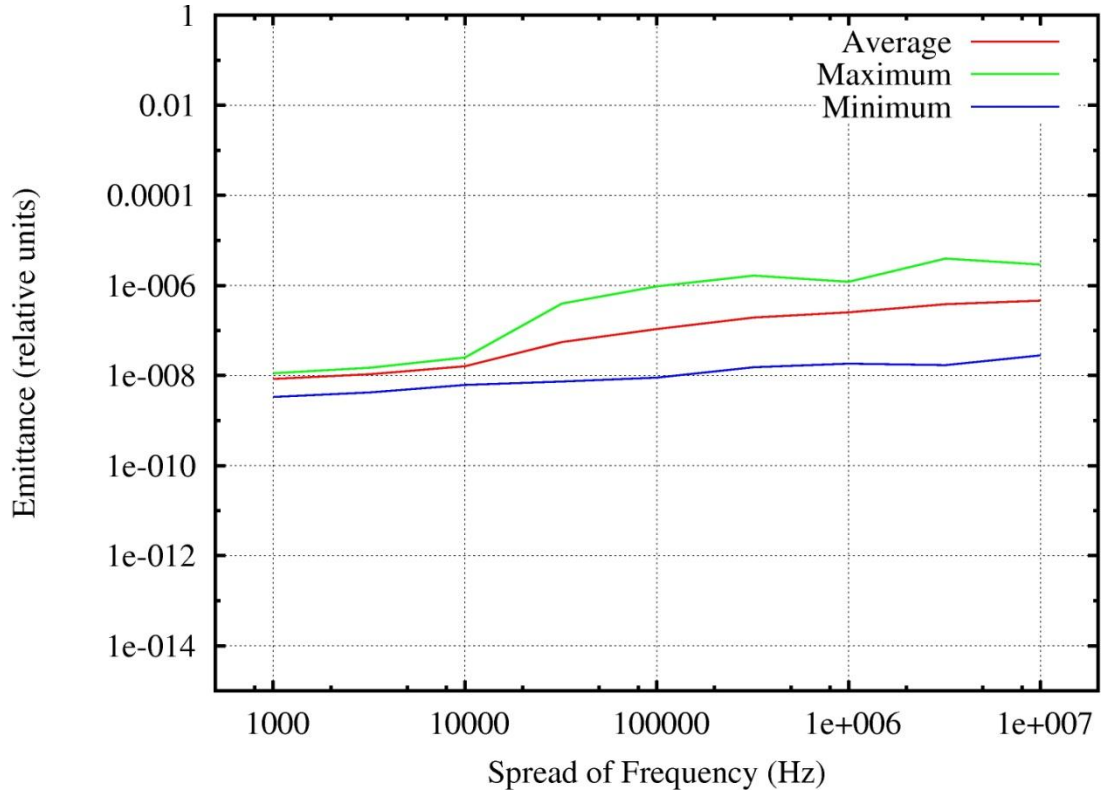

Figure 111: Longitudinal emittance dilution for $Q = 10^7$: real case

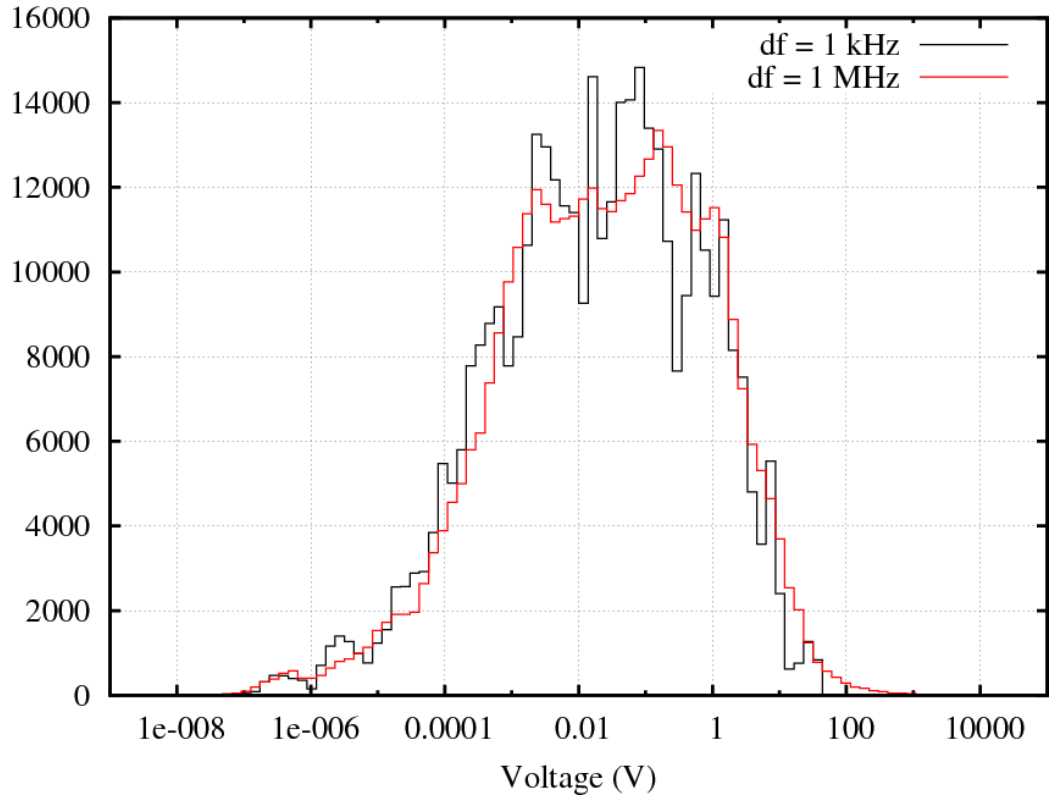

Figure 112: Monopole HOM voltage distribution for all real modes

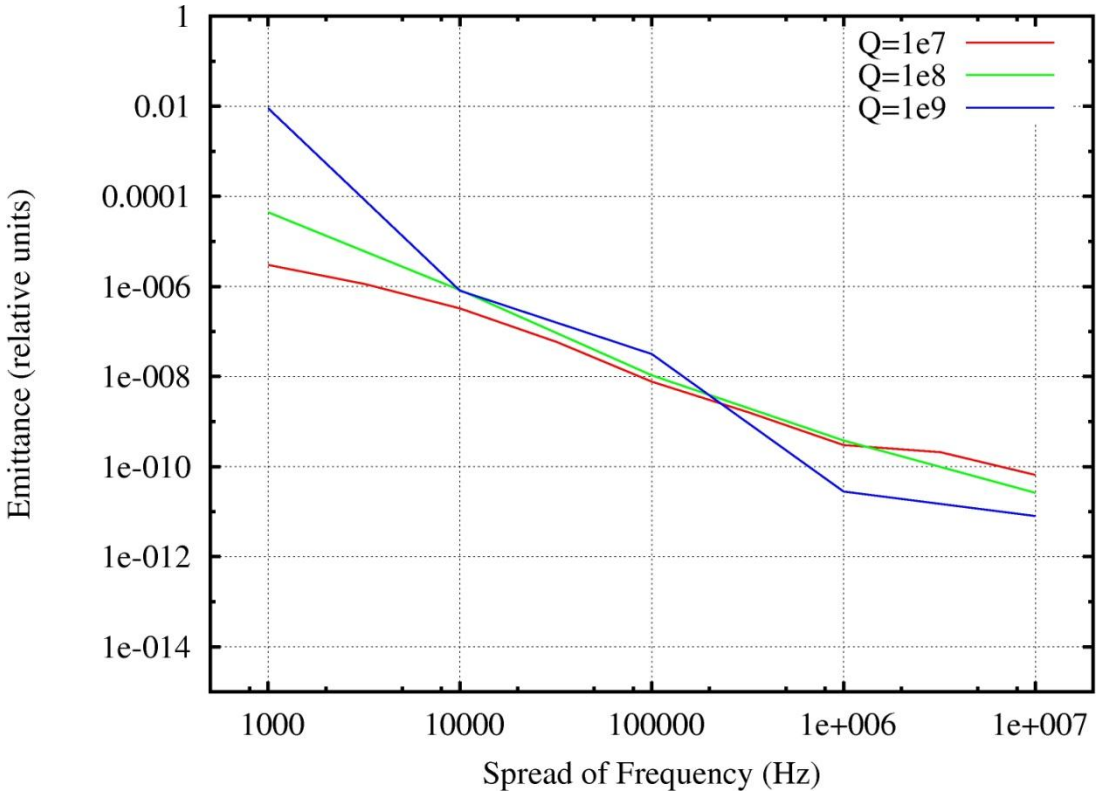

Figure 113: Transverse emittance dilution for the resonant case

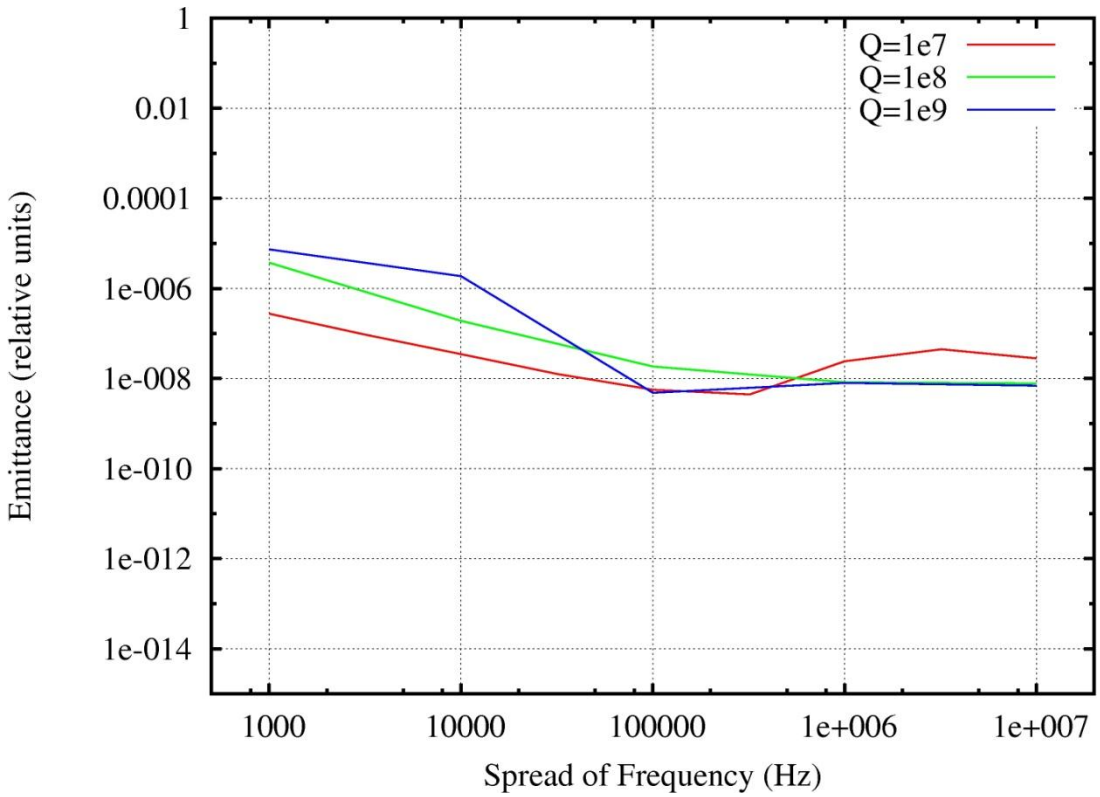

Figure 114: Longitudinal emittance dilution for the resonant case

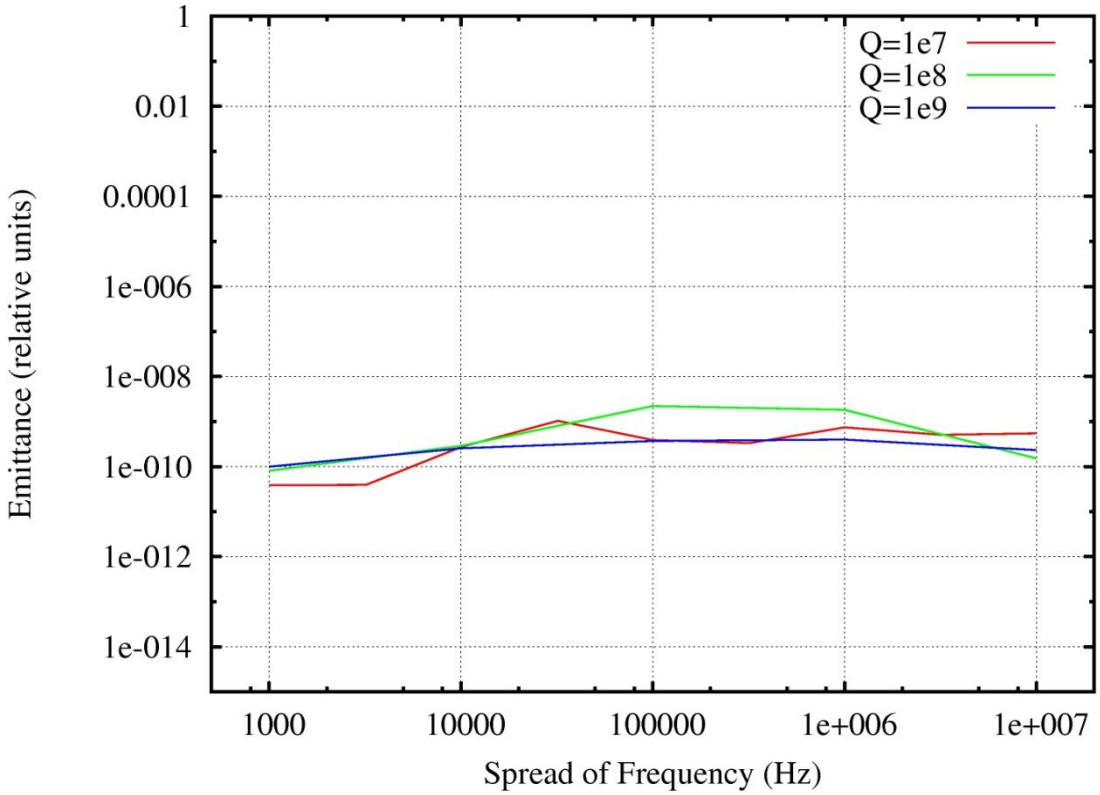

Figure 115: Transverse emittance dilution for the real case

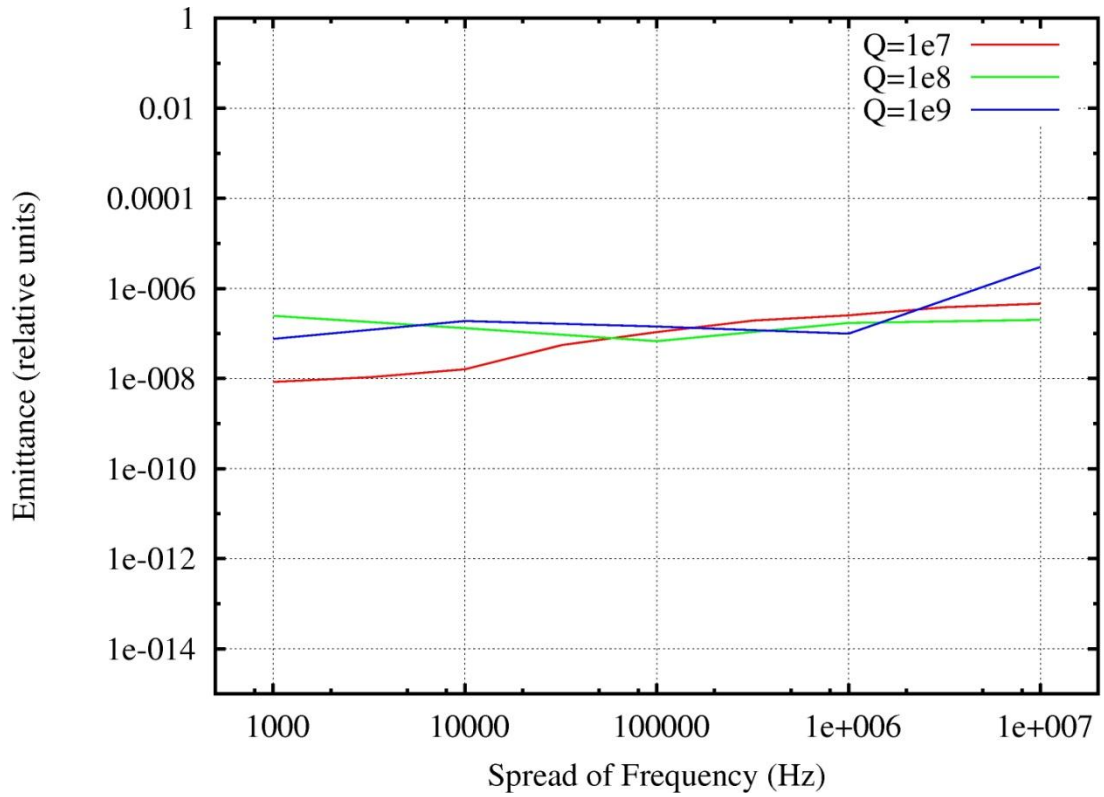

Figure 116: Longitudinal emittance dilution for the real case

Conclusion

The results of the calculations show that losses caused by longitudinal high order modes with frequencies below beam-pipe cutoff frequency should not look like an issue for both LE650 and HE650 sections. This fact is explained by small probability (less than 0.01%) for HOM to be close enough to a resonance, i.e. to cause losses more than $1\ W$. Besides it is shown that losses in Project X due to HOMs are smaller than these losses in SNS, which demonstrated that HOM losses is not an issue. Moreover it is shown that if it happens that a HOM is close to a resonant, HOM frequency shift by about $100\ Hz$ is enough to reduce power of losses up to acceptable level. It is shown that we can shift HOM frequency by detuning of the accelerating mode and tuning it back.

Range of quality factors of HOMs from 10^7 to 10^{10} is studied. Energy range from $150\ MeV$ to $550\ MeV$ is studied for LE650 section. Energy range from $500\ MeV$ to $3\ GeV$ is studied for HE650 section. The results can tell us that it is possible to get rid of HOM dampers in $650\ MHz$ sections as an expensive and complicated part of superconducting acceleration structure. Moreover HOM dampers can cause additional problems like multipacting, leak of power of the accelerating mode; they require additional hardware like cables, feedthrough, connectors, loads, etc. Experience of the existing proton SC linac (SNS) shows that HOM dampers may cause cavity performance degradation during long-term operation [10]. On the other hand, SNS linac experience does not show necessity of HOM dampers.

Emittance dilution caused by beam break-up effect and klystron instabilities is also studied. Simulations show that this dilution is significantly smaller than initial emittance of the beam, and induced HOM voltages are quite small too. There is no collective effects because of small impedances of HOMs, their dependence on beta, different HOM frequencies for different sections. It is another argument for the idea to get rid of HOM dampers at LE650 and HE650 sections of the Project X linac.

References

[1] "Project X Initial Configuration Document–2", Edited by P. Derwent. http://projectx-docdb.fnal.gov/cgi-bin/ShowDocument?docid=230

[2] N. Solyak, S. Nagaitsev, V. Lebedev, J.-F. Ostiguy, N. Perunov, E. Gianfelice-Wendt, I. Gonin, G. Romanov, S. Kazakov, V. Yakovlev, "The Concept Design of the CW Linac of the Project X", Proceedings of IPAC'10, Kyoto, Japan, June 2010. http://accelconf.web.cern.ch/AccelConf/IPAC10/papers/MOPEC081.pdf

[3] S. Nagaitsev, "Project X", Project X Collaboration Meeting, September 8–9, 2010. http://projectx-docdb.fnal.gov/cgi-bin/ShowDocument?docid=722

[4] N. Solyak, V. Yakovlev, "Assumptions about Q values in CW Linac". http://projectx-docdb.fnal.gov/cgi-bin/ShowDocument?docid=590

[5] D. G. Myakishev, V. P. Yakovlev, "The New Possibilities of SuperLANS Code for Evaluation of Axisymmetric Cavities", Proceedings of the 1995 Particle Accelerator Conference and International Conference on High-Energy Accelerators. http://accelconf.web.cern.ch/Accelconf/p95/ARTICLES/MPC/MPC17.PDF

[6] J. L. Altman, "Microwave Circuits", Princeton, NJ: Van Nostrand, 1964.

[7] N. Solyak, A. Vostrikov, T. Khabiboulline, A. Saini, V. Yakovlev, "Longitudinal and Transverse Effects of HOMs in the Project X Linac", Proceedings of IPAC'10, Kyoto, Japan, June 2010. http://accelconf.web.cern.ch/AccelConf/IPAC10/papers/tupea020.pdf

[8] J. Tuckmantel, "HOM Dampers or not in SUPERCONDUCTING RF Proton Linacs", CERN BE-Note-2009-009 RF: Geneva, Switzerland, 2009.

[9] V. Yakovlev, N. Solyak, A. Vostrikov, T. Khabiboulline, I. Gonin, A. Saini, A. Lunin, S. Kazakov, "HOMs in 650 MHz Section of the Project X Linac", Project X Collaboration Meeting, September 8, 2010. http://projectx-docdb.fnal.gov/cgi-bin/ShowDocument?docid=699

[10] S.-H. Kim, SPL HOM Workshop, June 25–26, 2009.

Appendix

Table 6: Monopole modes in LE650 and HE650 cavities at geometrical beta

LE650, $\beta = 0.61$		HE650, $\beta = 0.90$	
HOM frequency, MHz	$R/Q\,, Ohm$	HOM frequency, MHz	$R/Q\,, Ohm$
645.582	0.0007054	645.115	$4.406 \cdot 10^{-5}$
646.808	0.004786	646.459	0.001267
648.319	0.006974	648.128	0.0003662
649.535	0.013804	649.482	0.0013326
650	352.4	650	606.8
1447.8	0.05452	1229.02	0.15568
1451.52	0.02708	1231.64	1.693
1456.96	0.01627	1235.16	3.242
1462.94	0.009588	1238.62	22.06
1467.72	0.0008248	1241.14	129.12
1614.79	0.3624	1395.25	0.04508
1615.95	0.7368	1399.09	0.00447
1618.81	4.044	1404.67	0.002138
1622.04	2.212	1410.57	0.019682
1624.45	0.10906	1415.06	0.0007462
2130.63	0.02106	1817.7	4.732
2136.71	0.0248	1826.42	3.428
2147.08	0.013418	1840.26	0.0006238
2160.84	0.010474	1856.83	0.012982
2176.31	$3.74 \cdot 10^{-5}$	1871.33	0.00499
2191.31	0.02318	1988.36	0.003864
2205.1	0.003454	1988.37	0.07228
2216.4	0.19996	1988.38	0.7774
2224.86	0.2252	1988.4	0.956
2230.17	0.02138	1988.4	11.918
2723.49	0.004128	2097.9	0.07944
2731.8	0.3962	2110.8	1.0164
2747.25	0.06802	2133.3	1.9492
2767.17	1.8246	2159.38	12.17
2785.25	6.102	2180.82	2.852

Table 7: Dipole modes in LE650 and HE650 cavities at geometrical beta

LE650, $\beta = 0.61$		HE650, $\beta = 0.90$	
HOM frequency, MHz	$R/Q\,, Ohm$	HOM frequency, MHz	$R/Q\,, Ohm$
970.708	327.924	943.213	56.3804
974.021	11633.32	946.556	18248.82
978.551	25323.0	950.284	37168.2
982.966	8892.84	952.825	5900.64
986.007	11.66744	964.719	7841.64
1293.2	21108.4	964.72	8912.12
1311.84	305.588	975.929	394.964
1338.56	351.634	979.933	2212.88
1367.0	231.176	985.758	1661.9
1389.08	13.62298	991.008	84.4398
1696.14	10.19004	1376.07	61283.2
1696.69	2361.52	1383.62	19679.32
1697.68	9176.28	1396.57	515.35
1698.91	3067.56	1415.04	5570.88
1738.2	838.062	1436.66	709.434
1738.22	2468.36	1486.31	10.62286
1774.49	899.398	1522.78	1005.514
1776.53	965.602	1557.86	856.422
1778.09	39.7472	1574.28	19.66722
1778.9	26.0028	1582.89	1561.826
1882.07	6.66118	1582.91	137.2114
1883.37	10.15634	1601.57	103.7466
1886.87	25.015	1614.93	4049.66
1892.73	13.64816	1649.1	825.246
1899.61	63.3648	1685.55	11.95344
2063.3	2115.8	1731.21	787.816
2090.56	1675.18	1731.23	19.69914
2123.31	660.008	1732.4	367.712
2149.06	559.884	1734.52	73.152
2180.25	492.796	1743.16	4.9943

Table 8: Dimensions of the 650 MHz cavities

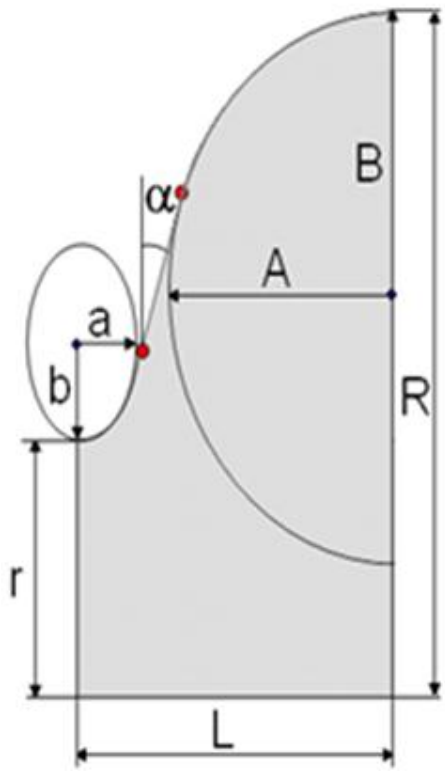

Dimension	LE650		HE650	
	Regular cell	End cell	Regular cell	End cell
r, mm	41.5	41.5	50	50
R, mm	195	195	200.3	200.3
L, mm	70.3	71.4	103.8	107.0
A, mm	54	54	82.5	82.5
B, mm	58	58	84	84.5
a, mm	14	14	18	20
b, mm	25	25	38	39.5
$\alpha, °$	2	2.7	5.2	7

Table 9: RF parameters of the 650 MHz cavities

Geometrical beta	0.61	0.90
R/Q, Ohm (for optimal beta)[2]	378	638
G-factor, Ohm	191	255
Maximum energy gain per cavity, MeV	11.7	19.3
Gradient, MeV/m	16.6	18.7
Maximum surface electric field, MV/m	37.5	37.3
E_{pk}/E_{acc}	2.26	2
Maximum surface magnetic field, mT	70	70
B_{pk}/E_{acc}	4.21	3.75
Coupling, %	0.68	0.75

[2] Note that the value of optimal beta is more than the value of geometrical beta for both types of cavity (see Figures 91 and 107).

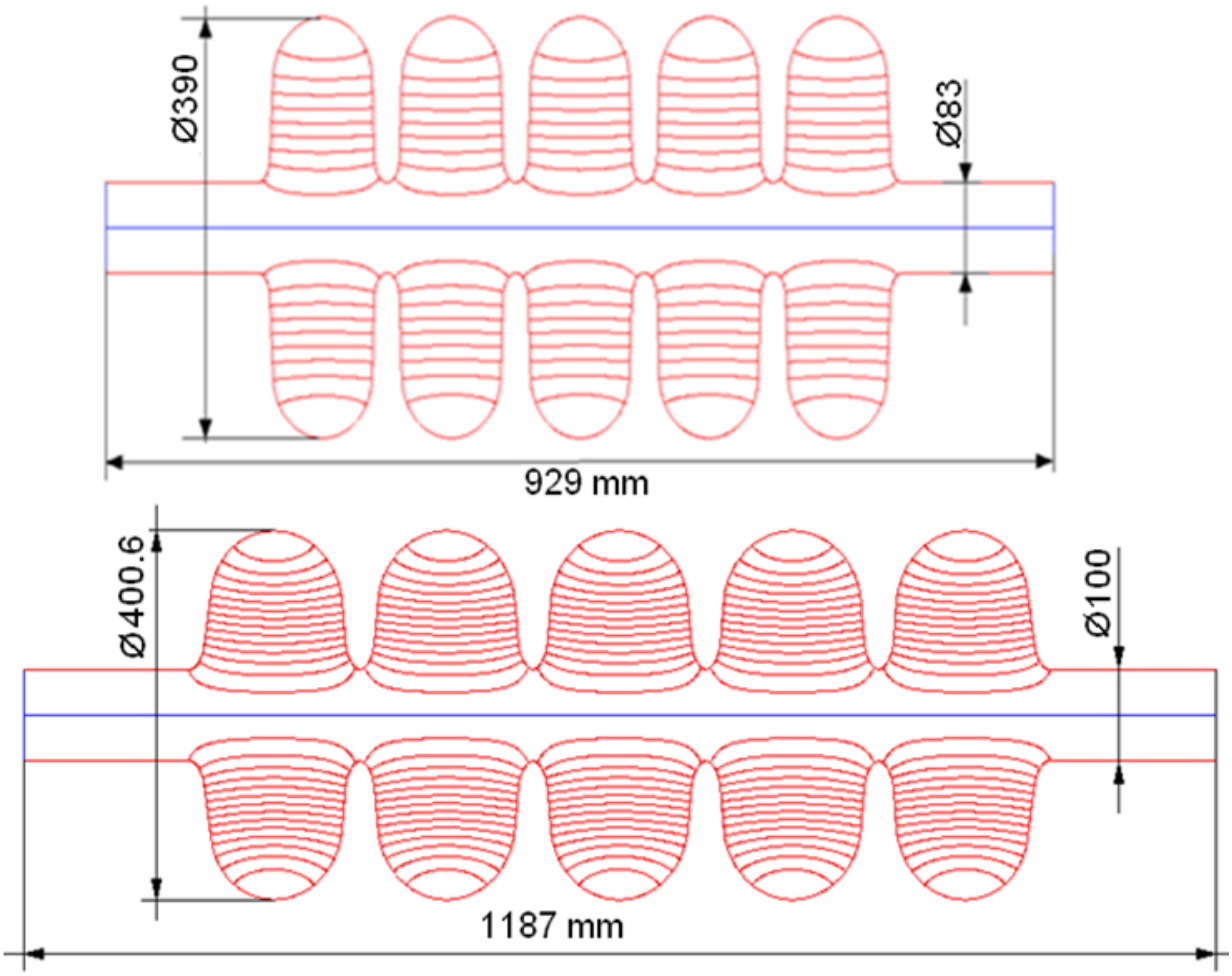

Figure 117: Layout of 650 MHz cavities: LE650 (top) and HE650 (bottom)

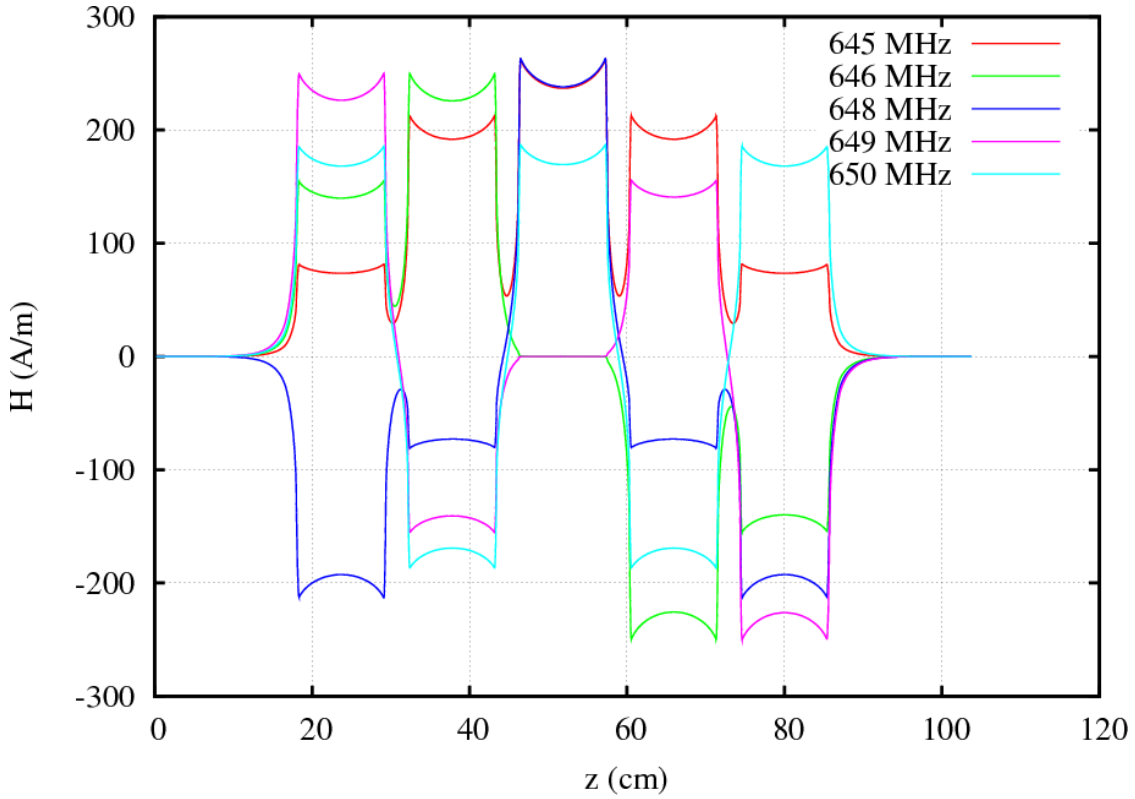

Figure 118: Surface magnetic field vs. cavity length for LE650, passband #1

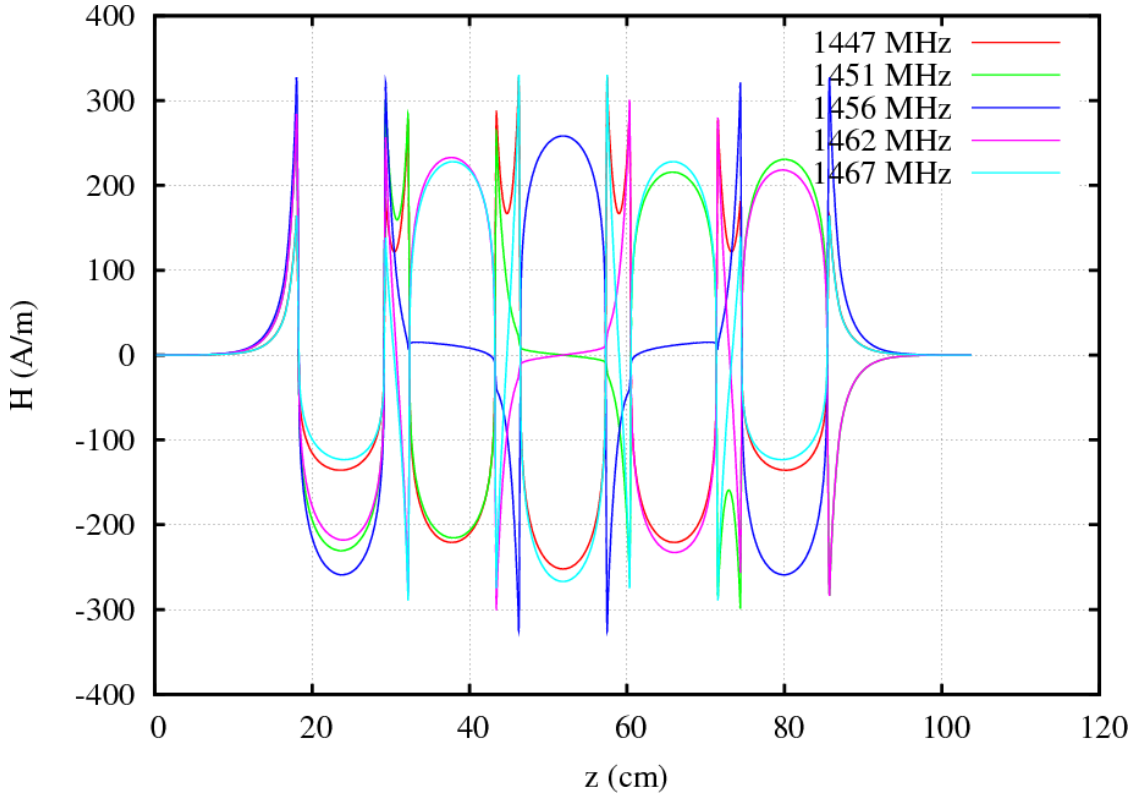

Figure 119: Surface magnetic field vs. cavity length for LE650, passband #2

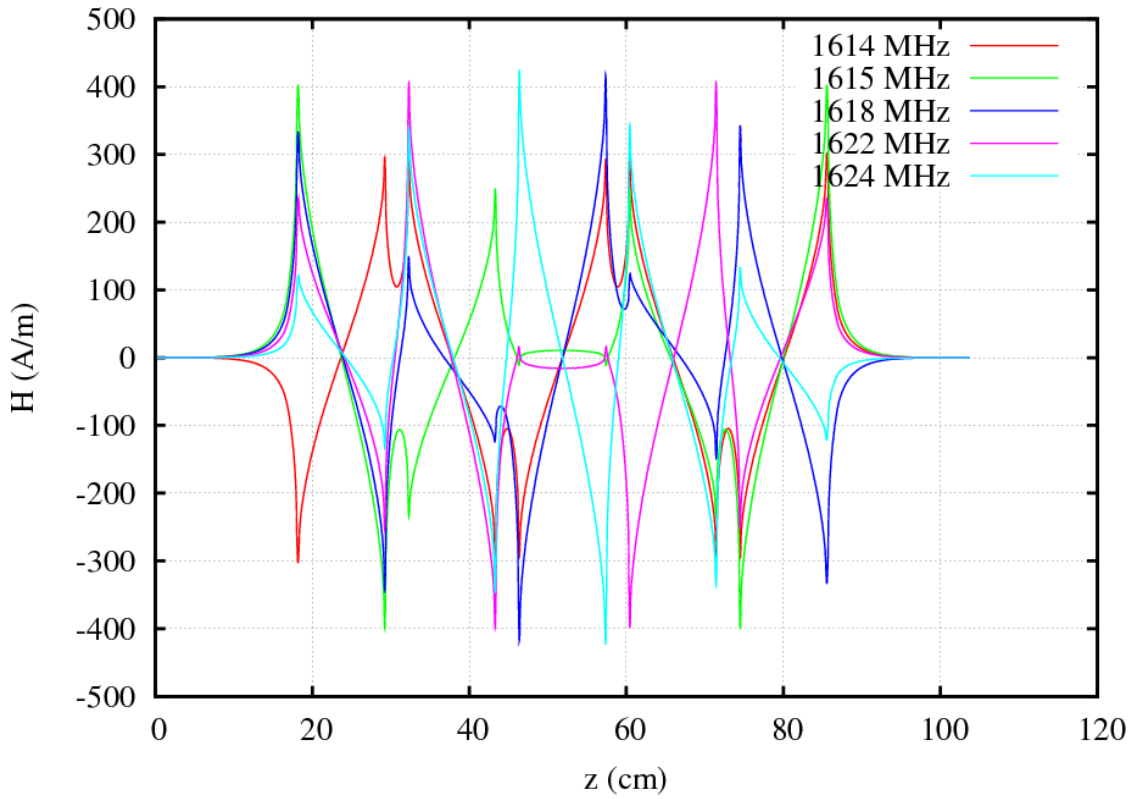

Figure 120: Surface magnetic field vs. cavity length for LE650, passband #3

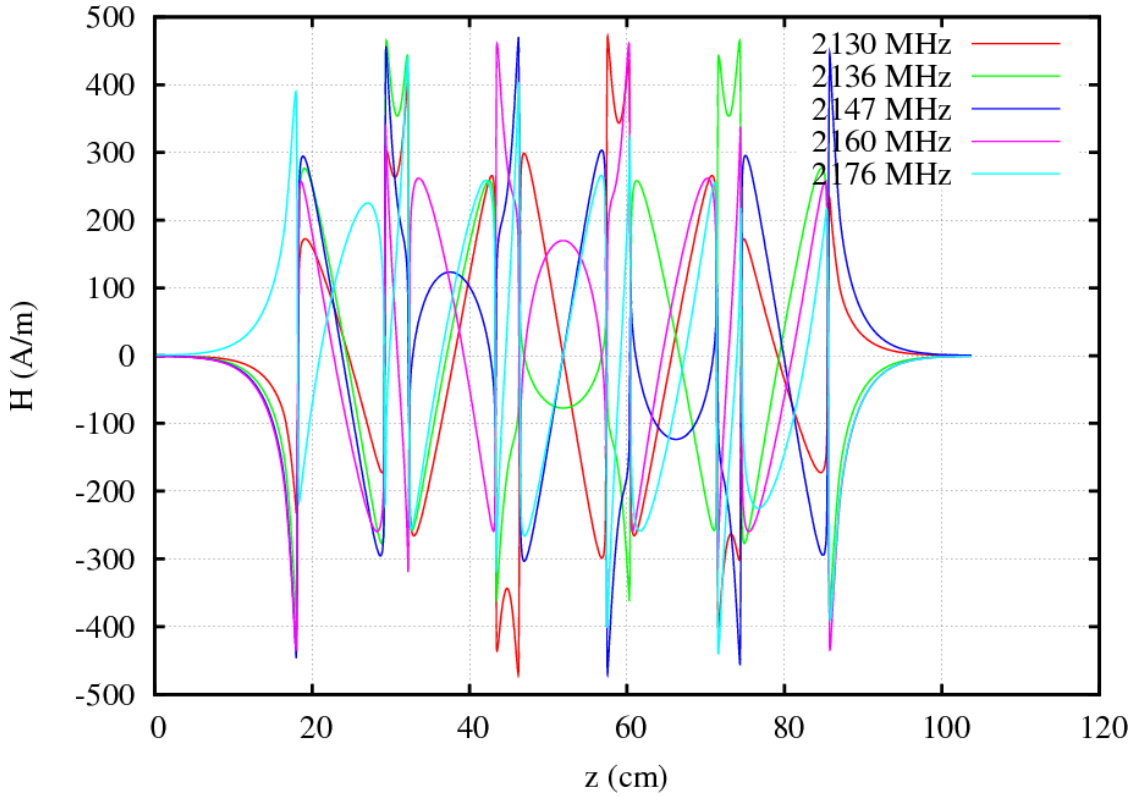

Figure 121: Surface magnetic field vs. cavity length for LE650, passband #4

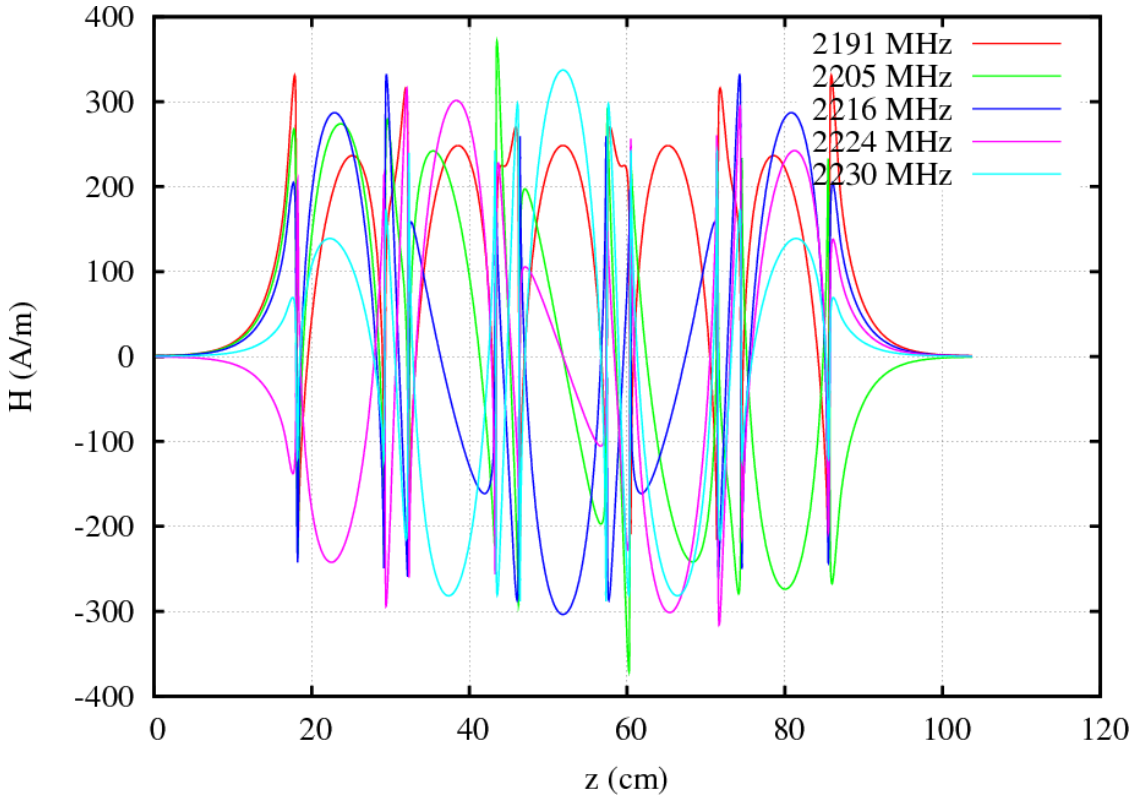

Figure 122: Surface magnetic field vs. cavity length for LE650, passband #5

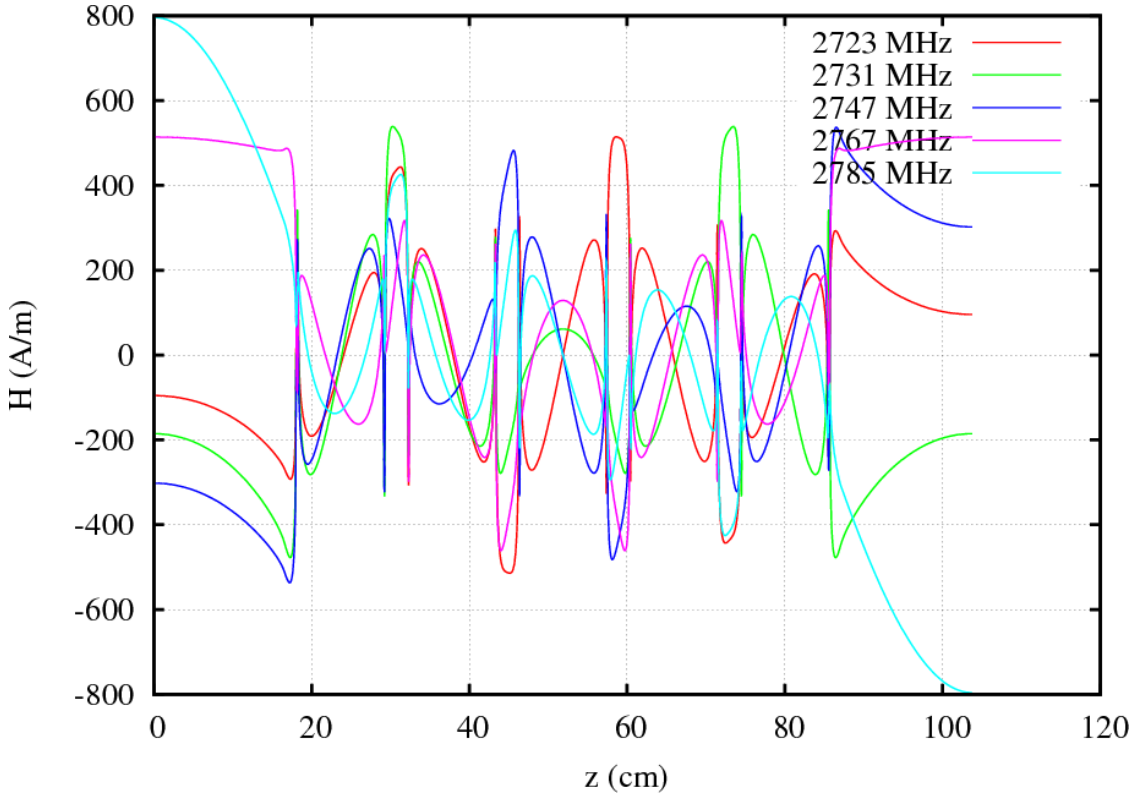

Figure 123: Surface magnetic field vs. cavity length for LE650, passband #6

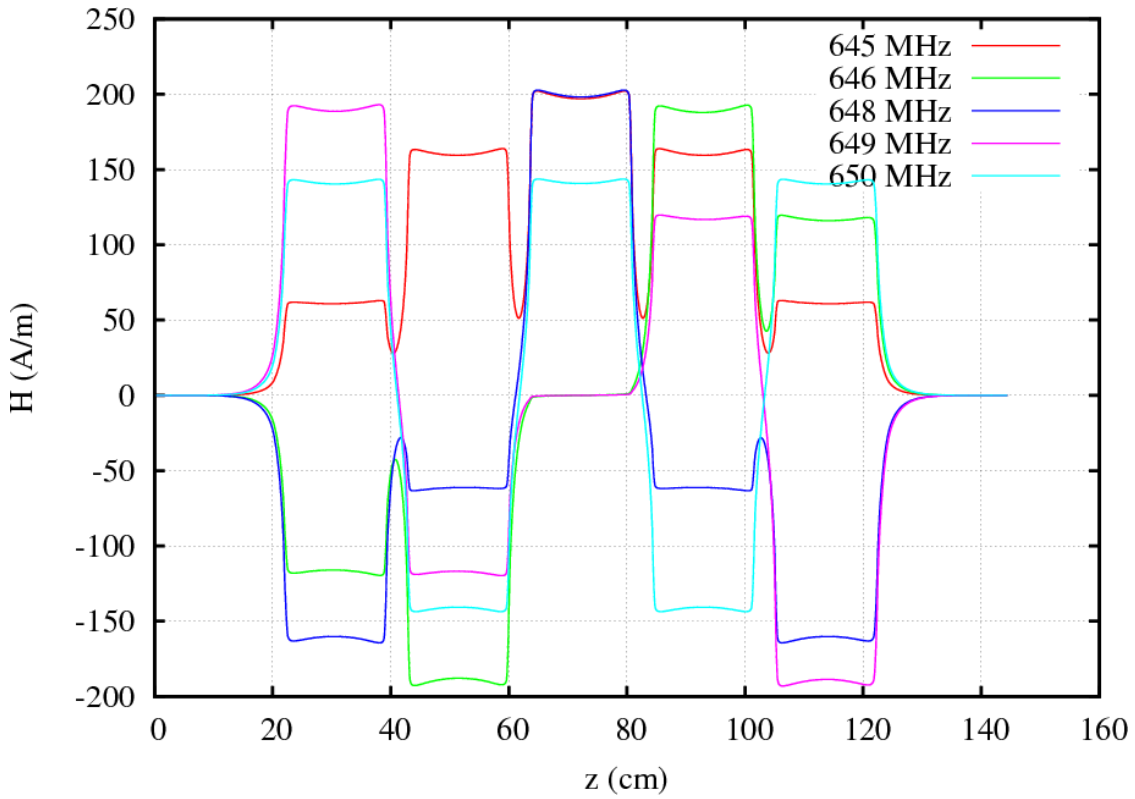

Figure 124: Surface magnetic field vs. cavity length for HE650, passband #1

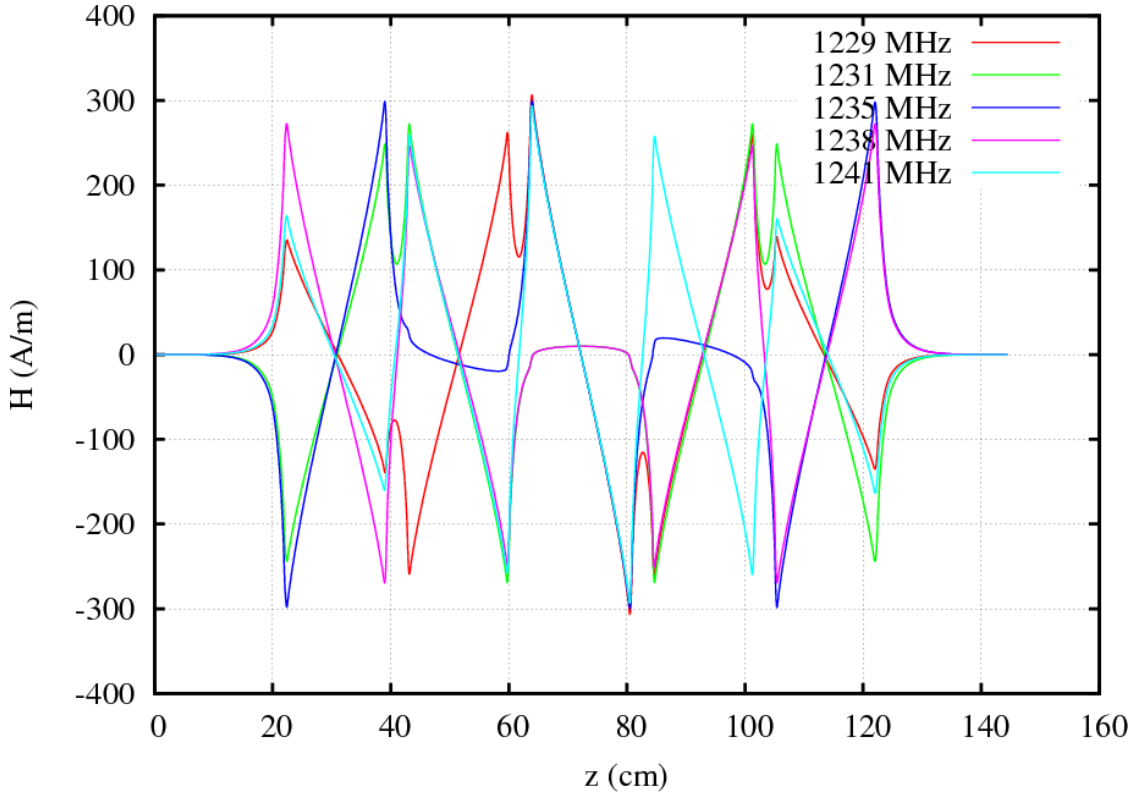

Figure 125: Surface magnetic field vs. cavity length for HE650, passband #2

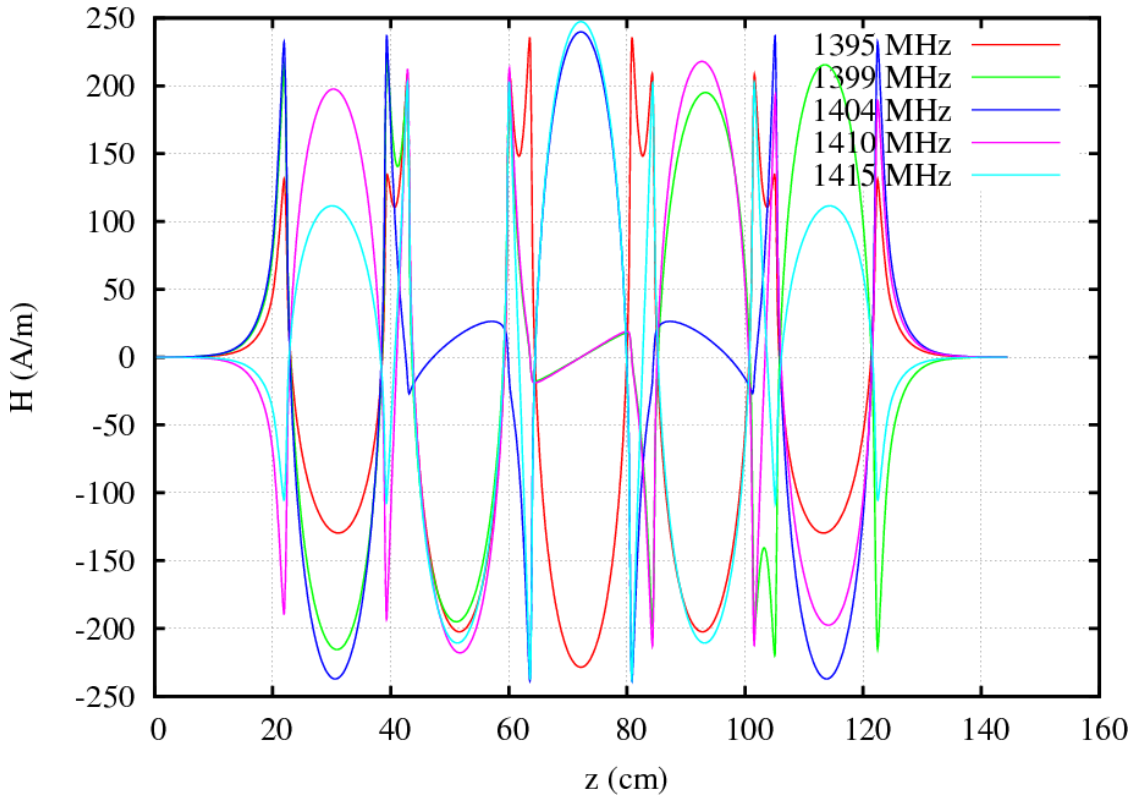

Figure 126: Surface magnetic field vs. cavity length for HE650, passband #3

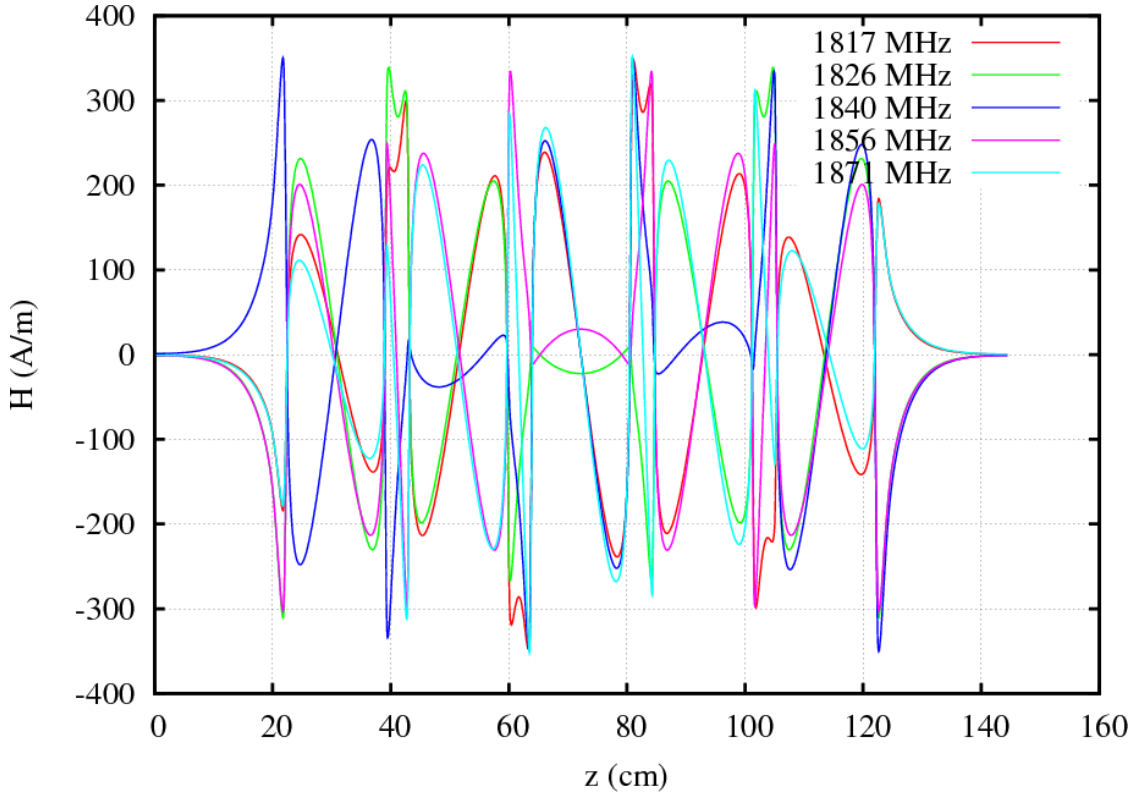

Figure 127: Surface magnetic field vs. cavity length for HE650, passband #4

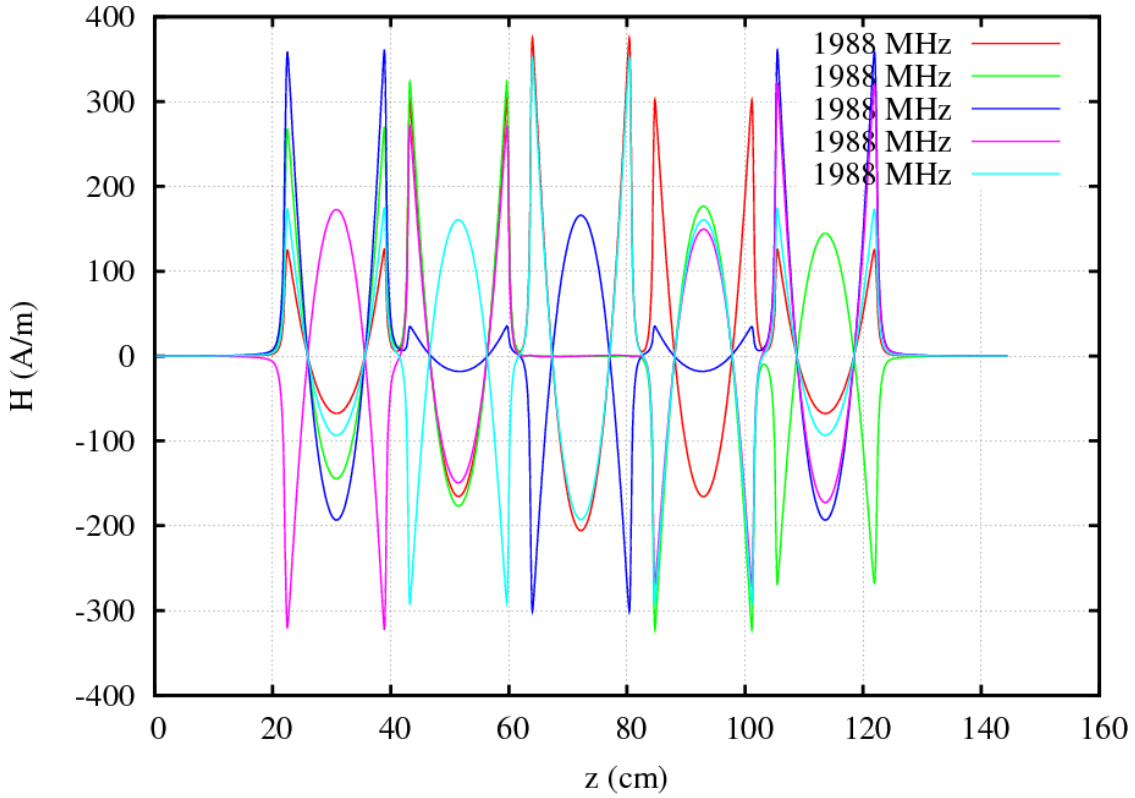

Figure 128: Surface magnetic field vs. cavity length for HE650, passband #5

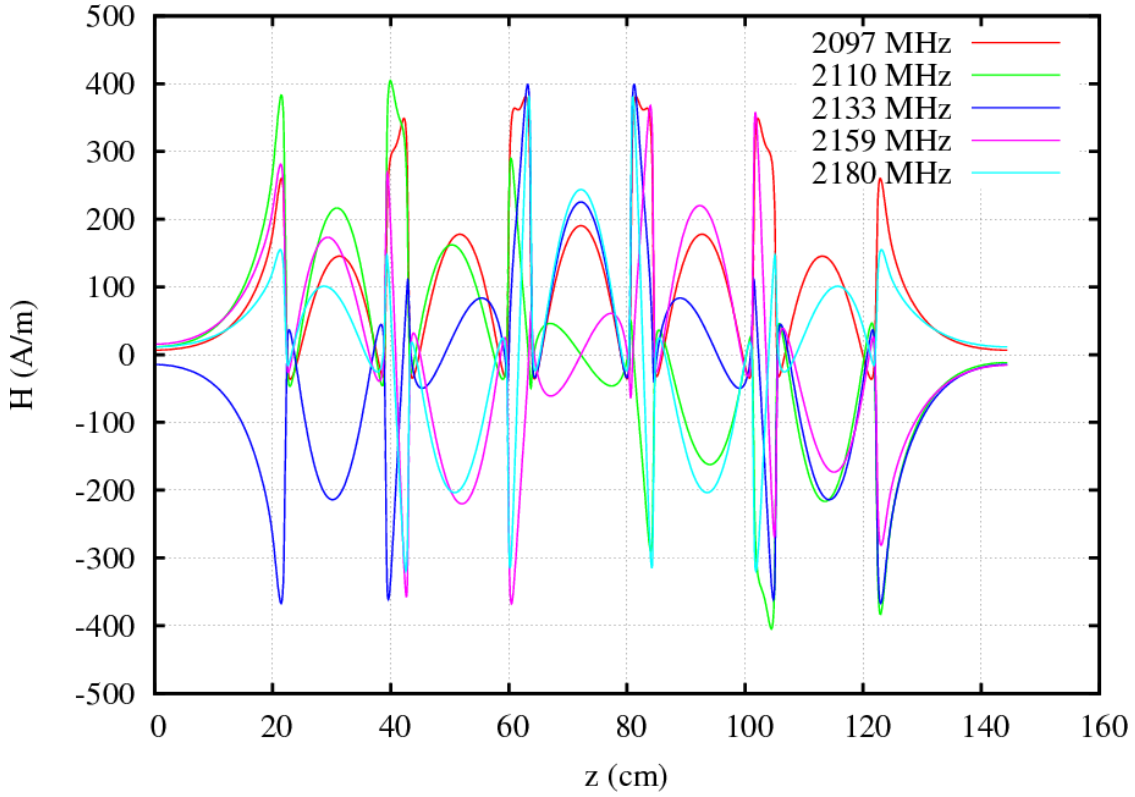

Figure 129: Surface magnetic field vs. cavity length for HE650, passband #6

R/Q Dependences on Beta at LE650:

Monopole Modes ##1 – 6

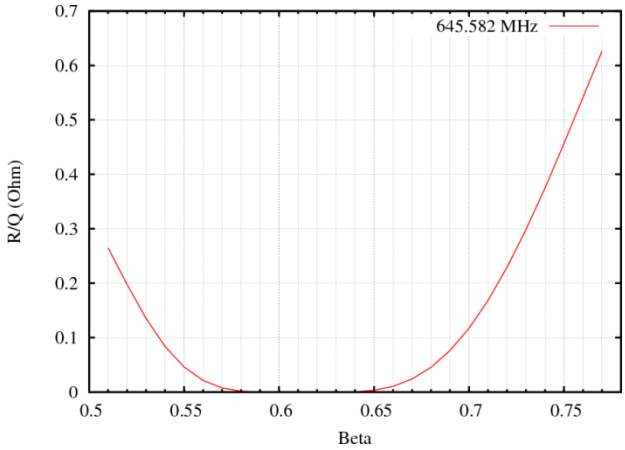

Figure 130: R/Q dependence on beta for $645.582\ MHz$ mode at LE650

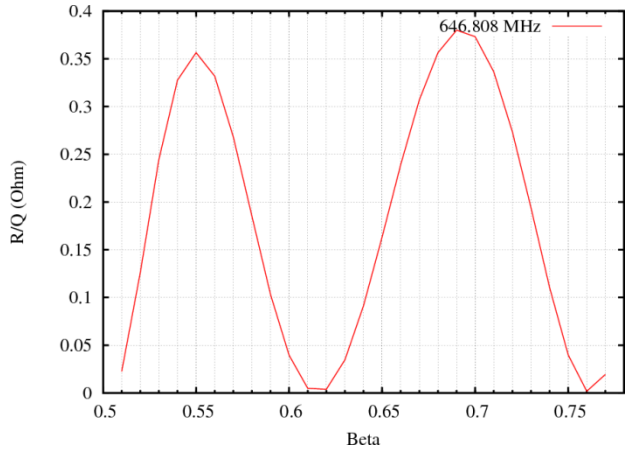

Figure 131: R/Q dependence on beta for $646.808\ MHz$ mode at LE650

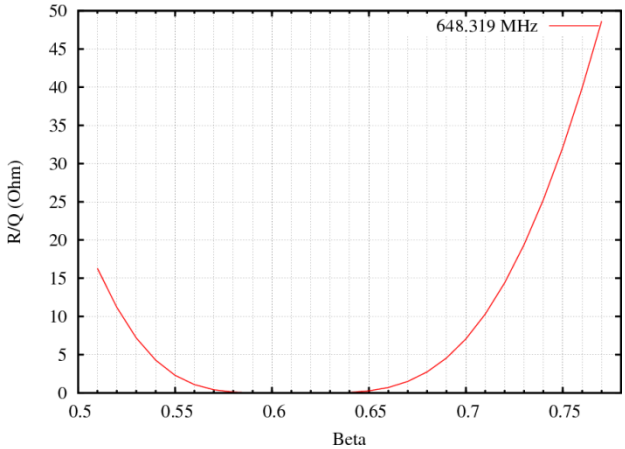

Figure 132: R/Q dependence on beta for $648.319\ MHz$ mode at LE650

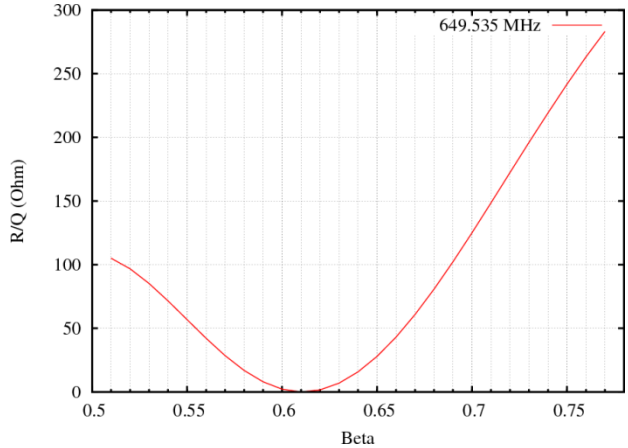

Figure 133: R/Q dependence on beta for $649.535\ MHz$ mode at LE650

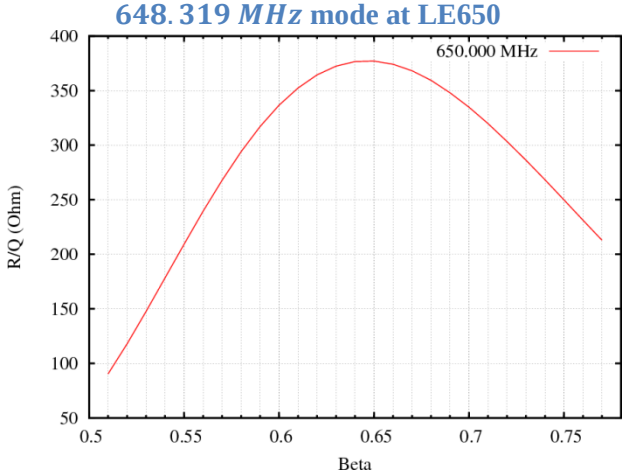

Figure 134: R/Q dependence on beta for $650\ MHz$ mode at LE650

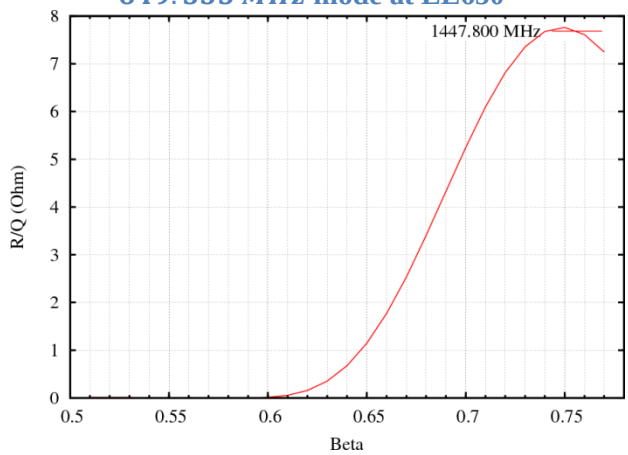

Figure 135: R/Q dependence on beta for $1447.800\ MHz$ mode at LE650

R/Q Dependences on Beta at LE650:

Monopole Modes ##7 – 12

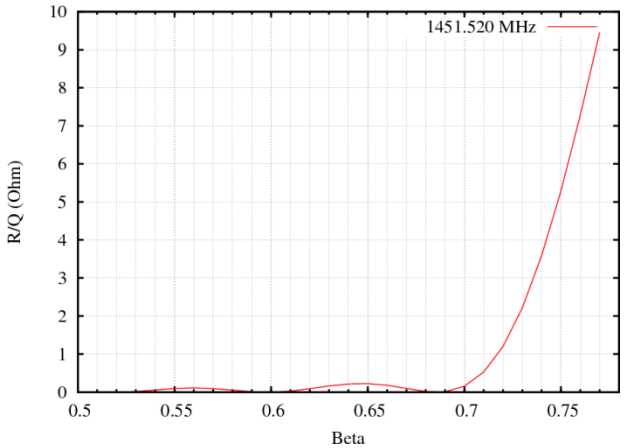

Figure 136: R/Q dependence on beta for $1451.520\ MHz$ mode at LE650

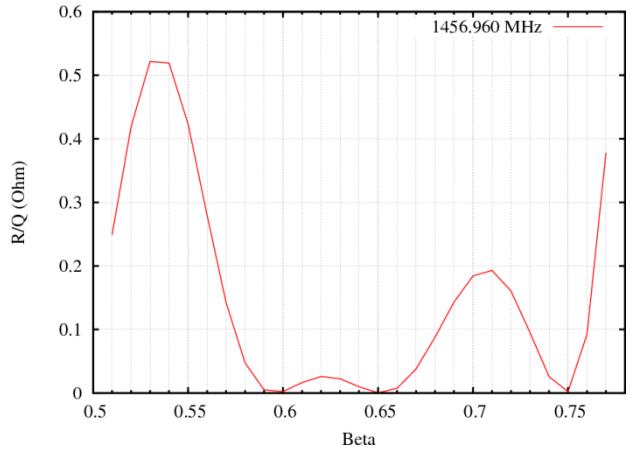

Figure 137: R/Q dependence on beta for $1456.960\ MHz$ mode at LE650

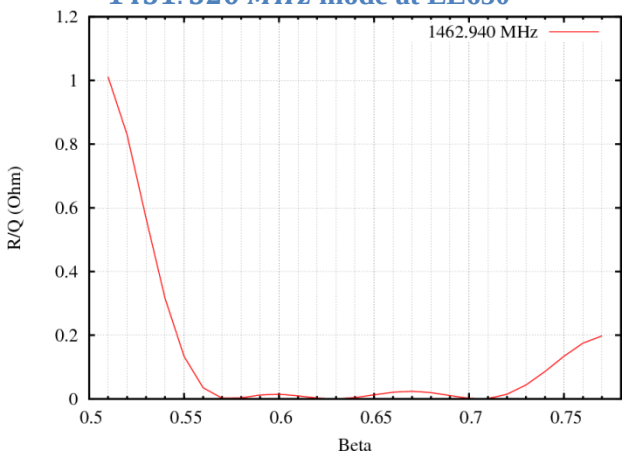

Figure 138: R/Q dependence on beta for $1462.940\ MHz$ mode at LE650

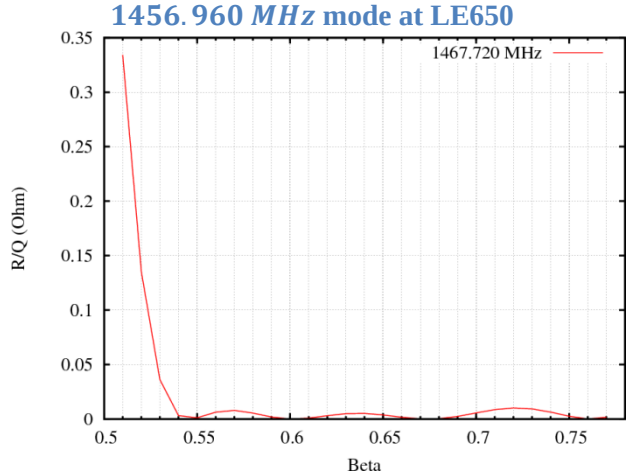

Figure 139: R/Q dependence on beta for $1467.720\ MHz$ mode at LE650

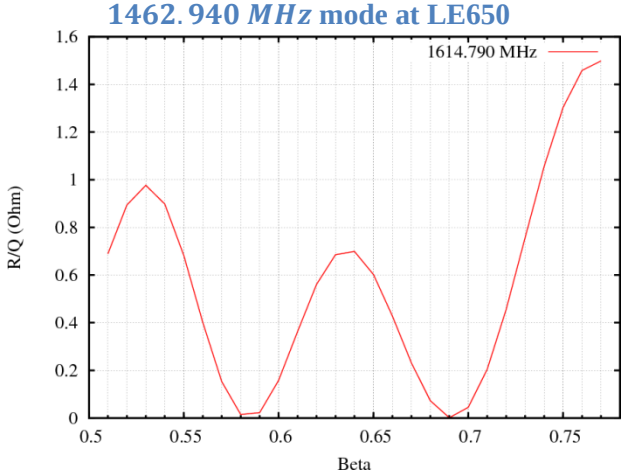

Figure 140: R/Q dependence on beta for $1614.790\ MHz$ mode at LE650

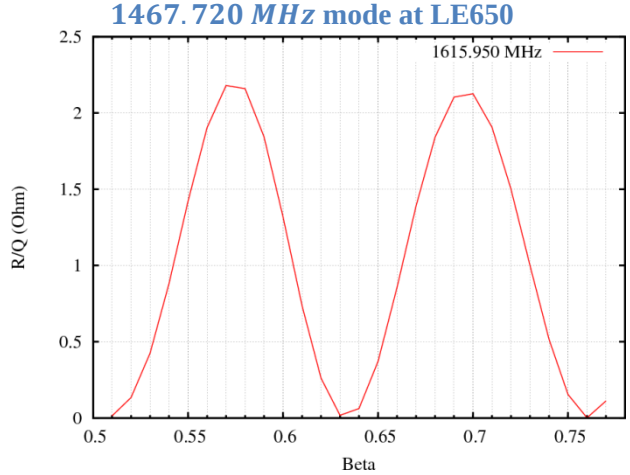

Figure 141: R/Q dependence on beta for $1615.950\ MHz$ mode at LE650

R/Q Dependences on Beta at LE650:

Monopole Modes ##13 – 18

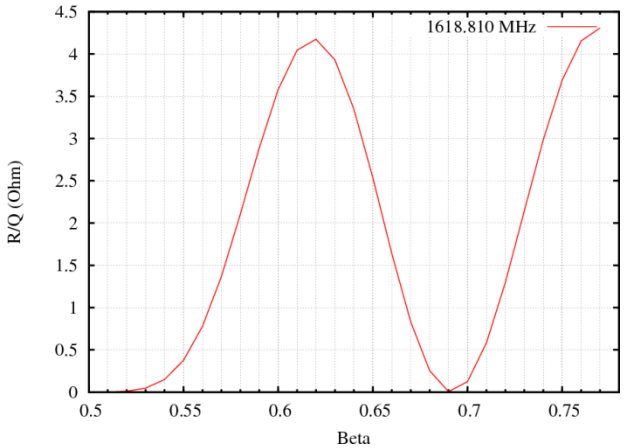

Figure 142: R/Q dependence on beta for $1618.810\ MHz$ mode at LE650

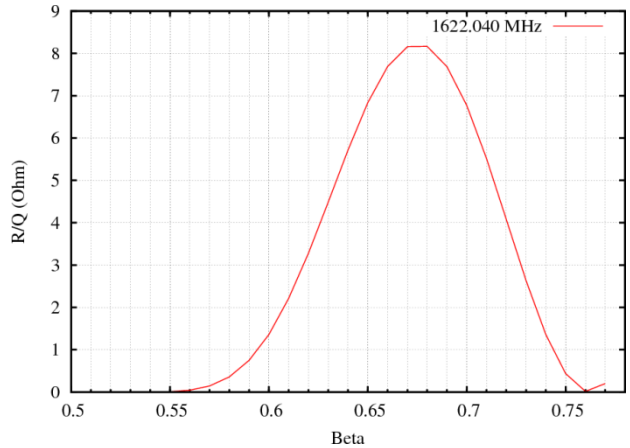

Figure 143: R/Q dependence on beta for $1622.040\ MHz$ mode at LE650

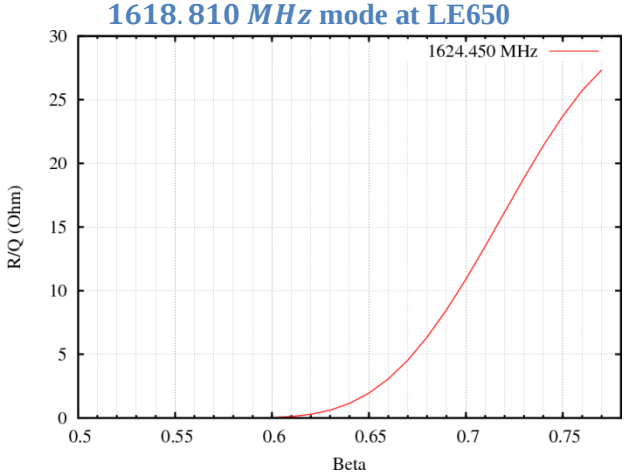

Figure 144: R/Q dependence on beta for $1624.450\ MHz$ mode at LE650

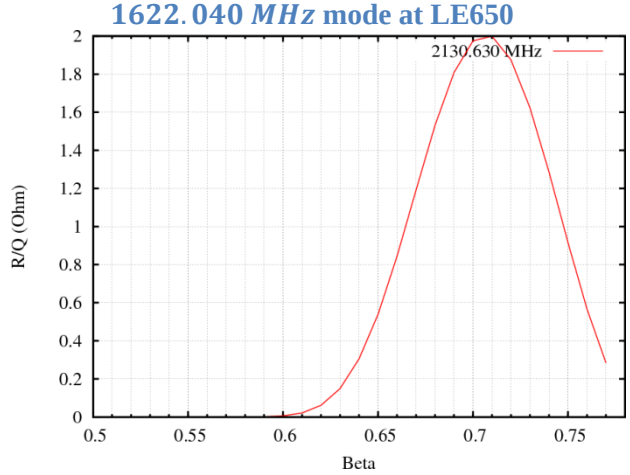

Figure 145: R/Q dependence on beta for $2130.630\ MHz$ mode at LE650

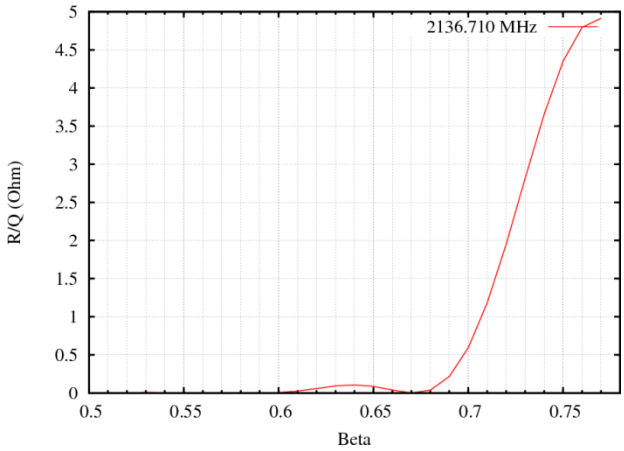

Figure 146: R/Q dependence on beta for $2136.710\ MHz$ mode at LE650

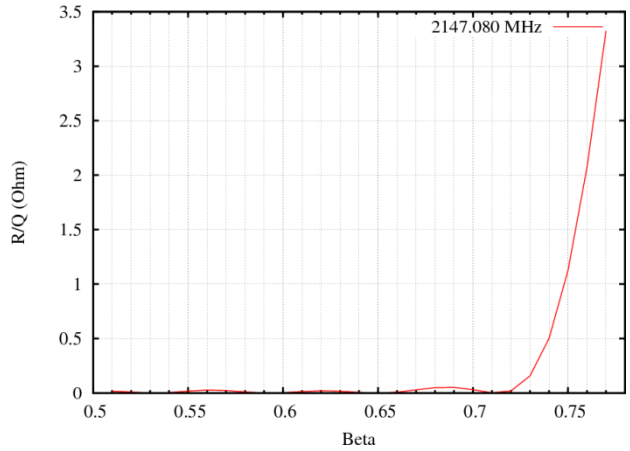

Figure 147: R/Q dependence on beta for $2147.080\ MHz$ mode at LE650

R/Q Dependences on Beta at LE650:

Monopole Modes ##19 – 24

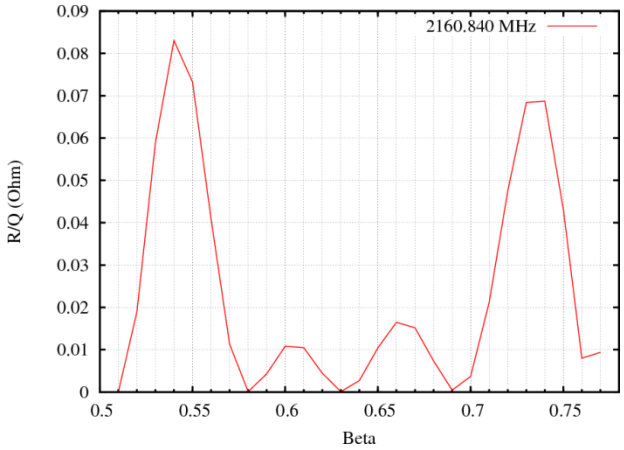

Figure 148: R/Q dependence on beta for $2160.840\ MHz$ mode at LE650

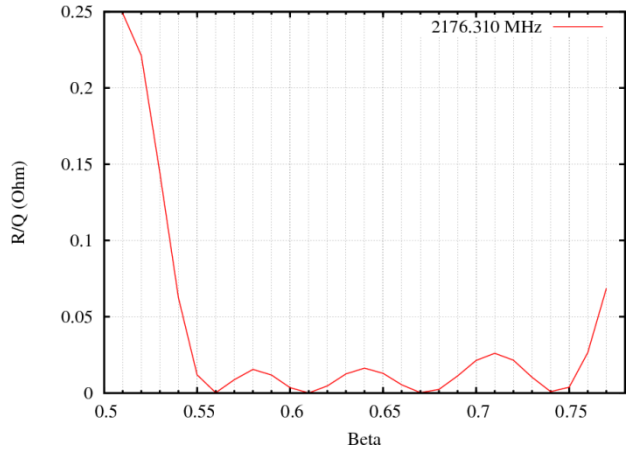

Figure 149: R/Q dependence on beta for $2176.310\ MHz$ mode at LE650

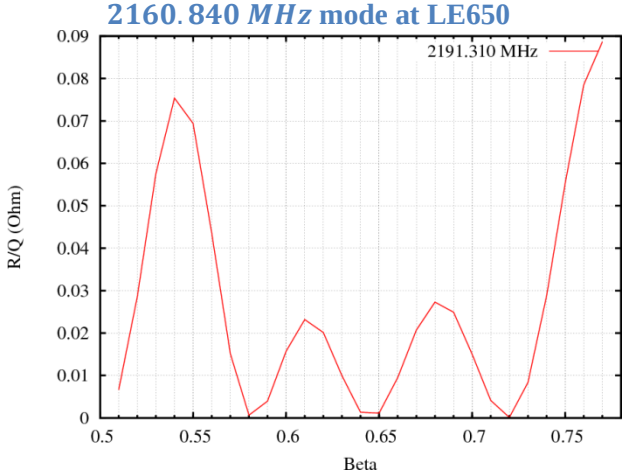

Figure 150: R/Q dependence on beta for $2191.310\ MHz$ mode at LE650

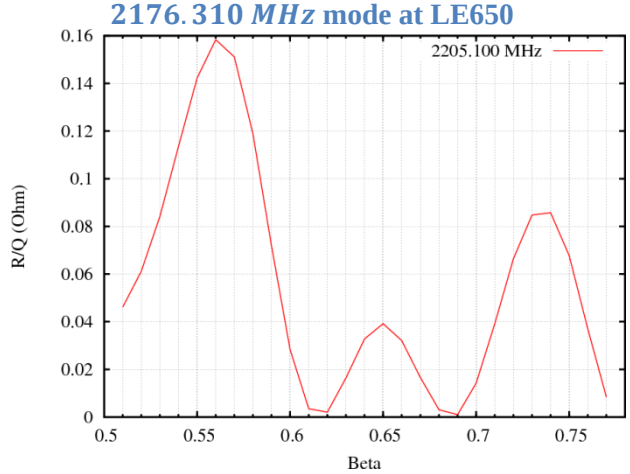

Figure 151: R/Q dependence on beta for $2205.100\ MHz$ mode at LE650

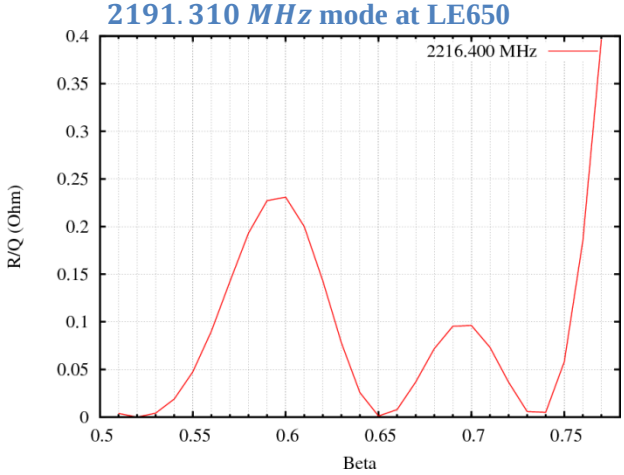

Figure 152: R/Q dependence on beta for $2216.400\ MHz$ mode at LE650

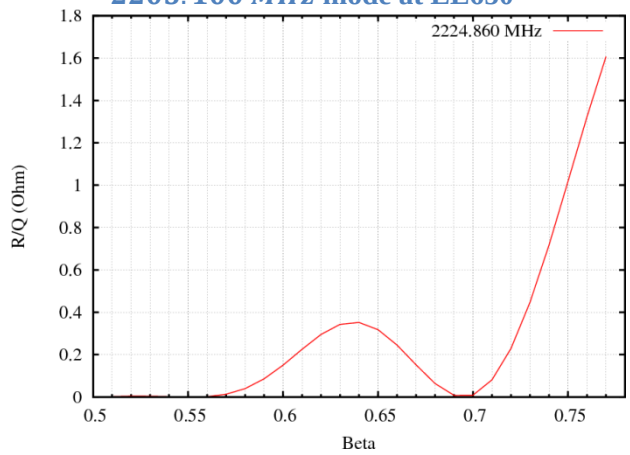

Figure 153: R/Q dependence on beta for $2224.860\ MHz$ mode at LE650

R/Q Dependences on Beta at LE650:

Monopole Modes ##25 – 30

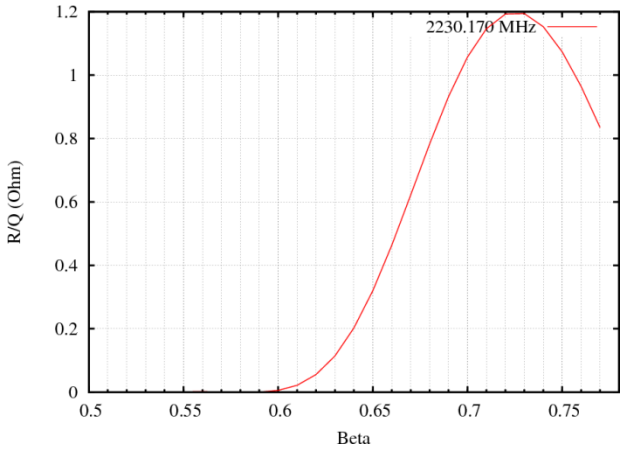

Figure 154: R/Q dependence on beta for $2230.170\ MHz$ mode at LE650

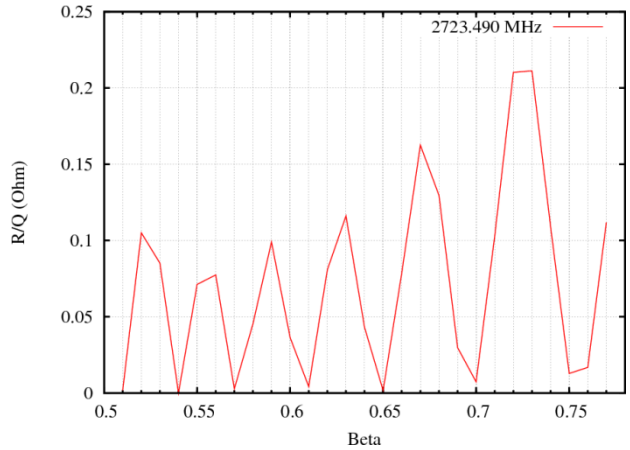

Figure 155: R/Q dependence on beta for $2723.490\ MHz$ mode at LE650

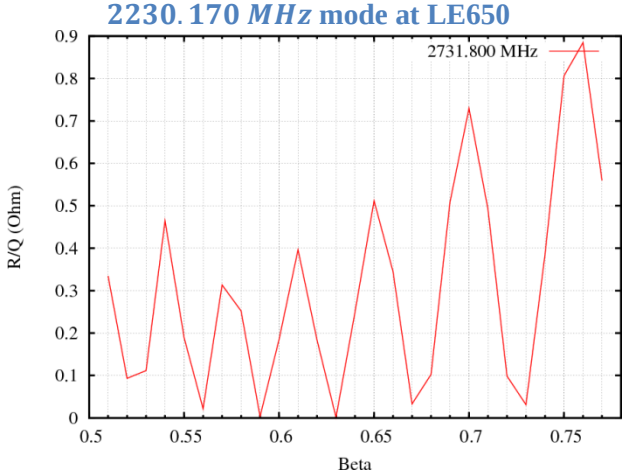

Figure 156: R/Q dependence on beta for $2731.800\ MHz$ mode at LE650

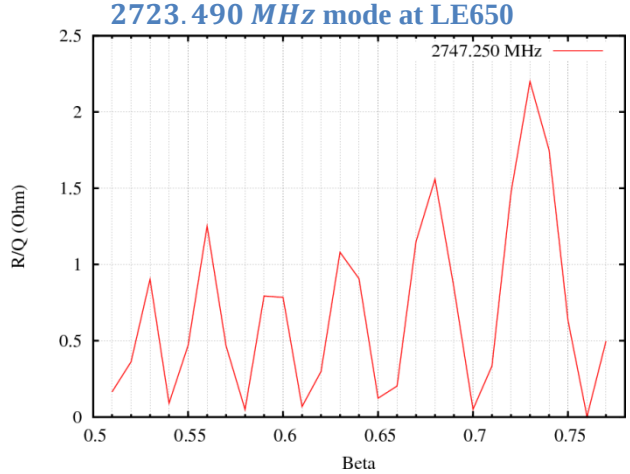

Figure 157: R/Q dependence on beta for $2747.250\ MHz$ mode at LE650

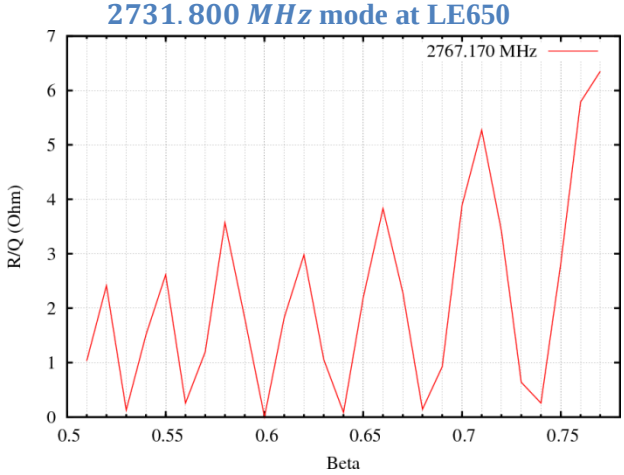

Figure 158: R/Q dependence on beta for $2767.170\ MHz$ mode at LE650

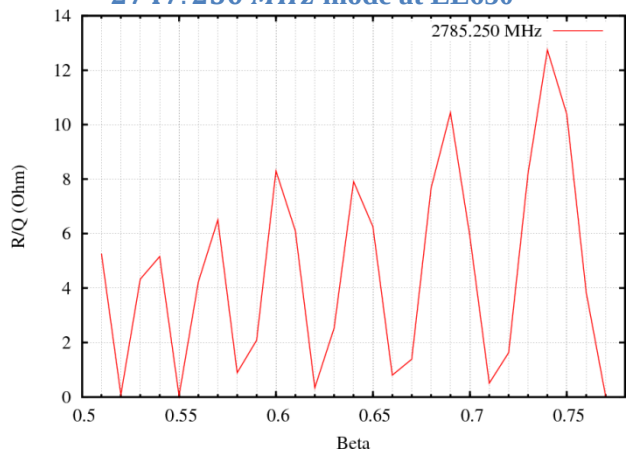

Figure 159: R/Q dependence on beta for $2785.250\ MHz$ mode at LE650

R/Q Dependences on Beta at LE650:

Dipole Modes ##1 – 6

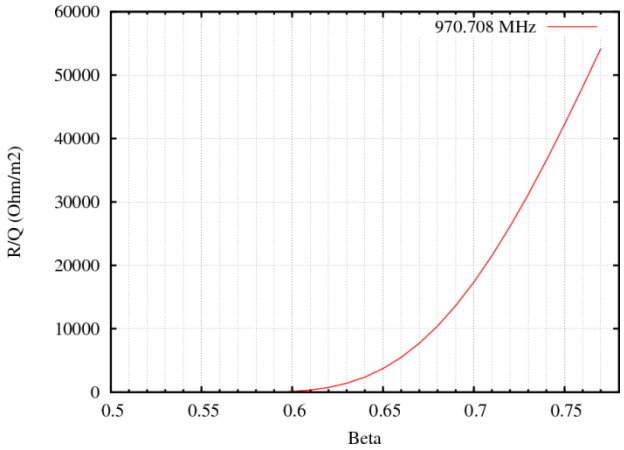

Figure 160: R/Q dependence on beta for $970.708\ MHz$ mode at LE650

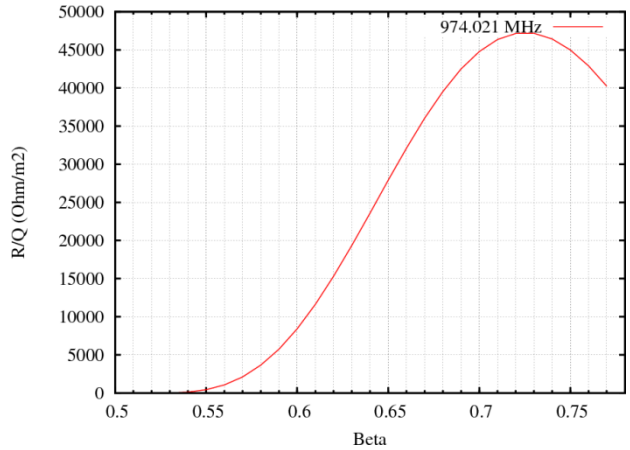

Figure 161: R/Q dependence on beta for $974.021\ MHz$ mode at LE650

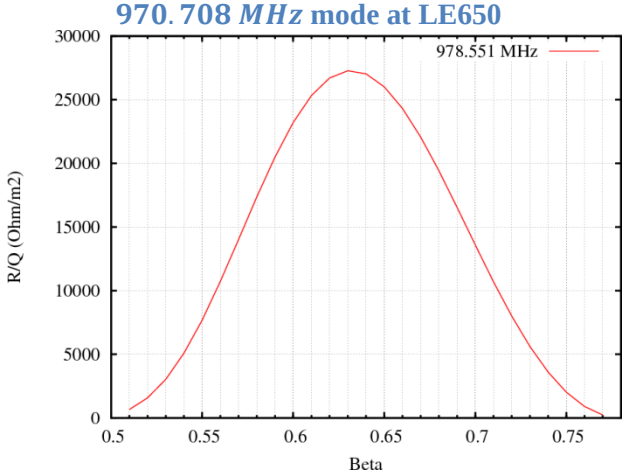

Figure 162: R/Q dependence on beta for $978.551\ MHz$ mode at LE650

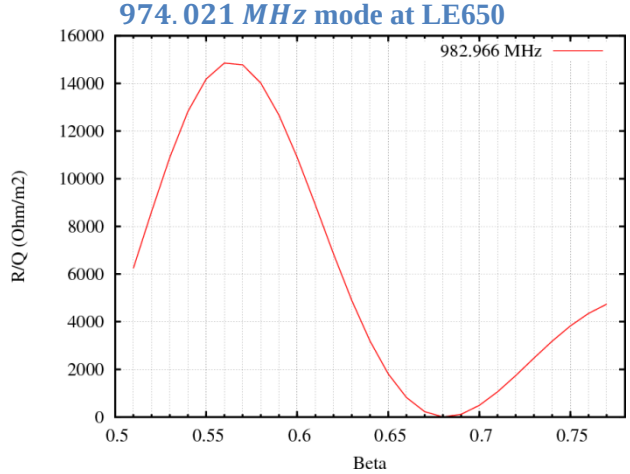

Figure 163: R/Q dependence on beta for $982.966\ MHz$ mode at LE650

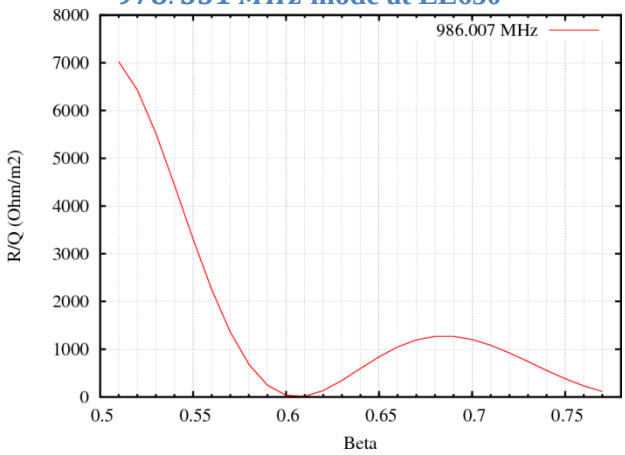

Figure 164: R/Q dependence on beta for $986.007\ MHz$ mode at LE650

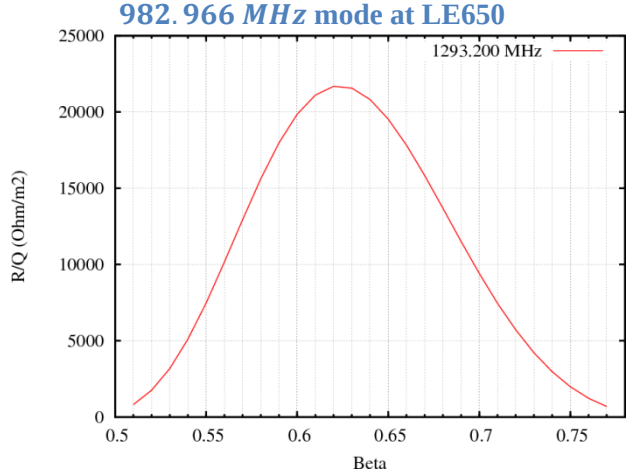

Figure 165: R/Q dependence on beta for $1293.200\ MHz$ mode at LE650

R/Q Dependences on Beta at LE650:

Dipole Modes ##7 – 12

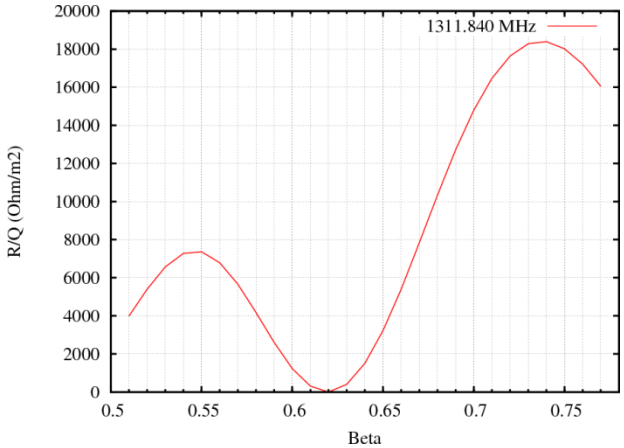

Figure 166: R/Q dependence on beta for $1311.840\ MHz$ mode at LE650

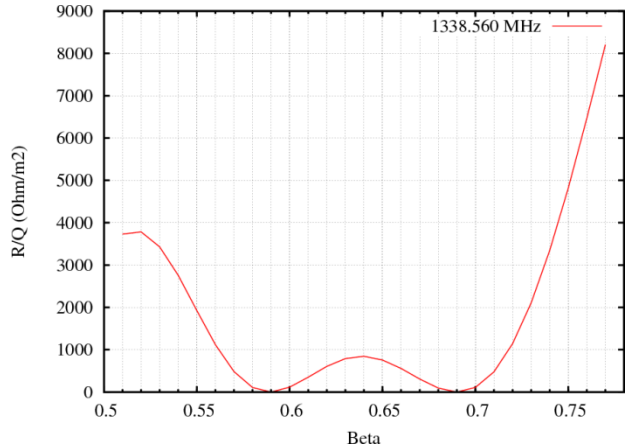

Figure 167: R/Q dependence on beta for $1338.560\ MHz$ mode at LE650

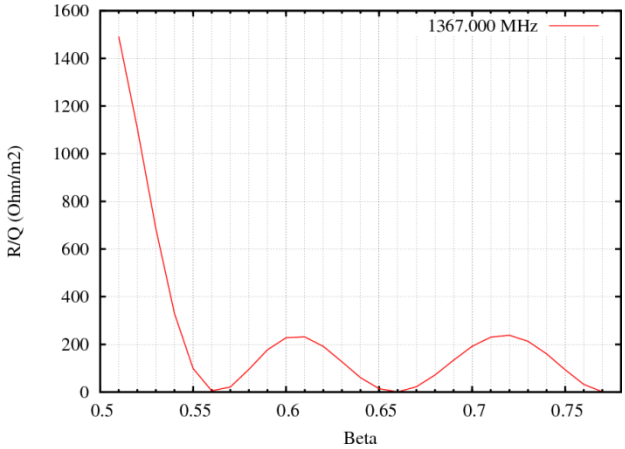

Figure 168: R/Q dependence on beta for $1367.000\ MHz$ mode at LE650

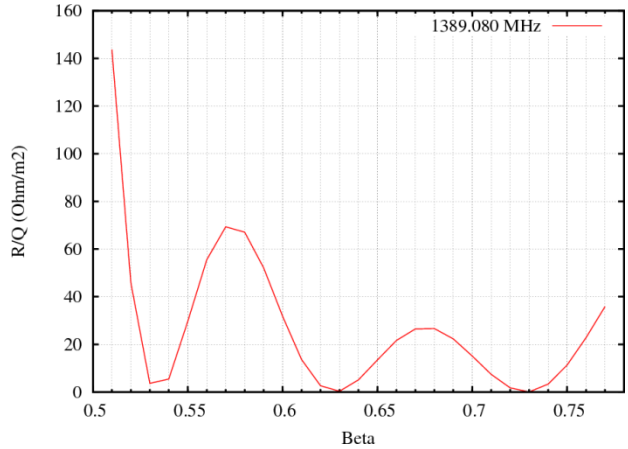

Figure 169: R/Q dependence on beta for $1389.080\ MHz$ mode at LE650

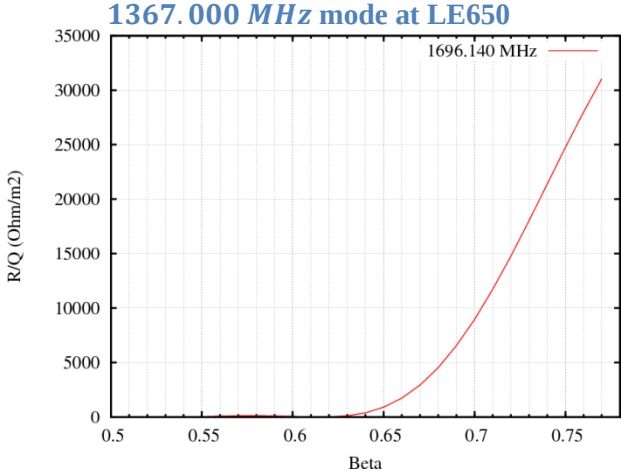

Figure 170: R/Q dependence on beta for $1696.140\ MHz$ mode at LE650

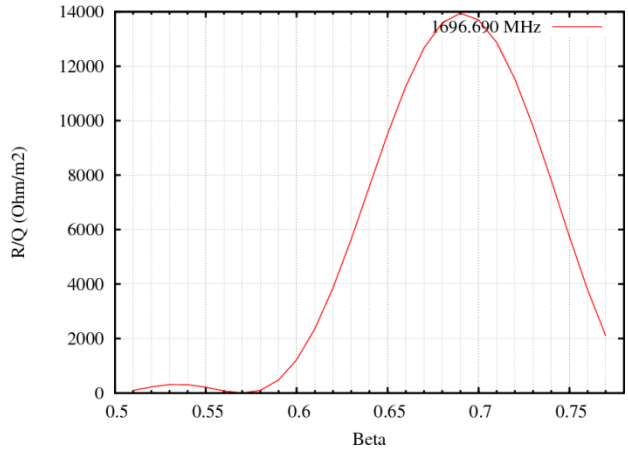

Figure 171: R/Q dependence on beta for $1696.690\ MHz$ mode at LE650

R/Q Dependences on Beta at LE650:

Dipole Modes ##13 – 18

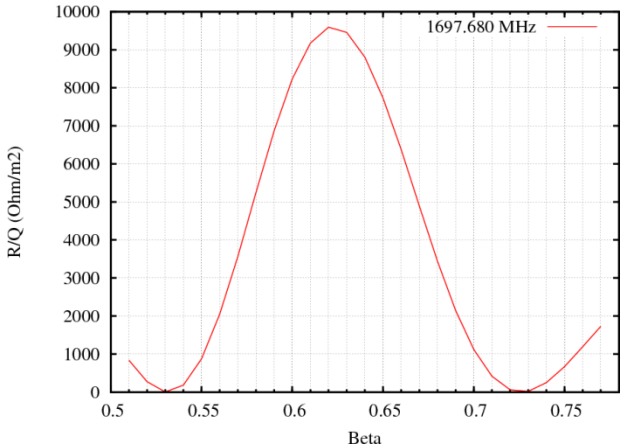

Figure 172: R/Q dependence on beta for $1697.680\ MHz$ mode at LE650

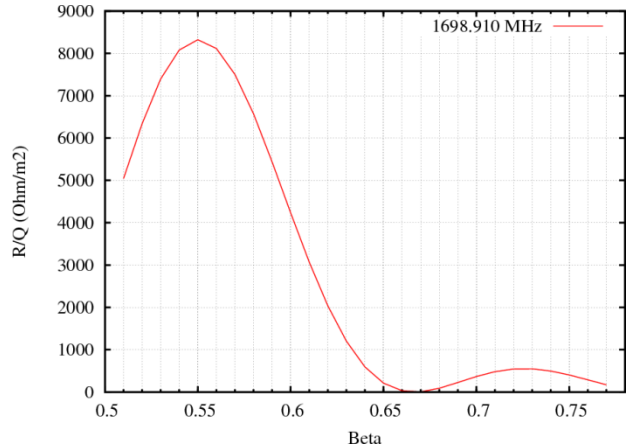

Figure 173: R/Q dependence on beta for $1698.910\ MHz$ mode at LE650

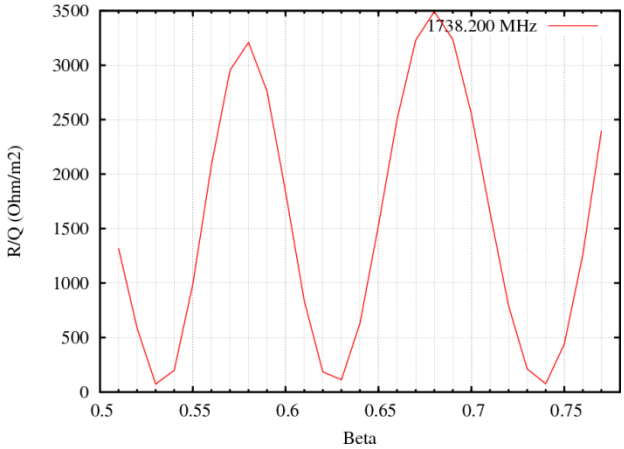

Figure 174: R/Q dependence on beta for $1738.200\ MHz$ mode at LE650

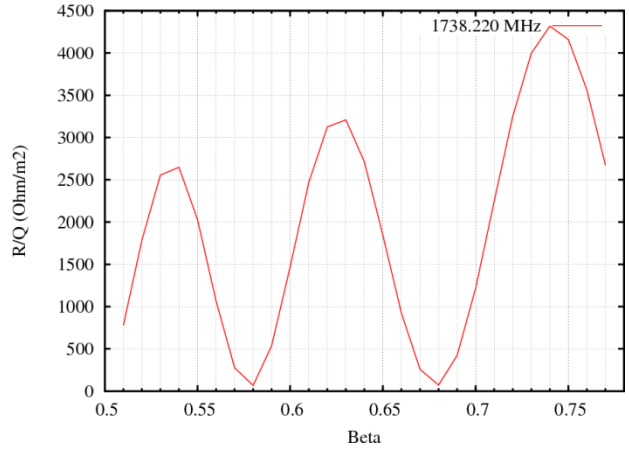

Figure 175: R/Q dependence on beta for $1738.220\ MHz$ mode at LE650

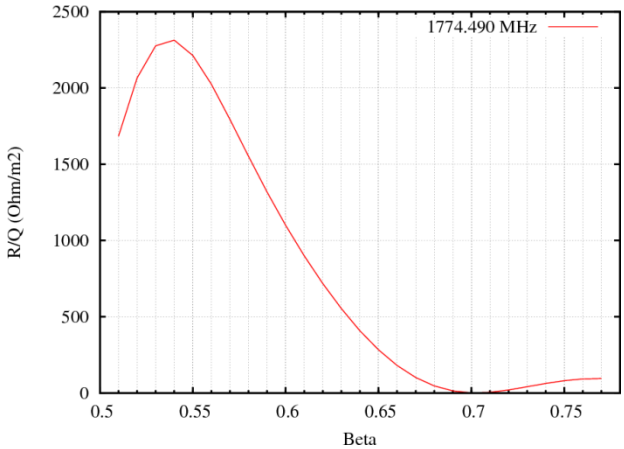

Figure 176: R/Q dependence on beta for $1774.490\ MHz$ mode at LE650

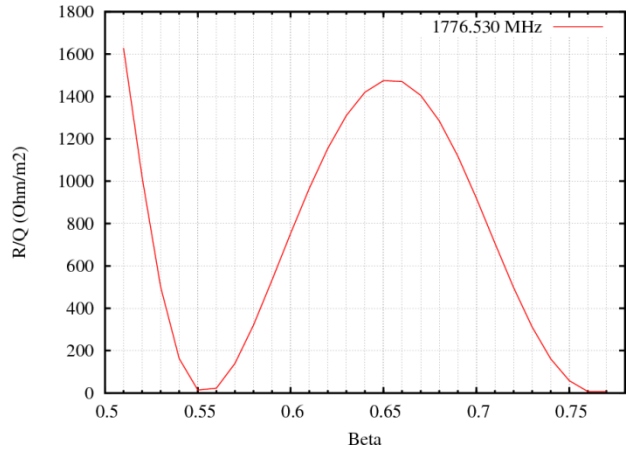

Figure 177: R/Q dependence on beta for $1776.530\ MHz$ mode at LE650

R/Q Dependences on Beta at LE650:

Dipole Modes ##19 – 24

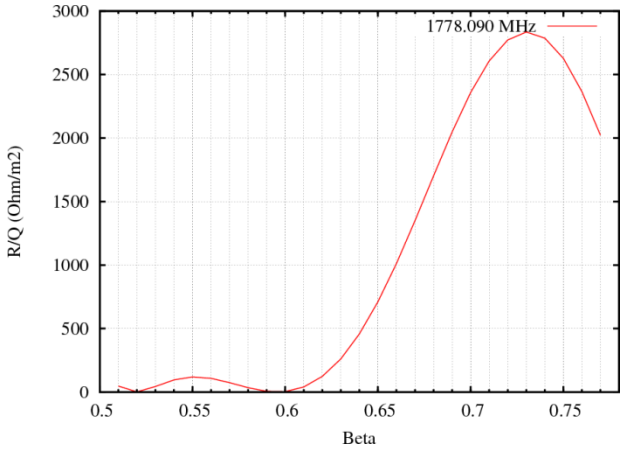

Figure 178: R/Q dependence on beta for $1778.090\ MHz$ mode at LE650

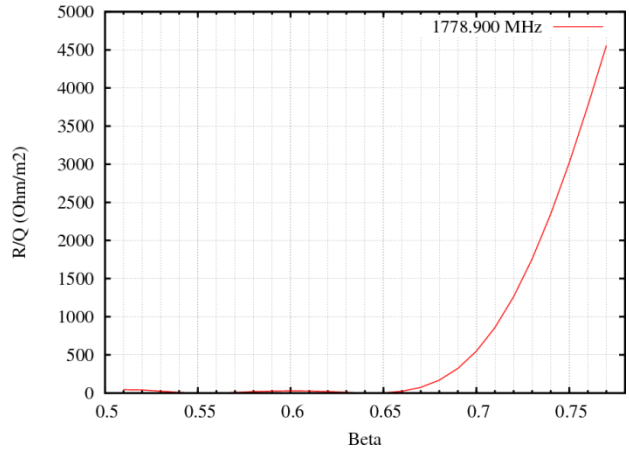

Figure 179: R/Q dependence on beta for $1778.900\ MHz$ mode at LE650

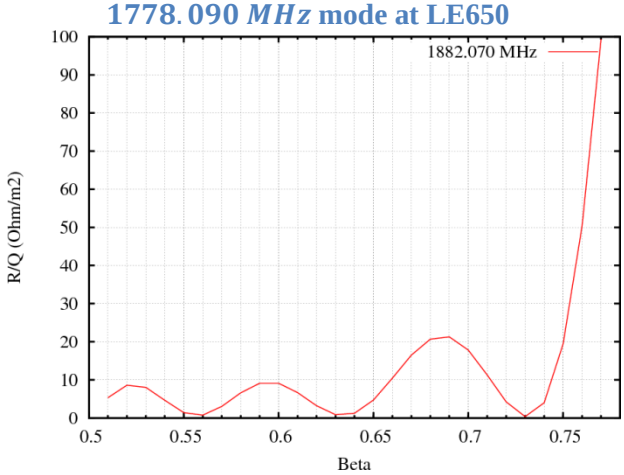

Figure 180: R/Q dependence on beta for $1882.070\ MHz$ mode at LE650

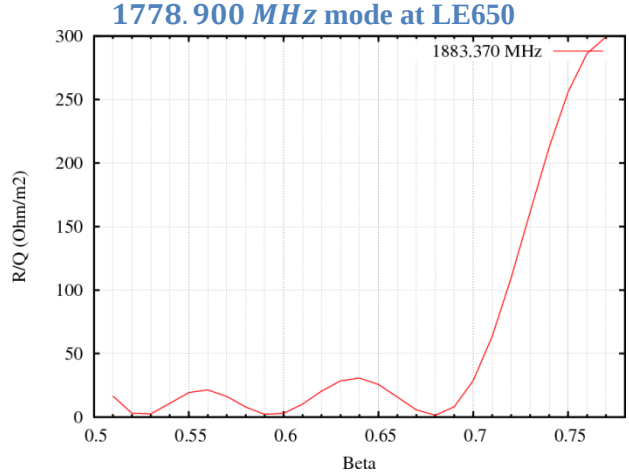

Figure 181: R/Q dependence on beta for $1883.370\ MHz$ mode at LE650

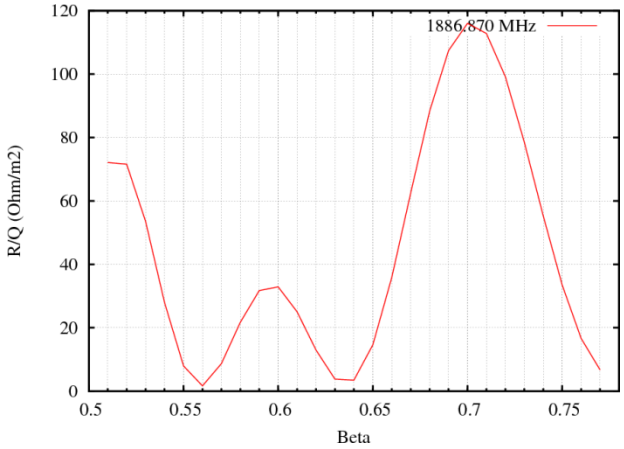

Figure 182: R/Q dependence on beta for $1886.870\ MHz$ mode at LE650

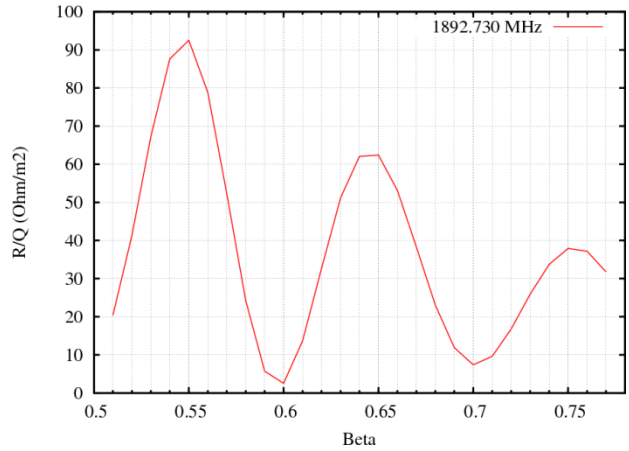

Figure 183: R/Q dependence on beta for $1892.730\ MHz$ mode at LE650

R/Q Dependences on Beta at LE650:

Dipole Modes ##25 – 30

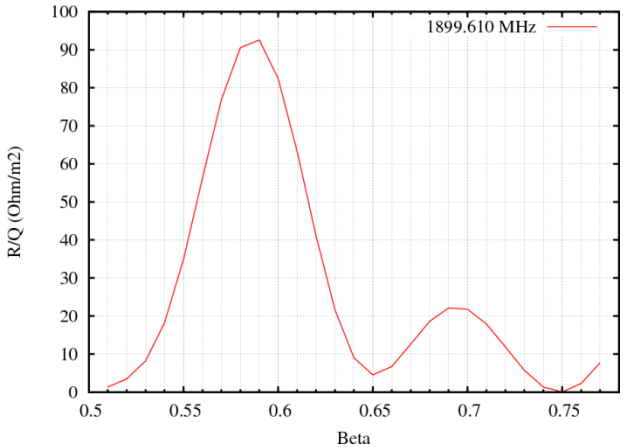

Figure 184: R/Q dependence on beta for $1899.610\ MHz$ mode at LE650

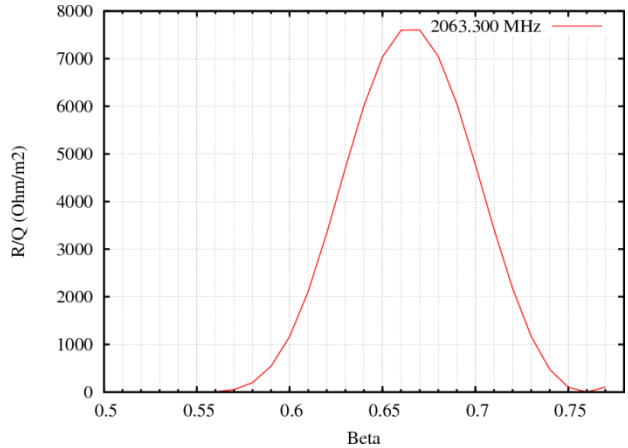

Figure 185: R/Q dependence on beta for $2063.300\ MHz$ mode at LE650

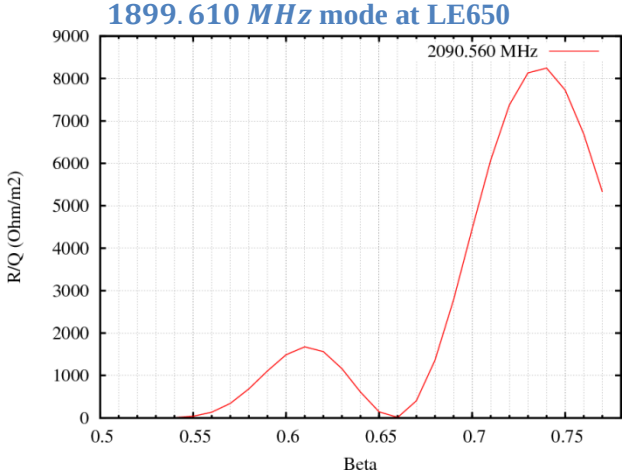

Figure 186: R/Q dependence on beta for $2090.560\ MHz$ mode at LE650

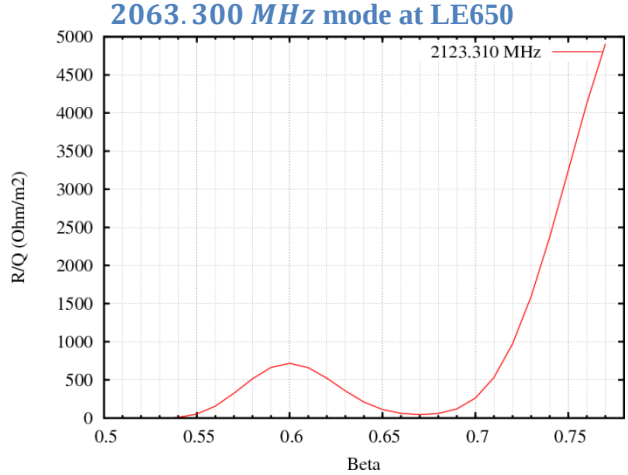

Figure 187: R/Q dependence on beta for $2123.310\ MHz$ mode at LE650

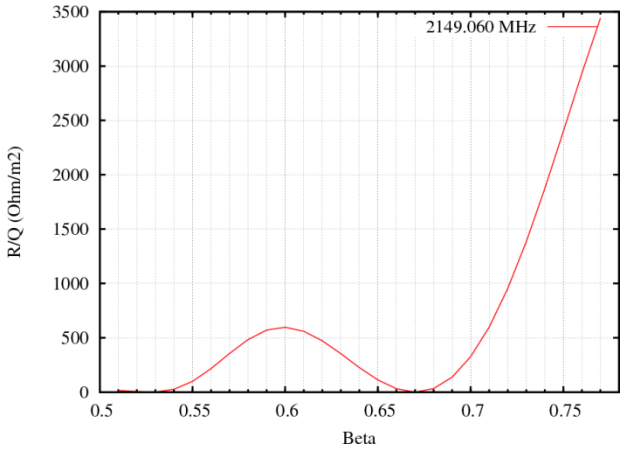

Figure 188: R/Q dependence on beta for $2149.060\ MHz$ mode at LE650

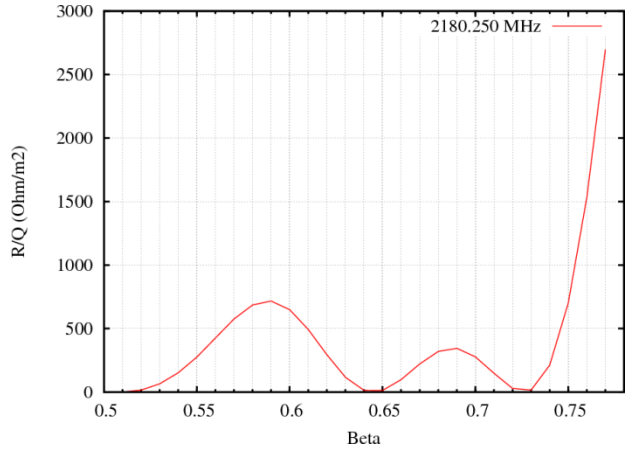

Figure 189: R/Q dependence on beta for $2180.250\ MHz$ mode at LE650

R/Q Dependences on Beta at HE650:

Monopole Modes ##1 – 6

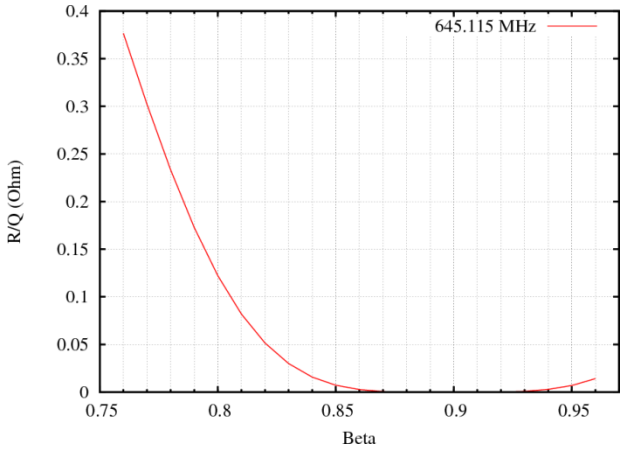

Figure 190: R/Q dependence on beta for $645.115\ MHz$ mode at HE650

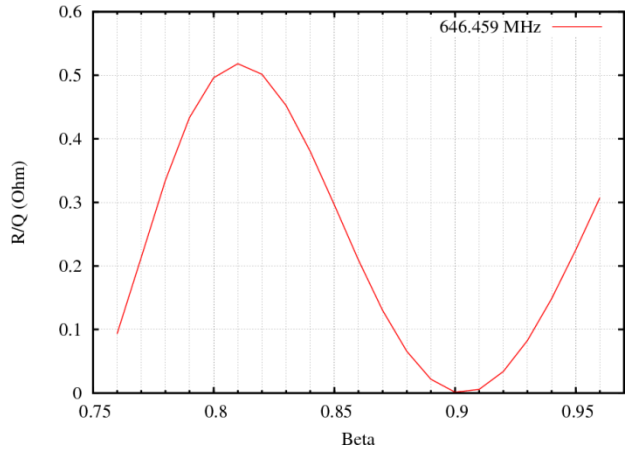

Figure 191: R/Q dependence on beta for $646.459\ MHz$ mode at HE650

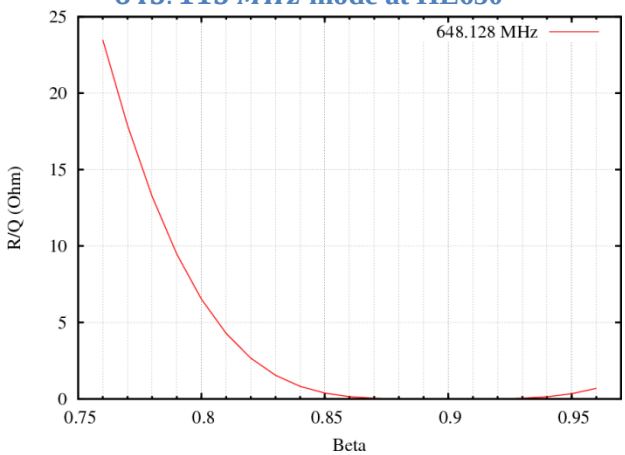

Figure 192: R/Q dependence on beta for $648.128\ MHz$ mode at HE650

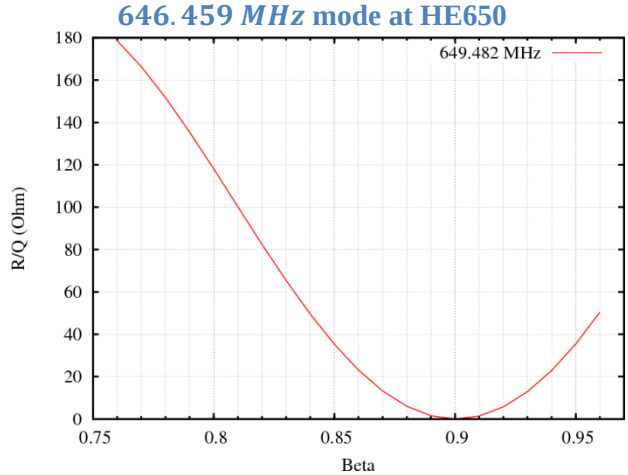

Figure 193: R/Q dependence on beta for $649.482\ MHz$ mode at HE650

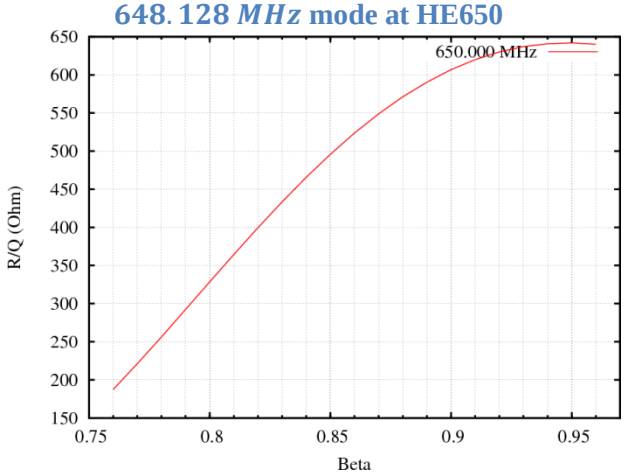

Figure 194: R/Q dependence on beta for $650\ MHz$ mode at HE650

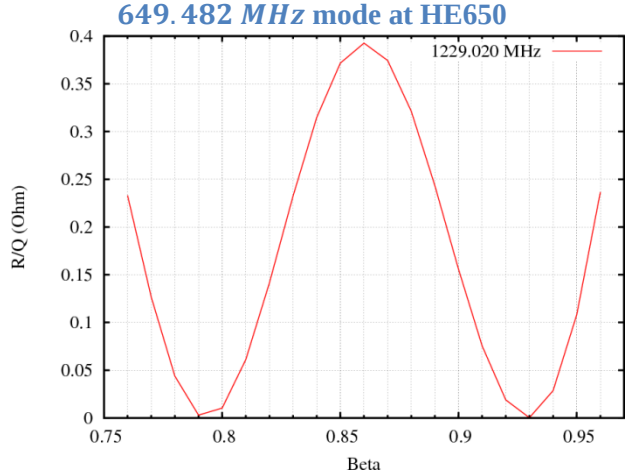

Figure 195: R/Q dependence on beta for $1229.020\ MHz$ mode at HE650

R/Q Dependences on Beta at HE650:

Monopole Modes ##7 – 12

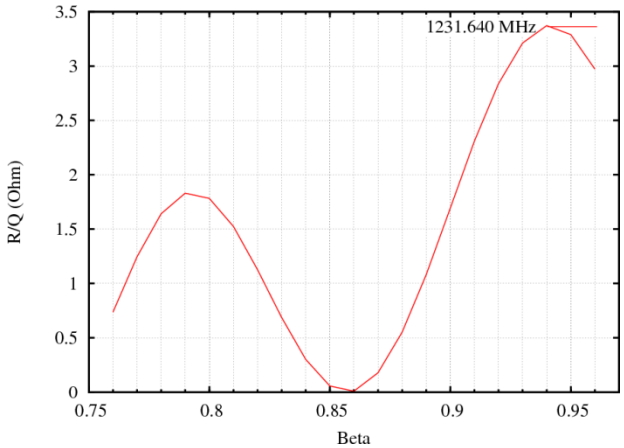

Figure 196: R/Q dependence on beta for $1231.640\ MHz$ mode at HE650

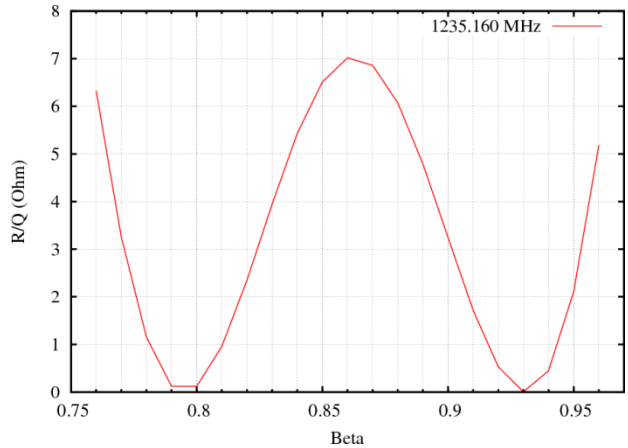

Figure 197: R/Q dependence on beta for $1235.160\ MHz$ mode at HE650

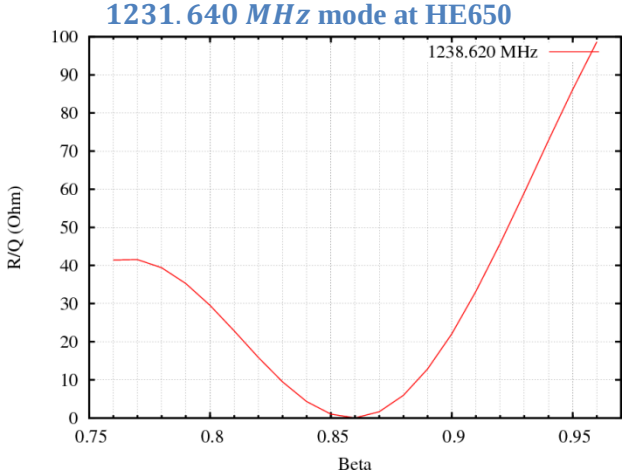

Figure 198: R/Q dependence on beta for $1238.620\ MHz$ mode at HE650

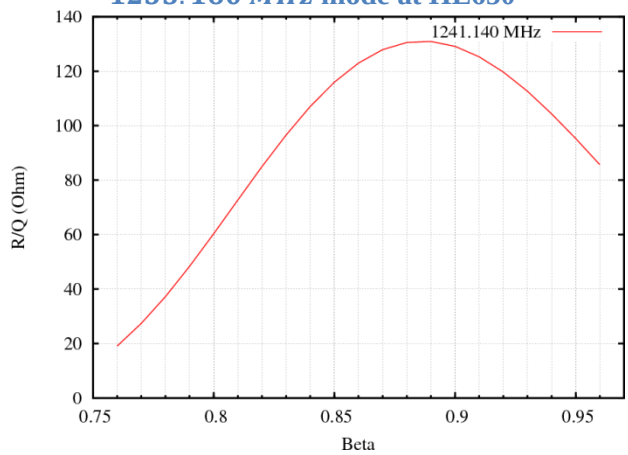

Figure 199: R/Q dependence on beta for $1241.140\ MHz$ mode at HE650

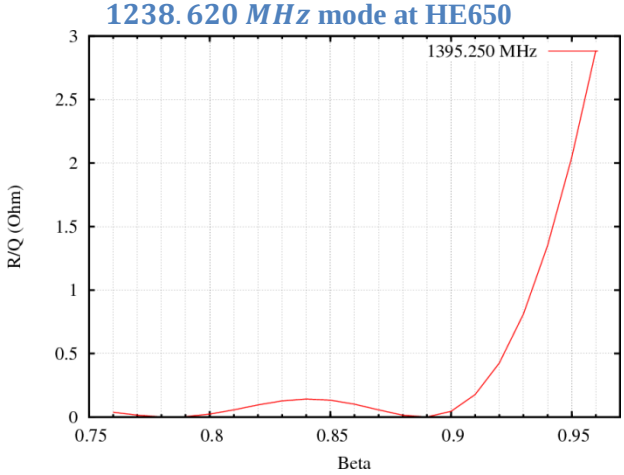

Figure 200: R/Q dependence on beta for $1395.250\ MHz$ mode at HE650

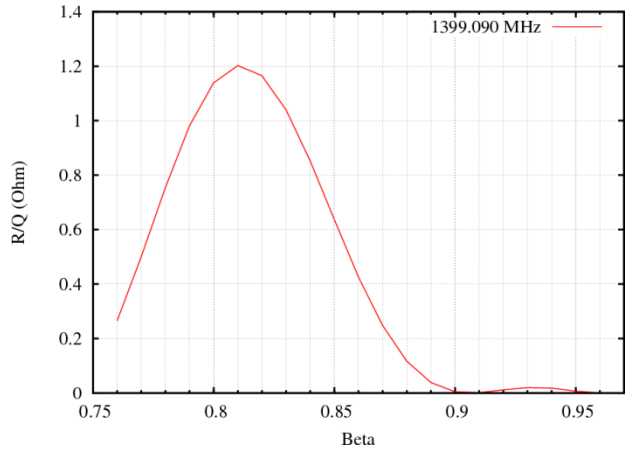

Figure 201: R/Q dependence on beta for $1399.090\ MHz$ mode at HE650

R/Q Dependences on Beta at HE650:

Monopole Modes ##13 – 18

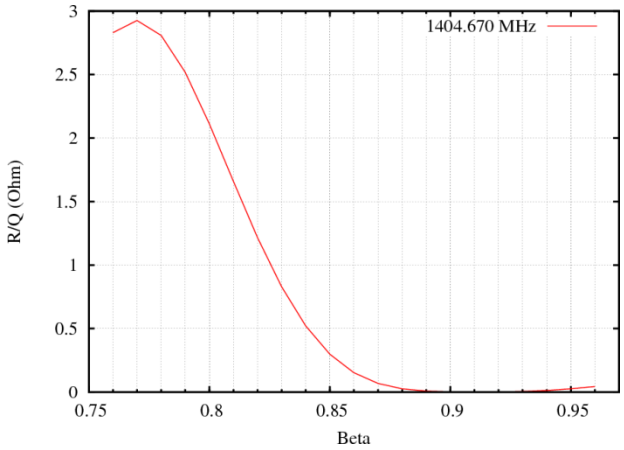

Figure 202: R/Q dependence on beta for $1404.670\ MHz$ mode at HE650

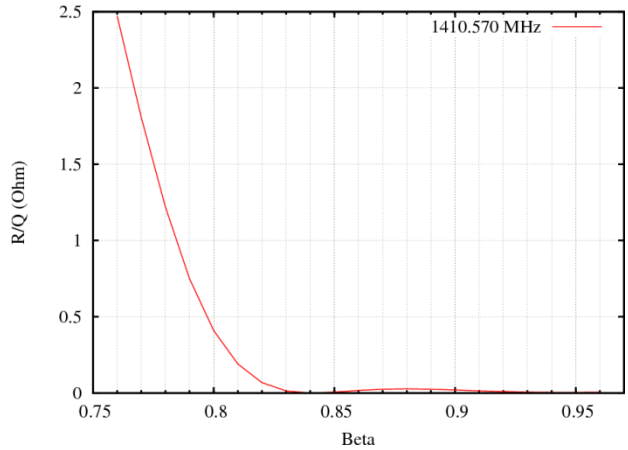

Figure 203: R/Q dependence on beta for $1410.570\ MHz$ mode at HE650

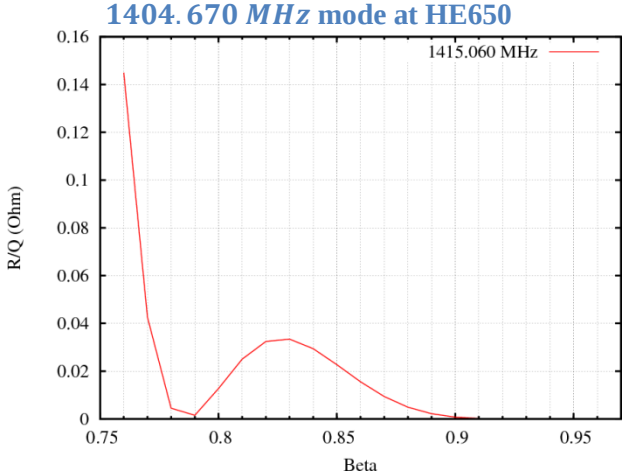

Figure 204: R/Q dependence on beta for $1415.060\ MHz$ mode at HE650

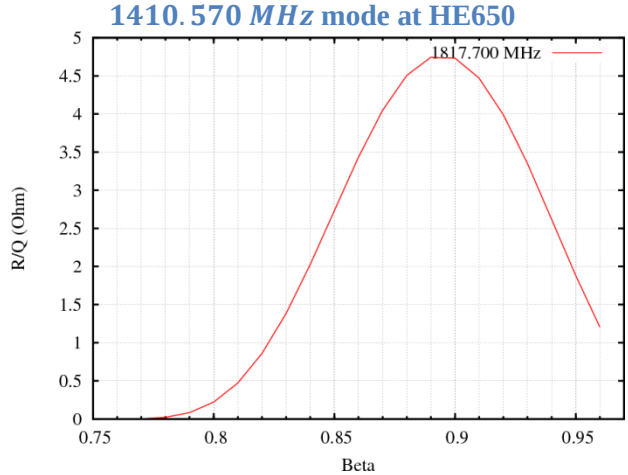

Figure 205: R/Q dependence on beta for $1817.700\ MHz$ mode at HE650

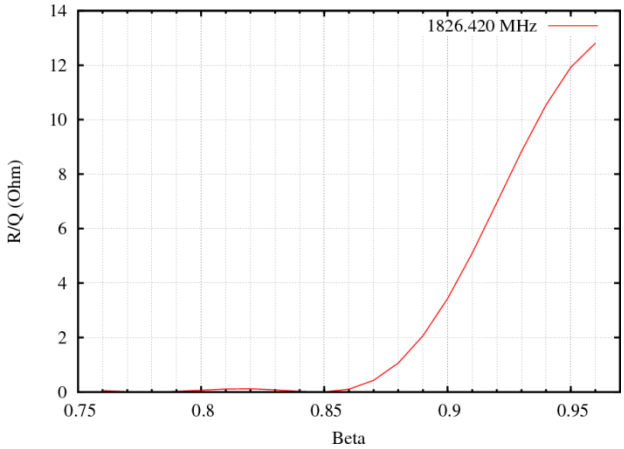

Figure 206: R/Q dependence on beta for $1826.420\ MHz$ mode at HE650

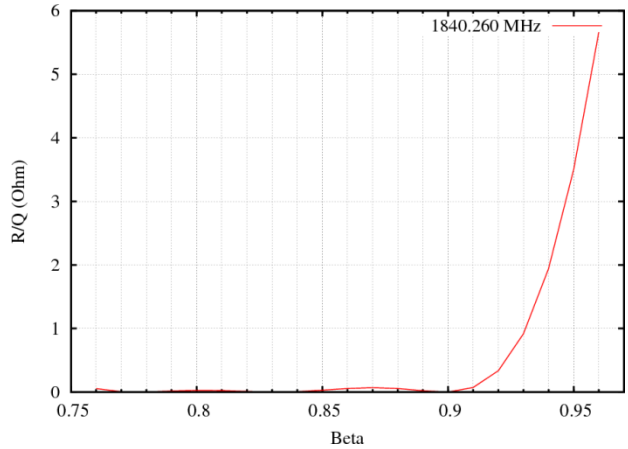

Figure 207: R/Q dependence on beta for $1840.260\ MHz$ mode at HE650

R/Q Dependences on Beta at HE650:

Monopole Modes ##19 – 24

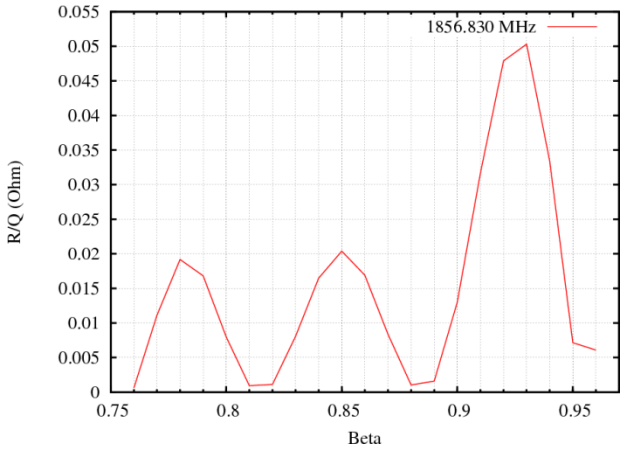

Figure 208: R/Q dependence on beta for $1856.830\ MHz$ mode at HE650

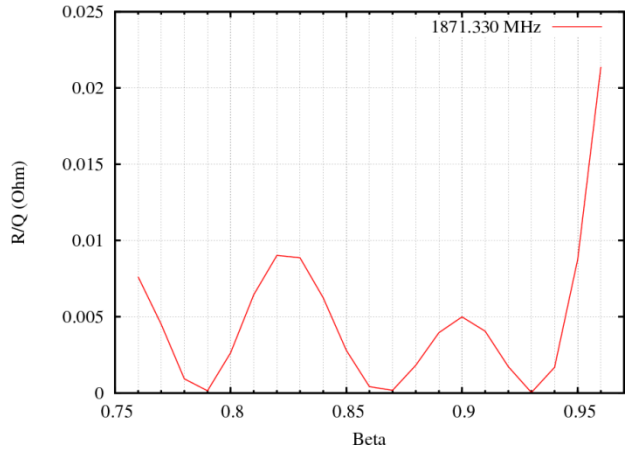

Figure 209: R/Q dependence on beta for $1871.330\ MHz$ mode at HE650

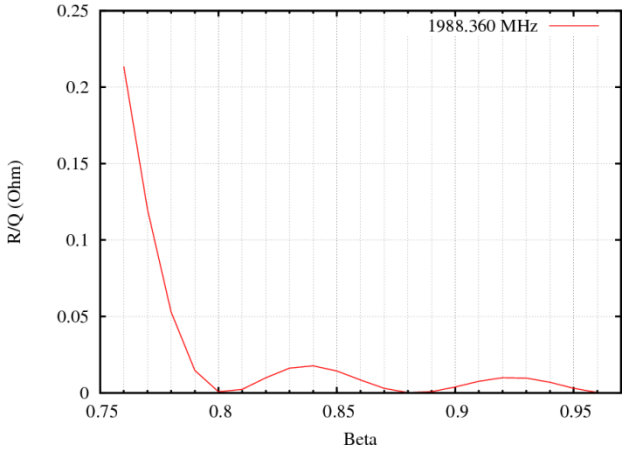

Figure 210: R/Q dependence on beta for $1988.360\ MHz$ mode at HE650

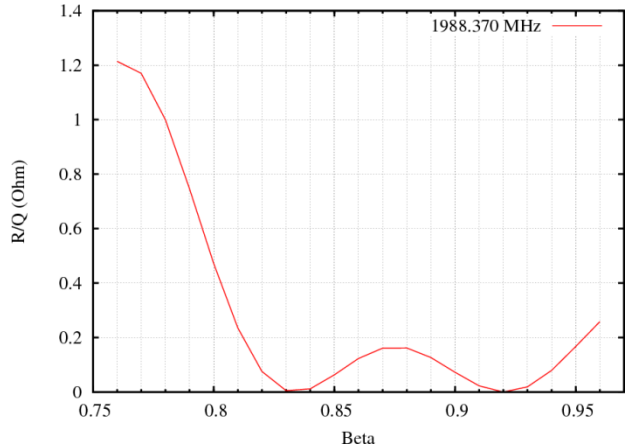

Figure 211: R/Q dependence on beta for $1988.370\ MHz$ mode at HE650

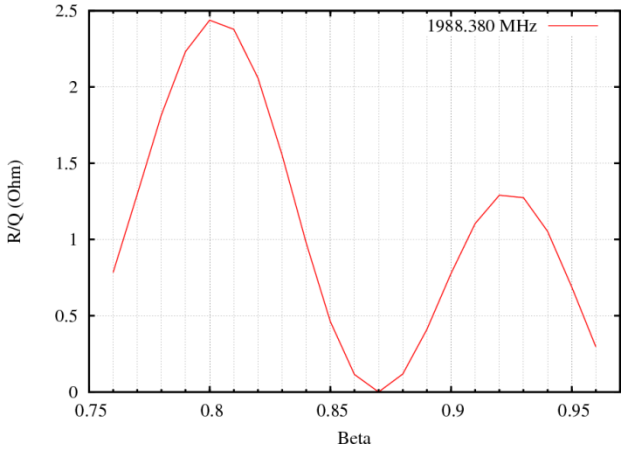

Figure 212: R/Q dependence on beta for $1988.380\ MHz$ mode at HE650

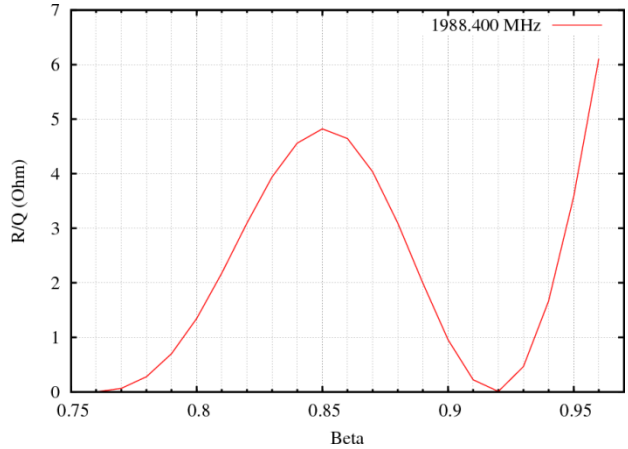

Figure 213: R/Q dependence on beta for $1988.400\ MHz$ mode at HE650

R/Q Dependences on Beta at HE650:

Monopole Modes ##25 – 30

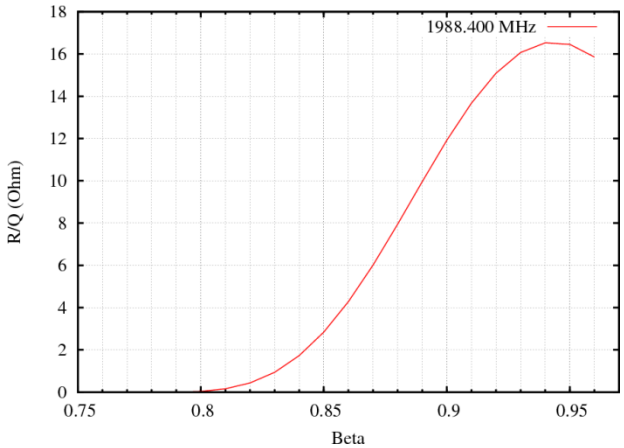

Figure 214: R/Q dependence on beta for $1988.400\ MHz$ mode at HE650

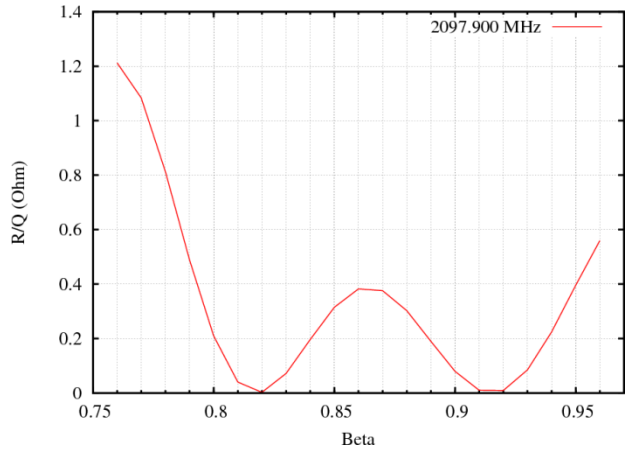

Figure 215: R/Q dependence on beta for $2097.900\ MHz$ mode at HE650

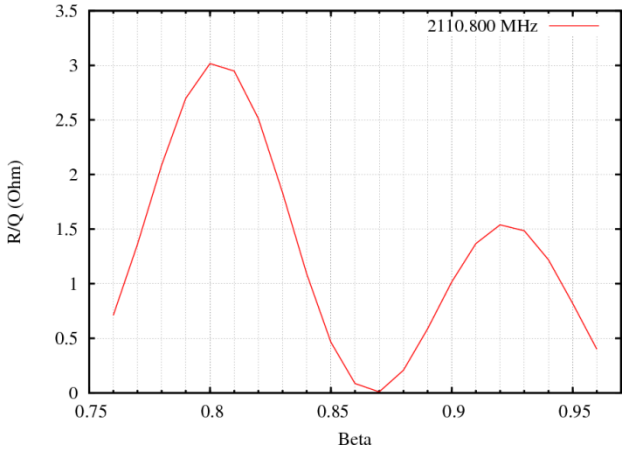

Figure 216: R/Q dependence on beta for $2110.800\ MHz$ mode at HE650

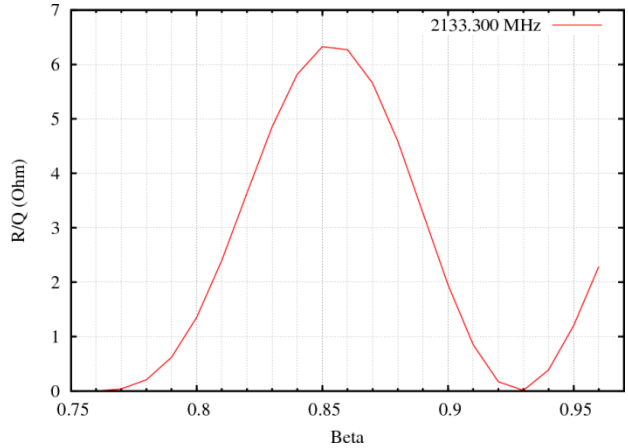

Figure 217: R/Q dependence on beta for $2133.300\ MHz$ mode at HE650

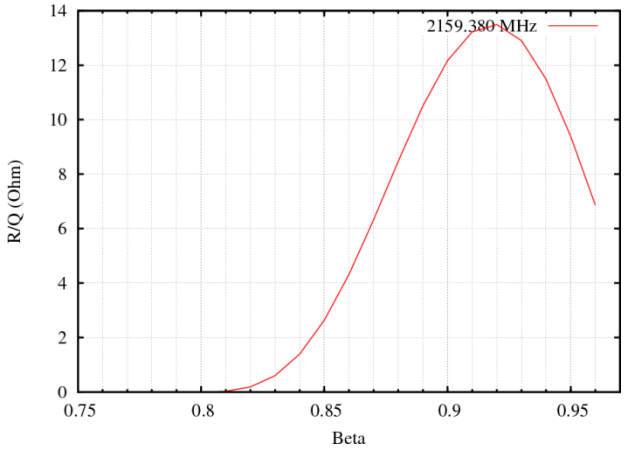

Figure 218: R/Q dependence on beta for $2159.380\ MHz$ mode at HE650

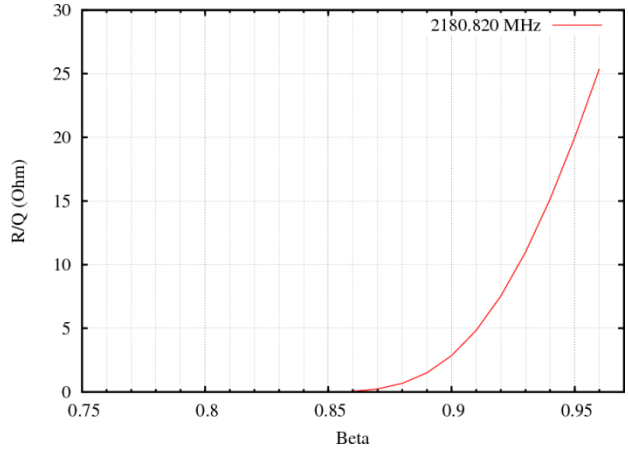

Figure 219: R/Q dependence on beta for $2180.820\ MHz$ mode at HE650

R/Q Dependences on Beta at HE650:

Dipole Modes ##1 – 6

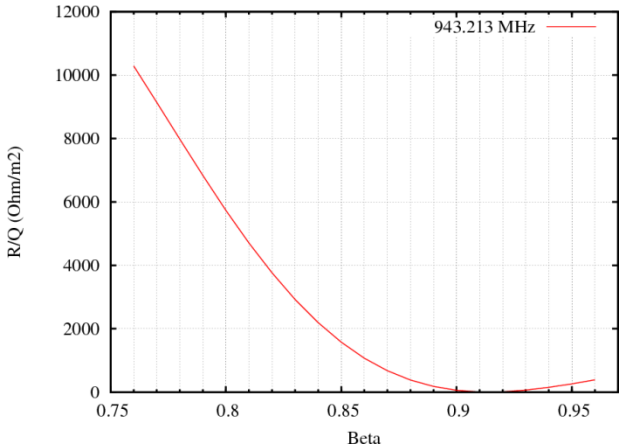

Figure 220: R/Q dependence on beta for $943.213\ MHz$ mode at HE650

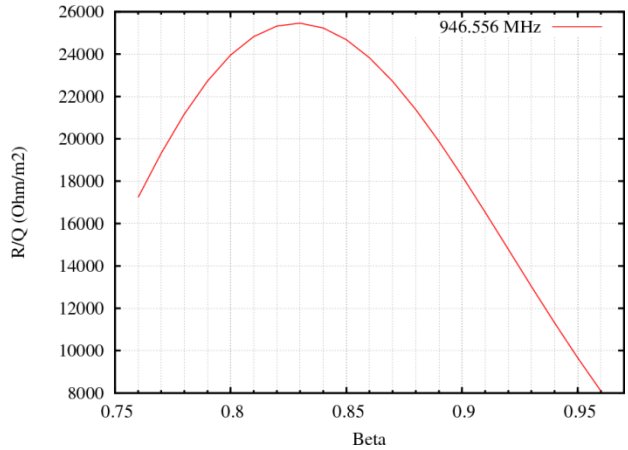

Figure 221: R/Q dependence on beta for $946.556\ MHz$ mode at HE650

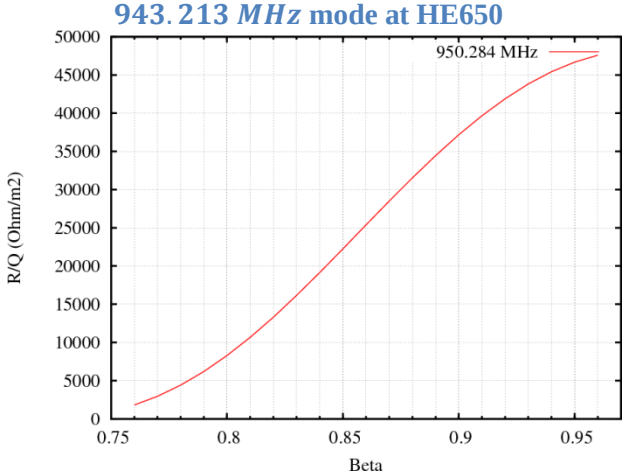

Figure 222: R/Q dependence on beta for $950.284\ MHz$ mode at HE650

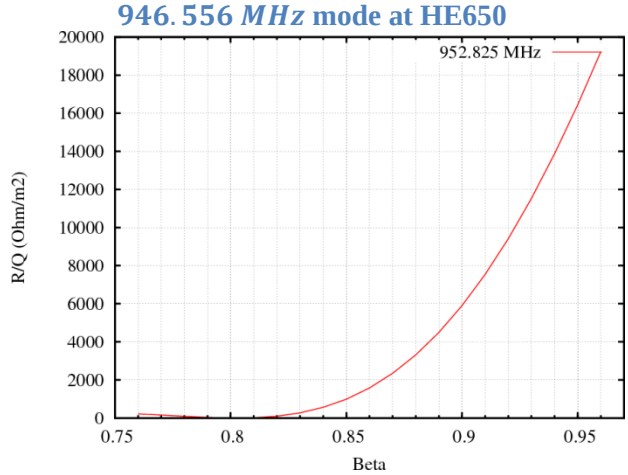

Figure 223: R/Q dependence on beta for $952.825\ MHz$ mode at HE650

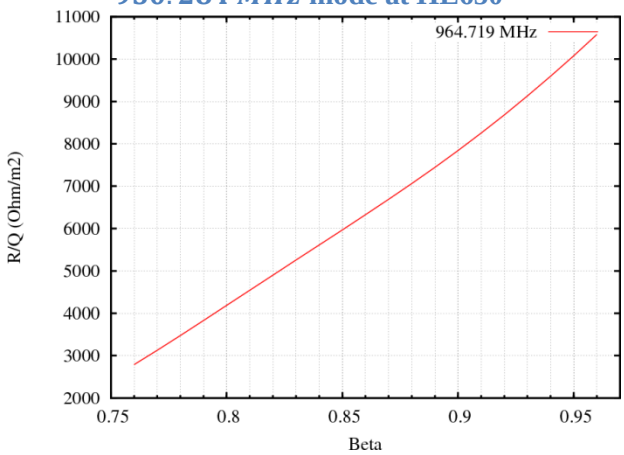

Figure 224: R/Q dependence on beta for $964.719\ MHz$ mode at HE650

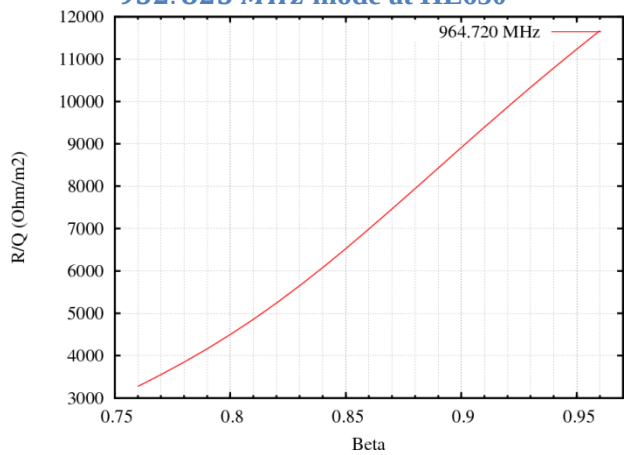

Figure 225: R/Q dependence on beta for $964.720\ MHz$ mode at HE650

R/Q Dependences on Beta at HE650:

Dipole Modes ##7 – 12

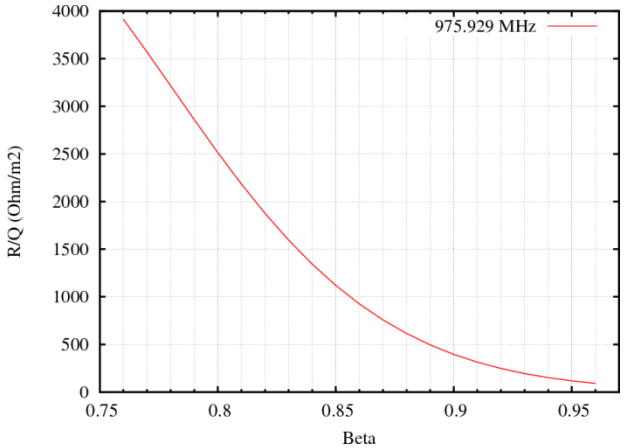

Figure 226: R/Q dependence on beta for $975.929\ MHz$ mode at HE650

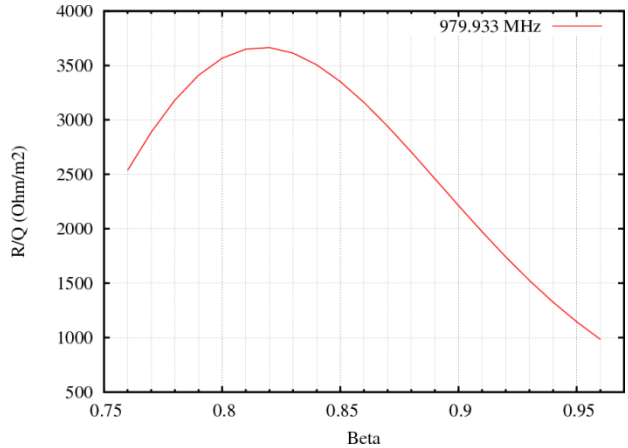

Figure 227: R/Q dependence on beta for $979.933\ MHz$ mode at HE650

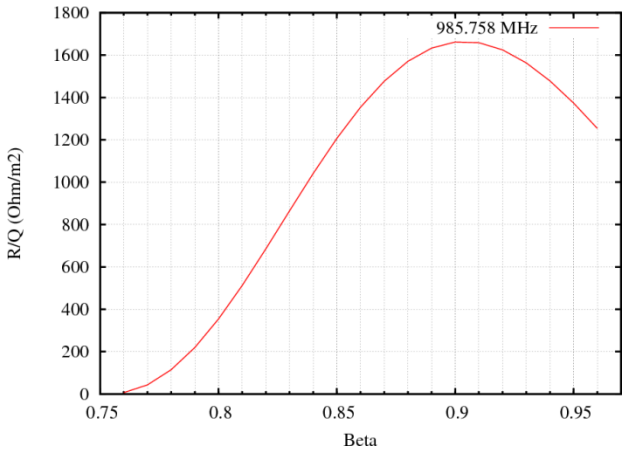

Figure 228: R/Q dependence on beta for $985.758\ MHz$ mode at HE650

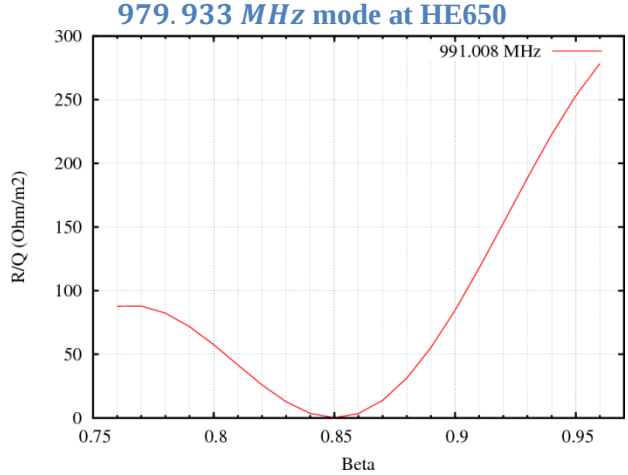

Figure 229: R/Q dependence on beta for $991.008\ MHz$ mode at HE650

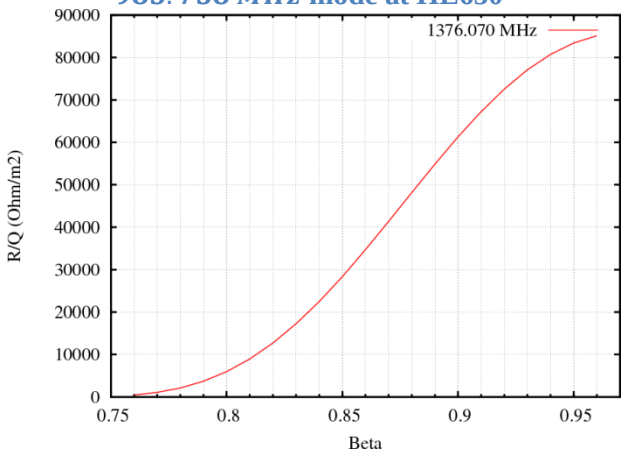

Figure 230: R/Q dependence on beta for $1376.070\ MHz$ mode at HE650

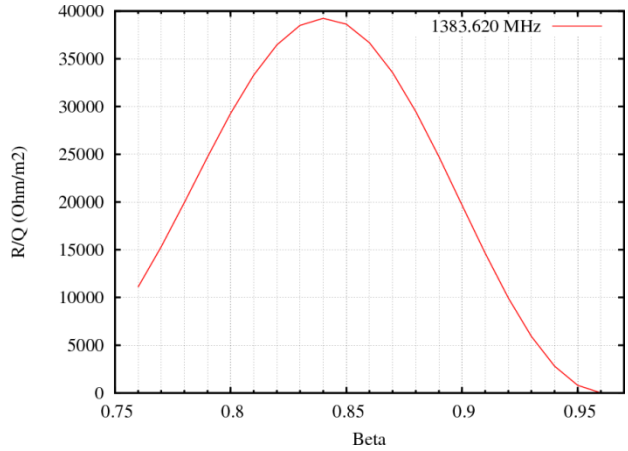

Figure 231: R/Q dependence on beta for $1383.620\ MHz$ mode at HE650

R/Q Dependences on Beta at HE650:

Dipole Modes ##13 – 18

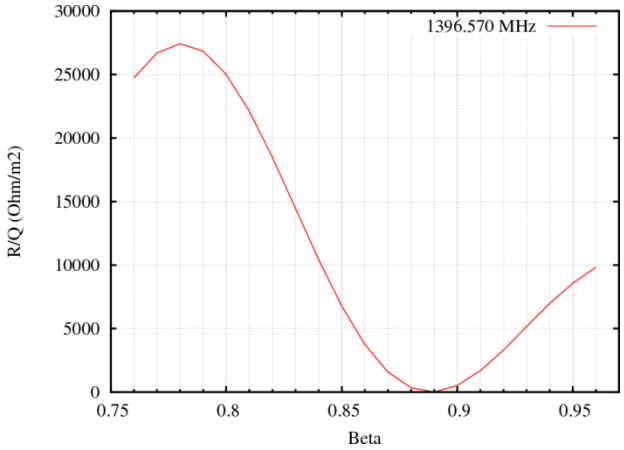

Figure 232: R/Q dependence on beta for $1396.570\ MHz$ mode at HE650

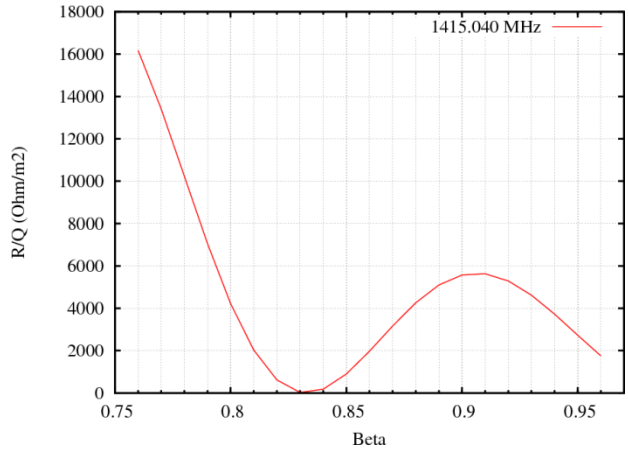

Figure 233: R/Q dependence on beta for $1415.040\ MHz$ mode at HE650

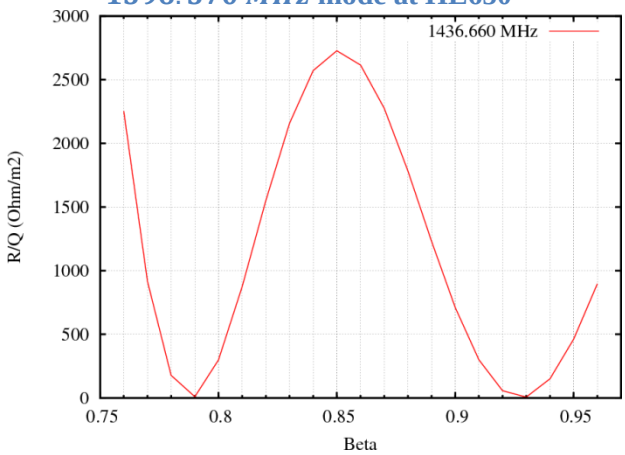

Figure 234: R/Q dependence on beta for $1436.660\ MHz$ mode at HE650

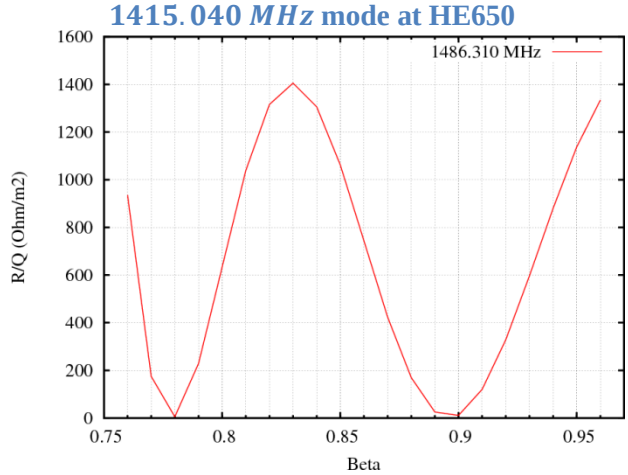

Figure 235: R/Q dependence on beta for $1486.310\ MHz$ mode at HE650

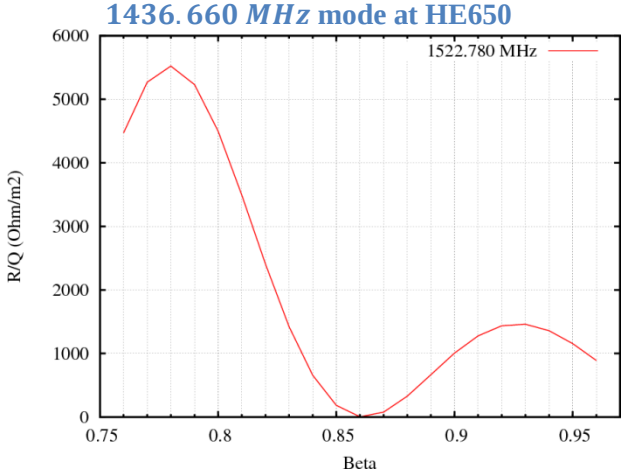

Figure 236: R/Q dependence on beta for $1522.780\ MHz$ mode at HE650

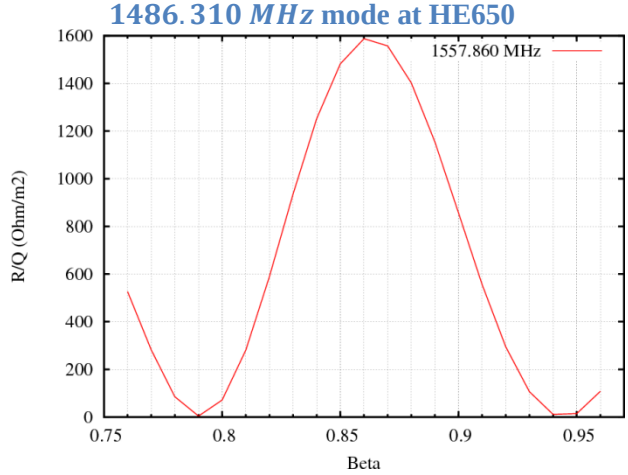

Figure 237: R/Q dependence on beta for $1557.860\ MHz$ mode at HE650

R/Q Dependences on Beta at HE650:

Dipole Modes ##19 – 24

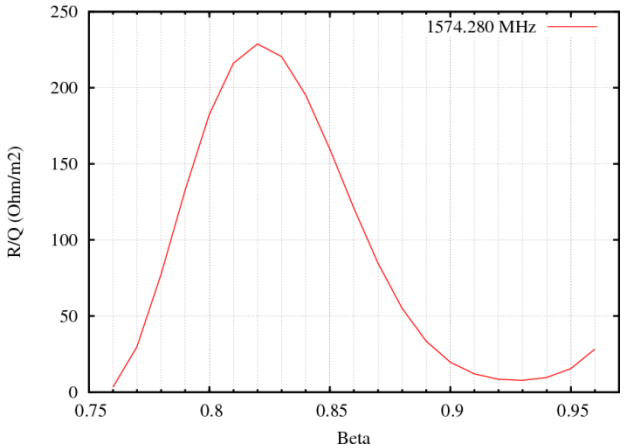

Figure 238: R/Q dependence on beta for $1574.280\ MHz$ mode at HE650

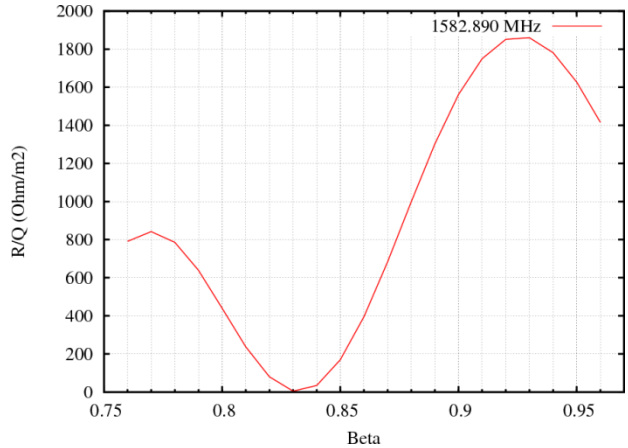

Figure 239: R/Q dependence on beta for $1582.890\ MHz$ mode at HE650

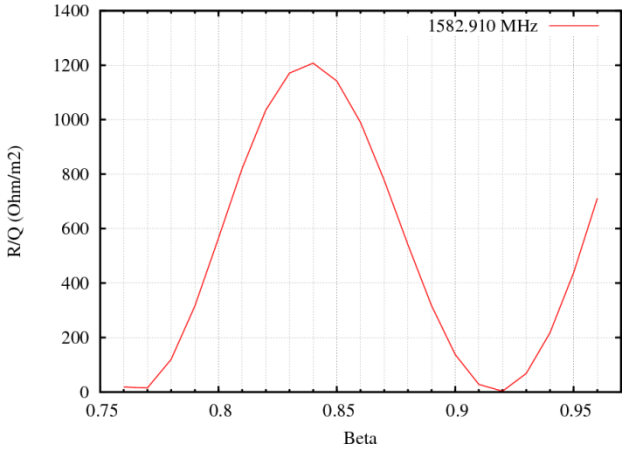

Figure 240: R/Q dependence on beta for $1582.910\ MHz$ mode at HE650

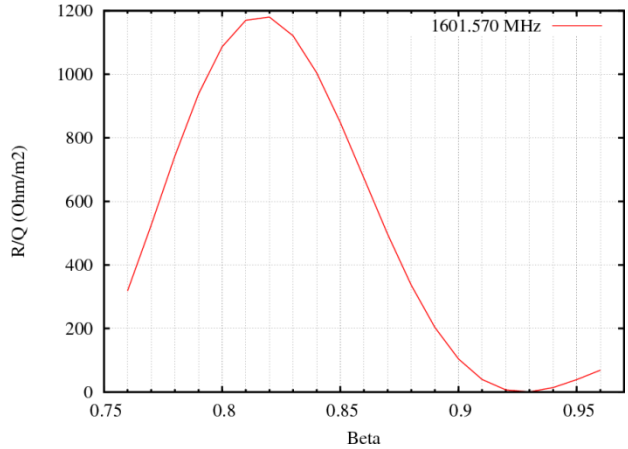

Figure 241: R/Q dependence on beta for $1601.570\ MHz$ mode at HE650

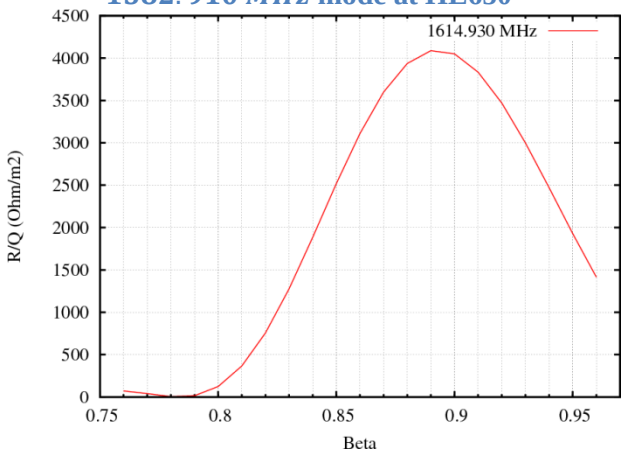

Figure 242: R/Q dependence on beta for $1614.930\ MHz$ mode at HE650

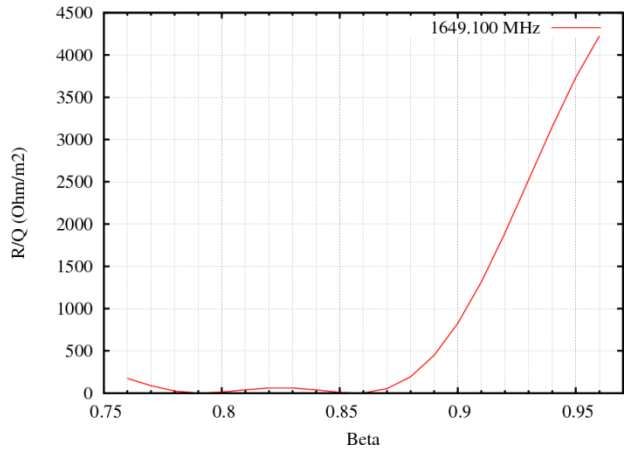

Figure 243: R/Q dependence on beta for $1649.100\ MHz$ mode at HE650

R/Q Dependences on Beta at HE650:

Dipole Modes ##25 – 30

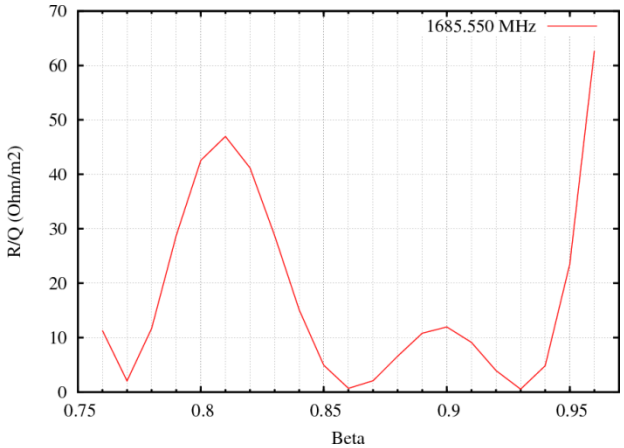

Figure 244: R/Q dependence on beta for $1685.550\ MHz$ mode at HE650

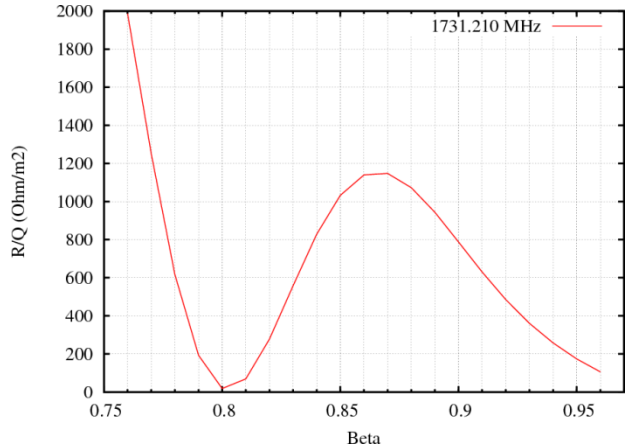

Figure 245: R/Q dependence on beta for $1731.210\ MHz$ mode at HE650

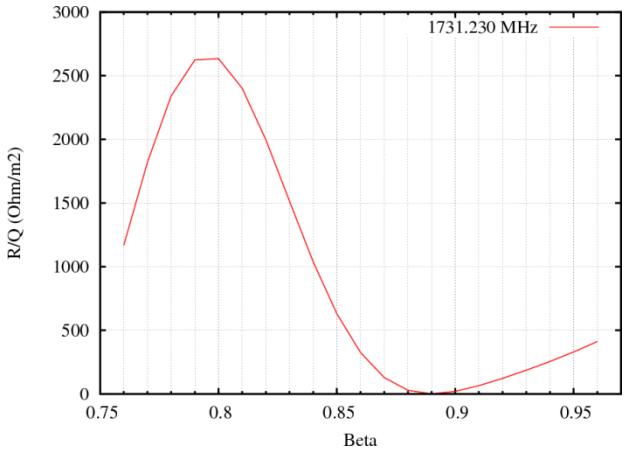

Figure 246: R/Q dependence on beta for $1731.230\ MHz$ mode at HE650

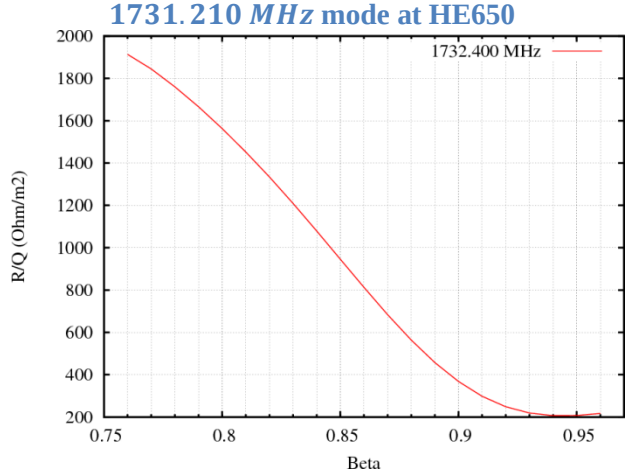

Figure 247: R/Q dependence on beta for $1732.400\ MHz$ mode at HE650

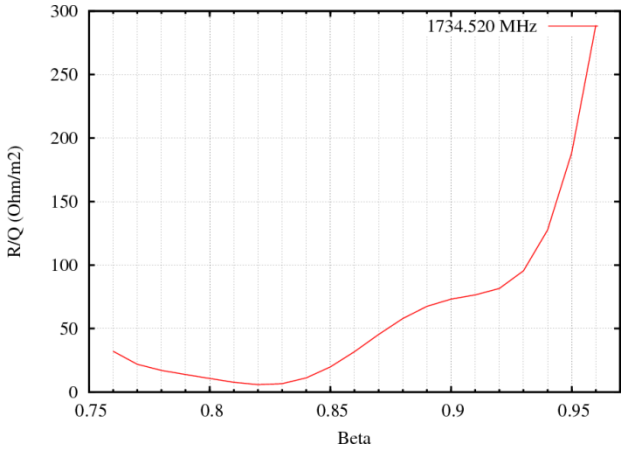

Figure 248: R/Q dependence on beta for $1734.520\ MHz$ mode at HE650

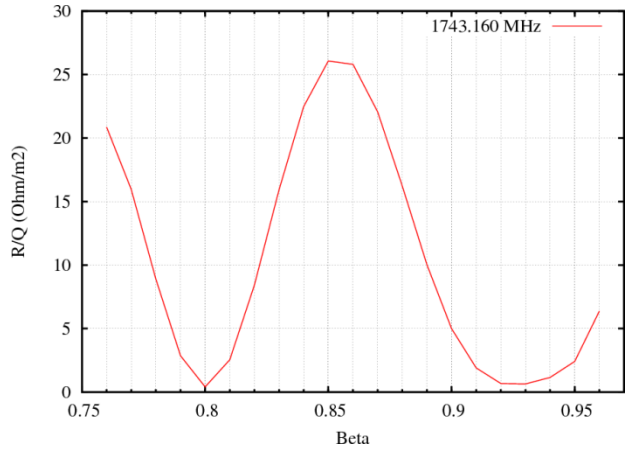

Figure 249: R/Q dependence on beta for $1743.160\ MHz$ mode at HE650

Alternative Spectrum

Alternative operation scenario of the Project X at 162.5 MHz frequency was suggested. Beam structure for this case is similar to the reference design one. It also contains three components: Muon, Kaon and other pulses. Muon pulses frequency is 81.25 MHz, and they are 10 % chopped at the frequency of 1 MHz. Kaon and other pulses frequencies are 20.3 MHz and 10.15 MHz correspondingly. Number of particles per bunch is bigger than it is at the reference design: 160 Mparticles compare with 120 Mparticels for the reference design. The beam structure is shown on the Figure 250.

Figure 250: Alternative beam structure. Muon pulses are shown in red. Kaon pulses are shown in blue. Other pulses are shown in green.

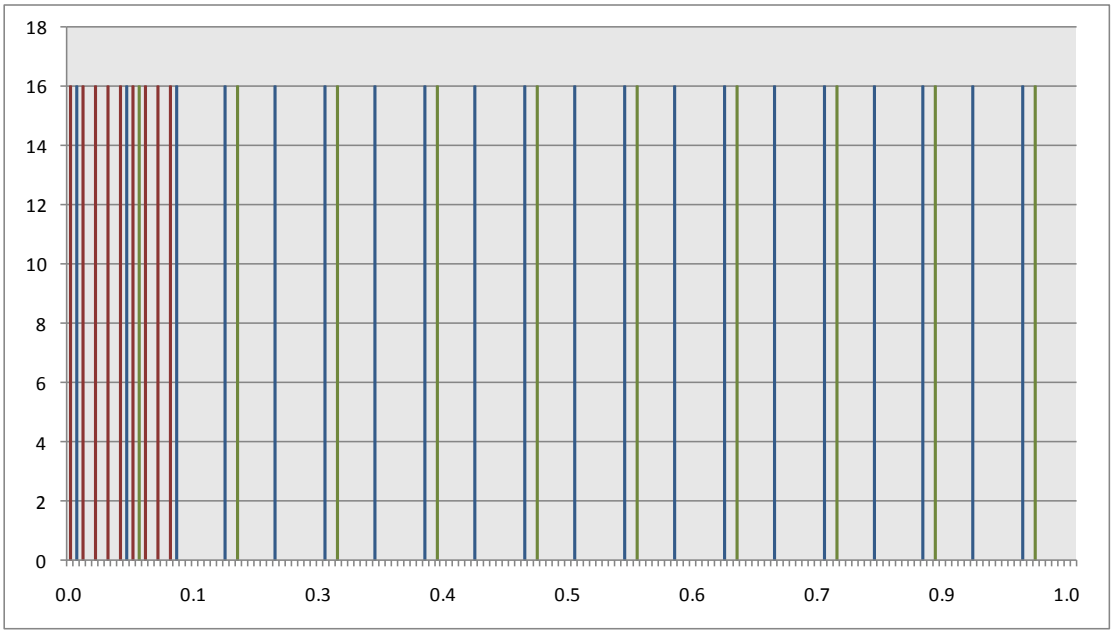

The same spectrum calculations as for the reference design were made for the alternative case, see Fgure 251. It is turned out that there is no new spectrum lines at the alternative spectrum which the reference design does not have. The strongest lines kept the same, but there are some lines which have larger amplitudes than they have at the reference design. There is no significant visual differences in the spectra, but separate losses calculations for the alternative one were made. They are described in the main part of the paper.
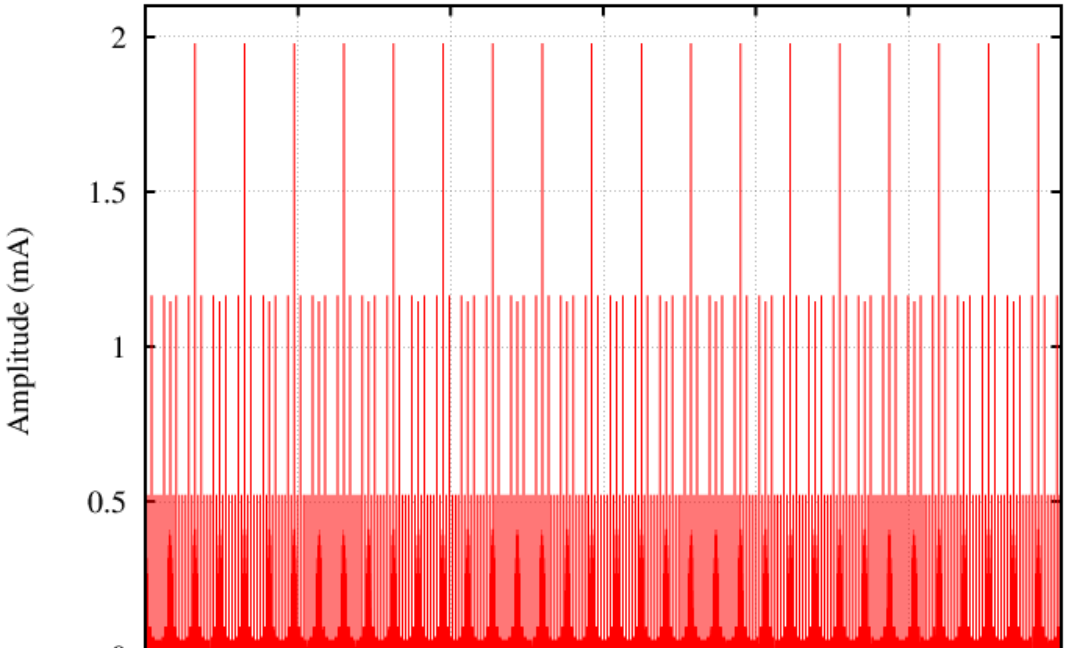
Figure 251: Alternative beam spectrum.